

THE
American Journal of
ANATOMY

MANAGING EDITOR

DONALD DUNCAN

THE UNIVERSITY OF TEXAS
MEDICAL BRANCH
GALVESTON TEXAS

ASSOCIATE EDITORS

BURTON L BAKER
UNIVERSITY OF MICHIGAN

RICHARD J BLANDAU
UNIVERSITY OF WASHINGTON

DON W FAWCETT
HARVARD UNIVERSITY

C P LEBLOND
MCGILL UNIVERSITY

HARLAND W MOSSMAN
UNIVERSITY OF WISCONSIN

VOLUME 108

JANUARY, MARCH MAY 1961

PUBLISHED BY

THE WISTAR INSTITUTE OF ANATOMY AND BIOLOGY
PHILADELPHIA PA

CONTENTS

No 1 JANUARY 1961

D A N HOYTE The Postnatal Growth of the Ear Capsule in the Rabbit	1
D B MOFFAT The Development of the Anterior Cerebral Artery and its Related Vessels in the Rat	17
W M FEAGANS L F CAVAZOS AND A T EWALD A Morphological and Histochemical Study of Estrogen-Induced Lesions in the Hamster Male Reproductive Tract	31
B PERCY Y CLEMMONT AND C P LEELEND The Wave of the Seminiferous Epithelium in the Rat	47
Y CLEMMONT AND CLAIRE HUCKINS Microscopic Anatomy of the Sex Cords and Seminiferous Tubules in Growing and Adult Male Albino Rats	79
MELVIN L MOSS Osteogenesis of Acellular Teleost Fish Bone	99
HELGE ANDERSEN AND FREDE BRØ-RASMUSSEN Histochemical Studies on the Histogenesis of the Joints in Human Fetuses with Special Reference to the Development of the Joint Cavities in the Hand and Foot	111

No 2 MARCH 1961

DOUGLAS B WEBSTER The Ear Apparatus of the Kangaroo Rat, <i>Dipodomys</i>	123
RICHARD F McLAUGHLIN WALTER S TYLER AND ROBERT O CANADA A Study of the Subgross Pulmonary Anatomy in Various Mammals	149
GERALD P BODEY OLGA MIRONOWSKA AND GEORGE O GUY Studies on Adrenal Transplantation. I Homologous and Autogenous Transplants	167
ADOLPH I COHEN Electron Microscopic Observations of the Internal Limiting Membrane and Optic Fiber Layer of the Retina of the Rhesus Monkey (<i>Macaca</i>)	179
CHARLES G BATTIG AND FRANK N LOW The Ultrastructure of Human Cardiac Muscle and its Associated Tissue Space	199

CONTENTS

No 3 MAY 1961

CATHRINE E STEVENS HOOPER Use of Colchicine for the Measurement of Mitotic Rate in the Intestinal Epithelium	231
J A KEEN A Study of the Arterial Variations in the Limbs with Special Reference to Symmetry of Vascular Patterns	245
HOWARD H CHAUNCEY AND GIULIANO QUINTARELLI Localization of Acid Phosphatase Nonspecific Esterases and β D Galactosidase in Parotid and Submaxillary Glands of Domestic and Laboratory Animals	263
JULIAN F HAYNES AND ALLEN C ENDERS The Composition of the Anal Glands of <i>Dasypus notemcinctus</i>	295
HAROLD F PARKS On the Fine Structure of the Parotid Gland of Mouse and Rat	303
SHEILA DONAHUE AND GEORGE D PAPPAS The Fine Structure of Capillaries in the Cerebral Cortex of the Rat at Various Stages of Development	331
Index to Volume 108	349

The Postnatal Growth of the Ear Capsule in the Rabbit

D A N HOYTE

Department of Anatomy University College of the West Indies Jamaica

A comprehensive account of the development and growth of the human ear capsule was given by Bast and Anson (49). They reviewed extensively earlier works concerned with the number, the situation, the mode and time of appearance, the spread, the comparative anatomy and the homologies of the centers of ossifications of the temporal bone. According to these authors "ossification in any part of the (otic) capsule does not begin until the part of the internal ear covered by said portion of the capsule has attained its maximum size" (p 206). However during intrauterine life there was certainly circumferential growth of the periotic bone at least in the region of the cochlea. Here the periosteal bone surrounding it in its turn the initial encapsulating bone which was replacing the cartilage of the otic capsule increased in thickness all around the circumference until the 27th week of intrauterine life but not thereafter (it subsequently increased in density not in size). On the internal aspect flanking the membranous cochlea a thin layer of bone appeared increasing in thickness very little if at all. "Throughout life it remains as a thin layer which is fairly uniform in thickness in all parts of the capsule" (Ibid p 223). The modiolus developed in membrane from the 20th week of intrauterine life independently of the cochlear capsule which it joined about the 22nd week. It is not clear from their description whether the periestabular and pericanalic ular portions of the otic capsule took part in the circumferential deposit of subperiosteal bone. The semicircular canals themselves only increased in size while they were enclosed in cartilage attaining maximum size about mid term when their capsule began to ossify. They did not accept that there was any real increase in size of the canals after this time.

Of the increase in size of the bony external acoustic meatus Bast and Anson had only this to say (ibid p 165)

"the tympanic ring expands from a C shaped element in the early fetus to a large structure of similar form in the adult. Growth must take place on the outside of the C shaped bone and it is here that the osteogenic layer is active. On the inner surface of the C the cambium layer is inactive and the osteoblasts seem to have been replaced by osteoclasts which actively resorb bone."

Resorption of this concave aspect was also described by Kolliker (1873).

Bateman (54) found from a study of the graylethal and microphthalmic mutants of the mouse that the periotic bone and the tympanic bulla grew for the most part circumferentially and thought that in the periotic as in the bulla this expansion must be accompanied by internal erosion. The oval and round windows were narrowed after their formation by "internal accretion of bone within their circumference up to about 10 days of age and after that were enlarged again by "internal erosion". His inferences were made from a study of the gross patterns of failure of accretion or of resorption in these animals as compared with normal controls and with Kolliker's (1873) descriptions of erosion. Mellanby (47) described osteoclastic widening of the internal acoustic meatus in puppies as a normal feature. He was able to cause excessive bone formation here by keeping the animals on a diet deficient in vitamin A and a reversal to marked osteoclastic activity by returning them to a normal diet. Vitamin A deficient animals also carried to excess the normal deposition of subperiosteal bone upon the endocranial aspect of the ear capsule but not upon the tympanic aspect. Again the ex-

cess bone was attacked by osteoclasts when the vitamin was added to the diet.

The development of the ear ossicles was reviewed and further described by Bast and Anson (*loc cit supra*). "The ossicles are all alike in the matter of longitudinal growth since they lack secondary or epiphyseal centers they do not lengthen when once fully formed in perichondrial bone" (p. 352). Bateman (51) described various areas and patterns of growth and erosion in the ossicles of the mouse but gave no idea of the amount of growth. His illustrations of the ossicles however show very little difference in size between mutant animals and controls and serve to emphasize that as in the human actual postnatal growth as distinct from ossification of preformed structures is minimal.

The purpose of this paper is to show at one and the same time all the features of the postnatal growth of the ear capsule in an experimental animal and to demonstrate the sites of deposition and of resorption of bone by direct examination rather than by inference. The crux of this method rests in the fact that all the animals used were normally growing animals of the same species kept under the same experimental conditions (Hoyt '60).

MATERIALS AND METHODS

A total of 15 rabbits (Copenhagen White and Chinchilla) was used in this investigation. A single intraperitoneal injection of alizarin red (Schour '36) was given to each of a series of animals ranging in age from birth to 25 days. The animals were sacrificed at intervals varying from 12 hours to 103 days thereafter. Of the skulls of these animals 38 were prepared as gross macerated dry specimens (16 partly or completely disarticulated) and 1 intact heads were serially sectioned in the undecalcified state (Roberts and Hoyt '58). The heads of the remaining three animals un.injected served as histological controls and were decalcified and serially sectioned.

RESULTS

The gross appearance of the periotic bone and tympanic bulla is shown in figures 16-22. A key to the text figures and other illustrations is given in table I below.

1 Microscopic appearances at birth (one specimen injected at one day surviving a further 18 hours one control aged one day)

A large part of the periotic was still cartilaginous. Only the middle part of the bone was becoming ossified in the areas of the cochlea vestibule and vestibular ends of the semicircular canals. The lateral cartilaginous portion contained the whole of the parafloccular fossa and the curved portions of the semicircular canals. There was a thin layer of red subperiosteal bone covering the exterior of the periotic both on its endocranial and tympanic surfaces but only in a few places had the internal cavities developed bony walls. Further details are given below.

Cochlea. Most of the tympanic and endocranial aspects of this part of the bone showed a thin red layer of bone. Ossification was proceeding from without inwards replacing the cartilage of the wall. Only in a few places in the interior of the cochlea had a similar shell of subperiosteal bone developed. In some places where ossification in the cartilage approached the internal surface osteoclasts were seen (in serial sections counterstained with toluidine blue or hematoxylin and eosin). Rapid and progressive erosion was not however a marked feature of cochlear growth in this series. The modiolus was fibrous.

Vestibule. Much of the internal wall was ossified though where the ampullae open there was little or no subperiosteal bone covering the deeper developing endochondral bone. The roof of the vestibule (floor of the parafloccular fossa) was completely cartilaginous except medially where it forms the limbus fossae parafloccularis contains the aqueductus vestibuli and covers the crus commune. Here endochondral ossification was taking place.

Internal acoustic meatus. (The shallow depression common to the separate openings of the 7th and 8th nerve canals.) The meatus and the walls of the canals were ossified in continuity with the flat subperiosteal growth of the endocranial aspect of the periotic but already along the course of the 7th nerve canal and at the mouth of the 8th nerve canal resorption could be seen.

TABLE 1

Key

Bones		
AS alisphenoid	Inter interparietal	Sq squamosal
BO basioccipital	M malleus	SO supraoccipital
BS basisphenoid	Pa parietal	St stapes
ExO exoccipital	Pc periotic	TB tympanic bulla
Fr frontal	PS presphenoid	Zy zygomatic
I incus		

Features

aq coch aquaeductus cochleae	oc occipital condyle
aq vest aquaeductus vestibuli	pf parafoveal fossa
cc carotid canal	plf foramen lacerum posterius
crc crus commune	pop paroccipital process
crsta crista ampullaris	post s c posterior semicircular canal
eam external acoustic meatus	pth post tympanic hook of squamosal
Ec (groove for) auditory (pharyngo-tympanic) tube	smf stylomastoid foramen
f coch fenestra cochleae (rotunda)	sup s c superior semicircular canal
fo foramen ovale	tent tentorium cerebelli
fp footplate of stapes	tent r tentorial ridge
f vest fenestra vestibuli (ovalis)	vest vestibule
gt sup p (hiatus for) greater superficial petrosal nerve	ZyT zygomatic process of squamosal
iam internal acoustic meatus	V trigeminal nerve root
lat s c lateral semicircular canal	V G trigeminal ganglion
lpf limbus fossae parafoveolaris	V3 mandibular nerve branches
memb tympanic membrane	VII facial nerve
mlf foramen lacerum medium	VIII stato-acoustic nerve
mM manubrium of malleus	VIII (c) cochlear nerve
obt f obturator foramen of stapes	VIII (V) vestibular nerve
	2nd memb secondary tympanic membrane

Symbols

—————	Surface of alizarin stained bones (flat subperiosteal growth)
	Surface of alizarin-stained bones (spreading trabecular growth) (if in relation to cartilage = endochondral ossification)
- - - - -	Interruption of alizarin stained surfaces by diploic resorption
—————	Resorption (if covered by new bone = a reversal line)
—————	New surface growth (flat subperiosteal growth)
	New surface growth (spreading trabecular growth) (if in relation to cartilage = endochondral ossification)
x x x x	Osteoclasts
□	Cartilage
▨	Areas of endochondral bone

Flat subperiosteal growth = flat lamellae of bone parallel to the surface

Spreading trabecular growth = bony spicules at an angle to the periosteal surface (possibly a more rapid form of growth)

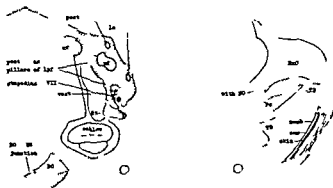


Fig 1 horizontal section of periotic through fenestra vestibuli (rabbit day of age survival three days) $\times 9$

Fig 2 horizontal section through lowest part of periotic (same

Tympanic bulla At this stage the bulla is represented by the narrow tympanic ring enclosing the drum and there is a wide gap inferiorly between it and the basioccipital bone. In this gap can be seen the lowest part of the cochlea. The tympanic ring showed resorption within its concavity except at the exact attachment of the drum to a little spur of bone near the medial part of the ring (fig 2). In coronal sections the ring usually appears in two parts with the skin lined wall of the external acoustic meatus stretched between them and separated from the drum by a slit like space.

In the one-day-old rabbit control examination of sections confirmed the presence of cartilage and of ossification in relation to that cartilage as shown in the alizarin stained specimen. Figure 23 shows marked osteoclastic activity within the bulla and the simultaneous external osteoblastic activity. Growth is therefore centrifugal.

2 Microscopic appearances at 4 days
(one specimen injected at one day
surviving a further three days
one control aged 4 days)

Ossification had proceeded much further in the body of the periotic bone. In the postero-superior portion (mastoid parafloccular fossa) there were patches of bone formation spreading into the anterior and posterior pillars of the limbus fossae parafloccularis (fig 1) (the limbus is completed later by the meeting of these two bony pillars) and laterally along the course of the lateral and posterior semicircular canals.

Cochlea There was a layer of red flat subperiosteal growth both externally and internally. Only the proximal part of the modiolus and the adjacent part of the spiral lamina were red. In the control specimen the spiral lamina was seen to be developing here in membrane. The base of the modiolus in the depths of the 8th nerve canal was formed in cartilage (this is of course part of the cochlear wall) and from here bone formation had spread a little way distally in membrane.

Vestibule There was a layer of flat subperiosteal bone on both internal and external (endocranial) aspects.

Tympanic bulla The ring was much wider with extensive resorption on its concave internal aspect and spreading trabecular growth externally (fig 2).

3 Microscopic appearances at 8 days
(specimen injected at one day
surviving a further 7 days)

The whole periotic tympanic complex was ossified (though the external acoustic meatus was not yet complete).

The endocranial surfaces of the periotic showed a distinct layer of new bone. In some areas a rapid spreading trabecular growth. In others flat subperiosteal growth. The tentorial ridge separating the middle from the posterior cranial fossa was becoming increasingly prominent.

The tympanic aspect showed stasis generally especially over the ampulla and adjacent part of the lateral semicircular canal but excepting the inferior aspect of the roof (Tegmen tympani) where resorption was the rule. This resorption here was especially marked in relation to the canal for the tensor tympani muscle. This canal enters above the bony pharyngotympanic tube at the antero-superior medial end of the bulla. It is roofed in by the tegmen and floored by the bulla (fig 3). The rapid centrifugal expansion of the bulla forming its floor occasioned a correlated resorption of the canal roof with reciprocal deposition on the endocranial aspect of the tegmen. (It is interesting to note that these extensive surface adjustments can occur in a canal from whose bony walls muscle fibers arise all the time.) So rapid was this erosion of the tegmen that by this period 7 days after injection it was almost entirely formed by new bone of endocranial origin. There was resorption along the course of the open facial canal but the closely related fossa for the stapedius muscle at the time of injection wholly cartilaginous consisted now of new white bone.

The postero-superior surface of the periotic showed stasis over the ampullae of the superior and lateral semicircular canals and resorption more laterally (fig 7). Elsewhere the walls of the parafloccular fossa and the courses of the canals therein were new. The posterior surface of the mastoid portion articulating with

the exoccipital was for the most part covered with new bone though a little resorption was seen opposite to the entry of the crus commune and posterior end of the lateral semicircular canal into the vestibule (figs 11 and 12)

Cochlea The tympanic aspect had remained static—a thin shell of red subperiosteal bone. The medial (posterior fossa) surface was covered with a thin white layer of new bone deposited upon the red. This new bone covered the inferior surface of the cochlea where it abuts upon the basioccipital medially and the bulla laterally (fig 5). Internally the thin red layer of bone showed some small areas of resorption. There was a good deal of new bone present inside the cochlea also of two-fold origin. Some had arisen from extension of endochondral ossification in the capsule covering the bony canal of the cochlea separating each turn of the canal from the next. The remainder represented the spread of intra-membranous ossification in the modiolus and spiral lamina from the base towards the apex. There had not been growth in the true sense—merely ossification of pre-existing structures.

Vestibule The originally ossified red internal surfaces had remained static for the most part though occasional small areas of resorption were seen (fig 7). Where the walls were at the time of injection still cartilaginous there was now a layer of new white bone e.g. in the crus commune.

Tympanic bulla (figs 3, 5 and 11) Widespread and rapid internal erosion had left very little of the old red bone—in some areas none at all. The bulla was complete but the lateral wall of the developing external acoustic meatus was still incomplete. The oldest (red) part of the bulla was at and near to the attachments of the drum. The growth of the bulla medially had narrowed the foramen lacrum posterius.

4 Microscopic appearances in older animals

Having thus established the trends of growth and development of the ear capsule in these specimens above it is instructive to follow the sequence of changes

in older specimens. Comparisons are made here in a series of annotated diagrams drawn from histological sections of similar regions in the younger animals and in two older ones—one a 16-day-old rabbit injected at birth the other a 22-day-old control.

The distribution of osteoclasts in the control specimens (fig 23) agreed closely with areas of resorption noted in the alizarin stained specimens. Sometimes osteoclasts were distributed more widely as noted in the remarks to figure 10 above but this does not mean that they were in active for their resorptive activity can be demonstrated if a series of animals be injected at differing intervals after birth (see under "Gross appearances" below). Marked similarities in the distribution of old and new bone in the periotic were seen in the alizarin-stained specimens and their normal controls. In the controls "old" bone was woven bone of endochondral origin easily recognized in hematoxylin and eosin stained sections by its patchy basophilia (Ham 57) and by the remnants of calcified cartilage (Bast and Anson 49) contrasting markedly with the regularly lamellated bone of subperiosteal origin. Figures 6 and 12 show the relative distribution of the two types of bone and should be compared with figures 5 and 11 respectively. Figure 24 shows a photomicrograph taken from area P of figure 12.

5 Gross appearances

These were studied in the series of skulls intact or disarticulated mentioned previously. Their interpretation was facilitated by examination of serial sections of the material described above and by examination of the dried bones at low magnification under a binocular microscope.

Periotic bone endocranial surfaces By the 6th day of life in an animal injected on the second day new white bone was being deposited generally on both the medial (posterior fossa) and antero-superior (middle fossa) aspects. This endocranial deposition was a constant feature throughout the series except within the internal acoustic meatus by the entrances to the 7th and 8th nerve canals each of which remained red though separated from the

Tympanic bulla At this stage the bulla is represented by the narrow tympanic ring enclosing the drum and there is a wide gap inferiorly between it and the basioccipital bone. In this gap can be seen the lowest part of the cochlea. The tympanic ring showed resorption within its concavity except at the exact attachment of the drum to a little spur of bone near the medial part of the ring (fig 2). In coronal sections the ring usually appears in two parts with the skin lined wall of the external acoustic meatus stretched between them and separated from the drum by a slit like space.

In the one-day-old rabbit control examination of sections confirmed the presence of cartilage and of ossification in relation to that cartilage as shown in the alizarin stained specimen. Figure 23 shows marked osteoclastic activity within the bulla and the simultaneous external osteoblastic activity. Growth is therefore centrifugal.

2 Microscopic appearances at 4 days
(one specimen injected at one day
surviving a further three days
one control aged 4 days)

Ossification had proceeded much further in the body of the petiotic bone. In the postero superior portion (mastoid parafloccular fossa) there were patches of bone formation spreading into the anterior and posterior pillars of the limbus fossae parafloccularis (fig 1) (the limbus is completed later by the meeting of these two bony pillars) and laterally along the course of the lateral and posterior semicircular canals.

Cochlea There was a layer of red flat subperiosteal growth both externally and internally. Only the proximal part of the modiolus and the adjacent part of the spiral lamina were red. In the control specimen the spiral lamina was seen to be developing here in membrane. The base of the modiolus in the depths of the 8th nerve canal was formed in cartilage (this is of course part of the cochlear wall) and from here bone formation had spread a little way distally in membrane.

Vestibule There was a layer of flat subperiosteal bone on both internal and external (endocranial) aspects.

Tympanic bulla The ring was much wider with extensive resorption on its concave internal aspect and spreading trabecular growth externally (fig 2).

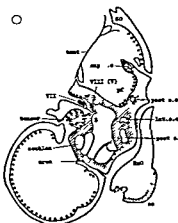
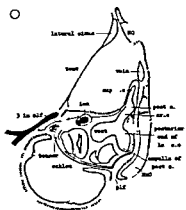
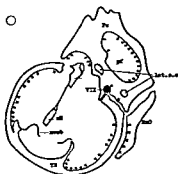
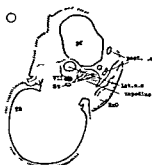
3 Microscopic appearances at 8 days
(specimen injected at one day
surviving a further 7 days)

The whole petiotic tympanic complex was ossified (though the external acoustic meatus was not yet complete).

The endocranial surfaces of the petiotic showed a distinct layer of new bone. In some areas a rapid spreading trabecular growth in others flat subperiosteal growth. The tentorial ridge separating the middle from the posterior cranial fossa was becoming increasingly prominent.

The tympanic aspect showed stasis generally especially over the ampulla and adjacent part of the lateral semicircular canal but excepting the inferior aspect of the roof (Tegmen tympani) where resorption was the rule. This resorption here was especially marked in relation to the canal for the tensor tympani muscle. This canal enters above the bony pharyngotympanic tube at the antero-superior medial end of the bulla. It is roofed in by the tegmen and floored by the bulla (fig 3). The rapid centrifugal expansion of the bulla forming its floor occasioned a correlated resorption of the canal roof with reciprocal deposition on the endocranial aspect of the tegmen. (It is interesting to note that these extensive surface adjustments can occur in a canal from whose bony walls muscle fibers arise all the time). So rapid was this erosion of the tegmen that by this period 7 days after injection it was almost entirely formed by new bone of endocranial origin. There was resorption along the course of the open facial canal but the closely related fossa for the stapedius muscle at the time of injection wholly cartilaginous consisted now of new white bone.

The postero superior surface of the petiotic showed stasis over the ampullae of the superior and lateral semicircular canals and resorption more laterally (fig 7). Elsewhere the walls of the parafloccular fossa and the courses of the canals therein were new. The posterior surface of the mastoid portion articulating with



Figures 7 to 12

other by a ridge of new bone. The periotic extended by growth at its edges anteriorly (petrosquamous fissure) and inferiorly and posteriorly where it presents as a rounded border abutting on the foramen lacerum posterius. The tentorial ridge developed rapidly by surface deposition on the red bone converting the rounded border (birth to three days) into a sharp one (6 to 10 days) and thereafter appearing as a more and more prominent and irregular ridge till it formed a ledge of bone overhanging the posterior fossa (40 days onwards).

The walls of the parafloccular fossa cartilaginous at birth were replaced by bone and the limbus fossae was completed by 7 days. In specimens injected about birth therefore no red bone was seen in the walls of the fossa except below just at and within the limbus. Specimens injected between 5 and 7 days and between 18 and 25 days showed that red stained bone was deposited on the walls of the fossa external to the white bone existing at that time was covered over in its turn by a further ectocranial deposition of white bone (by 6 days after injection at these times) was quickly exposed on the internal aspect by resorption and finally was removed from the internal aspect by continued and rapid resorption leaving the walls again white. The only traces of red bone persisting here under these conditions were along the courses of the semicircular canals (see below).

Tympanic surface The medial wall of the tympanum presents the promontory of the cochlea (fig 20) with the vestibular (oval) and cochlear (round) windows in relationships similar to those found in man. Above the promontory is a depression lodging the tensor tympani muscle in life made into a canal by the bulla and around a process of the bulla here the muscle tendon turns to its insertion on the malleus. The roof of the depression is the tegmen tympani. Below the front of the promontory is the periotic wall of the carotid canal. Almost directly above the oval window the facial canal opens into a groove lying between that window and the lateral semicircular canal. This latter canal near its ampullary end and the ampulla of the superior canal above it make promi-

nent bulges in the medial wall of the tympanum above and behind the oval window. The facial nerve groove turns vertically downwards to score the front of the base of the mastoid process where it again forms a closed canal completed by the bulla. The nerve leaves the skull at the so-called stylomastoid foramen (actually tympano-mastoid in the rabbit). Behind the cochlear window is a deep depression lodging the stapedius muscle.

The remarkable feature of this wall was the persistence of the red stain in the central portion especially over the cochlea. Even 82 days afterwards in an animal injected at birth this red portion was virtually unchanged though a film of new bone could be made out under the dissecting microscope. The tensor tympani canal the under aspect of the tegmen and the stapedial fossa became white by removal of the old red bone while the bulges made by the ampullae of the superior and lateral semicircular canals became white covered by a thin film of new bone. The groove for the upper part of the internal carotid artery developed prominent white lips of new bone. (The lower part is trapped by and taken into the bulla by the medial spread of that bone above it lies in the petrotympanic fissure).

Posterior surface This surface of the periotic articulating with the exoccipital showed generalized deposition of new bone except for a few persistent irregular areas of red bone either static or slowly resorbing.

Semicircular canals These are best seen in the walls of the parafloccular fossa through the widely open limbus (fig 16). Apart from their ampullae they showed no ossification at birth and were therefore not stained by alizarin injected at that time. The ridges marking their presence however were evident by 10 days. In an animal injected at 5 days of age and allowed to survive for a further 6 days their course was shown by curved red lines. Forty days afterwards in an animal injected at 7 days these curving lines were still distinctly red on transillumination though covered with a thin film of white on the aspect facing into the fossa where they make prominent ridges. Similarly three animals injected

at 18 days (surviving for a further 25 days) and at 25 days (surviving a further 57 and 73 days) respectively showed considerable persistence of the red stain in these curving canals. Even their ampullary ends red stained in animals injected at birth still showed red bone on transillumination 82 days later.

The picture is one of canals becoming more and more prominent inside the parafloccular fossa as that fossa expands centrifugally leaving them "marooned" on its internal walls. The canals themselves thickened their walls by external deposition but did not increase their internal diameters so much as to remove the red bone from their interiors except within their ampullae where some of it was apparently removed (fig. 7).

Tympanic bulla external aspect. From birth to the 7th day of life the tympanic membrane is exposed on the lateral surface held by the concavity of the tympanic ring. Between 7 and 11 days the drum is hidden by the growth of the ring to form a lateral plate. The bone encroaches from in front and behind the two processes thus formed meet by 11 days and the line of their junction has disappeared by 15 days. From 11 days onwards the bony external acoustic meatus develops as a tube directed upwards backwards and slightly outwards (fig. 17).

From the appearance of a bony lateral wall to the bulla there was deposition of new bone on its superficial aspect. The bony meatus grew by addition of bone at its free margin. Inferiorly the tympanic ring quickly grew medially so that by 6 days of age it had narrowed the foramen lacerum posterius to a mere slit had met and started to enclose the internal carotid artery. This inferior aspect too was covered externally by new bone.

Internal aspect. Injected at birth the tympanic ring became wholly red to the naked eye. By 11 days apart from the superficial closure of the processes of new bone to complete the lateral wall of the bulla there had developed from the ring a thick flat crescentic plate of bone (fig. 21) forming the lower part of the lateral wall of the external acoustic meatus and standing up in relief from it. The greater curvature of the crescent presented a nar-

row medially directed flange of bone—the original part of the ring holding the tympanic membrane (fig. 6). The membrane was still attached to this flange inclining medially above to attach to the medial wall of the bony meatus. The deepest part of the meatus is thus a mere slit between the membrane and this crescent of bone. The concavity of the ring (or flange) and this crescent persist virtually unchanged from this time (11 days). Elsewhere the interior of the bulla showed rapid and progressive resorption with the result that this crescent became more and more prominent. Once formed the interior of the bony meatus showed resorption also but less marked than that within the bulla so that some red bone remained within it 57 and 73 days after injection at 25 days.

6 The ear ossicles

The findings here agree in almost every respect with those of Bast and Anson (49) and need not therefore be elaborated in detail. Figures 13A and 13B below (and also figs. 1, 3 and 9) show some features of these bones. The cartilaginous primordia of the malleus (ossified as far as the base of the manubrium) and incus (ossified nearly to the neck by the lenticular process) were already nearly full sized at birth. The bone present at that time extended later merely to the natural limits of the cartilage models and gradually consolidated to form the typical dense structure of these ossicles. Actual surface growth and remodelling were minimal.

The endochondral bone of the stapes however while growing also to the natural limits of the cartilage model underwent profound changes as in the human. Each crus commencing as a solid pillar of cartilage developed on the second day of life a center of ossification at its junction with the footplate. This ossification appeared here as a subperiosteal shell of bone with invasion of the cartilage deep to it spreading from here in three directions—proximally along the crus towards the neck, distally and centripetally into the footplate and distally and centrifugally towards the edge of the footplate, the periosteal splint keeping pace with the underlying endochondral ossification. No

other by a ridge of new bone. The petrotic extended by growth at its edges anteriorly (petrosquamous fissure) and inferiorly and posteriorly where it presents as a rounded border abutting on the foramen lacerum posterius. The tentorial ridge developed rapidly by surface deposition on the red bone converting the rounded border (birth to three days) into a sharp one (6 to 10 days) and thereafter appearing as a more and more prominent and irregular ridge till it formed a ledge of bone overhanging the posterior fossa (40 days onwards).

The walls of the parafloccular fossa cartilaginous at birth were replaced by bone and the limbus fossae was completed by 7 days. In specimens injected about birth therefore no red bone was seen in the walls of the fossa except below just at and within the limbus. Specimens injected between 5 and 7 days and between 18 and 25 days showed that red stained bone was deposited on the walls of the fossa external to the white bone existing at that time was covered over in its turn by a further ectocranial deposition of bone (by 6 days after injection at these times) was quickly exposed on the internal aspect by resorption and finally was removed from the internal aspect by continued and rapid resorption leaving the walls again white. The only traces of red bone persisting here under these conditions were along the courses of the semicircular canals (see below).

Tympanic surface The medial wall of the tympanum presents the promontory of the cochlea (fig 20) with the vestibular (oval) and cochlear (round) windows in relationships similar to those found in man. Above the promontory is a depression lodging the tensor tympani muscle in life made into a canal by the bulla and around a process of the bulla here the muscle tendon turns to its insertion on the malleus. The roof of the depression is the tegmen tympani. Below the front of the promontory is the petrotic wall of the carotid canal. Almost directly above the oval window the facial canal opens into a groove lying between that window and the lateral semicircular canal. This latter canal near its ampullary end and the ampulla of the superior canal above it make promi-

nent bulges in the medial wall of the tympanum above and behind the oval window. The facial nerve groove turns vertically downwards to score the front of the base of the mastoid process where it again forms a closed canal completed by the bulla. The nerve leaves the skull at the so-called stylomastoid foramen (actually tympano-mastoid in the rabbit). Behind the cochlear window is a deep depression lodging the stapedius muscle.

The remarkable feature of this wall was the persistence of the red stain in the central portion especially over the cochlea. Even 82 days afterwards in an animal injected at birth this red portion was virtually unchanged though a film of new bone could be made out under the dissecting microscope. The tensor tympani canal the under aspect of the tegmen and the stapedial fossa became white by removal of the old red bone while the bulges made by the ampullae of the superior and lateral semicircular canals became white covered by a thin film of new bone. The groove for the upper part of the internal carotid artery developed prominent white lips of new bone. (The lower part is trapped by and taken into the bulla by the medial spread of that bone above it lies in the petrotympanic fissure).

Posterior surface This surface of the petrotic articulating with the exoccipital showed generalized deposition of new bone except for a few persistent irregular areas of red bone either static or slowly resorbing.

Semicircular canals These are best seen in the walls of the parafloccular fossa through the widely open limbus (fig 16). Apart from their ampullae they showed no ossification at birth and were therefore not stained by alizarin injected at that time. The ridges marking their presence however were evident by 10 days. In an animal injected at 5 days of age and allowed to survive for a further 6 days their course was shown by curved red lines. Forty days afterwards in an animal injected at 7 days these curving lines were still distinctly red on transillumination though covered with a thin film of white on the aspect facing into the fossa where they make prominent ridges. Similarly three animals injected

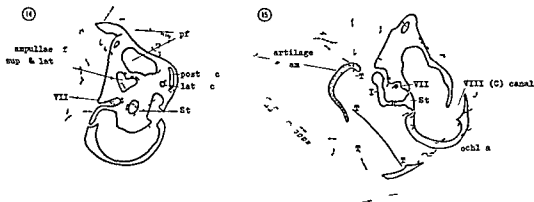
cretion especially upon the endocranial aspect and at the sutural surfaces of the bone and only slightly upon the tympanic aspect. This must be accounted a growth phenomenon in terms of the increase in size of the whole skull. Adding markedly to the dimensions of the petrotic is the centrifugal expansion of the parafloccular fossa while the expansion of the tympanic bulla and of the external acoustic meatus add their quota to the growth of the whole ear capsule. The size of the tympanum is added to by resorption from the inferior aspect of the tegmen tympani by enlargement of the tensor tympani canal and by erosion in the stapedial fossa. Local increases occur too in the facial nerve canal and in their course through the petrotic bone from the medial surface both 7th and 8th nerve canals are widened by resorption.

One must except from this progressive expansion of the bulla however the attachments of the tympanic membrane which remain virtually unchanged in size from birth (but see fig 15 below). As far as can be determined from observations which were qualitative rather than quantitative there is no significant increase in the size of the drum. Similarly one must except from the expansion of the parafloccular fossa the courses of the semicircular canals which therefore and for

a like reason become etched in relief upon the internal walls. The walls of the canals appear to thicken but no increase occurs in the size of their lumen.

It is worthy of note that in this series of rabbits there was a close correspondence between the intensity of erosion and the numbers of osteoclasts present. This does not support Bateman's (54) conclusions that "osteoclasts vary tremendously in their activity and mere numbers afford no guide to the intensity of erosion."

Figure 14 below represents the superimposition of outlines drawn from two actual sagittal sections through similar regions of the ear capsule in a 4-day-old and a 22-day-old control rabbit respectively. Superimposition was effected using three areas: the footplate of the stapes, the ampullae of the superior and lateral semicircular canals and the facial nerve canal (with the outline of the slightly smaller canal just within that of the larger). The coincidence of other points also ensures the validity of this comparison. These are the cut portions of the lateral and posterior semicircular canals, the floor of the parafloccular fossa and the antero-superior and postero-superior ends of the tympanic bulla. The diagram (fig 14) illustrates graphically the increase in size of the bulla cavity and of the parafloccular fossa and the encroach



Figs 14 and 15 Superimposition of outlines taken from sections of the ear capsule. The points of superimposition are detailed in the text.

Fig 14 sagittal sections from control rabbits 4 days old (solid outline) and 22 days old (interrupted outline) $\times 135$.

Fig 15 coronal sections from control rabbits one day old (solid outline) and 22 days old (interrupted outline) $\times 135$. TT represents the attachments of the tympanic membrane of the younger animal. TT' those of the older. In each case the distances are the same.

ment of the endocranial aspect of the petrotic bone upon the cranial cavity. This type of superimposition gives a good general idea of growth trends but cannot give exact proportions of growth since it does not allow for say angulation of the para-floccular fossa medially or laterally in relation to the rest of the bone.

Figure 15 represents a similar superimposition this time of outlines drawn from a 22-day-old upon those of a one-day-old rabbit. Exact correspondence of the stapes was found (in each case the plane of section was through the junction of the anterior crus and the footplate) and it can be seen that the facial nerve canal, the cochlea and the cochlear nerve canal all coincide. The size of the tympanic membrane has remained unaltered but it has been rotated to a more vertical plane. The distance between the attachment of the malleus to the drum (base of manubrium) and the promontory does not seem to have altered (in other similar superimpositions) and it is suggested therefore that rotation of the drum occurs about the point of manubrial attachment.

SUMMARY

1 The features of postnatal growth in the ear capsule of the rabbit are shown in a study of animals injected intra vitally with alizarin red at various periods after birth.

2 The histological appearances of sites of growth and of resorption are illustrated and compared with the findings in normal controls and with a series of gross specimens from other rabbits also injected with alizarin. This has allowed a detailed study of the contributions made to the growth of the ear capsule by deposition and resorption in a series of animals of the same species kept under the same conditions.

3 The cavities of the bony cochlea, vestibule and semicircular canals are full grown at birth. The growth of the exterior of the petrotic bone is circumferential.

4 The para-floccular fossa of the petrotic bone and the tympanic bulla expand centrifugally by internal resorption and

external deposition. The course of the semicircular canals remains static but the tympanic membrane also stationary in size rotates to a more vertical position about the fixed attachment of the manubrium of the malleus.

5 Of the ear ossicles the malleus and incus are full grown at birth and merely undergo ossification of the parts still remaining cartilaginous at that time. The stapes though full sized also changes its shape from a solid cartilaginous model to the typical thin outwardly crescentic crura, thin footplate and excavated head and neck of the adult bone.

6 Certain points within the ear capsule seen in sagittal or coronal section show remarkable constancy in their relations to each other and as fixed points may be used in superimposing the outlines of the capsule at different ages.

ACKNOWLEDGMENTS

I am grateful to Professor G A G Mitchell of the University of Manchester, England, for the facilities afforded to me to carry out this work, and to Professor W F Harper of the University College of the West Indies, Jamaica, for the time necessary to review and complete it.

LITERATURE CITED

- Bast T H and B J Anson 1949 *The Temporal Bone and the Ear*. Charles C Thomas, Springfield, Illinois.
- Bateman N 1954 Bone growth: a study of the grey lethal and microphthalmic mutants of the mouse. *J Anat Lond* 88: 212-262.
- Ham A W 1957 *Histology* third ed. Pitman, London.
- Harris H A 1933 *Bone Growth in Health and Disease*. Oxford University Press.
- Hoyle D A N 1960 Alizarin as an indicator of bone growth. *J Anat Lond* 94: 432-442.
- Kölliker A 1873 *Die normale Resorption des Knochengewebes und ihre Bedeutung für die Entstehung der typischen Knochenformen*. Leipzig.
- Mellanby E 1947 Vitamin A and bone growth. The reversibility of vitamin A-deficiency changes. *J Physiol* 105: 382-399.
- Roberts P A and D A N Hoyle 1958 The serial sectioning of undecalcified animal heads. *J Anat Lond* 92: 621-622.
- Schour I 1936 Measurements of bone growth by alizarin injections. *Proc Soc Exp Biol Med* 34: 140-141.

PLATES

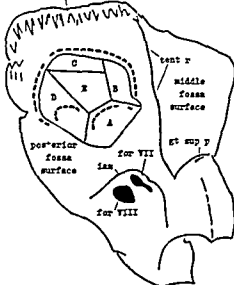


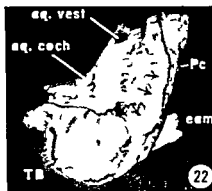
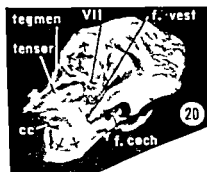
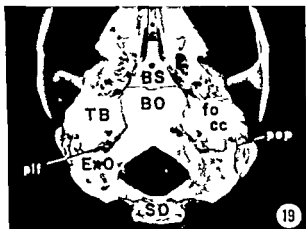
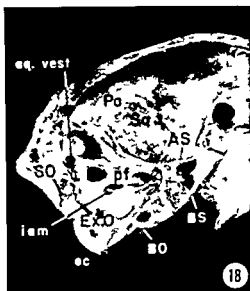
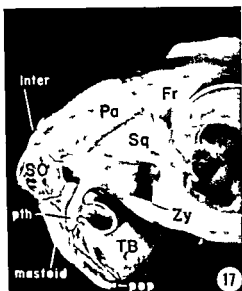
Fig 16 Plan of left periotic bone from the endocranial aspect (superomedial view) The parafloccular fossa is drawn as if one were looking into an irregular hollow cube The heavily dotted outlines represent the courses of the semicircular canals as follows

Surface A is the floor with the lateral semicircular canal (forms also the postero-superior surface of the main part of the periotic overlying the ampullary region of the vestibule) surface B is the anterior wall surface C is the roof surface D is the posterior wall with the posterior semicircular canal and articulates with the exoccipital surface E is the lateral (superficial) wall The superior semicircular canal occupies the margin of the fossa within the *limbus fossae parafloccularis* Surfaces B C and E underlie the continuous curve of the superficial (mastoid) portion of the bone

PLATE 1

EXPLANATION OF FIGURES

- 17 Lateral view of ear capsule posterior one third of adult rabbit skull
- 18 Medial (endocranial) view of ear capsule posterior one third of adult rabbit skull
- 19 Inferior view of ear capsule posterior one third of adult rabbit skull
- 20 Infero-lateral view of disarticulated left periotic bone This and the subsequent figures are from a Chinchilla rabbit injected with alizarin red at 18 days of age sacrificed 25 days later The medial wall of the tympanum was mostly red the superficial (mastoid) portion wholly white The arrows indicate the edge of the alizarin-stained bone
- 21 Medial view of disarticulated left tympanic bulla Arrows as in figure 20
- 22 Posterior view of right periotic bone and tympanic bulla disarticulated from exoccipital bone Apart from irregular patches of red the posterior surface of the periotic was white and the bulla was entirely white also Arrows as in figure 20





- 23 A portion of the tympanic ring in a one-day-old control rabbit showing osteoclasts on the internal surface $\times 90$
- 24 Inferior part of the cochlea lamellar subperiosteal bone deposited upon endochondral bone (area P in fig 12) (from a 22-day-old control rabbit) $\times 180$

The Development of the Anterior Cerebral Artery and its Related Vessels in the Rat¹

D B MOFFAT

Department of Anatomy University College Cardiff Great Britain

There is a vast and comprehensive literature concerning the distribution of arteries to the adult human brain but detailed investigations into the development of these important vessels are surprisingly few in number and often present conflicting opinions. This is probably due to the fact that this subject is usually studied by means of serial sectioning and reconstruction—an extremely time-consuming technique—so that the published results are based upon the study of a comparatively small number of embryos. By using animal material the vessels may be easily visualized by the injection of ink into the vascular system followed by dissection so that a large number of embryos may be examined in a very short time. This technique also has the advantage that a considerably more accurate picture of the arrangement of the arteries is given than is possible by reconstructions and this is particularly true in the case of dense vascular plexuses. The present study is based upon dissections of injected rat embryos and forms part of a detailed investigation into the development of the arterial system of the rat's brain. A necessary preliminary to the work was a survey of the pattern of the arteries in question in the brain of the adult rat since I have been unable to find the relevant data elsewhere although Greene (35) gives a general account of these vessels.

MATERIAL AND METHODS

The anterior cerebral artery and its related vessels were studied in dissections of the brains of 20 adult Wistar rats after the injection of Neoprene latex 572 into the arterial system.

For the embryological studies a series of accurately timed rat embryos was obtained by the usual methods and each

embryo was injected with India ink. The injection was made into the heart the umbilical vein or one of the vessels lying in the unopened membranes using mouth pressure. Full details of the technique have been given in previous papers (Moffat 57 and 59). After injection the embryos were fixed in formalin and dissected using fine glass needles and watchmakers forceps. In all 196 embryos were studied.

RESULTS

The anterior cerebral artery in the adult rat

Each internal carotid artery reaches the base of the brain by passing to the lateral side of the hypophysis and immediately gives off an infundibular artery which runs rostrad and mediad giving numerous branches which pass caudad to the region of the infundibulum and a few which pass cranial to reach the optic chiasma. The internal carotid then gives off the posterior communicating artery, the anterior choroidal artery, a branch to the optic nerve, the middle cerebral artery and the anterior cerebral artery. The anterior cerebral artery runs rostrad dorsal to the optic nerve and gives off a large olfactory artery which passes ventrad into the nose. Each anterior cerebral then gives a chiasmal branch which may anastomose with its fellow across the midline and which supplies mainly the dorsal aspect of the optic chiasma. The two anterior cerebral arteries then join at an acute angle to form a single midline vessel which passes dorsad and then caudad over the corpus callosum. Just before or just after the junction of the anterior cere

¹This work formed part of a thesis which has been approved for the award of the degree of M.D. in the University of London.

bral arteries a branch is given off on each side which runs around the caudal margin of the olfactory bulb to supply it and the adjacent part of the brain. This vessel also gives off a number of central branches. The midline anterior cerebral trunk supplies branches to the medial wall of the cerebral hemisphere and numerous small twigs to the corpus callosum before dividing into two again. Each terminal branch runs to the medial side of its own hemisphere, anastomoses with branches of the middle and posterior cerebral arteries and gives a slender branch which curves over the posterior aspect of the corpus callosum to end by supplying the anterior extremity of the choroid plexuses of the third and lateral ventricles, anastomosing with one of the choroidal branches of the posterior cerebral artery.

Embryological studies

The first definite branches of the primitive internal carotid arteries to the brain appear in embryos of 2-4 mm. At this stage the internal carotid gives off a prominent primitive maxillary artery which passes cranial ventral to the optic stalk and breaks up into a plexus on the forebrain (fig. 2). It also supplies some minute branches to the optic stalk. The internal carotid then divides into its caudal and cranial rami. The former is large but the latter is represented only by a short trunk which passes dorsal to the optic stalk and then breaks up into a number of tiny vessels. The side of the forebrain is thus covered by a dense capillary plexus but this plexus stops short of the midline both ventrally and dorsally. Figure 3 shows the ventral surface of the forebrain of a 3 mm embryo and is intended to indicate the wide midline nonvascular strip so that the anterior part of the circle of Willis is incomplete at this stage although the posterior portion formed by the caudal rami of the primitive internal carotid arteries is well seen.

In 4-6 mm embryos the primitive maxillary artery remains large and still plays a major part in the supply of the cranial pole of the brain. It can be seen in figure 4 which depicts the ventral surface of the forebrain in a 4.3 mm embryo. It

passes ventral to the large optic stalk and now gives a number of small medial branches which encroach upon the nonvascular strip and in places this strip is crossed by transverse communications between the two sides. In slightly older embryos of this stage the bilateral plexuses become continuous across the midline so that the whole of the ventral surface of the forebrain is covered with a network of vessels. The cranial ramus of the internal carotid artery is now well developed but since it runs dorsal to the optic stalk it is largely concealed in figure 4. It gives off the anterior choroidal artery, one or more vessels to the optic stalk and in older embryos of this stage the middle cerebral artery. It ends by contributing to the plexus on the ventral aspect of the forebrain.

The next stage in the development of the vessels is seen in embryos of 6-9 mm and a typical example of this stage is seen in figure 5 which shows the ventral aspect of the forebrain of a 7.6 mm embryo. During this stage the primitive maxillary artery begins to diminish in size until only its proximal part can be recognized and often even that cannot be found. The cranial ramus of the internal carotid artery however increases in size and after giving off the branches mentioned above now ends by passing ventrad into the region of the developing nasal cavity; this primitive olfactory artery has of course been divided in the specimen which is illustrated. Before entering the nasal cavity it gives off a few small branches to the forebrain. A new vessel is now appearing in the plexus which lies between the two primitive olfactory arteries. This leaves the primitive olfactory artery of each side at approximately right angles and runs mediad and caudad to become continuous with the cranial end of the primitive maxillary artery. It will be known here as the recurrent branch of the primitive olfactory artery and the specimen shown in figure 5 illustrates well the way in which it develops in the pre-existing capillary plexus. Usually the recurrent branch appears before the primitive maxillary artery has begun to diminish in size so that these two vessels together with the stem and cranial ramus

of the internal carotid artery form a complete wide arterial circle—the peri-optic ring—around the base of the optic stalk. This ring may be seen on the left side of the embryo shown in figure 6 and in side view in figure 8 although the recurrent branch in the latter embryo has a slightly atypical origin. At the same time changes are occurring in the capillary plexus between the two primitive olfactory arteries. In figure 5 the vessels of the plexus are already beginning to show a cranio-medial orientation so that they tend to pass towards the median longitudinal fissure of the brain while in figure 6 the vessels have become reduced in number to 5 or 6 on each side and are passing into the median longitudinal fissure where they unite to form a small midline vessel plexus form in places which closely follows the "neck" of the telencephalic outgrowth. Later still the 5 or 6 vessels become reduced still further in number (fig. 7).

An interesting anomaly is seen in figure 11 which depicts the right side of an 8.7 mm embryo. In this specimen and in 4 other similar embryos the cranial ramus of the internal carotid artery ends as the middle cerebral artery the proximal part of the primitive olfactory artery being represented only by a few tiny plexiform vessels. There is a large persistent primitive maxillary artery and a vessel corresponding to the recurrent branch of the primitive olfactory artery and these two vessels form the stem of origin of the primitive olfactory itself. In other words there has been a persistence of the ventral portion of the peri-optic ring in place of the usual dorsal portion.

In embryos of over 9 mm the primitive maxillary artery has disappeared and in its place there is now an infundibular artery which takes origin from the internal carotid and curves cranial and medial just cranial to the hypophysis giving off branches to the latter and a number of fine branches to the posterior part of the optic chiasma. It is not possible to say whether the proximal part of the infundibular artery represents the stem of origin of the primitive maxillary artery or whether it is an entirely new vessel.

The fate of the recurrent branch of the primitive olfactory artery may be seen in

figure 10. At this stage the cranial ramus of the internal carotid artery ends by dividing into two branches of approximately equal size. One of these which is divided in this specimen passes ventrad into the nasal cavity and will later form the olfactory branch of the anterior cerebral artery while the other consists of the stem of the recurrent branch. The more distal portion of the recurrent branch however has now diminished greatly in size and will form a chiasmal branch of the anterior cerebral artery. The vessels which were seen in previous stages to be passing towards the median longitudinal fissure from the recurrent branch have now been reduced in number until eventually only one on each side will remain to form part of the anterior cerebral artery and these unite in the fissure to form a single midline vessel which differentiates *in situ*. From these paired arteries or from the single midline artery arises a new branch which appears in the plexus on the ventral aspect of the forebrain. This artery which may be seen rather indistinctly on the left side of the embryo shown in figure 10 emerges from the median longitudinal fissure and runs laterad around the proximal part of the olfactory bulb giving branches to it and also one or more central branches which pierce the brain substance.

The further course of the anterior cerebral artery at this stage may be seen in figure 9 which shows a midline sagittal section of the brain of a 13.6 mm embryo. The anterior cerebral artery is relatively very large at this stage and it gives branches from its convex border to the medial surface of the cerebral hemisphere and from its concave border to the commissural plate. Near its termination the unpaired midline artery divides into left and right branches of which only the left remains in this specimen the right branch being adherent to the right cerebral hemisphere. The terminal branch gives one or more ascending branches to the medial wall of the hemisphere and one descending branch which can just be made out in the photograph and which passes to the cranial end of the choroidal fissure to supply the choroid plexuses of the third and lateral ventricles.

To sum up the adult anterior cerebral artery (fig 1) is formed from the stem of the primitive olfactory artery the proximal part of its recurrent branch one of the cranially directed branches of the latter and a single midline vessel which develops *in situ* between the two telencephalic vesicles. The distal portion of the primitive olfactory artery becomes the olfactory branch of the anterior cerebral while the distal part of the recurrent branch becomes a chiasmal branch of the anterior cerebral artery

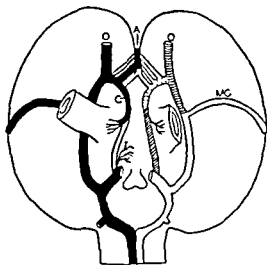


Fig 1 Diagram of the base of the brain to show the derivation of the anterior cerebral artery. The adult vessels are shown in solid black while the embryonic vessels are shown on the opposite side of the diagram. The optic stalk has been divided. MC middle cerebral artery. A anterior cerebral artery. O olfactory branch of anterior cerebral artery. C chiasmal branch of anterior cerebral artery. I infundibular artery. Horizontal hatching primitive olfactory artery. Stipple recurrent branch of primitive olfactory artery.

DISCUSSION

The primitive maxillary artery is a relatively large and important vessel up to the 6 mm stage and may in fact be as large as the continuation of the internal carotid artery. It is therefore surprising that it has been described by so few authors since it appears to be equally prominent in human embryos of the appropriate age. The artery was named by Sabin (17) who did not describe the artery but labeled it in a 6.5 mm pig

embryo in her plate 7. The term was retained by Padgett (48) who found this vessel prominent up to the 5-6 mm stage in human embryos. It supplies the cranial pole of the forebrain and the optic outgrowth. Rosenbauer (55) also used this term in describing the vessel in a 24 somite human embryo and it is therefore not intended to change it here in spite of its slightly misleading nature. The vessel has been mentioned or illustrated by other authors sometimes with inaccurate labeling. Piper (00) shows a vessel in a 6.8 mm human embryo which resembles the primitive maxillary artery but which is labeled the "a corporii callosi". Tandler (02) in his stage 2 describes and illustrates in his plate 3 figure 4 the "anterior branch" of the internal carotid artery which passed just in front of the stomodaeum and as Padgett (48) has pointed out this vessel must represent in fact the primitive maxillary artery although the anterior division of the internal carotid in a 5 mm human embryo is correctly described as passing dorsal to the optic outgrowth. Fuchs (05) who studied rabbit embryos described the appearance of the "erste Augenarterie" on the 9th day. This vessel passes ventral to the optic outgrowth and is succeeded by the "hypophthalmic artery" which is probably derived from it. Elze (07) described an unidentified vessel passing ventral to the optic outgrowth which appears to be a primitive maxillary artery.

The recurrent branch of the primitive olfactory artery on the other hand does not appear to have been described before although a number of authors have shown that the base of the optic outgrowth is almost or completely surrounded by an arterial ring. Thus Fuchs (05) mentioned an almost complete circle in this situation which in two embryos was in fact completed by capillaries while Elze (07) similarly illustrates an almost complete circle. More complete reconstructions are seen in Padgett's (48) paper and in her figure 3 which shows a 5.5-mm human embryo there is a large primitive maxillary artery which together with what appears to be a small recurrent branch of the primitive olfactory artery all but completes a peri-optic ring. Her figures

4(a) and (b) also show a stump of a recurrent branch and in the text the author writes "Before the cranial division of the carotid terminates at the olfactory pit it gives off mesial twigs in the path of the future anterior cerebral artery. It therefore seems possible that the recurrent branch is present in the human and this point deserves further study."

The ultimate fate of the primitive maxillary artery is difficult to determine. In the later stages of its regression its stem of origin can usually be recognized but in many embryos it disappears completely. Its place is taken by the infundibular artery which arises from the internal carotid at a similar level and turns medially cranial to the hypophysis to meet the corresponding vessel of the opposite side. It supplies numerous small branches to the optic chiasma and to the hypophysis. Its course and distribution are thus similar to the superior hypophyseal artery in the human but it is difficult to state whether its development is similar to that of this vessel. According to Padgett (48) the stem of the primitive maxillary artery forms one of the inferior hypophyseal arteries since she identified as the remains of the former vessel a branch of the internal carotid lying proximal to the ophthalmic artery i.e. arising from the future intra-cavernous portion of the internal carotid. The superior hypophyseal arteries she states are represented by "numerous plexiform branches from the carotid and posterior communicating arteries." However it does not seem certain that either Padgett's inferior hypophyseal arteries or the infundibular artery described in the present paper are necessarily derived from the primitive maxillary artery since Padgett too found that in embryos of 6 to 12 mm this vessel could not always be identified and when seen it could only be traced for a short distance. The difficulty is increased by the fact that in the rat there is no vessel corresponding to the ophthalmic artery in the human. The exact homologies of the hypophyseal arteries cannot therefore be established on the present evidence and it can only be stated that most if not all of the rat's infundibular artery is a new formation from the plexus of vessels around the

infundibulum and that its proximal part may perhaps represent the remains of the primitive maxillary artery.

The recurrent branch of the primitive olfactory artery is easier to follow into its adult condition. As may be seen from figures 1 and 10 its proximal part forms part of the anterior cerebral artery while its distal portion diminishes in size and becomes a chiasmal branch of the anterior cerebral. The diamond shaped area enclosed by the two anterior cerebral arteries and their chiasmal branches is often occupied by remnants of the original plexus in this situation so that this portion of the anterior cerebral artery is particularly liable to show "island formation."

There are a number of similarities between the appearance of this region in rat embryos and that in the human as described by Padgett (48). Thus the primitive olfactory artery has a similar history in both species up to the 18 mm stage of human development at which time the artery still terminates by entering the nasal cavity. In the human embryo at this stage the primitive olfactory artery is described as giving off a medially directed branch which represents the main part of the anterior cerebral artery and which breaks up into a plexus which reaches the midline. By this time however the relative sizes of the main trunk and the branch have become reversed so that the primitive olfactory artery now appears to be a branch of the anterior cerebral artery. (In the rat the two branches are of approximately equal size but for the sake of convenience human terminology has been applied in this paper.) In the 24 mm human embryo shown in Padgett's figure 8 the anterior cerebral arteries are fully formed but are still showing signs of their plexiform origin while the primitive olfactory artery is much reduced in size although it still supplies the nose. Padgett states that the stem of the latter vessel forms a small striate branch of the anterior cerebral while the medial striate or recurrent artery of Heubner is formed from components of the anastomosis between the primitive olfactory artery and its collateral anterior cerebral branches. In the rat the rather prominent branch of the anterior cerebral

artery which runs just caudal to the olfactory lobes seems to represent the recurrent artery of Heubner but this appears as a new vessel and is unrelated to the primitive olfactory artery

As has been stated remnants of the recurrent branch of the primitive olfactory artery persist in the rat to form chiasmal branches of the anterior cerebral artery and it is perhaps significant that such branches are also found in the human adult (Steele and Blunt '56 and Dawson '58) while Rubenstein ('44) described chiasmal branches from the anterior communicating artery

The segment of the anterior cerebral artery which lies between the two telencephalic vesicles is the last portion of this vessel to appear in both the rat and the human embryo. A single midline anterior cerebral artery (not to be confused with the artery of the corpus callosum) is common in animals and is occasionally found in the human. In a recent series of 350 human brains for instance Alpers Berry and Paddison ('59) found such a vessel in 2% of cases while Mitterwallner ('55) found it in 3.3% of 360 brains. It is however difficult to account for the figures quoted by Lessem ('05) who found a single anterior cerebral artery in 22 out of 32 fetal brains. According to de Vriese ('07) in the rabbit embryo there are two anterior cerebral arteries the smaller of which disappears along with a temporary artery of the corpus callosum leaving the remaining vessel to form the single midline anterior cerebral artery. There was no evidence of such duplication in the rat.

The choroidal branch of the anterior cerebral artery is of considerable interest. In the rat this vessel is relatively large and persists into adult life reaching the choroid plexus of the third ventricle by passing around the splenium of the corpus callosum. A similar branch is described by Bremer ('43) in a human embryo of 17.8 mm and by Padget ('48) in a 24 mm human embryo. At a later stage in a 39 mm embryo the latter author again found the choroidal branch but at this stage the vessel had a caudal loop before reaching the choroid plexus and she stated that no example is known of a similar branch persisting into adult life. I have

found a choroidal branch of the anterior cerebral artery in human fetuses of 102 and 131 mm while in another of 145 mm a long slender branch of the anterior cerebral artery could be traced round the splenium of the corpus callosum onto its under surface where it was lost.

There is some evidence that this choroidal branch may persist into adult life in animals other than the rat and in the human. Shellshear ('30) found in the chimpanzee a long branch of the anterior cerebral artery which passed around the splenium and then forwards to the region of the interventricular foramen. Critchley ('30) described a posterior pericallosal artery in the human which passes backwards to unite over the splenium of the corpus callosum with a branch of the posterior cerebral artery while more recently Lazorthes et al ('56) found an inconstant branch of the adult anterior cerebral artery which turns around the splenium and passes along with the posterior choroidal arteries to supply the tela choroidea of the third ventricle.

The embryo shown in figure 11 illustrates an anomaly which must be more common in the rat than in the human since five such embryos were found in the present investigation. In this specimen the stem of origin of the primitive olfactory artery is formed by a persistent primitive maxillary artery together with the recurrent branch that is to say the ventral portion of the peri-optic ring has persisted in place of the dorsal segment. Had this embryo reached adult life the anterior cerebral artery would have passed ventral to the optic nerve. Robinson ('59) found a right anterior cerebral artery in a human subject which showed just this course and suggested that the anomaly might be due to an enlargement of an anastomosis between the superior hypophyseal branches of the internal carotid artery proximal to its posterior communicating branch and the anterior cerebral artery. It is thought that the anomaly shown in the rat embryo suggests a more convincing explanation of the human anomaly although in a general way Robinson's interpretation is correct.

A case of persistence of the whole peri-optic ring can be seen in Watts ('34) fig

ure 6 which shows the circle of Willis in a chimpanzee. There is a communication between the two internal carotid arteries and from its left side a vessel passes for wards below the optic chiasma to join the anterior cerebral arteries. Bassett (49) described two cases of aneurysm of an anomalous vessel which left the internal carotid artery and passed ventral to the optic nerve. It seems possible that this vessel too represents a persisting primitive maxillary artery.

SUMMARY

The blood supply to the cranial pole of the brain is at first derived from the large primitive maxillary artery later reinforced by the cranial ramus of the internal carotid artery. At a later stage the latter vessel distal to the origin of the middle cerebral becomes a primitive olfactory artery which enters the nose and which gives off a recurrent branch. This branch usually connects up with the cranial end of the primitive maxillary artery to form a peri optic ring. A number of vessels pass cranial from the recurrent branch of the primitive olfactory artery to enter the median longitudinal fissure of the brain and one of these on each side enlarges to form a segment of the anterior cerebral artery. The unpaired portion of the anterior cerebral artery forms *in situ*. Thus the anterior cerebral is derived from the stem of the primitive olfactory artery the proximal part of its recurrent branch one of the cranially directed branches of the latter vessel and a single midline vessel which develops *in situ*. The distal part of the primitive olfactory artery becomes the olfactory branch of the anterior cerebral artery while the distal part of the recurrent branch becomes a chiasmal branch of the anterior cerebral.

ACKNOWLEDGMENTS

I should like to express my thanks to Mr A Welch for taking the photographs to Miss V E M Mahoney for technical assistance and to Miss A Jones for drawing figure 1.

I should also like to acknowledge here the constant advice and encouragement which I received during the course of this investigation from the late Professor J S Baxter.

LITERATURE CITED

- Alpers B J R G Berry and R M Paddison 1959 Anatomical studies of the circle of Willis in the normal brain A M A Arch Neur Psychiat 81 409-418
- Bassett R C 1949 Intracranial aneurysms I Some clinical observation concerning their development J Neurosurg 6 216-221
- Bremer J L 1943 Congenital aneurysms of the cerebral arteries an embryologic study Arch Path 35 819-831
- Critchley McD 1930 The anterior cerebral artery and its syndromes Brain 53 120-165
- Dawson B H 1938 The blood vessels of the human optic chiasma and their relation to those of the hypophysis and hypothalamus Ibid 81 207-217
- Elze C 1907 Beschreibung eines Menschlichen Embryo von ca. 7 mms Grosse Anat Hefte 35 409-492
- Fuchs H 1905 Zur Entwicklungsgeschichte des Wirbeltierauges I über die Entwicklung der Augengefässe des Kamochens Ibid 23 1-251
- Greene E C 1935 Anatomy of the rat Trans Am Phil Soc no 27 Philadelphia
- Lazorthes G J Gaubert and J Poulhes 1956 La distribution centrale et corticale de l'artere cerebrale anterieure etude anatomique et en cidences neurochirurgicales Neurochirurg Paris 2 237-253
- Lesern W H 1905 The comparative anatomy of the anterior cerebral artery The Post Grad uate 20 455-465
- von Mitterwallner F 1955 Variationsstatistische Untersuchungen an den basalen Hirnge fassen Acta Anat 24 51-87
- Moffat D B 1957 The development of the hindbrain arteries in the rat J Anat Lond 91 25-39
- 1959 Developmental changes in the aortic arch system of the rat Am J Anat 105 1-36
- Padget D H 1948 Development of the cranial arteries in the human embryo Cont Embryol Carnegie Inst 32 205-261
- Piper H 1900 Ein menschlicher Embryo von 68 mms Nackenlänge Arch Anat 95-132
- Robinson L R 1949 An unusual anterior cerebral artery J Anat Lond 93 131-133
- Rosenbauer K A 1955 Untersuchung eines menschlichen Embryos mit 24 Somiten unter besonderer Berücksichtigung des Blutgefässsystems Z Anat Entw 118 236-276
- Rubinstein H S 1944 Anterior communicating artery in man J Neuropath Exp Neur 3 196-198
- Sabin F 1917 Origin and development of the primitive vessels of the chick and of the pig Cont Embryol Carnegie Inst 6 61-124
- Shellshear J L 1930 The arterial supply of the cerebral cortex in the chimpanzee (Anthropithecus troglodytes) J Anat Lond 65 45-87
- Steele E J and M J Blunt 1936 The blood supply of the optic nerve and chiasma in man Ibid 90 486-493

Tandler J. 1922 Zur Entwicklungsgeschichte der Kopfarterien bei der Marmosa. Morph. Jb., 30 27-33
 de Vries E. 1922 Zur Entwicklungsgeschichte der Cerebrals Arterien. Verh. Anat. Ges. 21

Versammlung V. Morph. 1922 Anat. Anz., Ergänzungs., zum 30 125-129
 V. Anat. J. V. 1934 A comparative study of the anterior cerebral artery and the circle of Willis in primates. J. Anat., Lond. 69 534-570

PLATE 1

EXPLANATION OF FIGURES

All figures show rat embryos which have been injected with Indian ink and are unretouched.

- Right side of a 3.7mm embryo / 22. The primitive maxillary artery passes ventral to the optic outgrowth, dorsal to which the cranial ramus of the internal carotid artery is just beginning to form.
- Ventral surface of the fore- and mid-brain of a 3.0mm embryo / 30. The primitive maxillary arteries lie on either side of a wide midline mesencephalic strip.
- Ventral surface of the fore- and mid-brain of a 3.3mm embryo / 30. The internal carotid arteries lie on either side of the hypophysis and give off the primitive maxillary arteries. They then divide into a cranial and caudal ramus. The former pass dorsal to the divided optic stalk and the latter form the caudal portion of the circle of Willis. The midline mesencephalic strip is now crossed by a number of transverse vessels.
- Ventral surface of the fore- and mid-brain of a 3.6mm embryo / 27. The cranial ramus of the internal carotid artery is now large and after giving off the middle cerebral artery continues as the primitive ophthalmic artery which has been divided. A capillary plexus now covers the whole ventral surface of the fore brain and in this the recurrent branch of the primitive ophthalmic artery is just beginning to form. It links up with the cranial end of the primitive maxillary artery which is now much diminished in size.



PLATE 2

EXPLANATION OF FIGURES

- 6 Ventral surface of the fixation of a "1-mm embryo" / 21. On the left side of the brain the primitive maxillary and recurrent branch of the primitive maxillary artery are both large and help to form a peripheral ring around the divided optic stalk. The primitive maxillary artery has a series of branches which pass cranial towards the median longitudinal fissure of the brain.
- 7 Ventral surface of the fixation of a "2-mm embryo" / 22. The recurrent branch of the primitive maxillary artery gives off one or two small branches which pass to the median longitudinal fissure where they unite to form the median primitive maxillary artery. The primitive maxillary artery has been damaged on the left side and has regressed completely on the right.
- 8 Left side of the cranial end of a "2-mm embryo" / 23. The divided optic stalk is surrounded by a wide peripheral ring made up of the internal carotid artery, the cranial ramus, the recurrent branch of the primitive maxillary artery and the primitive maxillary artery.



PLATE 3

EXPLANATION OF FIGURES

- 9 Median sagittal section of the fore and mid brain of a 13.6-mm embryo $\times 21$. The midline unpaired portion of the anterior cerebral artery has remained adherent to the left cerebral hemisphere. It gives branches to the developing corpus callosum and to the medial surface of the hemisphere while the most proximal part of its choroidal branch can just be made out.
- 10 Ventral surface of the forebrain of an 11.7 mm embryo $\times 19$. The primitive olfactory arteries have been divided and on the left side one of the branches of the recurrent branch of the primitive olfactory has become enlarged to form part of the anterior cerebral artery. The distal portions of the recurrent branches have diminished in size to form chiasmal branches of the anterior cerebral artery.
- 11 Right side of the brain of an 8.7 mm embryo $\times 18$. The cranial ramus of the internal carotid terminates as the middle cerebral artery. The primitive maxillary and a vessel corresponding to the recurrent branch have persisted to form the stem of origin of the primitive olfactory artery. Compare with figure 8.



A Morphological and Histochemical Study of Estrogen Induced Lesions in the Hamster Male Reproductive Tract¹

W M FEAGANS L F CAVAZOS AND A T EWALD

Departments of Anatomy and Biophysics and Biometry Medical College of Virginia Richmond Virginia

Although there is considerable information on the influence of estrogens on the male reproductive tract in various mammalian species (Thorberg 48 Em mens and Parkes 47) few publications exist with reference to the hamster Bacon and Kirkman (55) suggested that prolonged estrogen treatment may induce endocrinopathic lesions in the hamster testis by direct action Ortiz (53) indicated that the response of the hamster male accessory glands to castration may differ from that in the rat In these studies morphological rather than histochemical or biochemical methods were utilized

The present investigation is concerned with the effects of a variety of estrogenic compounds on the cytochemistry of the male reproductive tract of the hamster

MATERIALS AND METHODS

Sexually mature male albino hamsters approximately 90 days of age were arbitrarily divided into 4 treated and one control group A cholesterol free 20 mg pellet of either estrone alpha estradiol ethinyl estradiol or stilbestrol was implanted in the subcutaneous tissue of the interscapular region The animals were killed by decapitation at 30 60 90 120 or 240 days following commencement of hormone treatment during the interval between May and November The pellet was recovered dissected free of the connective tissue capsule desiccated and weighed The absorption of estrogenic substance was expressed in units of mg per day Testes epididymides seminal vesicles and the bulbourethral glands were fixed in acetic alcohol formalin (4 C) buffered neutral formalin and the phospholipid fixative of Elftman (57)

In addition to hematoxylin and eosin staining the following histochemical reactions were utilized (1) The periodic acid Schiff method (PAS) was employed and controlled by hydrolysis of sections in diastase for removal of glycogen extraction with chloroform methanol for 16 hours at 60 C to remove glycolipids and staining without previous oxidation The counterstain when used was Weigert Lillies alum hematoxylin (2) A modification of the toluidine blue procedure of Kramer and Windrum (55) was used with a 0.1% solution of dye in 30% ethyl alcohol (pH 7.4) Controls were incubated for one hour at 56 C in a 0.01% ribonuclease solution in a phosphate buffer (pH 6.0) prior to staining (3) The Alcian blue 8 GS and Feulgen staining procedures were combined to demonstrate acidic carbohydrates and DNA respectively Sections were stained in 0.1% Alcian blue in 3% acetic acid for 30 minutes (pH 2.49) prior to Feulgen staining (4) Total lipids were demonstrated by Sudan black B and oil red O methods using propylene glycol (60 C) as solvents and staining for 30 and 60 minutes respectively Controls were treated for one hour at room temperature with an equal mixture of ethyl ether and chloroform prior to staining (5) Phospholipids were localized according to Elftmans (57) procedure (6) The Schultz reaction (Gomori 52) was used for identification of cholesterol

¹ Supported by U S P H S grant RG 6583 from the Division of General Medical Sciences

² Hormones generously furnished by Ciba Pharmaceutical Products Inc Division of Pharmacy Research and Development Mr Jack Cooper Director

A pathway analysis of the data was performed using multiple and simultaneous regression techniques (see review by Turner and Stevens (5)). It was assumed that the relation between organ weights and body weight follows the heterogeneity formula (Huxley (32)) and the following statistical model was developed:

$$Y_i = \sum_{j=1}^n a_{ij} X_j + \sum_{k=1}^m b_{ik} X_k + e_i \quad (1)$$

where Y_i is the i th response variable, the X_j 's are primary variables and X_k 's (corresponding to k of the heterogeneity formula) are unknown regression coefficients reflecting the magnitude of the effect produced by varying the respective primary variables.

Taking the logarithm of equation (1) the linear structural equation is

$$\log Y_i = \sum_{j=1}^n a_{ij} \log X_j + \sum_{k=1}^m b_{ik} \log X_k + e_i \quad (2)$$

where

$$a_{ij} = \log a_{ij}, \quad b_{ik} = \log b_{ik}, \quad e_i = \log e_i$$

$$e_i = \log e_i, \text{ and } e_i = \log e_i$$

The model equation is obtained by substituting X_j 's and X_k 's for a_{ij} 's and b_{ik} 's respectively and attaching the random residual error e_i . The X_j 's and X_k 's indicate the

measured variables. This equation is

$$Y_i = \beta_0 + \beta_1 X_1 + \beta_2 X_2 + \dots + \beta_n X_n + \beta_{n+1} X_{n+1} + \dots + \beta_{n+m} X_{n+m} + e_i \quad (3)$$

A family of such model equations was derived for all response variables and the estimates of the unknown parameters were calculated by the method of least squares. The computations were made on the IBM 650 using the program (062002.1-2-3) prepared at the North Carolina State College Computer Laboratory.

RESULTS

Testicular weight responses to estrogen are presented in table 1. This table shows the mean values of the absolute weights. In addition to the mean ratio where a correction has been made for initial and final body weights. Estrogens caused a uniform pattern of testicular atrophy (12 ± 1) although the final body weights varied erratically (table 2). Ethinyl estradiol was absorbed more rapidly than were the other estrogens (fig. 1).

Testis

Untreated controls

No seasonal variations in the weight and histology of the testis occurred. Spermatogenesis was active and spermatozoa

TABLE 1
Testis weights

	$\frac{n}{\text{animal}}$	20 D. W.	$\frac{n}{\text{animal}}$	60 D. W.	$\frac{n}{\text{animal}}$	20 D. W.	$\frac{n}{\text{animal}}$	60 D. W.	$\frac{n}{\text{animal}}$	240 D. W.
		6.76 ^a		611.60		770.4 ^a		626.7 ^a		612 ^a
Controls		211.4	1	277.6	4	671.3	8	278.3	3	274
Stilbestrol	3	6.6		581	4	37.4	3	41.8	3	48 ^a
		161		131 ^a		129.5		110.8		109.0
Alpha estradiol	3	7.63		381		57.6	2	37.3	0	
		187		169.4		157 ^a		16.9		
Ethinyl estradiol	3	69.10		48.47		47.83		59.1 ^a	3	364
		161.3		139.9		125 ^a		17.3		148 ^a
Estrone	6	4.41	0			4.43		41.4 ^a	3	99.27
		161.1				121.0		161.4		172

^a Mean of the ratio [combined testicular weights/initial body weight]/b (final body weight):b¹. Values of regression coefficients b_1 and b_2 are 1.07 and 1.31 respectively.

^b Mean of the combined testis weights in milligrams.

TABLE 2
Initial and final body weights (gm)

	No of animals	30 Days	No of animals	60 Days	No of animals	90 Days	No of animals	120 Days	No of animals	240 Days
Controls	6	102.0 ¹ 110.4	7	97.0 125.7	4	90.2 97.7	8	97.6 134.2	3	95.0 117.3
Sulbestrol	3	119.0 95.5	10	110.9 85.8	4	92.2 103.2	3	96.7 83.8	3	128.7 97.8
Alpha estradiol	4	128.0 106.5	8	104.4 101.8	5	115.4 91.3	3	86.3 102.4	0	
Ethinyl estradiol	3	128.3 112.3	12	95.0 88.5	7	105.3 89.1	7	84.0 93.7	3	111.7 93.5
Estrone	6	114.7 113.6	0		5	105.8 78.8	5	112.0 128.5	3	121.7 68.8
Mean initial body weight		1 Mean final body weight								

were numerous. In general the testicular morphology resembled that of other sexually mature rodents but the histochemical reactions of the untreated hamster testis are not comparable to those of the rat or guinea pig. A description therefore of the untreated controls precedes the experimental results.

The weakly stained PAS-positive Leydig cell cytoplasm was devoid of glycogen vacuolated and weakly basophilic with numerous toluidine blue positive granules present. Abundant droplets of sudanophilic lipid phospholipid and cholesterol occurred in these cells (fig. 7). The basement membrane and peritubular connective tissue of the seminiferous tubules was PAS reactive, moderately basophilic and Alcian blue positive. The Sertoli cell cytoplasm had considerable glycogen and many basophilic granules (residual bodies). These bodies were readily removed by ribonuclease hydrolysis. Lipid droplets were numerous and distributed in the basal cytoplasm of these cells. In contrast a weak Sertoli cell phospholipid reaction occurred in the perinuclear zone (Golgi?) and cell apex. Other than that associated with the acrosomal system the germinal cell cytoplasm had little PAS reactive material and was weakly basophilic. Some sudan

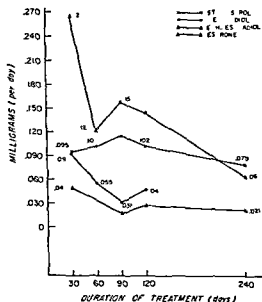


Fig. 1 Rate of absorption of estrogens from subcutaneous 20 mg pellets

ophilic lipids and phospholipid usually in the perinuclear or Golgi zone occurred in these cells.

Estrogen treated

After 30 days of estrogen treatment spermatogenic arrest had occurred at the

primary spermatocyte stage tubular diameter had decreased and the number of spermatogenic cells was reduced. The lumina of many tubules contained cellular detritus and desquamated germinal epithelial cells. Associated with intratubular changes was an apparent increase in the thickness of the basement membrane and peritubular connective tissue as revealed by the PAS technique.

Intratubular histochemical changes during early periods of estrogenization included lipid accumulation, decrease in basophilia and an increase in Sertoli cell glycogen.

An intense sudanophilic reaction was observed primarily in Sertoli cells and to a lesser degree in the spermatogenic cells present. Reactive material in Sertoli cells often appeared as large globules which on occasion were in the seminiferous tubule lumen. Fatty acids and cholesterol were markedly increased whereas there was only a slight increase in phospholipid. Cholesterol was confined to the tubules with little or no intratubular activity.

Concomitant with spermatogenic arrest an increase in Sertoli cell glycogen appeared up to 90 days of estrogen treatment but not thereafter. Many Sertoli cells had cytoplasmic diastase resistant PAS granules which increased in number with prolonged treatment whereas cytoplasmic glycogen decreased in spermatogonia. A few yellowish magenta granules (pigment) occurred in the spermatogonial cytoplasm although they appeared later

than in Sertoli cells (90 days of estrogenization).

A decrease in basophilic granules and an absence of residual bodies occurred in the seminiferous tubule lumen of all treated animals. The Sertoli cell cytoplasm particularly in early treatment groups demonstrated a decrease in basophilia which was removed by ribonuclease.

Inter-tubular changes in response to short term estrogen treatment were confined to a few Leydig cells with atrophy and nuclear pyknosis. Following 60 days of hormone treatment only a few atrophic Leydig cells were present. Other interstitial cells had yellowish-eosinophilic cytoplasmic inclusions which occurred initially in stilbestrol and ethinyl estradiol treated hamsters. These inclusions presumably pigment gave a greenish blue hue following toluidine blue staining with a slight reduction in orthochromasy after ribonuclease treatment. The granules were PAS positive and refractory to diastase or chloroform-methanol extraction. The number of cells containing pigment inclusions increased with prolonged estrogen treatment.

A similar mode of degeneration was observed within the tubules especially in Sertoli cells which gave positive reactions indicative of a lipofuscin pigment (table 3). This was particularly true in hamsters treated for 90 days or more. Formalin fixed paraffin-embedded sections following Sudan black B contained reactive granules in Sertoli cells, interstitial cells and a few spermatogonia. When destained

TABLE 3
Results of pigment staining

Staining procedure	Testis	Epididymis	Seminal vesicle
Sudan black B (MCD P)	+	+	+
Sudan black B (AAF I)	-	+	-
Sudan black B destained with alcohol-ether (3:1) for 1 hour at 60°C	-	-	-
Sections restained with Sudan black B	+	+	+
Ziehl-Neelsen (AAF I)	+	+	+
Toluidine blue pH 7.48 (AAF I)	+	+	+
Alcian blue pH 2.49 (AAF P)	-	-	-
PAS reaction (AAF P)	+	+	+
PAS reaction after diastase treatment	+	+	+

MCD Mercuric chloride dichromate fixative of Eftman

AAF Acetic alcohol formalin fixative

P Paraffin embedded tissue

with hot acetone and restained with Sudan black B this material remained sudanophilic

Following 90 days of estrogen a few tubules had undergone cystic formation or cavitation with a lining composed primarily of Sertoli cells. Pigment deposition which appeared to be antecedent to cavitation increased in many of the adjacent tubules. The dilated tubular segments associated with the longer treatment periods contained a homogenous fluid that gave a positive reaction to PAS and Alcian blue. There was no change in PAS after diastase or chloroform-methanol treatment nor was there any reduction in the toluidine blue orthochromasia in sections previously hydrolyzed by ribonuclease.

All testes treated for 240 days demonstrated (1) intense intratubular sudanophilia and positive Schultz reaction (2) intra and intertubular pigmentation of a lipofuscin type and (3) cystic tubular segments containing a fluid that was reactive to PAS, Alcian blue and orthochromatic to toluidine blue and nonreactive for lipids.

Cauda epididymidis

Untreated controls

An intense PAS reaction was localized in the basement membrane whereas the lamina propria and fibromuscular stroma (fig. 9) were moderately colored by the PAS and Alcian blue techniques. The columnar cell cytoplasm was weakly PAS positive and a few reactive granules some of which were glycogen were in the supranuclear cytoplasm. Furthermore this area was basophilic and contained small orthochromatic granules. This basophilia was reduced following ribonuclease. A diffuse sudanophilia occurred in the apical cytoplasm with discrete granules in the supranuclear and luminal portions of the cells. Large granules of phospholipid were also localized in the supranuclear zone. Stereocilia were weakly stained with the PAS and toluidine blue methods.

All epididymides examined contained spermatozoa and histologically appeared to be functional organs.

Estrogen treated

Three histological changes were common to all estrogen treated hamsters in the 30

day group with no distinguishable differences between the 4 hormone groups. First all sections of epididymides had a pronounced tubular atrophy with absence of spermatozoa. Secondly there was an apparent increase in the lamina propria and the fibromuscular components including the capsule of the cauda. Lastly ductal epithelial atrophy could be seen in several segments of the tubule. The ductal lumen had a weakly positive Alcian blue fluid containing many desquamated cells. Most of the denuded cells were of the germinal epithelium however some were of epididymal origin. The "secretion" within the lumen was intensely PAS positive and resistant to diastase or chloroform-methanol treatment.

The atrophied ductal epithelial cells had a small clear supranuclear zone with the remaining apical cytoplasm being orthochromatic to toluidine blue. Following ribonuclease a loss or reduction of cytoplasmic RNA occurred in the epididymal epithelium of all treated hamsters. Further diminution of cytoplasmic basophilia was not apparent with prolonged estrogenization. Glycogen was found in the epithelial cytoplasm but when compared with control epididymides a diminution in glycogen was evident. In addition to glycogen a few large PAS positive granules were in the supranuclear cytoplasm. The larger granules present in the 30 day group increased in number and size with further treatment in all estrogenized hamsters. Not infrequently this material was found in the perinuclear cytoplasm with pyramidal processes (fig. 10) streaming toward the luminal surface of the cell. Frozen sections stained with Sudan black B and oil red O demonstrated little change in lipid other than sudanophilic clusters which had a distribution similar to the large PAS positive granules. Results of further staining procedures (table 3) indicated that the large granulations were a lipofuscin pigment similar to that observed in the testes. The ductal cell pigment however was present after 30 days of estrogenization in contrast to that observed in the testes.

There was an apparent increase in the fibromuscular components of the cauda epididymidis up to and including the 90

dry group with no further increase in the 120 and 210 day estrogen treated hamsters. A strong PAS positive reaction was noted in the basement membrane lamina propria and fibromuscular elements.

Tubular epithelial cell involution continued during all treatment periods with the most severe atrophy occurring in epididymides of hamsters treated for 210 days with ethinyl estradiol. In this case the ductal epithelium consisted of flattened cells lining a lumen containing the homogenous fluid mass. Epididymides from the early treatment periods showed a few dilated tubular segments containing "hydropic" cellular elements in an intensely PAS positive fluid. This degenerative process comparable to the changes in testicular cytoarchitecture was considered to be cystic dilatation of the ductus.

Seminal vesicle

Untreated controls

The influence of estrogen treatment on seminal vesicle weights (including secretion) with respect to initial and final body weights is presented in figure 2. The ratio represents an adjusted organ weight where a correction was made for variations in body weights.

The epithelium had a fair to strong PAS reaction at the cell apex and a few glycogen granules were in the luminal cytoplasm. Pigment inclusions if present were PAS positive and resistant to chloroform-methanol and diastase. Furthermore the luminal cytoplasm was intensely orthochromatic (fig. 15) and the light areas had numerous basophilic (secretory or secretory) granules. Ribonuclease hydrolysis removed the cytoplasmic basophilia. A diffuse sudanophilia occurred in the apical cytoplasm. Lipid droplets varied in size with larger ones localized in the supranuclear zone. Some stained lipids were similar to pigment inclusions. Phospholipids were present in the light area of the supranuclear cytoplasm. The basement membrane smooth muscle of the lamina propria and the fibromuscular stroma reacted strongly with PAS were orthochromatic after toluidine blue and were stained by Alcian blue.

Estrogen treated

Seminal vesicle atrophy as reflected by reduction in organ weight (fig. 2) was readily apparent after 30 days of estrogenization. The gross involutional changes were caused by a reduction in luminal secretion accompanied by a slight reduction in epithelial height. The limited "secretion" in the lumina was weakly basophilic and intensely PAS positive. In the later treatment groups the "secretion" contained numerous desquamated cells many of which were engorged with pigment.

Toluidine blue orthochromasia of the epithelium decreased following 30 days of estrogen treatment. This diminution occurred by a reduction of basophilic granules in the supranuclear "light areas" and by narrowing of the basophilic zone of luminal cytoplasm. After 120 and 210 days of treatment no light areas were present in the secretory epithelium. An increase in cytoplasmic lipid including phospholipid was evident in all treated groups with the heaviest concentration of sudanophilic material in the supranuclear zone. In the 120 and 210-day treated animals the abundant cytoplasmic sudanophilia was the result of pigment affinity for the Sudan dye.

Increased cellular pigmentation rather than cellular atrophy appeared to reflect changes in the level of circulating androgen. This was particularly evident in the early treatment groups. Frequently the pigment would involve several cells with the nuclei being eccentrically located or fragmented. Desquamation of the epithelium was sequential to increased pigment. A positive reaction for pigment however was noted in many subepithelial macrophages. Results of staining techniques for seminal vesicle pigment are presented in table 3 and figure 16. Pigment when present in the seminal vesicle epithelium of the untreated controls gave reactions as indicated in table 3.

The seminal vesicle stroma similar to that of the cauda epididymidis appeared to be slightly increased. This apparent hyperplasia was accompanied by an increase in PAS reactivity metachromasia and number of mast cells. In view of the lack of distention due to reduction in se-

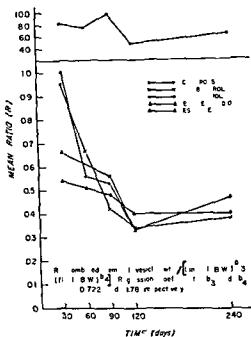


Fig 2 Effects of estrogens on seminal vesicle weight with respect to initial and final body weights

cretion this may not represent a true hyperplastic process

Bulbourethral gland

Untreated controls

The epithelium was pyramidal to columnar shaped with basal flattened nuclei and the stroma was a network of sparse connective tissue fibers primarily collagenous. Skeletal muscle with a delicate lamina of intervening collagenous fibers formed the capsule. The parenchyma gave an intense PAS cytoplasmic reaction and glycogen was inconsistently localized in the apical cytoplasm. Following toluidine blue there was a purple metachromasia in the epithelium and a distinct orthochromatic perinuclear cytoplasm (fig 17). Ribonuclease removed most of the cytoplasmic basophilia in the perinuclear zone. Alcian blue coloration corresponded to the toluidine blue metachromasia. Intense Alcian blue staining occurred in the secretory cell cytoplasm. The ductal secretion was PAS-positive orthochromatic with toluidine blue and strongly reactive following Alcian blue

Estrogen treated

Involutonal changes in the secretory elements of the bulbourethral glands appeared in all hamsters treated for 30 days and the severity of response did not progress with prolonged treatment. The epithelium was reduced to an irregular columnar type with a loss of cytoplasmic metachromasia and Alcian blue staining. The epithelial nuclei were spherical in contrast to the flattened nuclei of the control bulbourethral glands. Changes in total lipids and phospholipids were not readily apparent. Although there was no ductal epithelial hyperplasia an apparent increase in the stroma and mast cells was noted (fig 18).

Concurrent with parenchymal atrophy was a sizable reduction in PAS positive material. Staining was confined to the epithelium and ductal contents and the coloration presumably was a residual mucoid secretion.

DISCUSSION

The histological pattern of estrogen induced testicular degeneration as observed in the present study agrees essentially with the findings of Bacon and Kirkman (55). These investigators indicated that testicular pathology in the hamster could pursue two degenerative pathways which they termed "solid atrophy" and "cystic atrophy." The earliest and most common lesion solid atrophy was recognized by a reduction in tubular diameter with the seminiferous epithelium composed of lipid laden Sertoli cells and a few spermatogonia and primary spermatocytes. Cystic atrophy was associated with a loss of all spermatogenic elements and subsequent formation of dilated tubules lined by Sertoli cells.

The results of this investigation suggest an intermediate stage of degeneration. This stage has been designated as "pigmentation atrophy." Histologically it is characterized by the presence of a yellow pigment which accumulates preferentially in Sertoli cells although some pigment occurred in a few spermatogenic cells. This form of degenerative process was evident after 90 days of estrogenization and increased with further treatment. Sequentially intertubular pigmentation ap-

pears to occur before the intratubular changes. The reactivity of the pigment with the various histochemical stains indicated it was a type of lipofuscin (table 3).

Dietary deficiencies may favor the development of testicular pigment. Vitamin E deficiency in the rat (Furumachi, Tadice and Herranz 41), mouse (Menschikov, Munk, Rogalski, Rymaszewski and Szczepniak 52) and hamster (Mason and Mauer 57) will induce the formation of acid fast pigment.

Several questions must be answered to explain the pathogenesis of the testicular pigment observed in this investigation. Is this a specific alteration due to the direct or indirect action of estrogen or do dietary factors play a role in its formation? In this study considering the extreme weight losses encountered by the treated hamsters (table 2), nutritional inadequacies cannot be discounted.

The nature of the experimental design does not permit any definitive statement regarding the primary causative factor of "pigmentation atrophy." It is possible that the observed intratubular pigmentation is an expression of testicular degeneration which is associated with excessive estrogenic stimulation. Based on the results obtained in this investigation and that of other studies, the predicted pattern of intratubular degeneration after long term estrogen treatment would be: (1) solid atrophy, (2) pigmentation atrophy, (3) cystic atrophy and (4) replacement fibrosis (?). Solid atrophy is accompanied by an increase in intratubular glycogen and lipid with a slight reduction in tubular RNA. The immediate increase in Sertoli cell glycogen may be associated with non-utilization of this substance by spermatids and spermatozoa.

There is disagreement in the literature on the significance and localization of testicular cholesterol in the normal adult animal. Results of the present study suggest that the normal hamster testis is similar to the rat and guinea pig (McLampy and Cavazos 54) as well as man (Long and Engle 52) in that no intratubular cholesterol is present. Conversely Perlman (50) and Montagna and Hamilton (51) have reported tubular Schultz reactions in the testes of rat and man respectively. The presence of intratubular cholesterol might

reflect some measure of tubular epithelial dysfunction rather than a precursor of testicular hormone.

Bacon and Kirkman (55) proposed that cystic dilations of the seminiferous tubules are possibly related to disturbances of epididymal absorption as postulated by Mason and Shaver (52). According to these investigators, the results of Clubb (51) indicated that various segments of the hamster efferential and epididymal epithelium absorbed particulate matter from the tubular secretion. Furthermore, this material was transferred across the epithelium to the subepithelial macrophages. They suggested that the existence of acid fast pigment (lipofuscin) in these areas of prefferential absorption was from testicular origin in vitamin E deficient hamsters. Theoretically any alteration in the absorptive capacity of the efferential ducts would lead to an accumulation of intratubular fluid. According to Burgos de Oca and Montorzi (59) the non-ciliated cells of the efferential epithelium are primarily concerned with the absorptive phenomenon.

Changes in the absorptive mechanism of the efferential ducts may be the mechanism for formation of the cystic tubules here reported but it does not indicate the origin of the fluid. The homogenous mass in the lumina of the cystic tubules is possibly a mucoprotein. Similar reactions do not occur in the excretory products of the untreated control hamster testes. Although the cells lining the cystic tubules are strongly orthochromatic they do not resemble an actively secreting epithelium. Finally it must be assumed that the cystic fluid represents the products of cellular damage and necrosis.

Suppression of ICSH by exogenous estrogenization is evident by the presence of the typical "deficiency cells" in the testicular interstitium. With the disappearance or lack of identification of Leydig cells numerous pigmented macrophages occur in the intertubular areas. It is suggested that these phagocytic elements might be altered Leydig cells.

Estrogens will evoke epithelial atrophy and fibromuscular hyperplasia in the epididymis. The early epithelial histochemical changes as observed in this study resemble the postcastrational changes in

the rat epididymis (Cavazos 58 Maneely 58) With continued estrogen treatment however progressive cytolysis of the cauda epithelium results in accumulation of an acid fast pigment (table 3) Since this substance occurs in the epididymis before it does in the testis it is unlikely that these inclusions are absorbed luminal pigment from a testicular origin Presumably the pigment in the subepithelial macrophages is from the phagocytosis of disintegrating ductal cells

Lesions similar to testicular cystic tubules occur in the epididymides of treated hamsters Granados and Dam (48) reported epididymal cysts in mature hamster (220-240 days of age) which were associated with testicular hypoplasia The caudal cysts observed by Maneely (58) in gonadectomized rats were thought to be related to stasis of epididymal fluid It is possible that an abnormal epididymal absorptive or secretory process coupled with a blockage of the efferent system of the reproductive tract could account for these cysts

The present results and those of Ortiz (53) indicate that the rapidity of epithelial regression is not comparable to that noted in the castrate or estrogenized rat seminal vesicle In the hamster pronounced atrophy of the secretory epithelium is not evident until 120 days of treatment Glandular function may be arrested as indicated by loss of cytoplasmic basophilia and luminal secretion although the epithelial height is maintained The results of Ortiz (53) and those of the present study indicate that the presence of intracellular pigment may reflect the level of circulating androgen more clearly than the changes in cell height

A comparison of the epithelial involutions of the accessory glands of estrogenized hamsters indicates that the bulbourethral gland undergoes the greatest reduction in cell height Complete parenchymal atrophy with loss of secretory function is evident after 30 days of estrogenization In the gonadectomized rat castration atrophy of the bulbourethral gland was detected as early as 10 days (Heller 32) and the maximal state of atrophy was approximately 100 days postcastration

Ortiz (53) stated that the response of the hamster bulbourethral gland to castration was similar to the rat in that it underwent regression within 15 to 20 days post castration and as in the rat was a good indicator of the level of circulating androgen

SUMMARY

1 Sexually mature male hamsters were treated with subcutaneous pellets of alpha estradiol ethinyl estradiol estrone or stilbestrol for 30 60 90 120 and 240 days The induced involutional changes of the testis and accessory sex organs were examined histologically histochemically and statistically

2 Early atrophic tubular changes were characterized by heavy lipid accumulation an increase in Sertoli cell glycogen and a decrease in Sertoli cell RNA Prolonged estrogenization led to the deposition of tubular pigment followed by tubular cavitation The severity of testicular response was more dependent upon the quantity of estrogen absorbed than on the specific hormone administered The pathogenesis of the atrophic changes of the testis are discussed

3 The present study indicated that the estrogen induced atrophy of the seminal vesicle of the hamster was not accompanied by rapid epithelial regression Only the bulbourethral gland gave a pattern of immediate parenchymal atrophy associated with failing Leydig cell function No epithelial metaplastic alterations were observed in any of the accessories Conversely all the accessory organs demonstrated some degree of stromal hyperplasia

LITERATURE CITED

- Bacon R. L. and H. Kirkman 1955 The response of the testis of the hamster to chronic treatment with different estrogens *Endocrinology* 57 255-271
- Burgos M. H., H. Montes de Oca and M. M. Montorzi 1959 La incorporación de Fe-59 en los conductos eferentes del hamster *Rev. Soc. Argent. Biol.* 35 36-39
- Cavazos L. F. 1958 Effects of testosterone propionate on histochemical reactions of epithelium of rat ductus epididymidis *Anat. Rec.* 132 209-228
- Clubb R. W. 1951 A study of epididymal transport of India ink and related epithelial reactions Thesis Univ. Rochester (Cited by Mason and Shaver 1952.)
- Elftman H. 1957 Phospholipid fixation by dichromate sublimate *Stain Tech.* 32 29-31

- Emmens C W and A S Parkes 1947 Effects of exogenous estrogens on the male mammary Vitamins and Hormones 3 273-282
- Gomori C 1952 Microscopic Histochemistry Univ. of Chicago Press
- Granados H and H Dam 1948 Testicular hyperplasia and epididymal cysts in the Syrian hamster Nature 162 297
- Heller R F 1932 Cowper's gland and its reaction to castration and to different sex hormone conditions Am J Anat 30 73-77
- Huxley J S 1932 Problems of Relative Growth Lincoln MacVeach The Dial Press New York
- Kramer H and C M Windrum 1952 The metachromatic staining reactions J Histochem Cytochem 3 22-23
- Long M F and F TINGLE 1952 Cytochemistry of the human testis Ann N Y Acad Sci 5 619-628
- Maneely R B 1958 The effect of bilateral gonadectomy on the histology and histochemistry of the surviving epididymis in rats Acta Anat 32 361-380
- Mason A I and S I Mauer 1957 Reversible testis damage in the vitamin F deficient hamster Anat Rec 122 327-330
- Mason A I and S L Shaver 1952 Some functions of the caput epididymis Ann N Y Acad Sci 55 83-93
- McLampy R M and L F Cavazos 1954 Comparative study of lipids in vertebrate testes Proc Soc Exp Biol Med 87 297-303
- Menschik J M and Munk T Rogalski O Rymaszewski and J J Szczepniak 1952 Vitamin E studies on mice with special reference to the distribution and metabolism of lipids Ann N Y Acad Sci 52 94-107
- Montagna W and J B Hamilton 1951 Histochemical studies of human testes I The distribution of lipids Anat Rec 109 63-69
- Ortiz I 1953 The effects of castration on the reproductive system of the golden hamster Biol 117 65-77
- Perlman P I 1950 The functional significance of testis cholesterol in the rat Effects of hypophysectomy and cryptorchidism Endocrinology 47 311-316
- Pierantzi I J C Radice and M L Herratz 1949 Deposits of fluorescent pigment in the atrophic testes of vitamin F deficient rats Ann N Y Acad Sci 5 129-131
- Thorberg J V 1948 On the influence of sex steroid hormones on the male accessory genital system Acta Endocrinol 1 1-24
- Turner M E and C D Stevens 1957 The regression analysis of causal paths Biometrics 13 216-228
- Warren R P and J L R Aronson 1957 Sexual behavior in castrated adrenalectomized hamsters maintained on DCA Endocrinology 53 273-304

PLATE I

EXPLANATION OF FIGURES

- 3 Testis of untreated control hamster PAS counterstained with Weigert Lillie's hematoxylin. Spermatogenesis is apparent. 273
- 4 Testis of hamster treated with stilbestrol 210 days. PAS counterstained with Weigert Lillie's hematoxylin. Observe cystic tubules with intensely positive PAS luminal mass. Other tubules are undergoing the process of cavitation. 273
- 5 Testis of untreated control hamster, oil red O counterstained with Harris hematoxylin. Note sudanophilic droplets dispersed in the cytoplasm of Leydig cells. 676
- 6 Testis of hamster treated with stilbestrol for 90 days, oil red O counterstained with Harris hematoxylin. A heavy accumulation of tubular lipid is primarily localized in Sertoli cells. 676
- 7 Testis of untreated control hamster Sudan black B for localization of phospholipids in tissue fixed in dichromate-mercuric chloride solution of Elftman. Varying quantities of reactive material may be seen in the Sertoli cells, spermatogonia and spermatocytes. Note intense reaction in interstitial cells. 676
- 8 Testis of hamster treated with ethinyl estradiol for 120 days. Sudan black B for localization of phospholipids. Heaviest accumulation is in the Sertoli cell cytoplasm and cellular detritus. Some of coloration represents pigment staining. 676

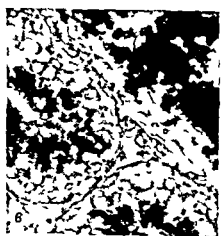


PLATE 2

EXPLANATION OF FIGURES

- 9 Cauda epididymidis of untreated control hamster PAS A diffuse reaction localized in the supranuclear cytoplasm of the ductal epithelium $\times 676$
- 10 Epididymus of hamster treated with ethinyl estradiol for 240 days PAS Note the intense PAS positive material located in ductal cells and lumen $\nearrow 676$
- 11 Cauda epididymidis of untreated control hamster toluidine blue Observe intense orthochromasia in the luminal and immediate supranuclear cytoplasm $\nearrow 676$
- 12 Cauda epididymidis of hamster treated with stilbestrol for 240 days Sudan black B staining of paraffin embedded tissue Cystic dilatation of ductus and pigment (arrows) are visible $\times 32$

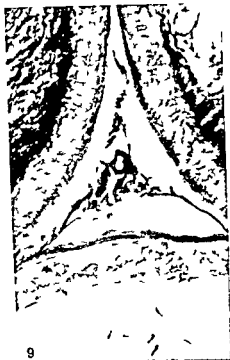
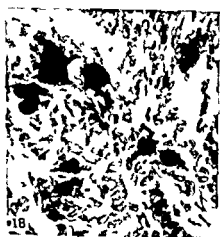
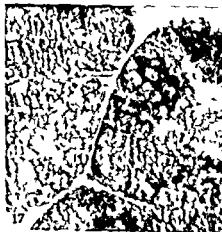


PLATE 3

EXPLANATION OF FIGURES

- 13 Testis of hamster treated with ethinyl estradiol for 240 days. Tissue fixed in AAF paraffin embedded prior to staining with Sudan black B. Three forms of degenerative lesions are represented in this section: A solid, B cystic and C pigmentation atrophy. / 39
- 14 Testis of hamster treated with alpha estradiol for 120 days. Ziehl-Neelsen procedure for lipofuscins. Principal localization of acid fast pigment occurs in Sertoli cells, tubular lumina and interstitial cells. / 676
- 15 Seminal vesicle of untreated control hamster toluidine blue. Characteristic supranuclear clear light areas are evident as well as occasional pigment inclusion (arrow). / 676
- 16 Seminal vesicle of hamster treated with estrone for 240 days. Sudan black B staining of paraffin embedded tissue. Note sudanophilic reaction in subepithelial macrophages and secretory epithelium. Luminal sudanophilia is confined primarily to desquamated cells. / 169
- 17 Bulbourethral gland of untreated control hamster toluidine blue. Acinar cells gave a strong metachromatic reaction. / 676
- 18 Bulbourethral gland of hamster treated for 60 days with alpha estradiol toluidine blue. Gland is characterized by drastic involution, stromal hyperplasia and mast cell infiltration. / 676



The Wave of the Seminiferous Epithelium in the Rat

B PEREY Y CLERMONT AND C P LEBLOND

Department of Anatomy McGill University Montreal Canada

Investigation of the manner in which germ cells are associated in the seminiferous epithelium of mammals led Von Ebner (1871) and Regaud (01) to define two important concepts one dealing with the evolution of germ cells in time—the *cycle*—and the other with their arrangement along the length of the tubules—the *wave*. Let us briefly describe these two concepts.

Sections of seminiferous tubules of rat show several concentric layers composed of cells at exactly the same step of development (fig 1). The layers of cells are combined in a predictable manner. For

instance groups of spermatids at a given step of development are always associated with the same groups of spermatocytes and spermatogonia. Thus definite cellular associations are formed.

The cellular associations encountered in the seminiferous epithelium of the rat may be classified into a limited number of types 8 according to Von Ebner (1871) or 14 according to our group (Leblond and Clermont 52a b). The latter classification has yielded precise and reproducible results over the past 10 years in our laboratory and will be used in the present investigation.

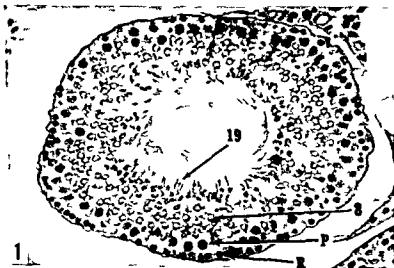


Fig 1 Cross section of a rat seminiferous tubule stained with PA Schiff hematoxylin $\times 300$

Most of the types of germ cells present in the seminiferous epithelium are visible. R indicates resting primary spermatocytes, P pachytene primary spermatocytes, 8 step 8 spermatids, and 19 step 19 spermatids on the verge of being released into the lumen to become spermatozoa (note their spiral tails). The cells of these 4 types are arranged into concentric layers as may be seen by looking along the direction of the arrows. Furthermore the cells of any given type have all the same appearance as they are all at the same step of development.

The various cell types together make up what is referred to as a "cellular association" (The seminiferous epithelium of the rat may consist of any one of 14 cellular associations. The one in this picture is known as cellular association VIII).

The evolution of the spermatids may be used as a guide to arrange the 14 typical cellular associations in an orderly sequence as done in figure 2. The implication is that the 14 cellular associations appear successively in any one area of the seminiferous epithelium and the sequence repeats itself time and time again. The succession of the 14 cellular associations constitutes the cycle of the seminiferous epithelium. The period during which each cellular association is present is a stage of the cycle. Thus a certain area of the seminiferous epithelium is said to be at a given stage of the cycle say stage VIII when cellular association VIII is present in that area (fig. 1). The duration of the cycle (that is the time between two successive appearances of the same cellular association in any one area of the tubule) was measured in the rat by means of radioautography using tritium labeled thymidine and found to be remarkably constant 12 ± 0.2 days (Clermont, Leblond and Messier 59).

The concept of "the cycle of the seminiferous epithelium" must be clearly distinguished from that of "the wave of the seminiferous epithelium". Whereas the cycle is concerned with the changes taking place in time in any one area of the seminiferous epithelium the concept of the wave refers to the arrangement of the cellular associations at any one time along the length of the seminiferous tubule.

Credit for formulating the wave concept belongs to Von Ebner. In 1871 he ex-

amined seminiferous tubules of rats along their length and observed an orderly series of cellular associations. For instance a portion of tubule displaying cellular association III would be followed by successive portions containing cellular associations IV, V, VI and so on. Each complete series of the recognized cellular associations may be called a wave ("Art einer Welle"). There would be several waves in each seminiferous tubule. Later (1888) Von Ebner found the length of the wave to average 3.2 cm.

The existence of waves was also observed by Benda (1887) in several mammals (mouse, guinea pig, rabbit, bull, ram, boar, dog and cat) and by Furst (1887) in marsupials. It remained for Regaud (1909) who studied the rat to emphasize the findings of his predecessors with the striking statement that "the wave is in space what the cycle is in time". He went on further by explaining that "the length of the wave is proportional to the duration of the cycle. Therefore stages of the cycle are represented by segments of tubule of a given length which is proportional to their duration". In order to explain some features of the wave and the clockwise pattern of the tails of maturing spermatids (fig. 1) Regaud (1909) postulated that the segments making up the wave follow a spiral course around the tubules—an idea endorsed by Von Ebner in 1902. Regaud explained the production of the wave by an "impulse" which would migrate along the tubules initiating spermatogenesis on

Fig. 2. Composition of the 14 cellular associations observed in the seminiferous epithelium in the rat. Each column consists of the various cell types making a cellular association (identified by Roman numeral at base). Each cellular association is defined by the step of development of the spermatids present. Whereas spermatids are classified into 19 steps according to the condition of nucleus and acrosomic structures in sections stained with the periodic acid Schiff hematoxylin technique, only the 14 first steps are used to define the 14 cellular associations.

The cellular associations succeed one another in time in any given area of seminiferous tubule according to the sequence indicated from left to right in the figure. (Following cellular association XIV, cellular association I reappears so that the sequence starts over again.) The succession of the 14 cellular associations makes up "the cycle of the seminiferous epithelium".

The cycle should not be confused with "spermatogenesis" which is the complete series of the changes taking place in germ cells during the evolution by which type A stem cells eventually become spermatozoa. This sequence can also be seen in the drawing if one reads from left to right starting with the bottom row. A indicates type A spermatogonia; In intermediate type spermatogonia B; type B spermatogonia R; resting primary spermatocytes L; leptotene primary spermatocytes Z; zygotene primary spermatocytes P; pachytene primary spermatocytes D; diakinesis of primary spermocytes II; secondary spermatocytes 1-19 steps of spermiogenesis. The subscript m next to a spermatogonium indicates the occurrence of mitosis.

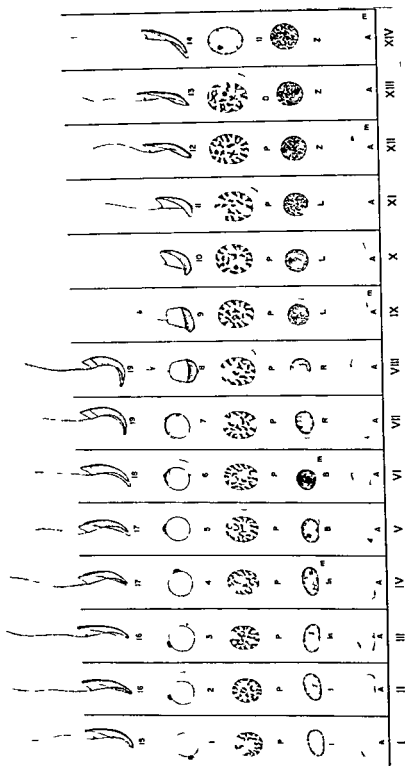


Figure 2

its way. However, Picaud's conclusions were reached from indirect evidence and without the help of measurements. Nevertheless, his views have been widely accepted up to the present time (Laylot and Baudrimont 26; Morel 47; Roosen Punge 50; Tobias 56). Perhaps the intricacy of his reasoning discouraged criticism.

The only substantial work on the wave during the last 50 years was that of Curtis (18) who investigated serial sections of mouse and rabbit testis. He confirmed that cellular associations with successive numbers usually follow one another along the length of the tubule. He added that the numbers decrease from the rete testis onwards. Curtis, however, emphasized that there were many irregularities in the distribution of the cellular associations. However, he did not feel that these irregularities were incompatible with the concept of the wave as proposed by Von Ebner (1888), a concept that he seems to have accepted without reservation.

The present study was designed to reinvestigate the wave of the seminiferous epithelium in the rat using the procedure described by our group for the study of the cycle (Leblond and Clermont 52a; Clermont and Perey 57). Two types of material were used: (1) portions of dissected tubules were sectioned along their length and (2) serial cross sections of a whole testis were prepared. Both methods lent themselves to the identification of the cellular associations encountered along the length of the tubules. Some laws governing the arrangement of the segments were formulated and the wave was redefined to fit the new observations.

MATERIAL AND METHODS

Longitudinal sections of seminiferous tubules

The testes of 5 albino rats weighing 250–300 gm were fixed in Zenker formal and the tubules were microdissected under water at a magnification of 45 diameters. A mounted sewing needle and small forceps were used to isolate the seminiferous tubules. Histological processing of the freed portions of tubules was difficult because of their extreme fragility. The problem was solved by placing each of them into a flat glass chamber built from ordinary histological slides (fig. 3). Free circulation of solutions in and out of the chambers could take place through the slits provided in the walls. Thus the chamber could be carried through water

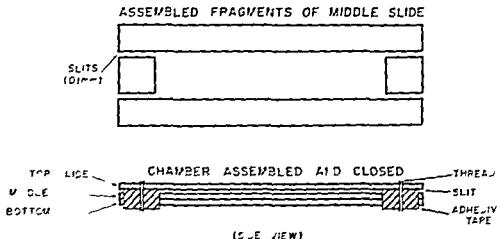


FIG. 3. Diagram of the glass chamber used to process isolated portions of seminiferous tubules through the x-ray and paraffin.

The lower figure is a side view showing that the chamber is constructed of three superimposed glass slides. The top and bottom slides are standard 1" x 3" histology glass slides, but the middle one is a middle slide cut into 4 pieces as shown in the top diagram. These 4 pieces are assembled over the bottom slide and fastened with adhesive tape. Then the dissected tubule is placed flat on the bottom slide in the space available between the pieces of the middle slide. Finally the top slide is adjusted over the others by means of thread at the slits provided for the circulation of fluids.

alcohol dioxane and melted paraffin with out any direct handling of the tubule

After passing through paraffin the chamber was allowed to cool and was taken apart leaving the tubule included in a small amount of paraffin over the bottom slide. Meanwhile a block of paraffin was prepared the surface of which was made flat by contact with a hot glass slide. The slide carrying its tubule was then reversed over this surface and the tubule was made to penetrate the block by rubbing a warm knife over the back of the slide. Gentle pressure was applied to flatten out the coils. When after a few minutes the slide was removed the tubule lay evenly at the surface of the block.

The microtome knife was adjusted as parallel to the surface as possible and the block was sectioned serially at $7\ \mu$. The sections were stained with periodic acid Schiff hematoxylin (figs 16-18). Measurements and results of microscopic analysis were recorded on low power photographs ($\times 30$) of the sections (figs 5-7, 9).

In this manner fragments of 34 tubules were obtained 21 of which included the junction of the tubule with the rete testis. Twenty two of the 34 fragments measuring from 13 to 128 mm were used for quantitative data. The combined length of these fragments was about 1 meter (1040 mm).

Serial sections of testis

One testis from an adult albino rat weighing 340 gm was fixed in Zenker formol. After impregnation in paraffin serial sections were made of the entire organ with the microtome set at $5\ \mu$. Since the fixed testis was 17 mm long 3400 sections were expected 3410 were actually obtained. The agreement between the two figures was so good that the mean thickness of the sections must have been very close to $5\ \mu$.

After staining with the periodic acid Schiff hematoxylin method a low power photograph was taken of every 20th section (i.e. every $100\ \mu$) giving a total of 170 photographs. Then each one of the tubular cross sections visible in each photograph was examined under the microscope for identification of the cellular association present according to the cri-

teria given by Clermont and Perey (57). The number of the cellular association was recorded on the picture of the corresponding cross section.

Individual seminiferous tubules were examined as follows. First the junction of a tubule to the rete testis was located and this tubule was given a code number (from 1-20). Then this tubule was followed from section to section throughout its course and a listing was made of the cellular associations encountered. Since it was known that the photographs were taken every $100\ \mu$ the length of tubule occupied by each cellular association could be calculated from the data. These lengths were corrected as described by Clermont and Huckins (61). Twenty complete seminiferous tubules were examined in the manner just described. Their combined length was 695 meters.

Several areas of the seminiferous tubules were reconstructed from the serial sections and mapped (figs 11 and 12) according to a technique described in detail elsewhere (Clermont and Leblond 59).

RESULTS

Observations made on longitudinally cut tubules

In describing any given region of the seminiferous tubule the portion nearer the rete testis will be referred to as proximal and that farther from the rete as distal.

Description of the junction between rete testis and seminiferous tubules

The junction was found to be a funnel like structure composed of two parts: the *tubulus rectus* opening into the rete testis and the *intermediate region* abutting on the seminiferous epithelium (fig 4). The tubulus rectus was a straight canal of variable length which like the rete itself was lined by a low cuboidal epithelium with a simple basement membrane. The intermediate region was a conical portion containing an epithelium composed of tall flame like cells with a nucleus characteristic of Sertoli cells and lined by the same type of complex basement membrane as that found around the seminiferous tubule proper (Clermont 58). The crowded bodies of the Sertoli cells made up a papilla

OPENING INTO RETE TESTIS

PROXIMAL

TUBULUS RECTUS
(LOW CUBOIDAL EPITHELIUM)

INTERMEDIATE REGION
(SERTOLI CELLS ONLY)

END OF SEMINIFEROUS
TUBULE PROPER
(TYPICAL
SEMINIFEROUS
EPITHELIUM)

DISTAL

Figure 4

PROXIMAL

DISTAL

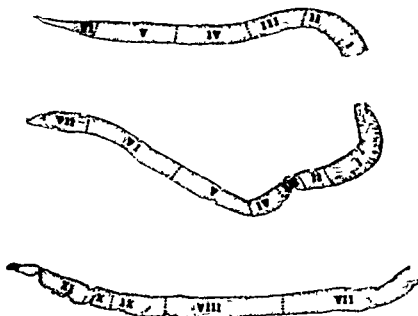


Fig 5 Low power photographs of three pieces of longitudinally cut tubules showing the junction with the rete testis $\times 20$

The junction between tubule and rete is seen at this magnification as a tapered end at left of each tubule. Next to the junction cellular association VI is seen at top VII in the middle and XI in the lowest tubule. The portion of tubule occupied by a cellular association is referred to a "segment".

Each segment is referred to by the same Roman numeral as the cellular association it contains. The limit is indicated by dotted lines. Note that in every tubule the numbers identifying the segments decrease from the rete testis (proximal end) to the distal portion of the tubules. This phenomenon is known as the "descent of the segmental order".

which projected into the tubulus rectus (fig 4) and may conceivably function as a valve allowing fluids and free cells to leave but not to enter the tubule.

Distally the intermediate region abruptly changed into the typical seminiferous epithelium (which may display any one of the 14 typical cellular associations e.g. XIII in fig 4).

Fig 4 Drawing of the region connecting a seminiferous tubule (base of picture) to the rete testis (top). The region includes two parts: the tubulus rectus lined by a low cuboidal epithelium and a funnel-shaped intermediate portion with an epithelium composed of Sertoli cells only. The apical extremities of these cells extend towards the tubulus rectus and form a papilla-like structure in the lumen. The seminiferous epithelium seen at the base shows cellular association XIII.

The segments

The cellular association seen next to the intermediate region extended around the circumference and over a certain length of the tubule. At a variable distance another type of cellular association was seen to be followed farther along the tubule by a third type and so on indefinitely (fig 5). The portion of tubule occupied by one type of cellular association was called a "segment" hence there were 14 types of segments which were each referred to by the number of their cellular association (I-XIV).

The limits of most segments were sharply demarcated. There was usually an abrupt change between a segment and the next one with no transition in between. The limit could usually be pinned down to

individual cells as illustrated by the junction XIII XIV in figure 18 (thick arrows). This was not evident however for the limit between segments IV-VIII where the subtle differences in spermatids from segment to segment did not make it easy to decide how abrupt the change was.

Nevertheless segmental limits were always precise enough to allow the length of segments to be measured. The results of such measurements expressed in millimeters (table 1) revealed wide variations in the length of any of the 14 types.

Continuity of the segmental order

When successive segments were compared it became evident that any two adjacent segments carried consecutive numbers (fig. 5) except for segments XIV and I which usually followed each other (fig. 6). However cellular associations XIV and I are as closely related as any two with consecutive numbers say XIII and XIV (Leblond and Clermont 52a). Hence if it is assumed that the list of consecutive numbers extends from I to

XIV and after XIV reverts to I then consecutive numbers were always carried by two adjacent segments. This feature was referred to as the "continuity of the segmental order".

Usually each segment was located between one with a more advanced and one with a less advanced type of cellular association. Thus in the tubule at the top of figure 5 segment IV is between segments V and III. On occasion however a segment was found between two which had both the next higher or both the next lower number. Thus in figure 6 the segment III seen near the base (shaded) is located between two segments II. Such an arrangement was in keeping with the continuity of the segmental order since any two adjacent segments carried consecutive numbers.

Descent of the segmental order

When the sequence of the segmental numbers was traced distally from the rete testis (fig. 5) it was found that any segment was usually followed by a segment with the next lower number (and segment I was usually followed by segment XIV). As a result the overall pattern of the segmental order was descending in a distal

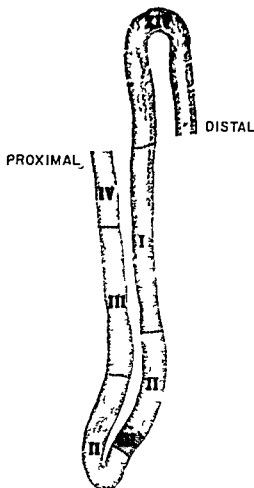


Fig. 6 Low power photograph of longitudinally cut tubule showing a modulation $\times 20$.

If the segmental order is followed in a distal direction it is seen to be descending at first (IV III II) ascending with the shaded segment (III) and then descending again (II I XIV). Such a fluctuation in the segmental order is referred to as a modulation.

direction. This feature was referred to as the "descent of the segmental order".

Irregularities in the descent of the segmental order: the modulations

While the overall pattern of the segmental order was that of a descent in a distal direction local irregularities were seen. Thus a segment could be followed by one with the next higher instead of the next lower number so that two or more segments were arranged in an ascending order in a distal direction. There

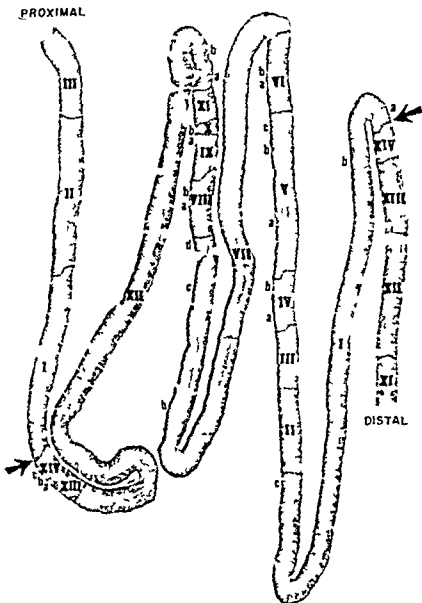


Fig 7 Low power photograph of longitudinally cut tubule showing a wave without modulation $\times 25$

Note the continuity of the segmental order the descent of the order in a distal direction and the variability in the length of segments of a given type (compare the two segments I also the two XII). No modulation was observed over this length of tubule. The limits of a wave may be taken to be the borderlines between segments XIV and I as indicated by two large arrows. (The small letters show where the microphotographs of the subsegments reproduced in fig. 8 were taken.)

after the descending pattern was resumed without breach in the continuity of the segmental order. For instance in figure 6 the usual descending order is seen at the left as far as the shadowed area where a segment III instead of the expected segment I follows a segment II. Close by the descent of the segmental order is resumed. In this case only one segment interfered with the usual order. In other cases several segments were involved (fig. 9). The shadowed segments in figures 6 and 9 constituted what was called a "modulation of the segmental order" or more simply a "modulation".

The limits of each modulation were arbitrarily determined as follows. The tubule under study (see fig. 9 for instance) was traced in the distal direction until the descending segmental order became ascending. At that point a modulation was said to begin. Farther on after the order became descending again a seg-

ment with the same number as that immediately preceding the modulation was encountered. There the modulation was taken to end. The modulation thus defined was always located between two segments with the same rank and was composed of an odd number of segments (one in fig. 6 and five in fig. 9).

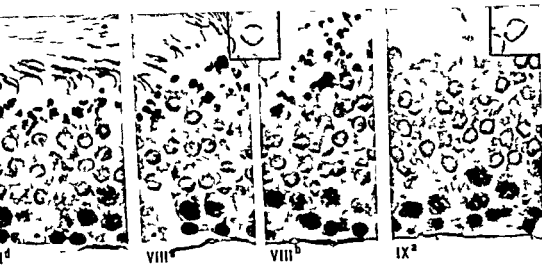
The wave of the seminiferous epithelium

The term "wave" as defined by Von Ebner (1888) and others referred to the complete series of the recognized cellular associations arranged consecutively along the length of the tubules. We had therefore expected to find waves consisting of a series of the 14 types of segments arranged in order from I to XIV. Such series have indeed been seen (fig. 7) but in most cases (80%) they were disturbed by the presence of modulations.

It is possible to define a "wave" under these conditions if we merely ignore all

Fig. 8. Microphotographs of the 14 types of segments (I-XIV) taken from the modulation-free wave seen in the longitudinally cut tubule of figure 7. Nine of the 14 segments have been subdivided into subsegments. (Small letters in fig. 7 indicate the sites where the photographs of the subsegments were taken.) PA Schiff hematoxylin / 600. Enlarged spermatids in the insets illustrate some of the criteria used in identifying subsegments.

- Ia The newly formed spermatids have small dark nuclei.
- Ib The nuclei of the young spermatids are larger and lighter than in segment Ia. Idiosome not visible.
- Ic Idiosome of young spermatids is apparent at left in the inset.
- II Several minute proacrosomic granules appear in the idiosome.
- III The small proacrosomic granules have fused into a larger and spherical acrosomic granule.
- IVa The acrosomic granule has a hemispherical shape and is applied onto the nucleus.
- IVb A pronounced flattening of the acrosomic granule on the nucleus is taking place.
- Va The head cap appears. It is often seen only on one side of the acrosomic granule.
- Vb The head cap is definite but covers less than a quarter of the nuclear circumference.
- Vc The head cap covers exactly one quarter of the nuclear circumference.
- VIa The head cap covers between one quarter and one third of the nuclear circumference.
- VIb The head cap covers one third of the nuclear circumference.
- VIIa The head cap covers more than one third of the nuclear circumference. Basophilic bodies are not seen in the cytoplasm of maturing spermatids.
- VIIb Spherical basophilic bodies appear in the distal cytoplasm of maturing spermatids.
- VIIc The basophilic (residual) bodies form a dense row just below the nuclei of maturing spermatids.
- VIIIa and b. The majority of head caps face towards the limiting membrane of the tubule. VIIIa and b are respectively before and after the release of spermatozoa.
- IXa The spermatid nuclei show a slight asymmetry.
- IXb The asymmetry of the spermatid nuclei is pronounced.
- X The nuclei of spermatids are slightly elongated.
- XI The spermatid nuclei are much elongated.
- XIIa The spermatid nuclei are less curved than at XI and less dark than in subsegment XIIb. The head has not reached maximal darkness and elongation.
- XIIb Spermatid nuclei are dark, nearly straight and narrow.
- XIII The apex of the spermatids is curved, pointed and lightly staining.
- XIVa Large division figures of primary spermatocytes (prophase excluded).
- XIVb Secondary spermatocytes resting or in prophase are present.
- XIVc Small division figures of secondary spermatocytes (prophase excluded).





I^a



I^b



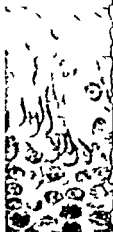
I^c



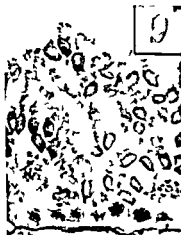
V^c



VI^a



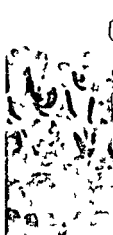
VI^b



IX^a



X



XI

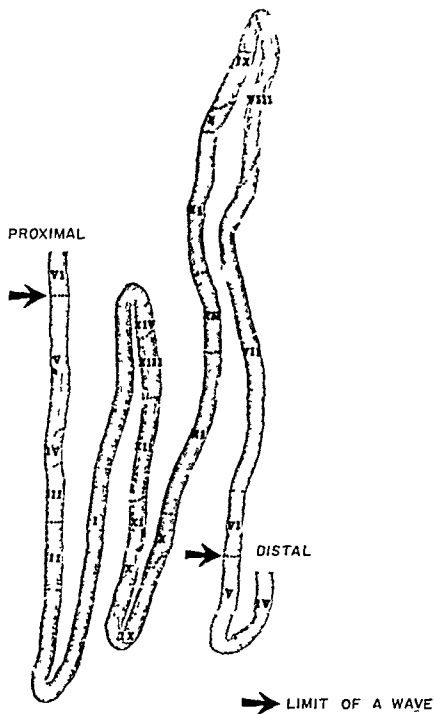


Figure 9

TABLE 1
Length of the segments measured on longitudinally cut tubules

Segmental number	Number of segments in a wave	Length of longest segment	Length of shortest segment	Average length of segment
		mm	mm	mm
I	56	7.2	0.10	2.6
II	53	4.5	0.17	1.2
III	59	5.0	0.06	0.6
IV	60	3.9	0.03	0.9
V	53	5.7	0.22	1.4
VI	50	6.2	0.10	1.5
VII	48	9.1	0.31	3.2
VIII	58	6.2	0.20	1.4
IX	65	3.1	0.06	0.8
X	68	1.9	0.02	0.4
XI	63	6.0	0.03	0.6
XII	54	6.8	0.07	1.5
XIII	56	7.1	0.07	0.9
XIV	56	3.3	0.07	0.8

segments involved in modulation. The wave is then a series of adjacent segments which includes the 14 possible types in addition to any segment which may be involved in modulation. This definition has been made rather broad so that the wave does not necessarily start with segment I and end with segment XIV but rather any segment outside a modulation may be considered to be the beginning of a wave (fig 9).

Thirty one waves were investigated in longitudinally cut tubules. Their average length expressed in centimeters was 2.33 cm (0.55-4.25 cm) and they contained an average of 1.35 modulations per wave (0 to 4).

Fig 9 Low power photograph of a longitudinally cut tubule showing a wave with a modulation. 20

Starting at the proximal end of the tubule the usual descending order of the segments is observed as far as the shaded area. There a segment X instead of the expected segment VIII follows segment IX. Farther on ascent of the segmental order continues with segments XI and XII but then reversion to a descending order take place with segments XI X IX VIII and so on. By definition (see text) the shaded segments constitute a "modulation" of the segmental order.

(The limits of a modulation would be different if the segmental order had been followed from the distal end in a proximal direction. The segmental order would be ascending up to segment XII become descending down to segment IX and then become ascending again.)

The portion of tubule between the two large arrows constitutes a wave with a modulation.

Subsegments

The precise recognition and delimitation of each segment made possible accurate experimental work such as that reported in table 1. However one may well wonder whether a detailed analysis of any segment would show morphological differences between its various parts. Such analysis revealed that 5 of the segments were reasonably uniform throughout (II III X XI XIII fig 8) but the others were not. Thus figure 17 represents two distinct parts of a segment VIII, one showing maturing spermatids at right and the other a spermatid free epithelium at left. Hence segment VIII may be said to consist of two subsegments referred to as VIIIa and VIIIb respectively. Two to 4 subsegments have been identified in segments I IV IX XII and XIV and are designated by the letters a b c up to d in figure 8.

Although subsegments were not so readily recognized they were usually as sharply limited as whole segments. In many cases they showed continuity and descent of the order (fig 10). However with short subsegments such as XIVa b and c the continuity of the order was often lacking. Thus in figure 18 the base showed continuity (XIII XIVa XIVb) but the top did not (XIII XIVb). It may be added that whereas segments usually extended around the circumference of the tubule subsegments may occupy only a

fraction of it (as does segment XIVa in fig 18)

Orientation of the tails of spermatids in the tubular lumen

The delicate tails sported by spermatids before they reach step 17 of spermiogenesis (fig 2) pointed at random either in the proximal or the distal direction of the tubule. However the spermatids at steps 17 18 19 of spermiogenesis seen in segments V-VIII had thick tails which always pointed distally that is away from the rete testis (fig 16 see also the mid row in fig 8). This was true even in segments involved in modulations (A change in the orientation of the tails occurred only when the maturing spermatids left the seminiferous epithelium to become spermatozoa as seen in the center of fig 17.)

Observations made on tubules reconstructed from serial sections

The normalcy of the single testis examined in serial sections was tested by comparing the frequency of occurrence of the 14 cellular associations in this organ and in a group of 6 testes investigated previously (Leblond and Clermont '52a). The two sets of results shown in the first two rows of table 2 were fairly similar. Hence the serially sectioned testis was taken to be a normal representative of the mature rat testis.

Junction of rete testis and seminiferous tubule

The frequency of occurrence of the 14 types of cellular associations at the junction with the rete testis (table 2 last row) was found to be approximately the same as anywhere else along the tubule (table 2 first row).

The segments

The reconstruction of tubules from serial sections revealed their zig zag shape with straight portions or limbs connected to one another by hairpin turns (see the previous article Clermont and Huckins '61). The segments were reconstructed using two-dimensional maps of the tubules (made by the method of Clermont and Leblond '59 p 240 which depicts a tubule as if it had been cut open along its length and laid down flat). Such maps confirmed that segmental boundaries were sharp and tended to be perpendicular to the axis of the tubule but were rather irregular (fig 11). Contrary to Regaud's ('01) assumption a spiral pattern was not seen.

The continuity of the segmental order was confirmed in all tubules examined (figs 11 13) and was even observed at the bifurcations described in the three branched tubules (Clermont and Huckins '61). On occasion however a segment could be found to occupy only part of the circumference of the tubule as in figure 11 where a minute area (marked by an arrow) is not covered by segment IX thus bringing segments VIII and X in contact. This failure of a segment to occupy the entire tubular circumference was encountered only in segments measuring less than 100 μ in length (usually segments III IV IX X XI or XIV). However when such segments failed to occupy a part of the tubular circumference this was only a small portion of it (fig 11) so that the continuity of the segmental order was preserved almost everywhere.

Examination of continuity at the subsegmental level was carried out using maps at a high magnification such as that in

PROXIMAL

DISTAL



Fig 10 Low power photograph of longitudinally cut tubule showing the location of a few subsegments. Note here continuity and descent of the subsegmental order from the proximal to the distal end.

TABLE 2
Frequency of occurrence of cellular associations

Cellular association	I	II	III	IV	V	VI	VII	VIII	IX	X	XI	XII	XIII	XIV	Total counts
Frequency as seen in tubular cross sections of the serially sectioned testis	139	57	23	33	52	85	227	57	28	25	34	147	41	51	6277
Mean Frequency as seen in tubular cross sections of 6 testes 6 (Leblond and Clermont table 2)	121	81	21	45	51	92	218	74	25	25	25	112	61	50	4041
Frequency as seen at the junction with rete in the serially sectioned testis 6	157	86	15	72	86	100	211	25	29	15	15	115	15	57	70

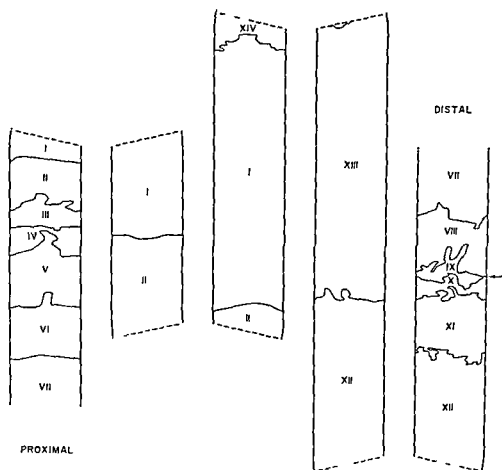


Fig 11 Two-dimensional map of a tubule showing a wave (from segment VII to the next segment VII) in which the limits of segments are indicated. To understand this map imagine that the tubule has been cut open along its length and laid down flat on the plane of the drawing. (Detailed reconstruction could be done along the limbs but not at the turns of the tubule.)

The segmental limits are seen as lines drawn across the tubule map. This means that the limits course around the circumference of the tubule. Note the irregularity and the variability in shape of the segmental limits.

At the point indicated by an arrow (right) segments VIII and X come in contact. In this case segment IX fails to occupy the whole circumference of the tubule.

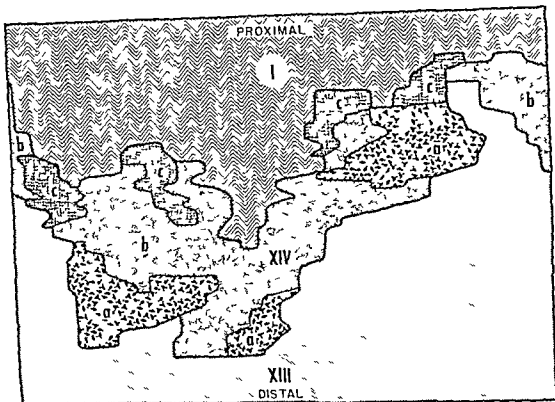


Fig 12 Two-dimensional map showing the area occupied by a segment XIV with its subsegments a b and c The tubule may be imagined as if it had been cut open along its length and laid down flat The two lateral edges of the figure would correspond to the line of cut Segment I is located on the proximal side of segment XIV and segment XIII on its distal side

Continuity of the subsegmental order would require that the series XIII XIVa XIVb XIVc and I be seen from base to top with every subsegment extending across the figure However many irregular interruptions are observed and therefore continuity does not exist at the subsegmental level

figure 12 which show the distribution of the subsegments a b and c of one segment XIV In this map subsegment c was in contact not only with subsegment b and segment I as expected but also with subsegment a and segment XIII The subsegment a at right has a small zone of contact with segment I and so on The presence of frequent cases of this type revealed that continuity was often lacking at the subsegmental level

The surface area covered by subsegments showed a fair amount of variation (fig 12) However the smallest subsegments such as the 4 subsegments c and the subsegment a at lower center in figure 12 had approximately the same surface area averaging 2035 μ

The descent of the segmental order over entire tubules The "site of reversal"

Examination of serial sections confirmed that the segmental order was descending from the rete testis distally (fig 13) However since most tubules have two extremities which both open into the rete testis (Clermont and Huckins 61) one would expect to observe along the tubules a point where the two descending segmental orders meet This was indeed found to be the case as a reversal of the segmental order took place abruptly in all tubules—a fact already shown in the mouse by Curtis (18) The region where this change occurred was called the "site of reversal"

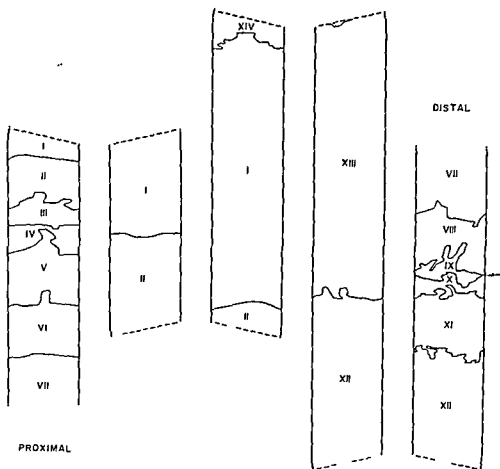


Fig 11 Two-dimensional map of a tubule showing a wave (from segment VII to the next segment VII) in which the limits of segments are indicated To understand this map imagine that the tubule has been cut open along its length and laid down flat on the plane of the drawing (Detailed reconstruction could be done along the limbs but not at the turns of the tubule)

The segmental limits are seen as lines drawn across the tubule map This means that the limits course around the circumference of the tubule Note the irregularity and the variability in shape of the segmental limits

At the point indicated by an arrow (right) segments VIII and X come in contact In this case segment IX fails to occupy the whole circumference of the tubule

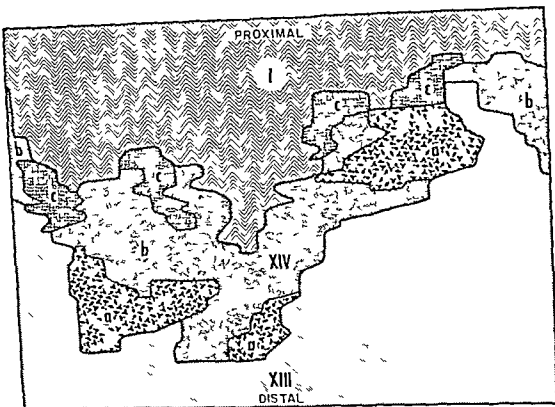


Fig 12 Two-dimensional map showing the area occupied by a segment XIV with its subsegments a b and c The tubule may be imagined as if it had been cut open along its length and laid down flat The two lateral edges of the figure would correspond to the line of cut Segment I is located on the proximal side of segment XIV and segment XIII on its distal side

Continuity of the subsegmental order would require that the series XIII XIVa XIVb XIVc and I be seen from base to top with every subsegment extending across the figure However many irregular interruptions are observed and therefore continuity does not exist at the subsegmental level

figure 12 which show the distribution of the subsegments a b and c of one segment XIV In this map subsegment c was in contact not only with subsegment b and segment I as expected but also with subsegment a and segment XIII The subsegment a at right has a small zone of contact with segment I and so on The presence of frequent cases of this type revealed that continuity was often lacking at the subsegmental level

The surface area covered by subsegments showed a fair amount of variation (fig 12) However the smallest subsegments such as the 4 subsegments c and the subsegment a at lower center in figure 12 had approximately the same surface area averaging 2035μ

The descent of the segmental order over entire tubules The "site of reversal"

Examination of serial sections confirmed that the segmental order was descending from the rete testis distally (fig 13) However since most tubules have two extremities which both open into the rete testis (Clermont and Huckins '61) one would expect to observe along the tubules a point where the two descending segmental orders meet This was indeed found to be the case as a reversal of the segmental order took place abruptly in all tubules—a fact already shown in the mouse by Curtis (18) The region where this change occurred was called the "site of reversal"

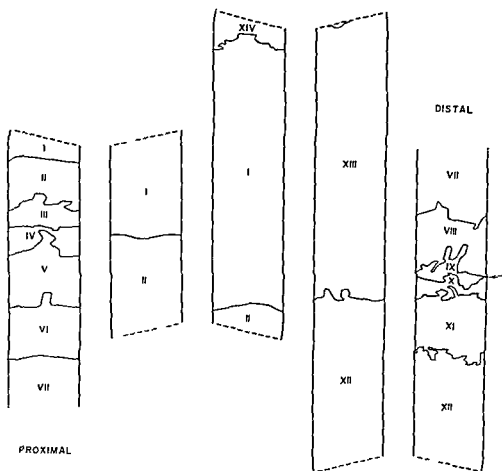


Fig 11 Two-dimensional map of a tubule showing a wave (from segment VII to the next segment VII) in which the limits of segments are indicated. To understand this map imagine that the tubule has been cut open along its length and laid down flat on the plane of the drawing. (Detailed reconstruction could be done along the limbs but not at the turns of the tubule.)

The segmental limits are seen as lines drawn across the tubule map. This means that the limits course around the circumference of the tubule. Note the irregularity and the variability in shape of the segmental limits.

At the point indicated by an arrow (right) segments VIII and X come in contact. In this case segment IX fails to occupy the whole circumference of the tubule.

TABLE 3
Position of the site of reversal along each seminiferous tubule

Code number of tubule	Length of tubule	Distance from the site of reversal to the rete testis		Distance from the site of reversal to the mid-point of tubule
		Longest side (L)	Shortest side (l)	
	cm	cm	cm	$\frac{L-l}{2}$
1	18.7	9.9	8.8	0.4
4	32.5	17.3	15.2	1.0
5	37.0	20.5	17.5	1.6
6	37.9	19.8	18.1	0.8
7	34.3	19.7	14.6	2.7
8	38.2	21.1	17.1	2.0
9	38.0	20.7	17.3	1.7
10	36.8	19.4	17.4	0.9
11	39.6	22.9	16.7	3.1
12	25.7	14.8	10.9	1.8
13	18.4	11.8	6.6	2.6
15	47.4	24.8	22.6	1.0
16	29.8	15.3	14.5	0.4
17	30.6	15.9	14.7	0.6
18	29.6	16.4	13.2	1.6
19	28.7	16.9	11.8	2.6
20	23.8	14.5	9.4	2.6
Averages	32.2			1.6

The site of reversal was clearly seen in diagrams in which the arrangement of the segments was plotted against tubular length for an entire tubule (fig 14)

Continuity of the segmental order was preserved in all of the 22 sites of reversal examined. No histological peculiarity seemed to differentiate these sites from other regions of the tubules.

The distance from any site of reversal to the two extremities of the tubules was found to be approximately the same (table 3). Indeed the site of reversal was distant from the mid point of the tubule by an average of only 1.6 cm (0.4-3.1 cm) which is about 5% of the mean

tubular length. As for the three branched tubules two of them had two sites of reversal each (nos 2, 3 of Clermont and Huckins '61) while the third one had only one (no 14). A site of reversal was also observed in the one blind ending tubule found (no 1).

Quantitative data on the wave

The number of waves per tubule varied from 7.9 to 15.4 and if branched tubules were disregarded averaged 12 (table 4). The number of waves was frequently different on both sides of the site of reversal (table 4 fig 14).

Fig 13 Diagrammatic representation of part of a tubule reconstructed from serial sections starting from the rete testis (at left)

In the top diagram the tubule is seen with its limbs and turns. The limits of the waves are indicated by arrows. The segments involved in "modulations" are shaded.

At the base of the figure the distribution of segments is represented graphically. Along the ordinate equal dimension is given to the 14 segments of the wave from I to XIV. On the abscissa, the tubular length in cm is given from the proximal towards the distal end. The segments are represented by horizontal lines proportional to their length and are connected by vertical lines (corresponding to segmental limits) to the preceding and following segments. Each limit between segments XIV and I was arbitrarily taken as the beginning of a wave (compare upper and lower diagram). The segments involved in modulation appear on the graph as spikes.

The first and second waves extend over a shorter length than those located distally.

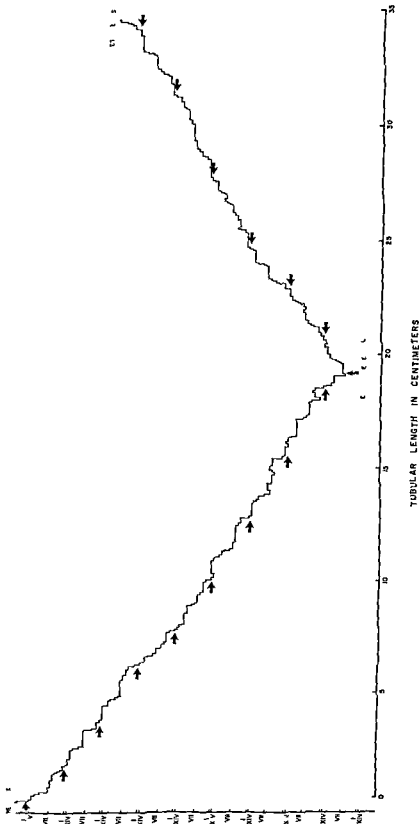


Fig. 14. Graphic representation of the distribution of segments and waves along a complete tubule. On the ordinate the successive waves are indicated with each one of the 14 segments being given the same dimension (only I, VII and XIV are written in). The tubular length in cm is given on the abscissa. Each segment is represented by a horizontal line proportional to its length and is connected to the preceding and following segments by vertical lines corresponding to segmental limits.

The beginnings of all segments I are indicated with arrows and may be taken as wave limits. Modulons are shown as spikes which may be seen in the 6th, 7th, 8th and 9th wave after the rete at left and in the first, second and 4th after the site of reversal at right.

TABLE 4

Number of waves per tubule and on each side of the site of reversal

C d n umber of tubule	Total number of waves	Number of waves on each side of site of reversal	
		Longest side	Short side
1	99	55	14
4	131	78	53
5	154	75	79
6	153	77	76
7	149	88	61
8	130	74	56
9	107	51	56
10	132	71	61
11	138	84	54
12	81	40	41
13	79	43	36
15	150	84	66
16	106	57	49
17	105	59	46
18	126	69	57
19	119	64	55
20	98	54	44
Average	121		

Measurements of the length of the waves were carried out in 20 complete tubules (table 5). The longest wave measured 6 cm and the shortest 0.7 cm. The mean wave length per tubule varied from 1.9 to 3.6 cm (table 5 last column).

A correlation between the length of a wave and its location within the tubule may be sought from the data in table 5 since the wave lengths were recorded for each tubule on two lines each one of which represented one side of the site of reversal. Each wave was placed in a different column according to the proximity to the rete (columns A B C D) or to the site of reversal (columns a b c d) which ever of the two was closer. Statistical analysis by the Student method revealed that the wave starting at the rete (A) was significantly shorter than the next one (B) with a p value < 0.001 whereas either one of them (A and B) was significantly shorter than any other wave in the tubule ($p < 0.001$). These size differences may also be seen in figure 13. No other significant variation was noted.

Quantitative data on the modulations

The frequency of modulations is illustrated by the data in table 6. Only 20 per cent of the waves did not show a modu-

lation while 28% had one, 20% had two, 15% had three and 17% had more than three modulations (up to 9). Within a tubule the frequency of modulations was found to be the same near the rete and near the reversal site.

When the number of segments per modulation was considered (table 6) it was found that 56% of the modulations were composed of one segment, 20% had three segments and 12% had more than 5 (up to 39). The number of segments per modulation was not different in the proximal and distal ends of the tubules.¹

The length of the segments involved in modulations was compared to that of segments measured outside modulations (table 7). The mean lengths did not differ significantly except for segments I, VII and XII which were shorter within than outside modulations.

Orientation of the tails in the tubular lumen

In serial sections the direction of the tails of maturing spermatids could only be observed in the hairpin turns taken by the tubules. In 125 such locations which included the maturing spermatids of segments V-VIII the tails pointed distally as already seen in longitudinal sections. This orientation of the tails towards the reversal site was true regardless of their distance from this site and even when the tails came from segments involved in modulations.

While the tails of maturing spermatids were always oriented towards the rete they were not pointing straight at it but curved in a clockwise direction thus producing the whorl-like appearance familiar to anyone who has examined sections of rat testis (fig. 1).

DISCUSSION

Concept of the wave of the seminiferous epithelium

The classics considered the wave of the seminiferous epithelium to be a complete

An interesting feature is the existence of large modulations containing smaller ones. About 30% of the modulations composed of 5 or more segments contained one or several smaller modulations. Such modulations found inside larger ones were usually composed of one or three segments.

TABLE 5

Length of waves (cm) seen in complete tubules¹

Code number of rubule	Rete				Reversal				Average wave length per tubule
	A	B	C	D	d	c	b	a	
1	1.8	2.3					2.2	1.9	
	1.4	1.6	2.2				2.3	2.0	1.9
2	1.1	1.7	1.8	2.4		2.5	3.2	2.3	
	1.0	1.8	3.2			2.6	2.4	1.9	2.2
2B							3.1	1.6	
	1.9	2.2	2.3			2.1	1.9	2.1	
3	2.7	3.1	1.8			2.1	2.9	1.4	
	1.4	2.7					2.1	2.4	2.5
3B		4.5	2.6				3.6	2.9	
	1.5	1.7	2.9	3.8		3.7	1.0	2.2	
4	1.7	2.3	2.4				3.4	4.4	
	1.4	1.8	2.3	2.0		1.6	2.7	2.3	2.6
5	0.7	0.9	1.9	3.5		2.5	2.3	2.6	
	1.9	3.5	3.1	3.0		2.4	3.3	2.7	2.4
6	1.2	1.1	2.1	3.1		5.5	1.6	2.1	
	1.7	3.7	1.6	2.0		2.2	2.8	3.0	2.4
7	1.2	2.2	3.0	1.2	2.3	3.2	2.3	3.2	
	1.5	2.9	3.3			2.7	2.0	2.0	2.3
8	1.6	2.5	2.2				5.9	3.6	
	2.2	2.3	2.4	3.6		4.0	3.3	2.3	3.0
9	2.8	2.8	4.7				3.5	2.4	
	2.1	3.3	5.9				4.6	4.0	3.6
10	1.0	1.5	3.0	3.1		4.1	4.3	2.8	
	2.5	2.1	2.6			3.3	3.2	3.6	2.8
11	2.4	1.9	3.8				4.5	2.7	
	1.4	1.5	2.1	1.8	3.5	3.9	3.6	4.2	2.9
12	4.3	3.0					4.5	2.8	
	1.5	2.2					6.0	1.2	3.2
13	1.3	1.9					4.5	3.5	
	1.6	1.5						3.1	2.5
14	1.0	1.5	3.1				3.4	3.6	
14B	0.7	1.6	3.3			3.2	2.5	2.8	2.6
	0.9	1.1	2.2	4.9	5.8				
15	1.6	1.7	1.8	3.4	4.2	4.2	3.5	3.6	
	1.3	3.4	3.9			3.5	4.2	4.9	3.2
16	0.8	2.4					3.5	5.4	
	1.7	2.4	2.9				2.5	3.2	2.7
17	1.2	2.3	3.1				2.5	3.3	
	1.1	2.8					3.4	5.0	2.7
18	2.0	1.8	3.7				2.4	2.6	
	0.9	1.7	2.6			3.5	1.7	3.0	2.4
19	2.2	2.8	3.6			2.8	2.1	2.6	
	1.1	2.3	2.1				2.0	2.6	2.4
20	1.2	2.5	2.9				4.0	2.5	
	0.8	1.0					3.1	3.8	2.4
Average wave length	1.5	2.2	2.8	2.9	4.0	3.1	3.1	2.9	Average length of all waves 2.6

¹The data for each tubule are given on two lines one for each side of the site of reversal. Additional lines are provided for the branched tubules (2B 3B and 14B)

TABLE 6
The modulations in complete tubules

Code number of tubule	Ave age number of modulations per cm of tubular length	Average number of segment per modulation
1	12	30
2+2B	15	21
3+3B	08	31
4	09	16
5	09	15
6	08	3.3
7	07	18
8	09	24
9	06	22
10	05	22
11	07	37
12	14	69
13	13	78
14+14B	07	27
15	06	22
16	03	19
17	04	28
18	07	30
19	06	28
20	05	25
Average	07	30

series of the various types of segments arranged consecutively (Von Ebner 1871 Regaud 01) The present work confirmed the existence of such typical waves with their 14 segments following the laws of

continuity and descent of the segmental order as illustrated in figure 7 However most waves were complicated by the presence of modulations (fig 9) Further more contrary to Regaud's views (01) the length of the segments was variable (table 1) and was not proportional to the duration of the stages of the cycle Thus in figure 7 segment VI has a length equal to about 2% of the wave while the duration of the corresponding stage VI calculated from the last column of table 7 is 9.2% of the cycle Finally when maps of tubules such as those in figures 11 and 12 were prepared no indication whatever was found of the spiral arrangement of the wave assumed by Regaud (01) Incidentally the corkscrew pattern of the tails of maturing spermatids (fig 1) one of Regaud's arguments for the spiral wave was found not to be associated with a spiral distribution of the cells Rather the tail twist appeared to be due to an intrinsic property of the tails themselves

In lieu of the typical waves postulated by the classics series of segments were found to be frequently interrupted by modulations The modulations consisted of segment(s) following the law of continuity but not that of the steady descent

TABLE 7
Length of segments within and outside modulations as measured in serial sections

Segmental number	Segmental length			Duration of corresponding stage (from Clermont et al. 59)
	Outside modulations ¹	Within modulation ²	P <	
	mm	mm		hours
I	25	12	0.001	34.8
II	11	09	0.2	23.3
III	03	03	0.5	6.0
IV	06	08	0.2	13.0
V	08	08	0.8	14.7
VI	13	13	0.8	26.5
VII	40	12	0.001	62.8
VIII	11	10	0.4	21.3
IX	05	06	0.3	7.1
X	04	04	0.5	7.1
XI	05	06	0.4	7.1
XII	21	13	0.01	32.3
XIII	06	09	0.2	17.6
XIV	07	08	0.7	14.1

Not corrected for obliquity of the tubules (as done in table 5) so that figures tend to be slightly smaller than the mean lengths measured in longitudinally cut tubules (table 1)

The segments measured were selected in such a way that they were separated from those showing ascent of the segmental order by as many segments as were ascending A total of 126-179 of each one of the 14 types of segments were measured

The segments measured were only those showing ascent of the segmental order 20-40 segments of each type were examined

TABLE 5

Length of waves (cm) seen in complete tubules¹

Code number of tubule	Rete				Reversal				Average wave length per tubule
	A	B	C	D	d	c	b	a	
1	18	23					22	19	
	14	16	22				23	20	19
2	11	17	18	24		25	32	23	
	10	18	32			26	24	19	22
2B							31	16	
	19	22	23			21	19	21	
3	27	31	18			21	29	14	
	14	27					21	24	25
3B		45	26				36	29	
	15	17	29	38		37	10	22	
4	17	23	24				34	44	
	14	18	23	20		16	27	23	26
5	07	09	19	35		25	23	26	
	19	35	31	30		24	33	27	24
6	12	11	21	31		55	16	21	
	17	37	16	20		22	28	30	24
7	12	22	30	12	23	32	23	32	
	15	29	33			27	20	20	23
8	16	25	22				59	36	
	22	23	24	36		40	33	23	30
9	28	28	47				35	24	
	21	33	59				46	40	36
10	10	15	30	31		41	43	28	
	25	21	26			33	32	36	28
11	24	19	38				45	27	
	14	15	21	18	35	39	36	42	29
12	43	30					45	28	
	15	22					60	12	32
13	13	19					45	35	
	16	15						31	25
14	10	15	31				34	36	
14B	07	16	33			32	25	28	26
	09	11	22	49	58				
15	16	17	18	34	42	42	35	36	
	13	34	39			35	42	49	32
16	08	24					35	54	
	17	24	29				25	32	27
17	12	23	31				25	33	
	11	28					34	50	27
18	20	18	37				24	26	
	09	17	26			35	17	30	24
19	22	28	36			28	21	26	
	11	23	21				20	26	24
20	12	25	29				40	25	
	08	10					31	38	24
Average wave length	15	22	28	29	40	31	31	29	Average length of all waves 26

¹ The data for each tubule are given on two lines one for each side of the site of reversal. Additional lines are provided for the branched tubules (2B 3B and 14B).

TABLE 6
The modulations in complete tubules

Code number of tubule	Average number of modulations per cm of tubular length	Average number of segments per modulation
1	1.2	3.0
2+2B	1.5	2.1
3+3B	0.8	3.1
4	0.9	1.6
5	0.9	1.5
6	0.8	3.3
7	0.7	1.8
8	0.9	2.4
9	0.6	2.2
10	0.5	2.2
11	0.7	3.7
12	1.4	6.9
13	1.3	7.8
14+14B	0.7	2.7
15	0.6	2.2
16	0.3	1.9
17	0.4	2.8
18	0.7	3.0
19	0.6	2.8
20	0.5	2.5
Average	0.7	3.0

continuity and descent of the segmental order as illustrated in figure 7. However most waves were complicated by the presence of modulations (fig. 9). Further more contrary to Regaud's views (01) the length of the segments was variable (table 1) and was not proportional to the duration of the stages of the cycle. Thus in figure 7 segment VI has a length equal to about 2% of the wave while the duration of the corresponding stage VI calculated from the last column of table 7 is 9.2% of the cycle. Finally when maps of tubules such as those in figures 11 and 12 were prepared no indication whatever was found of the spiral arrangement of the wave assumed by Regaud (01). Incidentally the corkscrew pattern of the tails of maturing spermatids (fig. 1) one of Regaud's arguments for the spiral wave was found not to be associated with a spiral distribution of the cells. Rather the tail twist appeared to be due to an intrinsic property of the tails themselves.

In lieu of the typical waves postulated by the classics series of segments were found to be frequently interrupted by modulations. The modulations consisted of segment(s) following the law of continuity but not that of the steady descent

TABLE 7
Length of segments within and outside modulations as measured in serial sections

Segmental number	Segmental length		P <	Duration of corresponding stage (from Clermont et al., 59)
	Outside modulations ¹	Within modulation		
I	2.5	1.2	0.001	34.8
II	1.1	0.9	0.2	23.3
III	0.3	0.3	0.5	6.0
IV	0.6	0.8	0.2	13.0
V	0.8	0.8	0.8	14.7
VI	1.3	1.3	0.8	26.5
VII	4.0	1.2	0.001	62.8
VIII	1.1	1.0	0.4	21.3
IX	0.5	0.6	0.3	7.1
X	0.4	0.4	0.5	7.1
XI	0.5	0.6	0.4	7.1
XII	2.1	1.3	0.01	32.3
XIII	0.6	0.9	0.2	17.6
XIV	0.7	0.8	0.7	14.1

¹ Not corrected for obliquity of the tubules (as done in table 5) so that figures tend to be slightly smaller than the mean lengths measured in longitudinally cut tubules (table 1).

The segments measured were selected in such a way that they were separated from those showing ascent of the segmental order by as many segments as were ascending. A total of 126-179 of each one of the 14 types of segments were measured.

² The segments measured were only those showing ascent of the segmental order 20-40 segments of each type were examined.

of the segmental order as illustrated in figure 9. To allow for the presence of frequent modulations (table 6) the wave was redefined above as "a series of adjacent segments which includes the 14 possible types in addition to the segments which may be involved in modulations." Using this operational definition it could be shown that the waves display extensive variations in length (table 5) and number per tubule (table 4). Eighty per cent of them contained modulations.

The variability in the features of the wave and the presence of modulations made it unlikely that the wave is triggered by an impulse progressing along the tubule as had been suggested by Regaud (01). In fact it seems unsafe to give the wave any dynamic connotation. We are rather inclined to return to Von Ebner's (1871) original view that the wave is a series of segments seen at a given instant of time.

Was there then any element of truth in Regaud's dictum that "the wave is in space what the cycle is in time?" A systematic comparison of wave and cycle was made and summarized in table 8. This led to the conclusion that the parallel drawn by Regaud between wave and cycle was only superficial: the wave is *not* in space what the cycle is in time.

Evolution of the segments in time

The changes in the segments with time might occur in various ways. The first possibility again arises from Regaud's theory of the wave (01). According to this theory the cells of any generation in a segment would be at more and more advanced steps of development from the distal to the proximal end. There they would transform into those of the segment with the next higher number (fig. 15A compare zero and three hours) so that the segmental boundary would migrate in a distal direction and all segmental boundaries would do so at the same constant speed (fig. 15A). However, this theory of the evolution of the segments with time is based on Regaud's erroneous premises. Indeed it has no support in fact and it is hoped that its influence on three generations of histologists will soon end.

The opposite possibility is that the segments—or subsegments when any—are homogeneous that is the cells of any given generation found along their length would all be at exactly the same step of development. They would eventually reach a stage when the whole length of the segment—or subsegment—suddenly changes to the next higher segment or subsegment. The time elapsing before this transformation occurs would depend

TABLE 8
Comparison between the cycle and wave of the seminiferous epithelium

Cycle	Wave
Similarities	
Cycle consists of 14 stages succeeding one another in time in any one area of the seminiferous tubule	Wave consists of at least 14 segments following one another in space along the length of the seminiferous tubule
Each stage is characterized by the presence of one of 14 cellular associations	Each segment is characterized by the presence of one of 14 cellular associations
Differences	
Duration of stages is constant (e.g. stage VIII lasts 21 hours)	Length of segments is variable (e.g. segment VIII varies from 0.2 to 6.2 mm)
Transition between stages is gradual	Boundaries of segments are sharp
Sequence of stages is irreversible	Series of segments may be altered by modulation
Duration of cycle is constant that is 12 ± 0.2 days	Length of wave is variable the extremes being 0.7 and 6.0 cm

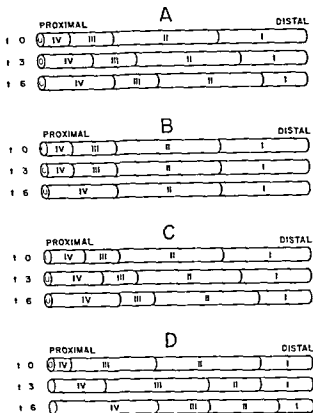


Fig 15 Diagrams of seminiferous tubules illustrating three theories on the evolution of the segments with time Regaud's theory (A) "Homogeneous segment" theory (B) "Unit segment" theory (C and D) For each theory three time intervals are represented $t = \text{zero}$, $t = 3$ and $t = 6$ indicating the time in hours The understanding of the diagrams is facilitated if it is recalled that stages II and III of the cycle last 23.3 and 6.0 hours respectively (see last column of table 7)

A Regaud's theory According to Regaud the length of the segments would be proportional to the duration of the corresponding stages of the cycle Within any segment e.g. segment III at time zero the stage of evolution of the cells would progress from the distal to the proximal end At this end cells would reach the next stage thus becoming part of the next segment (IV) Thus the segmental boundary would show a continuous migration in a distal direction (see $t = 3$ and $t = 6$) (According to Regaud the segmental boundaries do not extend straight across the tubule as indicated in the diagram but follow a spiral course—a feature omitted here for simplicity's sake)

B Homogeneous segment" theory If it is assumed that the segments of the B diagram make their appearance at time $t = \text{zero}$ this theory implies that the whole segment II suddenly changes to III after 23.3 hours and the whole segment III changes to IV after 6.0 hours Hence the diagram at $t = 3$ hours shows no change at all and at $t = 6$ hours a change only in segment III which becomes IV Note that the continuity of the segmental order is interrupted at this time

C and D "Unit segment" theory The postulated unit-segments (which are limited by dotted lines on the diagram) would be homogeneous and transform into the next unit segment at one stroke This is shown in diagram C which makes use of the same pattern of segment arrangement as at time $t = \text{zero}$ in diagram A and in diagram D which is less regularly arranged in keeping with usual observations Note the change in the size of segments II and III with time in diagram D

on the duration of the corresponding stage of the cycle. Thus since stage III lasts only 6 hours (Clermont et al. 59) segment III should stay only for that amount of time whereas since stage II lasts about 4 times as long as stage III segment II should persist for a correspondingly long time. A glance at the B diagrams makes it clear that short segments would often disappear (no segment III at 6 hours in fig 15B) and therefore continuity of the segmental order would not exist. Furthermore segment III would give rise to a segment IV in continuity with a previously existing segment IV (fig 15B 6 hours). The final segment IV would therefore not be homogeneous as far as the age of the cells is concerned—a fact contradicting the assumption made initially. Briefly the "homogeneous segment" hypothesis is incompatible with the observed facts.

A third hypothesis is that the segments—and perhaps the subsegments too—are composed of a series of small portions of seminiferous epithelium referred to as unit segments which alone are homogeneous (figs 15C and D). Sudden changes would be limited to unit segments. Thus in figure 15C one of the two unit segments postulated to exist in segment III has become part of segment IV by three hours and the other by 6 hours. As for segmental borderlines they would tend to migrate in distal direction as in Regaud's hypothesis but they would do so by jumping across unit segments either one at a time (compare zero three and 6 hours in diagram C) or far more often in an irregular fashion (diagram D) particularly so in modulations. The presence of unit segments would lead to changes in the size of the segments with time (compare segment III at zero three and 6 hours in diagram D). This hypothesis is compatible with the continuity of the segmental order (maintained in diagrams C and D) and will be tentatively adopted.

Since unit segments are homogeneous a reasoning similar to that presented above for the "homogeneous segment theory" leads to the conclusion that continuity may be lacking at the unit segment level. In this regard it may be recalled that the small subsegments observed

in this work often showed a lack of continuity. Thus at the top of figure 18 continuity would require the presence of a subsegment XIVa between XIII and XIVb (see also fig 12).

Now if unit segments really exist their size might well be that of the smallest subsegments observed which were shown above to have a surface area averaging $2035 \mu^2$.

It will be recalled that spermatogenesis is initiated at stage IX of the cycle when type A spermatogonia divide (cell A in column IX of fig 2). Unpublished observations indicated that in the rat as in the monkey (Clermont and Leblond 59) the spermatogonia about to divide are arranged in pairs along the wall of the seminiferous tubule. Two-dimensional maps of segment VII were then made on which several hundred type A spermatogonia were recorded. Measurements of the map surfaces indicated that one of these cells is present per $1090 \mu^2$ on the average. Hence the space occupied by a pair of type A cells— $2180 \mu^2$ —was quite similar to the presumptive size of a unit segment $2035 \mu^2$. It was therefore concluded that the territory occupied by a

Within modulations segmental boundaries may migrate in opposite directions. Hence the number of segments in a modulation may change with time. Indeed the modulation may disappear at times. Let us for instance consider a modulation made up of the underlined sequence in the series of segments XIII XII XI X IX X XI X IX VIII. After 21.3 hours (a time equal to the sum of the durations of the stages IX X and XI of the cycle but shorter than the duration of stage XII which is 32.3 hours) all the segments in and next to the modulation will be replaced by segment XII. No modulation would then be detectable. (The modulation would however reappear later.) Similarly since stages I and VII like stage XII have a rather long duration (last column table 7) segments I and VII are also likely to hide modulations.

A direct corollary of this is that the length of any segment I VII and XII may correspond to the sum of the lengths of a series of shorter segments involved in a potential but hidden modulation. This would explain why segments I VII and XII appeared to be long when measured outside modulations but relatively short within modulations (table 7).

The conclusion that there must be a number of modulations which are not visible at the time the animal is killed implies that the so-called modulation free waves may contain hidden modulations. Hence the figure of 20% modulation free waves given in the results is probably too high.

pair of type A spermatogonia corresponds to a unit segment. Presumably each one of the unit segments making up the wave consists of a pair of type A stem cells and their progeny.

Theories on the origin of the wave pattern

Formation of the wave with its characteristic continuity and descent of the segmental order may be explained by two kinds of hypotheses which although largely speculative may help in guiding future experimental work. (1) The wave pattern would be set once and for all during early development that is in fetal life or soon after birth (*embryological theory*). (2) The wave pattern would appear later in life and be maintained as a result of interactions between neighboring cells (*coordination theory*). From the outset it should be made clear that the wave pattern becomes established long before puberty (which occurs at about 45 days in the male rat). While at birth the seminiferous tubules have a uniform content of gonocytes and supporting cells (Clermont and Perey '57) the 12 day old rats showed spermatogonia and spermatocytes arranged into a wave in which modulations may already exist (Clermont and Huckins unpublished). Hence the visible pattern must be set during the first 12 days of life.

The embryological theory Clermont and Perey ('57) examined young rats soon after birth and found that in limited areas groups of type A cells arose from gonocyte mitoses. From these cells spermatogenesis started. The present hypothesis is that each early pair of type A cells constituted the oldest unit segment of a future wave. Then distally a new pair of type A cells would appear and build up the next unit segment and so on. Thus younger and younger unit segments would be added until the distance between any two of the oldest unit segments is covered by a full wave.

Modulations might arise just as the wave is formed or be induced later on in development by factors precipitating or delaying the differentiation of type A stem spermatogonia. It would seem that if modulations are set at the same time as the wave is the segments making up modulations need not differ in size from other seg-

ments. If however modulations were to arise from factors inducing a local change in an established wave (while maintaining continuity of the segmental order) the segments of the modulation would tend to be smaller than the others. The data (table 7) showed no difference between segments within and outside modulation (except for three segments for reasons explained in footnote 1 on p. 26) a finding in favor of the modulations being set at the same time as the wave is formed.

It remains to be seen whether the embryological theory alone can account for the maintenance of the continuity of the segmental order throughout life even in areas with modulations and at the site of reversal. Hence the next theory.

The coordination theory Liver cells are known to release to the circulation substances inhibiting their own proliferation (Such and Florian '58). Many other cell types also secrete inhibitory and/or stimulatory substances which enter the circulation and influence the corresponding cell population (Weiss '53). If such substances arise in the testis they are likely to be more concentrated within than outside the seminiferous tubules and perhaps they may diffuse predominantly in a given direction for instance by being carried in the luminal fluid which is known to flow towards the rete (Oslund '26, Toothill and Young '31). Hence inhibitory and/or stimulatory substances that may exist in the seminiferous tubules are likely to influence restricted groups of cells rather than whole populations.

Which cell type could be involved in the control of the seminiferous epithelium? Spermatocytes and spermatids may be rare or absent at times when the wave exists for instance in the 12-day old rat (Clermont and Huckins unpublished) and in the seminiferous epithelium undergoing regeneration after irradiation (Oakberg '55). Spermatogonia on the other hand are present. These cells are therefore likely to play a key role (although participation of Sertoli or interstitial cells may not be discounted).

Let us now assume that the released substances diffusing towards the rete inhibit only younger and/or stimulate only older spermatogonia. Such substances would favor the development of older cells on

their proximal side. Hence the randomness that might exist in the arrangement of the epithelium would be replaced gradually by a descent of the segmental order (Modulations would be in areas in which the rearrangement has not been completed).

The two theories proposed above may actually have to be combined to give a satisfactory account of the wave. Thus the pattern might be initiated as suggested by the embryological theory but maintained later by inhibitory and/or stimulatory substances as suggested by the coordination theory.

SUMMARY

The histology of the seminiferous epithelium along the length of the seminiferous tubules of the rat was examined using two methods. Longitudinal sections were made of dissected portions of seminiferous tubules obtained from the testis of 5 animals and serial cross sections of a whole testis were prepared and tubules reconstructed from them. All sections were stained with periodic acid Schiff and counterstained with hematoxylin.

The epithelium from any one area of seminiferous tubules is composed of several cell generations each one of which is at about the same stage of development. Such areas of epithelium extend over a variable length of the tubule and are referred to as *segments*. Assuming that the cycle of the seminiferous epithelium includes 14 stages which succeed one another in time in any given area, examination of tubules along their length at one given time might show 14 types of segments. These were indeed found. They were identified by Roman numerals (I–XIV) the segments with higher numbers being at a more advanced stage of development.

A segment is always adjacent to segments with the next higher or the next lower number (with the only exception of segments XIV and I which usually are located next to each other). The presence of consecutive numbers in adjacent segments is referred to as the *continuity of the segmental order*.

If a tubule is examined from the rete testis in a distal direction each segment

is usually followed by one whose epithelium is at a less advanced stage of development (i.e. with a lower number). In other words the numbering of the segments usually decreases from the rete testis on. This feature is called the *descent of the segmental order*.

Most tubules have an overall arch shape with both ends opening into the rete testis. The segmental order is descending from the rete testis along each branch of the tubule as far as a meeting point called the site of reversal. This site is located at approximately equal distance from the junction of each tubular end to the rete testis.

The segmental order always shows continuity with an overall descending pattern. In places one or more segments have ascending numbers although after a short distance the prevalent descending order is resumed. Such irregularities are called *modulations of the segmental order*. The number of segments per modulation varies from 1–7 or more with an average of three.

The segments found along the tubule may be arranged into distinct series called *waves of the seminiferous epithelium*. The wave is defined as a series of adjacent segments which includes the 14 possible types in addition to any segment which is involved in modulation. On the average the tubules contained 12 waves which measure 2.6 cm each (with a range of 0.7 to 6 cm). Statistical data show that the wave closest to the rete is shorter than the next one while these first two are shorter than all other waves. Twenty per cent of the waves have no modulation while 17% have more than three.

Segmental boundaries are sharply demarcated but are not arranged according to a spiral or any other regular pattern. Interpretation based on the size and arrangement of the segments is that they are composed of small *unit segments* which themselves consist of a pair of type A spermatogonia and/or their progeny. Within each unit segment cells develop synchronously but cells of neighboring unit segments are at a slightly more or slightly less advanced step of development although differences between the

unit segments are usually too slight for reliable identification

The arrangement of the unit segments into segments and of the segments into waves is probably determined embryologically although coordinating factors may play a role in maintaining the continuity and descent of the segmental order throughout life

ACKNOWLEDGMENT

This work was supported by a grant from The Population Council Inc. The technical assistance of Mrs M. Troitsky is acknowledged

LITERATURE CITED

- Benda C 1887 Untersuchungen über den Bau des funktionierenden Samenkanälchens einiger Säugetiere und Folgerungen für die Spermatogenese dieser Wirbelthierklasse Arch Mikr Anat 30 49
- Beylot E M and A Baudrimont 1926 Cahier de travaux pratiques d'histologie Vigot Freres ed Paris
- Clermont Y 1958 Contractile elements in the limiting membrane of the seminiferous tubule of the rat Exp Cell Res 15 438-440
- Clermont Y and C Huckins 1961 Microscopic anatomy of the sex cords and seminiferous tubules in growing and adult male albino rats Am J Anat 108 79-98
- Clermont Y and C P Leblond 1959 Differentiation and renewal of spermatogonia in the monkey *Macacus rhesus* Ibid 104 237-274
- Clermont Y C P Leblond and B Messier 1959 Durée du cycle de l'épithélium séminal du rat Arch Anat Micro Morph Exp 48 37-56
- Clermont Y and B Perey 1957 Quantitative study of the cell population of the seminiferous tubules in immature rats Am J Anat 100 241-267
- Clermont Y and B Perey 1957 The stages of the cycle of the seminiferous epithelium of the rat: practical definitions in PAS, hematoxylin and hematoxylin-eosin stained sections Rev Canad Biol 16 451-462
- Curtis G M 1918 The morphology of the mammalian seminiferous tubule Am J Anat 24 339-394
- Ebner V von 1871 Untersuchungen über den Bau der Samenkanälchen und die Entwicklung der Spermatozoen bei den Säugetieren und beim Menschen Rollets Untersuchungen aus dem Institut f. Phys u. Histol. in Graz s. 200 Separat Leipzig
- 1888 Zur Spermatogenese bei den Säugetieren Arch Mikr Anat Entwickl 31 236-292
- 1902 Die Geschlechtsorgane in A. Kollikers Handbuch der Gewebelehre des Menschen 6. Auflage 3. Band Leipzig
- Furst C 1887 Ueber die Entwicklung der Samenkorperchen bei den Beuteltieren Arch Mikr Anat 30 336
- Leblond C P and Y Clermont 1952a Spermatogenesis in rat, mouse, hamster and guinea pig as revealed by the periodic acid fuchsin-sulfurous acid technique Am J Anat 90 167-215
- Leblond C P and Y Clermont 1952b Definition of the stages of the cycle of the seminiferous epithelium in the rat Ann N Y Acad Sci 55 548-573
- Oakberg E F 1955 Degeneration of spermatogonia of the mouse following exposure to x-rays and stages in the mitotic cycle at which cell death occurs J Morphol 97 39-54
- Oslind R M 1926 Ligation of vasa efferentia in rats Am J Physiol 77 83-90
- Regaud C 1900 Direction helicoidale du mouvement spermatogénétique dans les tubes séminifères du rat C R Soc Biol 52 1042-1044
- 1901 Étude sur la structure des tubes séminifères et sur la spermatogénèse chez les mammifères Arch Anat Micro 4 101-156 231-380
- 1909 Études sur la structure des tubes séminifères et sur la spermatogénèse chez les mammifères Arch Anat Micro 11 291-431
- Roosen Runge E C and L O Giesel 1950 Quantitative studies on spermatogenesis in the albino rat Am J Anat 87 1-30
- Stich H F and M L Florian 1958 The presence of a mitosis inhibitor in the serum and liver of adult rats Canad J Biochem Physiol 36 855-859
- Tobias P V 1956 Chromosomes Sex-cells and Evolution in a Mammal Percy Lund Humphries & Co Ltd London
- Toothill M C and W C Young 1931 The time consumed by spermatozoa in passing through the ductus epididymidis of the guinea pig as determined by means of India ink injections Anat Rec 50 95-107
- Weiss P 1953 Some introductory remarks on the cellular basis of differentiation J Embryol Exp Morphol 1 part 3 181-211

PLATE 1

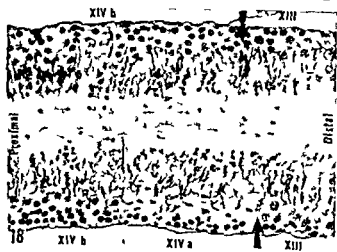
EXPLANATION OF FIGURES

Low power microphotographs ($\times 250$) of longitudinally cut tubules stained with the periodic acid Schiff hematoxylin technique

- 16 Portion of a segment VII. Note the common orientation of the tails of maturing spermatids toward the distal part of the tubule.
- 17 Portion of a segment VIII showing the junction of the subsegments VIIIA and b. At the top the junction is at about the middle of the picture (ascending arrow) whereas at the base the junction is at left (descending arrow). Hence proximally the picture shows the subsegment VIIIB the epithelium being free from spermatids while distally the picture shows the subsegment VIIIA with the epithelium containing maturing spermatids ready to be released from the seminiferous epithelium. Note that at the time of release the tails of the spermatids become oriented in a proximal direction.
- 18 Limit between segments XIV and XIII (thick arrows). In the segment XIV two subsegments could be recognized: subsegment XIVa with primary spermatocytes in division and subsegment XIVb showing secondary spermatocytes. The sharp limit between the two subsegments is indicated by a thin arrow.



16



18

Microscopic Anatomy of the Sex Cords and Seminiferous Tubules in Growing and Adult Male Albino Rats

Y CLERMONT AND CLAIRE HUCKINS

Department of Anatomy McGill University Montreal Canada

While it has long been known that the male sex cords of the embryonic gonad evolve into the seminiferous tubules of the adult testis (Allen 04 Felix 12) most of the work done in the past has been restricted to the early formation of the sex cords themselves and little attention has been given to the pattern of development of these cords into seminiferous tubules.

De Burlet and de Ruiter (20) working on embryonic mouse testis and Roosen Runge (57) working on embryonic rat testis reported that the sex cords appeared as a series of C shaped arches placed side by side in a way similar to the tracheal cartilaginous rings the plane of these arches being at right angles to the long axis of the organ. Some of the sex cords ran immediately below the tunica albuginea and were referred to as outer arches while others found in the core of the testis failed to reach the tunica albuginea and were referred to as inner arches. Analyses of the sex cords in other species (Bremer 11 Huber and Curtis 13 de Burlet 21 Gruenwald 34 Torrey 45) confirmed that they appeared as arches which either occurred singly or were anastomotically connected to form more complex structures. However the subsequent development of the sex cords into adult seminiferous tubules was not studied by these authors.

The reason why little effort was made to relate the sex cords of the embryo to the seminiferous tubules of the adult might simply be that very little was known about the morphology of the adult seminiferous tubules and particularly for the rat the literature yielded no information on the subject. The earliest attempts to describe adult mammalian seminiferous tubules made use of maceration and teasing

techniques (Sappey 1889). These methods however failed to preserve the integrity of complete tubules their *in situ* shape and the relationship of tubules to one another.

Curtis (18) was the first to apply the technique of reconstruction from serial sections to this problem. He described in an adult mouse testis two complete seminiferous tubules reconstructed in such a fashion. He observed that the tubules were highly convoluted that they followed within the testis a circular path which was perpendicular to the long axis of the organ and that they had a "basket like" shape. One of the tubules reconstructed was a simple arch with two openings into the rete testis the other branched along its course and thus had three openings into the rete. Hirota (52) by dissecting tubules from an adult mouse testis stated that all seminiferous tubules had at least two openings into the rete testis. Curtis (18) had also reported that in rabbit testes arched tubules were frequently linked together in tubule complexes and that branched tubules were common in this species. Later in 1934 Gruenwald reported similar findings in a number of species showing that the extent of linkage and of branching in the tubules was a species variable. Johnson (34) dissected human seminiferous tubules and found that most commonly they occurred as arches which were anastomotically connected. Only rarely did they appear as simple arches or as blind ending tubules.

Because of the length and extensive coiling of the adult tubules of the rat maceration and dissection could not provide fruitful information. Therefore it was felt that reconstruction of tubules from serial sections was an adequate method to yield

since in the embryos and at birth the stages of the cycle of the seminiferous epithelium were not identifiable only the position of the sex cord could be used to trace it through the serial sections. As before the code number of each cord was recorded on the corresponding photographic image.

Having completed the analysis of the sex cords and seminiferous tubules on photographs it was then possible to determine their length the course which they followed within the testis and their position relative to one another.

The lengths of sex cords were measured in several ways. In a few instances where the simple arched sex cords of the embryo outer testis ran parallel to the plane of cut so that the entire arch appeared on one section it was possible to run a map measure over the photographed section of the arch. From this measurement and knowing the magnification of the section the length of the cord was easily calculated. In most cases however it was necessary to reconstruct sex cords as plane figures on graph paper or as three dimensional models on sheets of acrylic plastic in order to determine their length and other morphological characteristics such as the direction of the limbs of the sex cord the course of the cords within the testis and the relationship of cords to one another.

RESULTS

17 day embryo

The 17-day embryonic testis appeared as an elongated and slightly crescentic organ running along the medial aspect of the mesonephros. Cross-sections of the testis showed each sex cord to be a simple arch. Some of them—the outer cords—followed an elliptical pathway immediately beneath the tunica albuginea (figs 1-3 O). Their two extremities were connected with an anastomotic series of delicate tubules the rete testis which they reached on its lateral aspects. Other sex cords—the inner cords—formed smaller arches located inside the outer ones and did not touch the tunica albuginea (figs 1-3 In). These smaller arches also had two extremities opening into the rete testis these connections being seen side by side on the internal aspect of the rete testis.

All these arched sex cords were distributed side by side along the length of the testis their plane of orientation being more or less perpendicular to the cranio-caudal axis of the organ (fig 10A). In the completely reconstructed testis at this age 21 sex cords were outer and 10 were inner. Furthermore of these 31 sex cords all had two openings into the rete testis except for 4 which branched along their course and therefore had three openings into the rete testis (table 1). The average length of the sex cords was 1.09 mm with outer cords having a greater length than inner ones (table 2).

19 day embryo

At 19 days of embryonic life the testis had become nearly spherical. Each sex cord persisted basically as a simple arch but showed some waviness and in places was twisted and folded upon itself (fig 6 O). Here again outer and inner sex cords could be distinguished (fig 4-6 O In).

The sex cords remained consecutive to one another but their initial parallel orientation was modified as a result of the rounding up of the testis into a sphere. Thus the sex cords now fanned out from the rete testis from the cranial to caudal pole (fig 10B). While the outer sex cords were closely packed together immediately beneath the tunica albuginea the inner sex cords were separated by some loose connective tissue (fig 4 L). The 4 testes reconstructed at this age contained 23, 25, 26 and 28 sex cords respectively. In three of these testes several branched cords were found (table 1). The sex cords had nearly doubled their length between 17 and 19 days when they averaged 1.79 mm again the inner cords were shorter than the outer ones (table 2).

Newborn animals

The newborn testis was an almost perfect sphere the long axis of which was only slightly greater than the diameter. Although the sex cords maintained their circular pathway around the testis they appeared strikingly different at that time. Each cord folded upon itself to give an average of 90 tiny convolutions (fig 9 O In) and therefore zigzagged back and

TABLE 1
Number of various types of sex cords

Age	Total number of tubules present	Types		Number of branched tubules
		Outer	Inner	
17 Day embryo	31	21	10	4
19 Day embryo	28	20	8	3
19 Day embryo	23	17	6	3
19 Day embryo	20	18	7	2
19 Day embryo	26	16	10	0
Newborn	20	17	3	3
Newborn	22	16	6	5

TABLE 2
Length of the unbranched sex cords

Age	Outer tubules		Inner tubules		Average length of all measured tubules \pm S.E.
	Number of tubules measured	Average length \pm S.E.	Number of tubules measured	Average length \pm S.E.	
		mm		mm	mm
17 Day embryo	13	1.19 ± 0.25	4	0.78 ± 0.16	1.09 ± 0.29
19 Day embryo	12	2.00 ± 0.25	8	1.47 ± 0.31	1.79 ± 0.38
Newborn	14	8.33 ± 1.62	5	5.92 ± 1.46	7.70 ± 1.88
12 Day	1	126.00			

Fig 1 Low power photograph of a section from a 17 day embryonic testis. The plane of section is perpendicular to the cranio-caudal axis of the organ and is almost parallel to the arches of the sex cords. On the lower part of the photograph the sex cords connect with the rete testis. A cross section of the mesonephric duct (MD) is seen at the right. PAS hematoxylin $\times 120$. Compare with figures 2 and 3.

Fig 2 An outline drawing of two complete sex cords from figure 1 showing an outer (O) and an inner (In) sex cord.

Fig 3 A diagrammatic three dimensional drawing of the outer (O) and inner (In) sex cords seen in figures 1 and 2. These cords appear as smooth arches with two connections to the rete testis.

Fig 4 Low power photograph of a section from a 19-day embryonic testis in which the plane of section is perpendicular to the long axis of the organ. Sex cords are cut obliquely or transversely and are therefore represented by numerous cross sections. In the central portion of the section an extensive area of loose connective tissue (L) is seen in the central part of the testis. PAS hematoxylin $\times 60$.

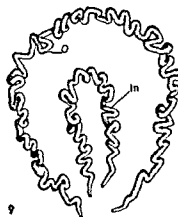
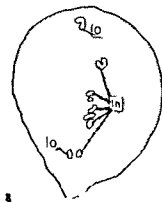
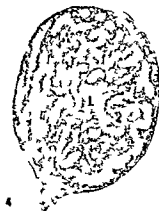
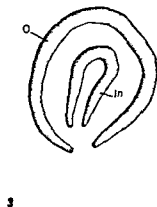
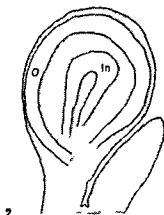
Fig 5 An outline drawing of figure 4 to show the position of an outer (O) and an inner (In) sex cord.

Fig 6 A diagrammatic three-dimensional drawing of an outer (O) and an inner (In) sex cord similar to those seen in figures 4 and 5. These arched sex cords show some folding upon themselves.

Fig 7 Low power photograph of a section from a newborn rat testis. Here the plane of section is more or less parallel to the long axis of the organ. Sex cords are cut obliquely or transversely and are therefore represented by numerous cross sections. In the central portion of the section an extensive area of loose connective tissue may be seen (L). The rete testis is at the base of the photograph. PAS hematoxylin $\times 60$.

Fig 8 An outline drawing of figure 7 to show the tubular sections belonging to an outer (O) and an inner (In) sex cord. Because the plane of section is perpendicular to the path of the sex cords they are seen only over a part of their course.

Fig 9 A diagrammatic three-dimensional drawing of an outer (O) and an inner (In) sex cord similar to those seen in figures 7 and 8. Note that the arched sex cords have been thrown into a number of tiny convolutions.



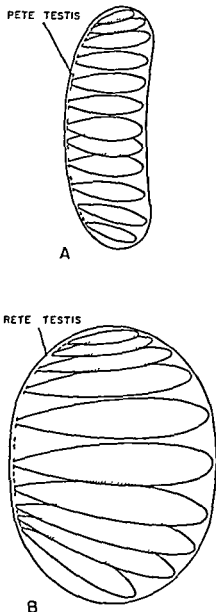


Fig 10 Two diagrammatic side views of a 17-day (A) and a 19-day (B) embryonic testis showing arches which represent the approximate distribution of outer sex cords. The broken line indicates the position of the rete testis. In diagram A the paths of the arched sex cords are more or less perpendicular to the long axis of the organ. In diagram B as the testis becomes more spherical the sex cords appear to fan out from the rete testis and are no longer perpendicular to the cranio-caudal axis of the organ.

forth in a more or less random direction although the general course of the limbs of the convolutions (i.e. the portion of the sex cord between the hairpin turns) tended to run toward the interior of the testis (fig 7).

The architecture of the organ consisted of outer and inner sex cords (figs 7-8). In distributed consecutively and fanning out from the rete testis in the manner described for the 19-day embryo (fig 10B). The outer sex cords became closely packed at the periphery of the testis with the convolutions of successive cords frequently interdigitating with one another. The inner sex cords were much less closely packed and were separated by an extensive amount of loose connective tissue (fig 7 L). Incidental inspection of older testes revealed that this remarkable feature persisted until 4 days after birth when the entire testis became filled with convolutions of tubules.

The two testes reconstructed in newborn rats had respectively 20 and 22 sex cords of which several were branched (table 1). There was a four fold lengthening of each sex cord between 19 embryonic days and birth; the outer cords remaining longer than the inner ones (table 2).

12 day rat

At 12 days the testis was elongated and ovoid and had grown to one fifth the size of the adult testis. Two "outer seminiferous tubules" (as the outer sex cords were called at this age) were reconstructed in an attempt to find a condition intermediate between that at birth and that in the adult. The tubule as a whole continued to follow a circular pathway around the testis but the limbs of the convoluted tubules underwent extensive elongation, some of these limbs being three or 4 times the length of others. When the course followed by an individual limb was examined in some detail it was found that the cranial end of each limb ran at first from the tunica albuginea toward the interior of the testis (fig 11) and then after a short distance the limb suddenly sloped caudally and gradually toward the cranio-caudal axis of the organ (fig 11). Thus most of the limbs of a tubule coursed back and forth in this fashion to give a tubule

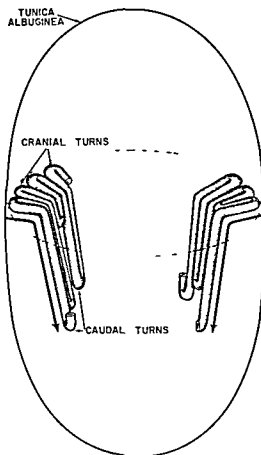


Fig 11 A diagrammatic representation of a few convolutions from an outer seminiferous tubule in a 12-day testis drawn from an oblique cranial view. A heavy continuous line represents the tunica albuginea and the outline of the testis while the broken line indicates the circular path followed by the tubule. The cranial hairpin turns of a tubule may be seen applied to the tunica albuginea. As indicated by the arrows the limbs of the convolutions run inward and caudally.

whose geometric pattern resembled a wide mouthed funnel with a broad rim around the mouth. The outer tubule measured had a length of 126 mm.

No "inner seminiferous tubule" was reconstructed in this animal.

Adult rat

All the seminiferous tubules reconstructed had a number of characteristics in common which we shall describe first as we consider a representative tubule (figs 12-13). Upon leaving the rete a

tubule usually ran caudally for a certain distance then after a hairpin turn it ran cranially. Thereafter the tubule kept on running back and forth caudally and cranially to form a large number of regular convolutions. The long limbs (i.e. the portions of tubules between the hairpin turns) of these elongated convolutions were more or less parallel to each other. This resulted in a fence or palisade like arrangement of the convolutions. Following the complete reconstruction of a tubule it soon became clear that its convolutions were distributed along a circular path within the testis and that its two extremities were connected with the rete testis (fig 13). It was finally noted that generally the cranial hairpin turns of the convolutions were closer to the tunica albuginea than were the caudal ones in such a manner that the circular palisade formed by the tubule was not straight or parallel to the axis of the testis but was sloped and at an angle with this axis (figs 12-13).

The completely reconstructed tubules assumed two main geometrical shapes: funnel and cone. The funnel shaped tubule showed the following pattern in serial sections. The tubular cross sections from the cranial end of the palisade were seen on the photographs to be close to or touching the tunica albuginea and were therefore "outer seminiferous tubules" (fig 14A). But in the more caudal sections of the testis the tubular cross sections were seen at a distance from the tunica albuginea and closer to the cranio-caudal axis of the testis (compare figs 14A, B and C) and finally those from the caudal end of the palisade were found even closer to the cranio-caudal axis of the testis but without reaching it (fig 14D). Thus the shape of the reconstructed tubule (fig 14E) could be likened to a funnel the wide part of which was orientated toward the cranial pole of the testis and usually touched the tunica albuginea.

In a cone shaped tubule the tubular cross sections from the cranial end of the palisade showed a typical circular path way in the serial photographs but these were at a distance from the tunica albuginea and were therefore "inner seminiferous tubules" (fig 15A). More cau

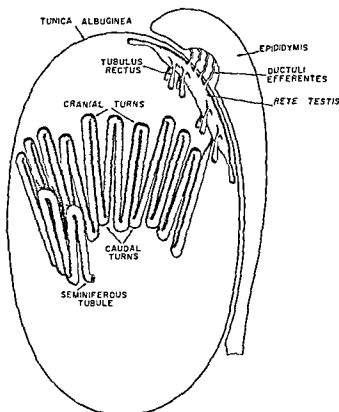


Fig 12 Diagrammatic representation of a portion of a seminiferous tubule from an adult rat testis and its connection to the excretory duct system. An outline of the testis seen from a lateral aspect is indicated by a continuous line which represents the tunica albuginea. Between the cranial and caudal hairpin turns of the convoluted tubule long limbs run more or less parallel to one another to give the tubule a palisade like appearance. The seminiferous tubule is connected to the rete testis by a short narrow tubulus rectus. The rete testis is an elongated sac applied to the inner surface of the tunica albuginea and connected to the ductus epididymis by 5 to 7 ductuli efferentes.

dally the cross sections of the limbs were seen closer to the cranio-caudal axis of the testis. Finally the tubular cross sections from the caudal end of the palisade appeared clustered together in the central portion of the testis (fig 15B). The geometrical shape of such a tubule was therefore a hollow cone with its base orientated toward the cranial extremity of the testis (fig 15C).

The distribution of the reconstructed tubules within the testis was represented diagrammatically in a longitudinal section along the axis of the organ (fig 16). In such a diagram the longitudinal sections of the tubules whether funnel (e.g. tubule 3) or cone (e.g. tubule 20) appeared as two more or less symmetrical zones on either

side of the midline. It was quite clear in the diagram that most of the funnel shaped tubules (tubules 3-12) were outer seminiferous tubules since they had cranial extremities which came close to or touched the tunica albuginea. As an exception tubule 8 had half of its tubular convolutions peripherally located (left) and the other half centrally located (right). All of these outer funnel shaped tubules were regularly inserted into each other. Although the cranially located tubules 1 and 2 were considered as outer tubules because of their contact with the tunica albuginea they did not assume the shape of funnels. Tubule 1 formed a solid structure around which the other tubules were concentrically arranged. Tubule 2 en-

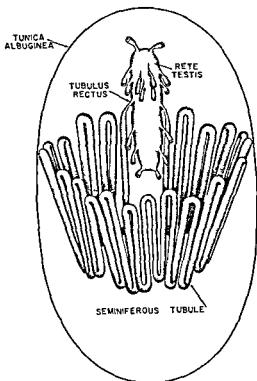


Fig. 13 Diagrammatic representation of a seminiferous tubule and its connection to the rete testis in a view looking into the testis from above and medially. The convoluted tubule is seen to follow a circular path within the testis and has two connections with the rete testis. The cranial portions of the palisade are closer to the tunica albuginea than are the caudal ones. Several tubuli recti are seen in the lateral and internal aspects of the rete testis.

circling tubule 1 had a narrow hollow cone-like shape. At the caudal extremity of the testis tubule 13 which was obviously an outer tubule had a wide shallow cup-like shape.

The cone shaped tubules (tubules 14-20 excluding 18) occupied the central portion of the testis and their cranial extremities were found at some distance from the tunica albuginea. These inner tubules were also regularly inserted into each other. Of these there was one (tubule 18) which assumed the shape of a funnel rather than that of a hollow cone.

Length of adult seminiferous tubules

An attempt was made to obtain values as accurate as possible for the tubular lengths. Since the number of sections traversed by a given limb of a tubule was known as well as the thickness of the section (5 μ) it was easy to obtain an initial estimate for the length of this limb.

An approximate value for the length of the whole tubule was then calculated by adding the lengths of all the limbs of this tubule. This measure did not include however the lengths of the short portions of tubules involved in hairpin turns which were cut longitudinally in the serial sections. Measurements on reconstructions of turns showed that approximately 500 μ per turn had to be added to the sum of the length of the limbs. The length of the tubule thus obtained was referred to as the crude tubular length (table 3).

This value would be a satisfactory approximation of the tubular length if the tubules were running parallel to the long axis of the testis and at right angles to the plane of sectioning. Reconstructions of complete tubules clearly indicated that this was not generally the case and that most of the tubules ran obliquely to the plane of sectioning. The angles made by the tubules and the axis of the testis were

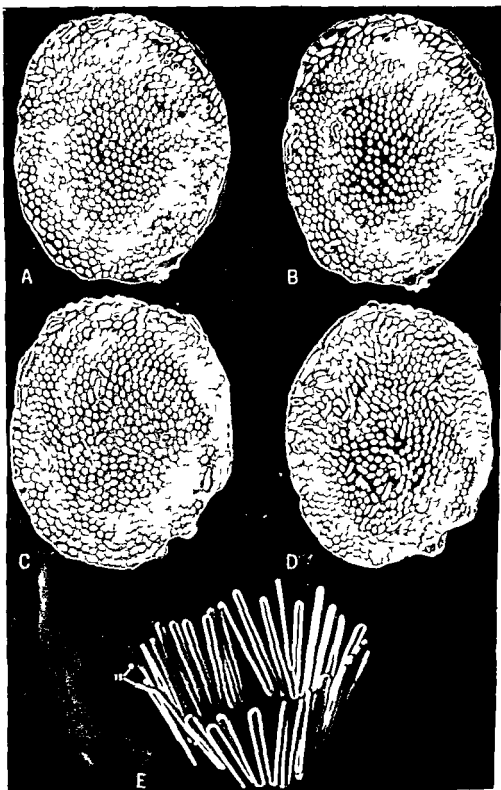


Figure 14

Fig 14 Pictures A B C and D are low power ($\times 16$) photographs of 4 transverse sections of adult rat testis taken at intervals of about 1.3 mm. Numerous tubular cross-sections are visible in the background and the rete testis is the space located along the lower border of photographs A and B. On each photograph the cross sections belonging to one tubule have been painted white. It is apparent from this that the tubule follows a circular pathway within the testis and that the cranial portions of the tubule (picture A) are near the tunica albuginea while the more caudal portions (pictures B C D) are progressively farther from the tunica albuginea.

Photograph E is of a tubule model reconstructed in plastic. The tubule was similar to the one seen in cross section in the preceding photographs. The position of the tubuli recti is indicated at (TR). The geometrical shape of this tubule is that of a funnel with its narrow part directed caudally.

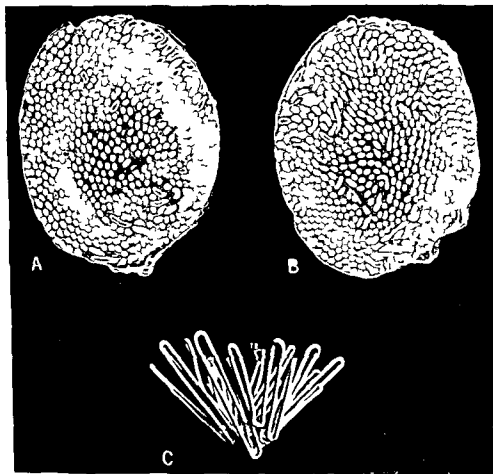


Fig 15 Pictures A and B are low power ($\times 16$) photographs of two transverse sections of adult rat testis taken at two levels 3 mm apart. The tubular cross sections painted in white belong to the same tubule. The cranial portions of the tubule (photograph A) follow a circular pathway around the testis but are at some distance from the tunica albuginea. At the more caudal level (photograph B) the caudal extremities of the tubuli are clustered together in the center of the testis. Photograph C is of a tubule model reconstructed in plastic and similar to the one seen in pictures A and B. The geometrical shape of this tubule is that of a hollow cone the apex of which is directed caudally. Tubuli recti are indicated (TR).

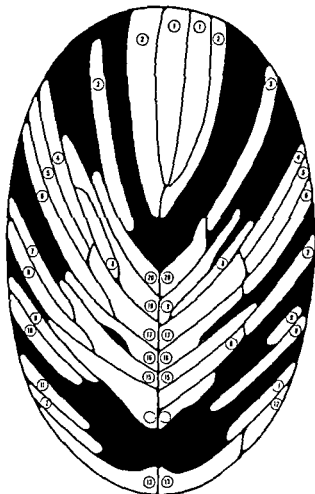


Fig 16 Diagrammatic representation of a longitudinal section along the axis of an adult testis showing the areas occupied by 20 reconstructed tubules. Each tubule appears as two zones (labeled with the tubule number) on either side of the midline. Outer tubules are indicated by white zones while inner ones are shown by pale gray zones. The black spaces around the labeled zones are occupied by tubules which were not reconstructed. The symmetrical distribution of the areas occupied by the tubules allows the funnels (which are mostly peripheral) or cones (which are mostly central) to insert into one another.

small at the cranial end of the organ but were progressively larger as the caudal extremity was approached (fig 16). Obviously the tubules running at an angle to the plane of section were longer than previously recorded and a correction had to be applied to the crude tubular length. Such a correcting factor could be determined if the angle made by the tubule and the perpendicular to the plane of section could be measured.

This information was obtained from the graphic representation of the tubules in a diagram of the testis cut longitudinally

(fig 17). Straight lines were run through the areas occupied by the tubule and the angles made by these lines and the perpendicular of the plane of section (a parallel to the long axis of the testis) were measured (α fig 17). A final tubular length (L) could be obtained by using the crude tubular length (l) and the secant of the angle according to the following formula $L = \sec \alpha \times l$ which is derived from $\sec \alpha = L/l$.

As can be seen in figure 17 the angles made by the tubule on both sides of the testis were generally different. To obtain

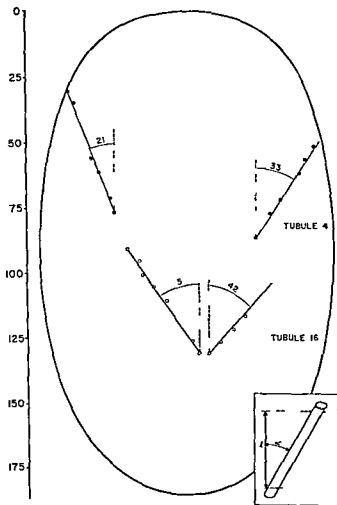


Fig 17 Diagram to illustrate the method used in correcting the crude tubular length. The numbers of the semiserial photographs are indicated on the right of the outline of a longitudinal section of the testis. The points correspond to the position of two tubules at various levels within the testis. The position of these points was determined as follows: the distances of the cross-sections of a given tubule from the tunica albuginea were measured on the photographs (Only those tubular cross-sections on a diameter of the section parallel to the rete testis were considered). Such distances were transposed to the diagrammatic outline of the longitudinal section of the testis as a series of points. It was possible to measure the angle (α) made by the straight line running through these points and a line parallel to the long axis of the organ (broken line). Note that the angles made by the tubules on either side of the testis differed. Knowing the crude tubular length (l) and angle it was possible to calculate the true tubular length (L) using the formula $L = \sec \alpha \cdot l$.

a better correction the tubules were divided approximately in halves (the so-called "site of reversal" served as a line of division see Perey Clermont and Le blond 61) and each tubular half was corrected by its corresponding factor. The

final tubular length (table 3 L) was the sum of these two corrected values. Obviously the above corrections did not take into account the local irregularities of the tubule such as a sudden waviness or a change of orientation of a given limb etc.

TABLE 3
Morphology and length of the seminiferous tubules of an adult rat

Tubule number	Morphological characteristics ¹	Number of ascending and descending limbs	Tubular length uncorrected (l)	Tubular length corrected (L)
			cm	cm
1	Solid cone unbranched one connection to R T	69	18.4	18.4
2	Hollow cone branched 3 connections to R T	168	46.5	46.5 ²
3	Funnel branched 3 connections to R T	203	50.0	54.7
4	Funnel unbranched 2 connections to R T	97	28.8	32.5
5	Funnel unbranched 2 connections to R T	124	32.3	38.0
6	Funnel unbranched 2 connections to R T	98	32.7	37.9
7	Funnel unbranched 2 connections to R T	94	29.8	34.3
8	Funnel unbranched 2 connections to R T	94	29.5	38.2
9	Funnel unbranched 2 connections to R T	86	25.6	38.0
10	Funnel unbranched 2 connections to R T	89	28.1	36.8
11	Funnel unbranched 2 connections to R T	104	28.4	39.6
12	Funnel, unbranched 2 connections to R T	86	17.7	25.7
13	Funnel unbranched 2 connections to R T	64	10.6	18.4
14	Hollow cone branched 3 connections to R T	115	25.8	45.4
15	Hollow cone unbranched 2 connections to R T	94	34.8	47.4
16	Hollow cone unbranched 2 connections to R T	74	22.7	29.8
17	Hollow cone unbranched 2 connections to R T	76	25.1	30.6
18	Hollow cone unbranched 2 connections to R T	83	24.9	29.6
19	Hollow cone unbranched 2 connections to R T	66	27.1	28.7
20	Hollow cone unbranched 2 connections to R T	58	21.8	23.9
Averages for unbranched tubules		85		32.2

¹ Location of tubules within the testis is given in figure 16

² The lengths for the various portions of the branched tubules 2 3 14 are given in figure 18

The values proposed here for each tubule were thus still considered as approximations (table 3). The average length of unbranched tubules was found to be 32.2 cm. The inner tubules had a tendency to be slightly shorter than the outer ones

(compare for example tubules 16-20 with tubules 4-11 in table 3) several tubules however did not follow this trend (tubules 1 12 13 15). The lengths of the various portions of the branched tubules were graphically represented in figure 18

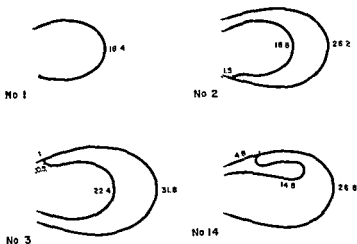


Fig 18 Diagrams showing the lengths in centimeters of the various parts of the three branched tubules (tubules 2 3 and 14) and the blind ending tubule (tubule 1) found in the adult testis. Each tubule and its branch were represented by single lines.

Correlation between the location of the tubules in the testis and of their respective openings into the rete testis

The rete testis of the rat formed an irregular flat cavernous sac (about 1 cm long and 0.2-0.3 cm wide) closely applied to the inner surface of the tunica albuginea (fig 12). On the side applied to the tunica albuginea the only tubular structures seen were the 5 to 7 ductuli efferentes which connected the rete testis to the ductus epididymis. Tubuli recti the short and narrow tubules which joined the seminiferous tubule proper with the rete testis opened either on the lateral edges of the rete testis or on its internal surface (fig 13).

A diagrammatic representation of the connections of the tubuli recti to the rete testis as seen from the interior of the testis is given in figure 19. This diagram revealed that the tubules located at the cranial extremity of the testis (e.g. 1 2 3) had their openings at the cranial extremity of the rete testis and likewise the tubules located caudally within the testis (e.g. 11 12 13) opened at the caudal tip of the rete. Furthermore the outer seminiferous tubules (e.g. 5-12) were usually connected to the rete testis on its lateral edges while the inner seminiferous tubules (e.g. 16 17 19 20) had their openings on the internal surface of the

rete although there were several exceptions to these rules (e.g. 18 at the top left). Finally the order in which the tubular openings appeared from the cranial to the caudal extremity of the rete corresponded grossly—although there were a few inversions—to the order in which the tubules were distributed within the testis (fig 19).

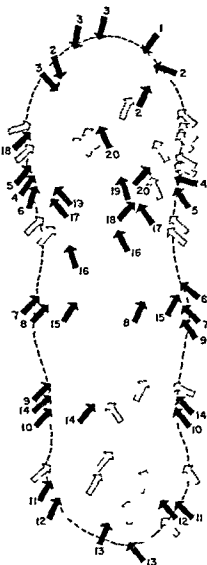
It was also found—and this is reflected in figure 19—that while most of the tubules had two openings into the rete testis tubule 1 had but one opening, and tubules 2 3 and 14 were branched tubules each having three connections with the rete testis. Tubule 1 was the only tubule to show a blind end. Examination of this terminal portion revealed that the ascending limb of the last convolution approached the rete but bypassed it and terminated cranially close to the tunica albuginea as a blind slightly distended pocket. The histology of this last limb was atypical: the seminiferous epithelium was composed of Sertoli cells, spermatogonia and a few spermatocytes, some of which were degenerating. The pocket-like extremity was filled with a dense mass of entangled spermatozoa (as if they had flowed toward the blind end to be trapped there). Such a structure observed here for the first time was considered as an anomaly.

DISCUSSION

The simple arch shape has been repeatedly described for mouse and rat sex cords (De Burllet and de Ruiter 20 Gruenwald 34 Roosen Runge 57) and the present investigation revealed that in the rat testis the full complement of such discrete and well formed C-shaped sex cords was present. Furthermore in rat embryos (figs 1-6) as in the mouse (De Burllet and de Ruiter 20) the sex cords formed two rows of consecutive arches, one internal to the other and referred to as inner and outer sex cords respectively.

It was of some interest to see if these basic morphological features were maintained throughout development and adulthood. From the present study it became apparent that despite an approximate 300-fold increase in tubule length from the 17th embryonic day to adulthood the basic plan of organization of the sex cords was maintained in the adult. Thus the growing sex cords generally preserved their smooth arch shape until birth when each cord folded upon itself to give a series of about 90 convolutions. Thereafter the number of convolutions no longer increased but the limbs located between the turns of the existing convolutions lengthened. The growth direction of the convolutions of the seminiferous tubules (as sex cords were called once spermatogenesis was initiated) was mostly inward and caudal so that these tubules progressively assumed the shape of slanted palisades. Consequently when taken as a whole each adult seminiferous tubule followed within the testis a circular or rather arch-shaped pathway which was approximately perpendicular to the cranio-caudal axis of the organ just as was the initial sex cord. Furthermore in the adult testis outer and inner tubules could be distinguished which were equivalent to outer and inner sex cords. Most of the outer tubules when considered as a whole assumed the geometrical shape of a funnel the mouth of which was cranially directed and which approached or touched the tunica albuginea. The inner tubules on the other hand occupied the central portion of the testis and had the geometrical shape of a hollow cone the mouth of the cone was also cranially directed.

Fig 19 Diagram showing the outline of the rete testis (broken line) and the connections of the seminiferous tubules (arrows) to the rete testis. The numbered black arrows belong to reconstructed tubules while the broken line arrows are those of tubules not reconstructed. In general outer tubules (1-13) were connected to the lateral aspects of the rete testis while inner tubules (14-20) were connected to the internal surface of the rete testis but there were a number of exceptions (e.g. tubules 8 14 etc.). Also the order of the tubule openings into the rete testis corresponded roughly to the order of the distribution of tubules within the testis although here were several inversions (compare with position of tubules within the testis in fig 16).



but remained at a distance from the tunica albuginea. All tubules retained their two connections with the rete testis (with one exception tubule 1 which was considered as an anomaly). It was observed that as the outer sex cords did in the embryonic testes the outer tubules usually opened into the lateral aspects of the rete testis whereas like the inner sex cords the inner tubules had their junctions on the internal surface of the rete. Additionally the few branched cords found in the testes of the embryonic series persisted as branched tubules in the adult testis.

The question arose as to how the tubules assumed the shapes of funnels or of hollow cones regularly inserted into one another and how the apices of these funnels and cones came to point caudally. Only a tentative and partial explanation can be proposed here. It may be recalled that at birth the rat testis was almost a perfect sphere which with time became elongated (fig 20). Measurements of the distance of the rete testis from the cranial and the caudal extremities of the organ revealed that during the post natal growth of the testis the direction of expansion was definitely caudal i.e. the distance from the caudal extremity of the rete testis to the caudal extremity of the testis increased at a much faster rate than the distance from the cranial extremity of the rete testis to the cranial end of the testis (fig 20). This would suggest that the cranial end of the testis covered by epididymis was more rigidly fixed and less extensible than the caudal extremity which lay free in the abdominal cavity.

Thus the growing tubules closely packed side by side and applied to the tunica albuginea would expand in the direction of least resistance. At first (from 0 to 4 days of age) this growth would occur in the direction of the central area of the testis where tubules were found to be less closely packed and separated by a large amount of loose connective tissue (fig 4). Then when this space was occupied and as the internal pressure due to tubular growth built up the tunica albuginea would expand but mainly in the caudal direction. The growing tubular limbs would follow this path of least resistance and thus become oriented caud-

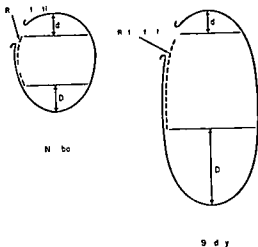


Fig 20 Diagrams showing the outlines of newborn and 9-day old testes from the lateral aspect. The position of the rete testis is indicated by a broken line. Between birth and 9 days there is extensive elongation of the testis with little change in diameter. Furthermore while the distance from the cranial end of the rete testis to the cranial extremity of the testis (d) does not change appreciably during this time the distance from the caudal end of the rete testis to the caudal extremity of the testis (D) increases considerably. This suggests that the lengthening of the testis was primarily in a caudal direction.

ally. The tubular morphology in the 12 day rat testis i.e. the inward path of the cranial portions of the tubule followed by a caudal and inward slope of the more caudal portions would seem to support this hypothesis (fig 11). (This particular angular shape of the tubular limbs observed at 12 days but not seen in the adult is apparently lost with the elongation of the tubules.) The final distribution of the tubules would thus be simply the consequence of the growth of tightly packed tubules within a membranous sac the tunica albuginea which appeared to expand more freely in the caudal direction.

It was clear however that despite the tremendous growth of the tubules their architectural plan in the adult reflected the distribution of the arched sex cords observed in embryos.

SUMMARY

The sex cords from 17 and 19-day rat embryos and of newborn rats as well as the seminiferous tubules from testes of 12-day and adult animals were recon-

structed from serial sections and their morphology and distribution within the testis was investigated.

In the 17-day embryo the full complement of distinct sex cords—20 to 31 per testis—were present. They appeared as a series of C-shaped arches which were distributed along the long axis of the testis in the same manner as the cartilaginous rings of the trachea and which were in a plane more or less perpendicular to the long axis of the organ. The cords were classified as outer when they ran immediately beneath the tunica albuginea or as inner when they formed smaller arches located at a distance from the tunica albuginea. At their extremities most sex cords had two connections with the primordium of the rete testis but a few branched cords (3-5 per testis) had additional connections.

In the 19-day embryonic testis the sex cords fanned out from the rete testis remaining as simple arches which showed some waviness and folding along their course. Sex cords were similarly distributed in testes of newborn rats but concomitant with their rapid lengthening they each folded themselves into a number—about 90—of tiny convolutions. Thereafter the number of convolutions remained constant as the limbs connecting successive convolutions lengthened. Reconstruction of two peripheral tubules from the 12-day testis revealed a considerable lengthening of these limbs so that the cranial turns of the tubule were applied to the tunica albuginea while caudal turns were placed more internally. The limbs between successive turns were there fore directed inward and caudally.

In the adult testis 20 seminiferous tubules were reconstructed. As was found in the more immature forms the tubules retained their two connections to the rete testis and followed a circular pathway within the testis. Likewise these tubules showed a number of convolutions in which the cranial hairpin turns were closer to the tunica albuginea than were the caudal ones. Adjacent long limbs between these turns were more or less parallel to one another and thus formed a sort of sloped palisade. In so doing the tubules assumed the geometrical shapes of funnels or of cones in which their wide parts were ori-

ented cranially and their narrow parts directed caudally. These funnels or cones more or less regularly inserted into one another. Furthermore both outer and inner tubules which had evolved from outer and inner sex cords respectively could be found. A definite correlation could be established between the position of a tubule in the testis and the site of its connections with the rete testis.

Although many morphological features were deeply modified during the extensive growth of sex cords into adult seminiferous tubules the architectural plan of the tubules in the adult testis reflected the distribution of sex cords in the embryo.

ACKNOWLEDGMENTS

This work was supported by a grant of the National Research Council of Canada to Dr C P Leblond.

LITERATURE CITED

- Allen, B M. 1904. The embryonic development of the ovary and testis of the mammals. *Am. J. Anat.* 3: 89-153.
- Bremer, J L. 1911. Morphology of the tubules of the human testis and epididymis. *Ibid.*, 11: 393-416.
- De Baurle, H. M. and H. J. de Pultre. 1920-21. Zur Entwicklung und Morphologie des Säugerhodens. I. Der Hoden von *Mus musculus*. *Anat. Hefte* 59: 321-384.
- De Baurle, H. M. 1921. Zur Entwicklung und Morphologie des Säugerhodens. II. Marsupialier. *Zschr. Ges. Anat.*, 61: 19-31.
- Clermont, Y., and B. Peray. 1957. Quantitative study of the cell population of the seminiferous tubules in immature rats. *Am. J. Anat.* 100: 241-258.
- 1957. The stages of the cycle of the seminiferous epithelium of the rat: practical definitions in PA Schiff hematoxylin and hematoxylin-eosin stained sections. *Rev. Canad. Biol.*, 16: 451-462.
- Curtis, G. M. 1918. The morphology of the mammalian seminiferous tubule. *Am. J. Anat.*, 24: 333-334.
- Felix, W. 1912. The development of the genital organs. In *Manual of Human Embryology*. Keibel and Mall, eds. J. P. Lippincott Co. chap. XIX, pp. 752-979.
- Gruenewald, P. 1934. Ueber Form und Verlauf der Keimstränge bei Embryonen der Säugetiere und des Menschen. Die Keimstränge des Hodens. *Zschr. Anat. Entwickl.*, 103: 1-19.
- 1936. Die Entwicklung der Keimstränge und der Bauplan der Keimdrüsen beim Menschen. *Arch. Gynäk.*, 189: 506-524.
- 1942. The development of the sex cords in the gonads of man and mammals. *Am. J. Anat.* 70: 359-397.

- Hirota S 1952 The morphology of the seminiferous tubules I The seminiferous tubules of the mouse Kyushu Mem Med. Sci 3 121-128
- 1952 The morphology of the seminiferous tubules II The seminiferous tubules of the monkey Ibid 3 129-136
- Huber G C and G M Curtis 1913 The morphology of the seminiferous tubules of mammalia. Anat Rec 7 207-219
- Johnson F P 1934 Dissections of human seminiferous tubules Ibid 59 187-199
- Leblond C P and Y Clermont 1952 Definition of the stages of the cycle of the seminiferous epithelium in the rat. Ann N Y Acad Sci. 55 548-573
- Perey B Y Clermont, and C P Leblond 1961 The wave of the seminiferous epithelium of the rat Am. J Anat 108 47-78
- Roosen Runge E. C 1957 The structure of the rete testis in the albino rat Anat Rec 127 357
- Sappey P C 1889 Traité d'Anatomie Descriptive Paris 4th ed 4

Osteogenesis of Acellular Teleost Fish Bone¹

MELVIN L. MOSS

Department of Anatomy Columbia University
College of Physicians and Surgeons New York

Bone in many higher Teleost fish is totally devoid of enclosed osteocytes (Moss 60). The existence of this unique skeletal tissue type poses many problems among which are those regarding its structure and osteogenesis.

Kolliker (1859) studied 289 species of fish and divided them into two groups on the basis of the presence in their skeletons of either cellular or acellular bone. This latter tissue he also termed "osteoid" additionally likening it incorrectly to dentin. Schmid Monnard (1883) in one of the first papers dealing with the histogenesis of acellular bone declared that "cell free" bone arose as a product of osteoblastic activity and that these osteoblasts frequently become "enclosed in the formed bone substance." Tretjakoff and Chinkus (27) were of the opinion that the only differentiating characteristic between cellular and acellular bone was the lack of cells a conclusion supported by Wisniewski (35). Ougaroff (31) while agreeing that cellular and acellular bones were similar both "in general and in detail" felt that there were some undescribed quantitative differences between these two tissues. A more recent morphologic description of this tissue is that of Enlow and Brown (56, 57, 58).

Acellular bone has long been known to the paleohistologist. The work of Stensio Gross Bystrow and Ørvig have established that both types of bone were present in the earliest Ordovician vertebrates (see Ørvig 51 for a recent comprehensive review and a most complete citation of the literature).

At the outset of a series of investigations concerning the structure and function of acellular bone it was felt that a study of its mode of osteogenesis was warranted.

MATERIALS AND METHODS

Two species of the Family Cichlidae were used *Tilapia macrocephalus* and *Aequidens latifrons* both maintained at 80 F in laboratory aquaria. These were obtained through the courtesy of Dr Lester Aronson, Department of Animal Behavior, American Museum of Natural History. Both species possess acellular bone. The lower jaw and the operculum were used exclusively in the present study. Several specimens of each size were obtained at 5 mm intervals of body length which ranged from 6 to 120 mm. These were fixed in neutral formalin embedded in paraffin and cut serially at 6 μ . All specimens larger than 30 mm were decalcified in a lactic acid nitric acid mixture. In the smaller specimens one series was similarly decalcified while another matching series was cut undecalcified.

Commercially obtained material was provided by *Fundulus heteroclitus*, a marine form having acellular bone and by *Carassius auratus* which has cellular bone. The age of these fish could not be determined. Supplementary material was obtained from *Salvelinus fontinalis*, *Scomberomorus maculatus* and *Porontus triacanthus*.

Stains. Selected sections of all fish were stained with hematoxylin and eosin. Alternate serial sections were stained with mucicarmine, thionine, von Kossa's silver nitrate, Prussian blue (McGee Russell 58), Alcian blue, Weigert's elastic and Foote's silver techniques. Sections were also stained by methylene blue extinction and periodic acid Schiff techniques. Additional unstained and undecalcified sections were studied by phase and polarization microscopy.

¹Aided in part by grants A 1930 and D-1206 National Institutes of Health.

1 Periosteal osteogenesis At sites of active bone growth the periosteum may be either single or multilayered (figs 8 9 10) Osteogenic cells are intensely basophilic and assume a wide variety of shapes In very rapidly growing areas it is occasionally possible to define an uncalcified layer of osteoid As in mammalian bone some osteoblasts become incorporated within a matrix of their own production It is precisely here that the differentiation between cellular and acellular bone begins At first and especially in very young *acellular* bone fish the enclosed osteoblasts (osteocytes) resemble cellular bone osteocytes (fig 11) Very rapidly these cells undergo nuclear pycnosis Their cell spaces (lacunae?) become filled with a faintly eosinophilic substance (fig 12) Gradually this cell space disappears and the area becomes indistinguishable from the surrounding matrix This obliteration was studied best in the chondroidal mode of osteogenesis and will be discussed further below Study of undecalcified sections make it certain that the surrounding matrix is calcified prior to the obliteration of the cell space The pericellular matrix is more intensely basophilic It is not clear whether this localized modification is homologous with a lacunar wall The periosteum of resting (non growing) bone surfaces becomes extremely attenuated In some instances there is a thin layer of elongated fusiform cells (fig 10) In others virtually no cell layer is seen (fig 4)

It is extremely difficult to observe the incorporation of osteoblastic cells in acellular bone formation In most cases even in fish undergoing rapid growth the impression persisted that the osteoblasts possibly played a role in the synthesis of the ground substance and its fibers (and also a role in the subsequent calcification?) in a manner somewhat analogous to that of odontoblasts in the formation of dentin That is the cells did not seem to be entrapped at all but rather were constantly "withdrawing" from the acellular bone matrix Of course no cytoplasmic processes were left behind so that the odontoblastic analogy is perhaps a bit too strong

2 Chondroidal osteogenesis Many articular areas in the lower jaw are covered with chondroid tissue (fig 13) The morphology of this tissue somewhat resembles mammalian articular cartilage (fig 14)

Chondroid is a multilayered tissue of variable thickness (5-30 cells thick) Superficial cells are roughly elliptical with their long axes parallel to the surface The cells gradually become more spherical as depth increases Deeper still the cells hypertrophy nuclear basophilia increases and the cytoplasm becomes lighter

In cellular bone osteogenesis these enlarged cells change insensibly into osteocytes as the surrounding matrix becomes calcified When calcification has occurred the size of the enclosed osteocytes become smaller and their shape identical with that produced by periosteal osteogenesis (fig 13)

In acellular chondroidal osteogenesis nuclear pycnosis occurs in the deeper layers identical with that observed in acellular periosteal osteogenesis Calcification of the matrix external to these pycnotic cells is followed by a "calcification" of the cell space (figs 14 15)

In the zone of calcification of the chondroid tissue of both skeletal types the periodic acid Schiff reaction becomes especially strong in the extracellular matrix The intensity of this reaction diminishes in the cellular bone following the transformation of the chondroid into bone while in the acellular bone this diminution occurs when the empty cell spaces begin to be "filled in" Our present data suggest an intracellular accumulation of calcium salts This is indicated in the following manner in undecalcified sections The cytoplasm of these cells becomes positively stained by von Kossa and Prussian blue techniques This stain is diffuse in the cytoplasm Unstained sections viewed under polarized light show birefringent "granules" These same "granules" appear dark as does bone when viewed with bright phase contrast All these signs disappear in decalcified sections

The most convincing demonstration of intracellular calcification was obtained by the method of Hiyama and Ichikawa (52) Tilapia injected 96 and 72 hours before sacrifice showed abundant extra

TABLE 1

Differential staining of chondroid tissue and other fish and rodent skeletal tissues

	Mucicarmine	Thionine	Methylene blue
Chondroid (fish various)	(-)	(-)	(±) at pH 4.66 (+) at pH 5.36
Hyalin cartilage (fish various) (rodent)	(+) (+)	(+) (+)	(+) at pH 2.8 (+) at pH 2.8
Secondary cartilage (rodent)	(+) in pericellular matrix only	(+) in pericellular matrix only	(+) at pH 2.62 in peri- cellular matrix (+) at pH 3.88 in all of the matrix
Bone (fish rat various)	(-)	(-)	(+) at pH range 4.66-5.36

cellular granules in the zone of calcification of the chondroid matrix and some intracellular granules in the deeper parts of this same layer. Tilapia injected 288, 216, 120 and 48 hours prior to sacrifice showed additionally many granules in the empty cell spaces of the deeper layers.

The superficial resemblance of chondroid to either piscine or mammalian cartilage is dispelled both by a careful morphological examination (fig. 16) and by its differential staining reactions (table 1). Chondroid differed from the secondary cartilage of the rat which also undergoes an analogous transformation (metaplasia) directly into bone (Moss '58, '60).

The methods of microscopy employed were incapable of demonstrating the sites of these cell spaces in more mature acellular bone. In the areas of newly calcified acellular matrix such "ghost sites" could still be visualized within the woven bone of the area (figs. 12, 16).

DISCUSSION

Bone. Little attention has been paid to acellular bone. Some may feel that this designation is a contradiction in terms. A survey of the comparative and phylogenetic aspects of the skeletal system (cf. Schaffer '30, Weidenreich '30, Petersen '30) reveals a wide spectrum of skeletal tissues including acellular bone which exhibit great diversity and blend insensibly into each other. Briefly they form a continuum rather than a series of discrete entities. While mammalian skeletal tissues themselves demonstrate some of

this diversity especially in pathological situations in general they are a group of evolved tissues whose histologic characteristics are rather specific and self-limiting. For examples of the newer concepts and hypotheses that arise when non-mammalian skeletal tissues are considered see Örvig ('51).

A brief review of earlier attempts at classification of piscine bone is useful. Kolliker (1858) spoke of (a) "true" bone as a tissue containing cells, (b) a bone tissue "like dentin" without cells (presumably containing uncalcified fibers) and of (c) an "osteoid" tissue which contained neither tubules nor cells. In addition he defined several other skeletal tissue types which are not of immediate concern. Tretjakoff ('24-'25) regarded Kolliker's "dentin bone" as "true bone" and classified piscine bone as (a) true bone which contained cells, (b) osteoid substance and (c) "pseudodentin" with and without cells. A more recent dichotomous classification is that of Bertin ('58) who spoke of osteoid tissue (without cells) and of "bone tissue proper" (with cells).

Most of this essentially semantic confusion arose from attempts to classify non-mammalian skeletal tissue types in terms applicable to mammals alone. Bone as a tissue may be either cellular or acellular (cf. Örvig '51). It consists of an essentially collagenous organic fiber matrix with associated mucoproteins and is calcified by hydroxyapatite salts. Despite these essential similarities there are undoubtedly differences. When compared with

cellular fish bone the acellular bone has crystallites of smaller size and also has a significantly greater amount of organic mass presumably collagen (Moss and Posner '60). These data reject the earlier contention of Tretjakoff and Chinkus ('27) that the only differentiation between cellular and acellular bone is the absence of cells and support the thesis of Ougaroff ('31).

Chondroid Chondroid tissue is generally composed of circumscribed compact masses of large separate vesicular cells which appear to have a high fluid content. These cells are non-capsulated separated by variable but usually sparse basophilic intercellular substance within which a fibrous framework exists. Generally the tissue resembles relatively young cartilage and has been variously termed pseudocartilage, prochondral tissue, vesicular supporting tissue, fibrohyaline tissue and pre-cartilage (cf. Studnicka '03). Schaffer ('30) describes 4 main types of chondroid tissue chiefly characterized by differing amount of mucoid rich intercellular substance.

Chondroid tissue stands in an intermediate position between chondroid (notochordal) and cartilaginous tissues. It is emphasized that a spectrum of tissues exists interconnecting these seemingly discrete entities.

Our present data (table 1) indicate that chondroid and cartilage may be functionally differentiated by the inability of the former to stain with mucicarmine and thionine and by its inability to bind methylene blue below a pH of 4.66.

The specific type of chondroid tissue we are presently concerned with has been described by Lubosch ('10) as a "vesicular tissue characteristic of the joint morphology of the bony fish. Nowhere else in joint histology does it play such a role. In certain places it especially forms a complete substitute for cartilage and carries out completely the varied functions of these sites." The mechanical role of this specific chondroid tissue is also agreed to by Petersen ('14). See Kaschforoff ('16) for further details.

Osteogenesis Periosteal osteogenesis is a basic vertebrate process essentially homologous in all forms. One point requires

attention. This is the apparent withdrawal of the periosteal layer during acellular bone formation. It was rare to find evidence of osteoblastic incorporation in the bone matrix during this type of osteogenesis. The impression exists that these cells produced consecutive layers of acellular bone and continuously withdrew from the front of matrix formation. It is stressed that no evidence of enclosed protoplasmic processes was observed which in any way resembled odontoblastic processes although Bertin ('58) does mention such a type of cell process in the "canaliculated" cellular bone of Holostean fish.

Chondroidal osteogenesis on the other hand does appear to be unique in fish. Superficially there is a similarity between the chondroidal osteogenesis and the transformation of mammalian secondary cartilage to bone (see Moss '58 for a recent review of this latter tissue). In both tissues there is a metaplasia of the original tissue cells into osteoblasts (osteocytes?) with concomitant alteration in the surrounding matrix and ground substance ending in the calcification of these extracellular areas. The differential staining reactions of these two tissues (table 1) probably allows us to claim that a basic disparity exists between them.

While there are sufficient mutually confirmatory reports extant concerning the transformation of secondary cartilage there is but one prior report of the transformation of chondroid into bone that of Loewenthal ('24) who further noted that chondroid may also transform into hyaline cartilage at appropriate sites.

The observed process of intracytoplasmic "mineralization" leading to the obliteration of enclosed cells in acellular osteogenesis appears to be similar to the obliteration of osteocytes observed by Belanger ('59) in early osteolathyrism in the rat and possibly to the process which produces the human "micropetrosis" described by Frost ('60). Whatever the actual mechanism proves to be these data extend the earlier position of Ougaroff ('31) who claimed that the osteoblastic (osteocytic?) cytoplasm became directly "transformed into bone matrix." We note in passing that certain unicellular organisms also possess the ability to undergo

an analogous intracellular hydroxyapatite calcification (Ennever and Snyder 60 Scott and Wright 60 Zander Hazen and Scott 60)

SUMMARY

The microscopic morphology of acellular fish bone tissue was described and compared with cellular fish bone tissue and found to differ at this level of observation only in the presence or absence of osteocytes. A series of non-osseous piscine tissues was also described with emphasis on a chondroid tissue type. Two modes of piscine osteogenesis were described: a perosteal and a chondroidal, both of which participated homologically in the formation of both cellular and acellular bone. The perosteal mode is identical with that observed in higher vertebrates with the possible exception that in acellular osteogenesis the periosteum may withdraw away from the site of bone matrix formation. Chondroidal osteogenesis involves a direct transformation from chondroidal to osseous tissue. In acellular bone formation this latter process was observed to include cellular pycnosis and hyperchromasia in areas of extracellular calcification. This was followed by obliteration of osteoblastic (osteocytic?) sites by a process of intracellular calcification.

LITERATURE CITED

- Amprino R. and G. Godina 1956 Osservazioni sul rinnovamento dell'osso in Pesci Teleostei. *Publ. Staz. Zool. Napoli* 28: 62-71.
- Belanger L. F. 1959 Observations on the manifestations of osteolathrism in the chick. *J. Bone Jt. Surg.* 41B: 581-589.
- Bertin L. 1908 *Tissus Squelettiques*. In *Traite de Zoologie* 13: 532-550. Masson et Cie Paris.
- Enlow D. H. and S. O. Brown 1956 A comparative histologic study of fossil and recent bone tissue. Part I. *Tex. J. Sci.* 8: 405-443.
- 1957 *Ibid* Part II. *Tex. J. Sci.* 9: 186-214.
- 1958 *Ibid* Part III. *Tex. J. Sci.* 10: 187-230.
- Ennever J. and W. E. Snyder 1960 Intracellular mineralization by filamentous microorganisms. *J. Dent. Res.* 39: 654-655.
- Frost H. M. 1960 Micropetrosis. *J. Bone Jt. Surg.* 42A: 144-150.
- Hayama Y. and R. Ichikawa 1962 A method to mark the time in the scale and other hard tissues of fishes to see their growth. *Jap. J. Ichthyol.* 2: 156-167.
- Kaschkaro D. N. 1916 Untersuchungen über das blasige Gewebe bei Knochenfischen. *Wiss. Mitt. Univ. Moskau Abt. Naturwissen.* Mitt. 38: 1-206.
- Kolliker A. 1859 On the different types in the microscopic structure of the skeleton of osseous fish. *Roy. Soc. Lond. Proceed.* 9: 656-688.
- Lowenthal N. 1924 Sur le tissu fibrohyalin et les bourrelets perostiques des poissons. *Bull. Histol. Appl.* 1: 529-549.
- Lubosch W. 1910 Bau und Entstehung der Wirbelgelenke. G. Fischer Jena.
- McCoe Russell S. M. 1958 Histochemical methods for calcium. *J. Histochem. Cytochem.* 6: 22-42.
- Moss M. L. 1958 Fusion of the frontal suture in the rat. *Am. J. Anat.* 102: 141-166.
- 1960 Inhibition and stimulation of sutural fusion in the rat calvaria. *Anat. Rec.* 136: 457-468.
- 1960 Osteogenesis and repair of acellular teleost bone. *Anat. Rec.* 136: 246-247.
- Moss M. L. and A. Posner 1961 X-ray diffraction study of acellular Teleost Bone. *Nature* 188: 1037-1038.
- Ougaroff A. A. 1931 Beitrag zur Kenntnis der Entwicklung des zellfreien Knochengewebes. *Zeit. Mikr. Anat. Forsch.* 26: 347-370.
- Orvig T. 1951 Histologic studies of Placoderms and fossil Elasmobranchs. *Ark. Zool.* 2: 321-406.
- Petersen H. 1914 Studien zur vergleichenden und allgemeinen Mechanik des Tierkörpers I. Das Kiefergelenk des Kabeljau *Gadus morhua*. *Arch. Entwickl. Mech.* 39: 1-51.
- 1930 Die Organe des Skelettsystems in Handb. d. Mikroskop. *Anat. d. Mensch.* 2(2): 521-678.
- Schaffer J. 1930 Die Stützgewebe. In *Handb. Mikr. Anat. Mensch.* 2(2): 1-390.
- Schmid Monnard C. 1883 Zur Histogenese des Knochens der Teleostier. *Zeit. Wiss. Zool.* 39: 97-136.
- Scott D. B., and D. N. Wright 1960 An electron microscope study of calcification. *J. Dent. Res.* 39: 709-710.
- Smith J. W. 1960 Collagen fiber patterns in mammalian bone. *J. Anat.* 94: 329-344.
- Studnicka F. K. 1903 Histologische und histogenetische Untersuchungen über das Knorpelvorknorpel und Chordogewebe. *Anat. Hefte* 21: 283-325.
- Tretjakoff D. 1924-1925 Das Knochengewebe bei den Pleuronectiden und den Plectognathen. *Anat. Anz.* 59: 379-387.
- Tretjakoff D. and F. Chinkus 1927 Das Knochengewebe der Fische. *Zeit. Anat. Entwickl.* 83: 363-396.
- Weidenreich F. 1930 Das Knochengewebe. In *Handb. Mikr. Anat. Mensch.* 2(2): 391-520.
- Wisniewski P. 1935 Über den Aufbau der Knochen des Innenskelets bei Cypriniden. *Anat. Anz.* 80: 161-204.
- Zander H. A. S. P. Hazen and D. B. Scott 1960 Mineralization of dental calculus. *Proc. Soc. Exp. Biol. Med.* 103: 257-260.

PLATES

PLATE 1

EXPLANATION OF FIGURES

The illustrations in both plates are of the lower jaw elements of the indicated fish

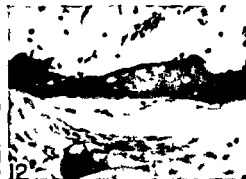
- 1 The basophilic cement line sharply delineates the base of the newly formed cellular bone. Note the osteoblastic cells on the left and the generally loose appearance of this tissue. *Salvelinus fontinalis* Approx $\times 100$
- 2 In addition to demonstrating the morphology of newly formed cellular fish bone this section shows the penetration of collagen fibers through the newly formed bone into the older osseous tissue. *Salvelinus fontinalis* Approx $\times 400$
- 3 The continuity of these lightly stained fiber bundles deep into cellular bone tissue is demonstrated. *Salvelinus fontinalis* Approx $\times 400$
- 4 Non growing acellular bone is shown. Note the absence of a periosteum. The horizontal striations do not stain as distinctly as the cement lines of the previous figures although they may represent homologous structures. *Scomberomorus maculatus* Approx $\times 400$
- 5 An example of extreme intrinsic vascularity in compact acellular bone. There are no osteons in this tissue. *Scomberomorus maculatus* Approx $\times 100$
- 6 A layer of acellular bone is seen lying horizontally beneath a rod of hyaline cartilage. Note that the skeletally active soft tissue layer lies between the cartilage and the bone. *Scomberomorus maculatus* Approx $\times 200$
- 7 Endochondral ossification. Note the general lack of trabeculae and the absence of a zone of calcification. A single cone of hypertrophic cartilage is seen with an attached area of cellular bone. *Carassius auratus* $\times 100$
- 8 Periosteal osteogenesis. A multilayered periosteum lies above an actively growing area of acellular bone. Note the absence of enclosed osteoblasts. *Tilapia macrocephala* Approx $\times 400$



PLATE 2

EXPLANATION OF FIGURES

- 9 Periosteal osteogenesis The periosteum of an actively growing area of cellular bone Note the enclosed osteocytes the area of uncalcified matrix and the inclusion of many collagenous fibers *Carassius auratus* Approx $\times 400$
- 10 Periosteal osteogenesis The tip of the growing acellular bone is surrounded by an active thickened periosteum while the relatively quiescent periosteum immediately to the left is more attenuated *Tilapia macrocephala* Approx $\times 400$
- 11 Periosteal osteogenesis Acellular bone formation is a very young form The bone shows enclosed osteoblasts which will quickly disappear *Tilapia macrocephala* Approx $\times 400$
- 12 Periosteal osteogenesis The cell spaces of this acellular bone are filled with a faintly eosinophilic matrix which stains positively for calcification *Tilapia macrocephala* Approx $\times 400$
- 13 Chondral osteogenesis of acellular bone Note the gradual transition of cell morphology of the chondral tissue The deepest cells show cellular changes and calcification *Tilapia macrocephala* Approx $\times 400$
- 14 Chondral osteogenesis of cellular bone These tissues are undoubtedly articular surfaces *Carassius auratus* Approx $\times 100$
- 15 Chondral osteogenesis of acellular bone The sequence of changes are especially well shown in this section *Poronotus triacanthus* Approx $\times 300$
- 16 The tinctorial differentiation between chondroid tissue (upper) and hyalin cartilage (lower) is illustrated *Tilapia macrocephala* Approx $\times 400$



Histochemical Studies on the Histogenesis of the Joints in Human Fetuses with Special Reference to the Development of the Joint Cavities in the Hand and Foot¹

HELGE ANDERSEN AND FREDE BRO RASMUSSEN
*Department of Anatomy University of Copenhagen
Nørre Alle 63 Copenhagen Denmark*

Since the publication of Bernays (1878) Schulins (1879) and Hagen Torn s (1882) classical studies on the development of the joints a number of comprehensive thorough and amply illustrated papers have appeared. The most important of the recent papers are those of Walmsley (40) Whillis (40) Haines (47) Gardner and Gray (50-53) Gray and Gardner (50-51) and Gray Gardner and O'Rahilly (57).

A common feature of these and most other studies is that apparently very little attention has been given to the histological technique. Careful perusal of the papers and illustrations indicates that a number of the results regarding the formation of the joint cavities are undoubtedly misinterpretations of artifacts caused by shrinkage of the tissues during the preparation of the sections.

Furthermore, no study using the most recent histochemical staining methods appears to have been reported. We have therefore made a renewed study of the development of the joints, concentrating primarily on techniques. As the object of our study we chose the formation of the joint cavities in the hands and feet, i.e. fairly simple joint cavities.

MATERIAL AND METHODS

Material. The material comprises 25 human fetuses removed from the uterine cavity by Caesarean section in the course of sterilization operations. According to crown rump length the material may be grouped as follows: 12 mm (1), 30 mm (1), 48 mm (1), 61 mm (1), 63 mm (1), 65 mm (2), 75 mm (1), 78 mm (1), 80 mm (1), 90 mm (1), 99 mm (1), 102 mm

(2), 108 mm (1), 110 mm (1), 118 mm (1), 125 mm (1), 127 mm (1), 135 mm (1), 148 mm (1), 160 mm (2), 170 mm (1), 179 mm (1).

Hands and feet were used to study a) interphalangeal joints, b) metacarpo and metatarsophalangeal joints, c) carpometacarpal joints, d) tarsometatarsal joints, e) intercarpal joints, f) intertarsal joints, g) radiocarpal joints and h) talocrural joints.

The following requirements must be made on the material used:

1. It must be as freshly removed as possible in order to reflect the conditions in the living body as accurately as practicable.

2. Any artificial bending of the joints must be avoided, since this will inevitably create a joint space. Moreover, any cutting out of tissue pieces must be done very carefully and far from the joints to be studied. If small tissue pieces are desired during the sectioning and subsequent flattening of the sections, it is recommended to cut out these pieces after embedding the tissue in paraffin. Using a sharp razor blade we have successfully practiced this procedure without causing distortion in the tissue.

Fixation. The specimens were fixed as soon as possible, although experiments have shown that even a period of 6 hours at room temperature before fixation apparently does not affect the histochemical reactions used in the present study (Andersen 60).

— This work was supported by grants from The Association for the Aid of the Crippled Children, New York, and from the King Christian X Foundation, Copenhagen, Denmark.

As a fixative we used Lillie's acetic acid alcohol formalin (consisting of 10 ml 40% formaldehyde 5 ml glacial acetic acid and 85 ml 100% ethanol) (Lillie 49). The choice of this fixative mixture was made for the following reasons:

1 Each component of a fixative mixture should as far as possible compensate for a defect in another. Ethanol results in severe shrinkage of the tissue and does not fix chromatin whereas acetic acid compensates for both these defects. Acetic acid does not fix cytoplasm and karyoplasm while ethanol fixes both. Ethanol fixes cytoplasm and karyoplasm in a fairly coarse network whereas formaldehyde gives a more even fixation of these components and involves less shrinkage of the tissues (Baker 58).

2 Lillie (54) reports that this mixture of fixatives is excellent for glycogen preservation if possible superior to Carnoy.

3 This fixative affords good fixation of the acid mucopolysaccharides in fetal tissue (Andersen 61).

4 No rinsing is required after the fixation since all three components are freely miscible with a dehydrating medium such as ethanol.

It may be a disadvantage to use a mixture of fixatives where different components penetrate the tissue at different rates. Normally this disadvantage may be compensated for by the use of small tissue pieces but this procedure was not practicable in the present study in which the main stress was to avoid any unnecessary damage to the tissue. In return the three components in the mixture used are fairly rapidly penetrating tissue fixatives (Baker 58).

In order to control the ability of the fixative mixture used in the present study to fix acid mucopolysaccharides we used cetyl pyridinium chloride which according to Williams and Jackson (56) is a good fixative for these substances prior to metachromatic staining and staining with periodic acid Schiff reagent. In the opinion of these authors this fixation is superior to 4% aqueous formalin and Carnoy's fluid. Cetyl pyridinium chloride is used as an 0.5% solution in 4% aqueous formaldehyde. It forms very insoluble complexes with the acid mucopolysac-

charides and is recommended by Pearse (60) as a fixative for these substances. Fixation period was 48 hours. On comparison with Lillie's fixative mixture we did not find striking differences.

Decalcification As soon as ossification processes began to manifest themselves decalcification was performed using a medium consisting of 2% citric acid and 20% sodium citrate (equal parts) with pH of about 6.0 (Andersen and Balslev Jørgensen 60; Andersen 61). This decalcification apparently involves no loss of metachromasia even after the lapse of 30 days. A decalcification period of 12-18 hours is sufficient depending on the fetal size and rinsing of the decalcifying medium for ½ to one hour is fully sufficient. Nuclear staining was not affected. Apparently there was no difference between specimens which were decalcified and those which were not decalcified.

Embedding and sectioning Shrinkage of the tissue may occur not only during fixation but also during dehydration and embedding. In order to investigate this aspect three experimental series were set up.

I Dehydration through 70% 96% and absolute alcohol to xylene followed by embedding in paraffin as usual.

II Dehydration in an apparatus allowing the alcohol concentration to increase only by a drop per second. Correspondingly the apparatus gives an even transition from ethanol to xylene. From xylene the tissue passes through xylene paraffin mixtures to paraffin containing 5% bees wax (at 58).

III In order to evade the effect of alcohol the tissue was dehydrated for 5-6 hours in a mixture of Carbowax 4000 and 1500 (9:1) at 58°C (Blank and McCarthy 54). According to these authors even 4 days action of molten Carbowax does not cause evident distortion in the tissue. After dehydration the tissue was passed through xylene xylene paraffin mixtures to paraffin as in experiment II in order to evade the difficulties of floating out Carbowax embedded sections.

After trimming of blocks the specimens were cut into sections of 7-15 μ which were prevented from curling by breathing

on them during the entire cutting process and by supporting them by a fine brush

In each series the sections were flattened as follows (a) On the surface of a thermostat regulated water bath at 37 C (b) Directly on the "Meyer-coated" slides by a drop of 37 C aqueous 0.1% sodium chromate (Heard 57) (c) Directly on the "Meyer coated" slides without using any particular floating medium

The sections were dried as follows (1) In a desiccator at 40 C (2) at room temperature and (3) at room temperature under a glass case holding a dish with phosphorus pentoxide

The best results with a minimum of distortion were obtained by dehydration methods II and III when the sections were flattened with 37 C aqueous 0.1% sodium chromate or directly on the "Meyer-coated" slides without a flattening medium. Small sections are fairly easy to flatten by this procedure whereas larger sections did not flatten completely. As already mentioned this difficulty was overcome by cutting the tissue into smaller pieces after embedding in paraffin. Except in the very small fetuses flattening on the thermostat regulated water bath at 37 C would inevitably give rise to artificial joint spaces: the cartilages bending and becoming retracted from the joint area. By a thorough control of each step of the preparation it was found that the vulnerable step was the drying of the flattened sections. Too rapid drying of the heterogeneous tissue resulted in shrinkage leading to artificial joint spaces. The best results were obtained by drying at room temperature.

Staining 1 Metachromatic staining was with 0.1% azure A in 30% ethanol (Kramer and Windrum 55). These authors recommend a staining period of 10 minutes for demonstrating small quantities of acid mucopolysaccharides and a shorter staining period for demonstrating larger amounts of mucopolysaccharides. With the stain (G.T. Gurr) used in the present study the optimum staining period has been found to be one minute (Andersen and Balslev Jørgensen 60 Andersen 60 and 61).

2 Staining with 0.1% Alcian blue in 3% acetic acid (pH 2.7-3.0) (Mowry 56) followed by ordinary periodic acid

Schiff. Between the periodic acid and the Schiff reagent the specimens were washed for 5 minutes in water. This precaution is adequate for preventing recolorization of Schiff's reagent due to periodate (Hale 57).

3 Staining with periodic acid Schiff reagent (Pearse 60) to demonstrate partly connective tissue and partly glycogen. For this purpose celloidin-coated sections were used (1% celloidin in ether/alcohol) in order to prevent the periodic acid from removing the glycogen. These specimens were not decalcified.

4 Staining with hematoxylin eosin (Romeis 48).

5 Phase contrast microscopy

With metachromatic staining shrinkage may occur occasionally since after staining the sections pass from distilled water directly to absolute alcohol. The other staining methods did not involve any shrinkage during the staining procedure and the subsequent mounting. As a mounting medium we used DePex highly diluted with xylene in order to avoid distortions in the sections during the rapid drying of DePex. The influences of staining upon the sections were observed by direct microscopy of the non-deparaffinized sections and by phase-contrast microscopy.

In order to ascertain which substances were responsible for the metachromatic reaction in the sections we performed an extraction test with hyaluronidase using 1 mg per ml 0.9% NaCl at 37 C for 15 hours. By way of further control sections were incubated in 0.9% NaCl without enzyme at 37 C for 15 hours. The alcohol resistance of the metachromatic reaction was studied by passing the sections briefly through 70% ethanol and 96% ethanol (one minute) after the staining.

In order to control the presence of glycogen digestion tests with human saliva were run for 15 hours at room temperature followed by periodic acid Schiff staining. The sections were not celloidin-coated until after the treatment with saliva since celloidin would prevent the action of the enzyme.

OBSERVATIONS

At the site of the future joint there is in early stages the so-called interzone in

serted between the adjoining cartilages. This interzone is three layered consisting of two chondrogenous layers each continuing in the perichondrium of the cartilages and in an intermediate layer of loose avascular mesenchyme which continues peripherally in a vascular mesenchyme the so called synovial mesenchyme. The latter extends wedge shaped in between the adjoining chondrogenous layers. The cells of the intermediate layer of the interzone are arranged with their long axes at right angles to the long axes of the adjoining cartilages and here mitotic figures are not as abundant as in the two chondrogenous layers. The latter which are at the site of the subsequent joint surfaces show pronounced γ metachromasia in the intercellular substance and this metachromasia merges evenly into the fainter metachromasia of the intermediate layer. A similar appearance is seen with Alcian blue which stains the intercellular substance a bright blue. In the early developmental stages the intermediate layer of the interzone consists of a zone which is 3-4 cells thick but in later phases this layer is occupied from both sides by the chondrogenous layers its cells being converted to chondroblasts depositing highly γ metachromatic substances around them (fig 1). The same result is found with Alcian blue. Thus the cartilages bordering on the joint grow appositionally in all directions partly through the chondrogenous layers in the interzone and partly by the aid of the ordi-

nary perichondrium. At later developmental stages the intermediate layer has been occupied from both sides by the chondrogenous layers and the two chondrogenous layers touching in the central area of the joint. At the same time the two chondrogenous layers cease to exist at this site as growth zones for the adjoining cartilages and are incorporated in the joint cartilages which are now in contact by smooth surfaces (fig 2). In the peripheral area of the joint the cartilages remain covered for some time still with a chondrogenous layer. From this layer the peripheral segments of the future joint surface undergo continuous appositional growth in order to keep up with the growth of the fetus as a whole. After the disappearance of the chondrogenous layer the central area of joint cartilage undergoes only interstitial growth. In the case of the foot this coincides closely with the occurrence of vascular canals in the cartilages (at 80 mm c.r. length). In the carpus the vascular cartilage canals (at 100 mm c.r. length) do not appear until long after the central parts of the chondrogenous layers have been incorporated in the joint cartilage. This must be related to the fact that in the hand the cartilages remain for a long time of an order of magnitude which permits the necessary supply to the inside of the cartilages by the perichondral vessels securing interstitial growth. Periodic acid-Schiff stains the intercellular substance of the intermediate layer only very faintly and the same applies to the intercellular



Fig 1. Sagittal section through the talocrural joint at 65 mm crown rump length. The intermediate layer of the interzone is almost completely incorporated in the two chondrogenous layers. Staining 0.1% azure A in 30% ethanol. 100

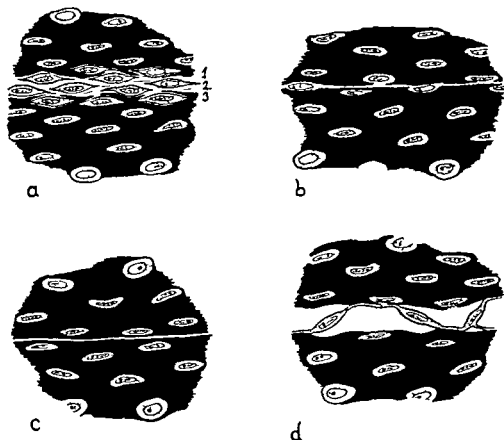


Fig 2 Schematic representation of the formation of joint cavities a Three layered interzone 1 chondrogenous layer 2 intermediate layer 3 chondrogenous layer b The intermediate layer of the interzone has been almost completely incorporated in the two chondrogenous layers c The newly formed joint cavity d Artificial rupture occurring at stage b

substance in the chondrogenous layers. On the other hand this staining method gives a strong reaction for glycogen in the cells of the chondrogenous layers and also in the cells of the intermediate layer which are gradually converted to chondroblasts and incorporated in the chondrogenous layers. The synovial mesenchyme stretching wedge shaped in between the chondrogenous layers in the peripheral parts of the joint gradually shows increased vascularity. The numerous vessels are embedded in a ground substance which stains a bright blue with Alcian blue and is metachromatic and PAS-positive. It is not particularly cellular but at 110 mm the first slightly granulated mast cells begin to appear. This corresponds rather accu-

ately to previous findings (Andersen '61). No glycogen is seen in the cells of the synovial mesenchyme.

The joints of the foot from the talocrural joint and to the distal point develop at approximately the same time. Between 60 and 78 mm c.r. length the formation of the joint cavities is completed in the central areas (fig 3) whence they spread peripherally where the vascular synovial mesenchyme projects wedge shaped into the joint cavity. In comparison the joints of the hand from the radiocarpal joint and towards the distal point are somewhat ahead in development the joint cavities appearing at a crown rump length of between 50 and 65 mm.



Fig. 3. Sagittal section through the talonavicular joint at 78 mm crown-rump length. The intermediate layer of the interzone has been incorporated in the two chondrogenous layers and a joint cavity is visible. 0.1% azure A in 20% ethanol. $\times 425$.

DISCUSSION

In a 5-week-old human embryo the skeletal blastema in the limbs forms a coherent cord of condensed mesenchyme in which the differentiation of the prechondral and later the chondral centers of the individual bones takes place. Gradually as the centers develop and approach each other parts of the non-differentiated blastema are left between them: the so-called interzone.

At the outset the interzone consists of a homogenous tissue but as already mentioned it soon becomes three-layered. This phenomenon is seen in all joints: the separation into three layers appearing first in the large and proximal joints of the extremities. So far there seems to be agreement between the various groups of investigators. The disagreement concerns the formation and time of formation of the joint cavities.

In the present series we found three-layered interzones in the hand at the 30 mm stage. Haines (4) found three-

layered interzones in the carpal and in most intercarpal joints at 25 mm and in all interphalangeal joints at 27 mm where as Whillis (40) found three-layered interzones at the 30 mm stage. In a comprehensive study on the development of the hand Gray Gardner and O'Pahilly (57) found somewhat varying times of appearance of the interzones in the individual joints. On the whole however their results are comparable with those mentioned above. On the other hand there is a marked conflict of opinion regarding the times at which the joint cavities appear. Lewis (52) did not find any joint cavities before 20 mm. Martin (39) found joint cavities in all joints of the hand at 31 mm and Leboucq (1884) stated that all joint cavities were present towards the end of the 4th month. Haines found complete separation of the joint surfaces in the metacarpophalangeal joints at 45 mm whereas the cavities of the wrists and intercarpal joints did not appear until after the 50 mm stage. Beau-Sommelet

and Cavotte (52) found radiocarpal cavities at 25 mm and almost complete cavitation at 65 mm. Gray Gardner and O'Rahilly found cavitation in the joints of the hand between 30 mm and 50 mm but they state at the same time that not all the cavities were constantly present until about 65 mm. In many places they found contact between the different cartilaginous elements after the formation of joint cavities had started. Unlike Whillis however they never found fusion of the joint surfaces.

Practically all authors agree that the primordia of the joint cavities start at the peripheral parts of the joints from which they spread into the intermediate layer of the interzone by a process of liquefaction. Faldino (21) on the other hand has stated that the joint cavities start centrally in the radiocarpal joint at 35 mm (although at 41 mm he found none) centrally in the intercarpal joints at 45 mm and in the interphalangeal joints after 61 mm. Faldino's view that the joint cavities

appear in the central part of the interzone has found practically no support in the literature neither in regard to the joints of the hand and feet nor to the large joints.

Our studies have not supported either the primary appearance of the joint cavities at the periphery or the liquefaction in the intermediate layer. This must be seen in the light of the histological technique and the use of modern histochemical reactions. As mentioned above little attention has been given to the technique so far although a few authors are aware of the numerous technical difficulties. As early as 1897 Hultkrantz called attention to the fact that in one section the joint cavities may be open while in a neighboring section they prove to be closed. Haines states that "cartilages are notorious for their liability to expand and contract as they pass from one solution to another both in the celloidin and paraffin techniques." He adds that in the early stages it is relatively easy to find out what are

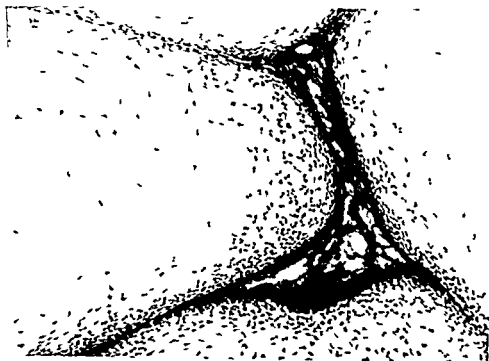


Fig. 4 Frontal section, right hand 12 mm crown-rump length, showing vascular synovial fold in space between lunate, capitate, hamate and triquetrum. No artificial rupture. Hematoxylin-eosin. 200

artifacts but during the latter stages this difficulty is enormously increased. To Haines' addition we must agree but as to what are natural occurrences and what are artifacts our experience brings us in conflict with Haines, Whillis as well as Gray, Gardner and O'Rahilly. By numerous methodical studies of sections from the same hands and feet we have formed the opinion that any primary occurrence of the joint cavity in a peripheral situation may be interpreted as an artifact. Especially the drying of the sections prior to deparaffinization and staining (and this was the more distinct the longer the crown rump length) gave rise to the formation of peripheral joint cavities of exactly the same appearance as Haines' figures 28, 43 and 45 as well as Gray, Gardner and O'Rahilly's figures 14, 30 and 50 (which ought to be compared with our figure 4) and Whillis' figure 5. When adhering to a gentle technique in all stages of preparation we never see peripheral joint cavities. Moreover, in contradistinction to Haines we never found signs of

the cartilage expanding in the course of preparation and causing compression of the loose intermediate tissue in the interzone. On the other hand we observed that at times the cartilages might retract from the intermediate layer of the interzone and this results in major or minor concavities of the cartilages (fig. 5).

According to numerous authors the formation of the joint cavities is preceded by a liquefaction process peripherally as well as centrally. These liquefaction processes are said to comprise the intercellular ground substance leaving a cellular network of scattered strands with irregularly arranged nuclei. Some of the cells in the inner part of the cavities are said to show signs of cell death and the synovial fluid is said to contain remnants of cellular debris. In our study we did not find any signs of such liquefaction. On the contrary, the histochemical reactions used by us show that the cells of the intermediate layer are able to deposit gradually an amorphous cartilaginous ground substance, presumably chondroitin sulphate.

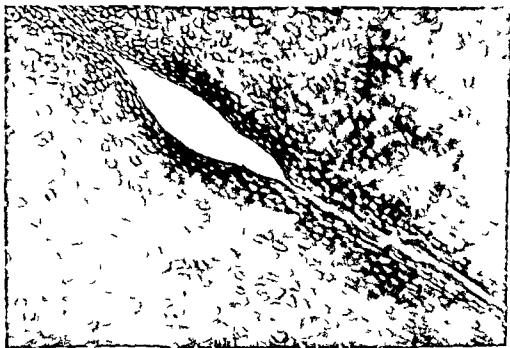


Fig. 5. Sagittal section through the joint between the calcaneus and the cuboid bone at 65 mm crown rump length. Artificial retraction of the two cartilages. 0.1 azure A in 30% ethanol $\times 180$.

A and C as they are incorporated in the chondrogenous layer of the interzone. Furthermore PAS staining reveals that gradually these cells store glycogen in their cytoplasm like the other chondrogenous cells as well as the cartilage cells. With thionine staining Whillis reported less staining affinity in the so-called zone of liquefaction no such signs were found by us using metachromatic staining. Regrettably Whillis does not mention the staining concentration solvent staining time or after treatment. Hematoxylin eosin stained sections do not afford any information about the intercellular ground substance in sites where the liquefaction is reported to take place. On the other hand metachromatic staining shows a metachromatic ground substance in these sites.

The cellular strands arching from one joint surface to another and interpreted by the above mentioned authors as a normal occurrence represent in our experience artificial distortions at a stage when

the intermediate layer of the interzone is present only as one single layer of cells (cf fig 2d and fig 6).

It is agreed by most authors that the vascular synovial mesenchyme participates in the formation of the synovial apparatus including synovial and sub synovial tissue as well as in the formation of intracapsular structures such as ligaments. At the same time it must be presumed that the increasing vascularization taking place in this tissue after the 30 mm stage is of significance to the supply of the chondrogenous layers in the avascular interzone so long as cavitation has not taken place. When cavitation has occurred the synovial fluid may be formed by transudation from these vessels. As to the composition of this early synovial fluid the present study does not provide any information. According to Meyer (57) sulphated mucopolysaccharides have never been isolated from the synovial fluid although the latter does contain small



Fig 6 Sagittal section through the talonavicular joint at 65 mm crown rump length. Artificial rupture with the formation of a false joint cavity at a stage while a single cellular layer is still persisting in the intermediate layer of the interzone. 0.1% azure A in 30% ethanol $\times 600$.

amounts of sulphate. The only polysaccharide which has been isolated from the synovial fluid is hyaluronic acid. According to *in vitro* experiments (Meyer 57) testicular hyaluronidase will remove chondroitin sulfate A and C both of which have been demonstrated in hyaline cartilage. The same applies to hyaluronic acid which has never been demonstrated in hyaline cartilage. We therefore carried out an extraction test with hyaluronidase although Pearse (60) states that neither bacterial nor testicular hyaluronidase will remove the mucopolysaccharides from hyaline cartilage and that this applies particularly when the sections have been fixed in media containing formalin and alcohol. He adds that mucopolysaccharides in tissue sections cannot be expected to be as easily accessible to enzymic action as in *in vitro* experiments. The control experiments showed that 15 hours treatment with hyaluronidase caused a marked loss of metachromatic substances in cartilage chondrogenous layers intermediate layer in the interzone and in the synovial mesenchyme. In other words the mucopolysaccharides in fetal tissue must be more accessible than those in adult tissue to enzymic action.

In an attempt to establish the character of the substance or substances which caused the marked metachromasia in the articular area the alcohol resistance of the metachromasia was investigated. This test is based on Sylven's (41) finding that by treatment with diluted alcohol a distinction may be made between metachromasia caused by high molecular sulfated polysaccharides and metachromasia caused by sulfate free chromotropes (hyaluronic acid) in observation which has been supported to some extent by Kramer and Windrum (55). The present experiments showed that treatment of the sections with 70% and 96% ethanol after metachromatic staining did not influence the staining result. It would seem therefore that the metachromatic substances in the articular area are due to chondroitin sulfate A and C although it has not been finally proved that alcohol resistance is an exclusive indication of polysaccharide ester sulfate. The metachromasia of the hyaluronates is also alcohol resistant

under certain circumstances. However hyaluronic acid is a much weaker chromotrope than chondroitin sulfates. Meyer (47) has demonstrated that a concentration of hyaluronate in the tissues of 1% is required for obtaining metachromasia whereas Sylven and Malmgren (52) report 2-5%. According to Schubert and Hamerman (56) it is doubtful whether this concentration is attained in tissues and they doubt whether hyaluronates do cause metachromasia. Finally hyaluronic acid appears to be a product of the least differentiated fibroblasts (Meyer 57) while the highly metachromatic substances in the present work were made up of chondroblasts (in the chondrogenous layers of the interzone) or of cells which gradually become chondroblasts (in the intermediate layer of the interzone).

But as also indicated by the faintly positive reaction with periodic acid Schiff the interzone must be the site of formation of other substances besides chondroitin sulfate A and C. According to Pearse (60) recent studies have shown that hyaluronic acid as well as chondroitin sulfates are PAS negative. Moreover Pearse reports that continued experiments have shown that a faint PAS positive reaction in an intensely metachromatic tissue indicates the presence of carbohydrate protein complexes of the type neutral mucopolysaccharides and mucoproteins as well as glycoproteins. We are now studying a possible process of secretion from the synovial mesenchyme as a link in a study of the larger joints and carrying out electron microscopic investigations.

According to Mowry (56) Alcian blue appears to be sensitive for the coloration of glucuronic groups whereas Wagner and Shapiro (57) do not consider it a specific histochemical reagent stating that positive staining strongly indicates the presence of acid polysaccharides.

SUMMARY AND CONCLUSIONS

On the basis of our investigations we conclude that the joint cavities start centrally in the joints after the intermediate layer of the interzone in this site has been incorporated in the two chondrogenous layers which in turn are incorporated

in the two joint surfaces ceasing to exist as chondrogenous layers. From the central articular area the joint cavity spreads to the peripheral parts of the joint. This explanation of the participation of the interzone in the formation of the joint cavity is in fair accord with Fell's *in vitro* experiments (Fell 56). It is only in the peripheral areas of the joint surfaces that the chondrogenous layers still persist giving rise to appositional growth of the marginal areas of the joint surfaces whereas the central areas show only interstitial growth. During the development of the joint fairly large quantities of chondroitin sulfates A and C are formed while hyaluronic acid was not demonstrable in the layers of the interzone. The conditions for the appearance of the joint cavities of the foot are present at a crown rump length of about 60-78 mm whereas in the case of the hand the corresponding conditions are present at a stage as early as 50-65 mm.

Histochemical studies of the histogenesis of the joints especially the formation of the joint cavities were carried out on the hands and feet of 25 human fetuses ranging in crown rump length from 12-179 mm. In order to avoid artifacts the various phases of the histological technique were accurately investigated. The most vulnerable step was found to be the drying of the flattened sections after cutting. The following histochemical staining methods were used: Metachromatic staining with 0.1% azure A in 30% ethanol staining with 0.1% Alcian blue in 3% acetic acid followed by ordinary PAS staining with periodic acid Schiff reagent, hematoxylin-eosin and phase contrast microscopy. The investigations revealed that the formation of the joint cavity starts centrally in the joints after the intermediate layer of the interzone at this site has become incorporated in the two chondrogenous layers of the interzone. Thereupon the two chondrogenous layers cease to exist as distinct entities in the center of the joint being incorporated into the joint cartilage while they persist for some time in the peripheral parts of the joint surfaces securing appositional growth of these structures. From the center of the joint the joint cavity gradually

spreads to the periphery of the joint. In the course of the joint formation fairly large quantities of chondroitin sulfate A and C form in the three layers of the interzone and the cavity formation was not preceded by any sign of liquefaction or degeneration in the intermediate layers of the interzone.

LITERATURE CITED

- Andersen H. 1960 Postmortem autolysis in human fetuses and its influence on some histochemical reactions. *Acta Path Microbiol Scand* 50: 225-227.
- 1961 Histochemical Studies on the Histogenesis of the Nails. *Acta Morph Neerl Scand* 3: 322-330.
- Andersen H. and J. Balslev Jørgensen. 1960 Decalcification and staining of archaeological bones with histochemical interpretation of metachromasia. *Stain Tech* 35: S1-96.
- Baker J. R. 1958 Principles of Biological Microtechnique. John Wiley and Sons Inc. New York.
- Leau A. J. Sommelet and J. Cayotte. 1952 Recherches sur le développement de l'articulation du poignet chez l'homme. In: *Recueil des Travaux de la Laboratoire d'Anatomie de la Faculté de Médecine de Nancy*. Georges Thomas. Nancy. pp. 27-40.
- Blank and McCarthy. 1954 cited by R. D. Lillie in *Histopathologic Technique and Practical Histochemistry*. McGraw Hill Book Company. New York.
- Faldino G. 1921 Ricerche sullo sviluppo delle articolazioni. *Chir d Org di Mov* 5: 609-631.
- Fell H. B. 1956 Skeletal development in tissue culture. In: *The Biochemistry and Physiology of Bone*. C. H. Bourne. ed. Academic Press. Inc. New York. chap. XIV.
- Gardner E. and D. J. Gray. 1950 Prenatal development of the human hip joint. *Am J Anat* 87: 163-212.
- 1953 Prenatal development of the human shoulder and acromioclavicular joints. *Ibid* 92: 219-276.
- Gray D. J. and E. Gardner. 1950 Prenatal development of the human knee and superior tibiofibular joints. *Ibid* 86: 235-288.
- 1951 Prenatal development of the human elbow joint. *Ibid* 88: 429-470.
- Gray D. J., E. Gardner and R. O'Rahilly. 1957 The prenatal development of the skeleton and joints of the human hand. *Ibid* 101: 169-224.
- Hagen Torn O. 1882 Entwicklung und Bau der Synovialmembranen. *Arch Mikr Anat* 21: 591-663.
- Haines R. W. 1947 The development of joints. *J Anat* 81: 33-55.
- Hale A. I. 1957 The Histochemistry of Polysaccharides. *Intern Rev Cytol* 6: 193-263.
- Heard O. O. 1957 Methods used by C. H. Heuser in preparing and sectioning early embryos. *Contrib Embryol* 36: 1-18.

- Hultkrantz J W 1897 Das Ellenbogengelenk und seine Mechanik Eine anatomische Studie G Fischer Jena 153 pp
- Kramer H and G M Windrum 1955 The metachromatic staining reaction J Histochem Cytochem 3 227-237
- Leboucq H 1884 Recherches sur la morphologie du carpe chez les mammifères Arch Biol 5 35-102
- Lewis W H 1902 The development of the arm in man Am J Anat 1 145-184
- Lillie R D 1949 On the destruction of cytoplasmatic basophilia (ribonucleic acid) and of the metachromatic basophilia of cartilage by the glycogen splitting enzyme maltodiastase A histochemical study Anat Rec 103 611-633
- 1954 Histopathologic Technique and Practical Histochemistry McGraw Hill Book Company New York
- Martin P 1929 Contribution à l'étude des articulations des membres chez l'embryon humain Thèse Université de Lausanne 56 pp
- Meyer K 1947 The biological significance of hyaluronic acid and hyaluronidase Physiol Rev 27 335-359
- 1957 The acid mucopolysaccharides of connective tissue In Connective Tissue A Symposium Blackwell Scientific Publications Oxford
- Mowry R W 1956 Alcian blue technics for the histochemical study of acidic carbohydrates J Histochem Cytochem 4 407
- Pearse A G E 1960 Histochemistry Theoretical and Applied 2nd ed J & A Churchill Ltd London
- Romeis B 1948 Mikroskopische Technik Leibniz Verl München
- Schubert M and D Hamerman 1956 Metachromasia chemical theory and histochemical use J Histochem Cytochem 4 159-189
- Schulin K 1879 Ueber die Entwicklung und weitere Ausbildung der Gelenke des menschlichen Körpers Arch Anat Physiol Anat Abth 240-274
- Sylvén B 1941 Über das vorkommen von Hochmolekularen Esterschwefelsäuren in granulationsgewebe und bei der epithelregeneration Acta Cir Scand 86 Suppl 66 1-151
- Sylvén B and H Malmgren 1952 On the alleged metachromasia of hyaluronic acid Lab Invest 1 413-430
- Wagner B M and Shapiro 1957 Application of Alcian Blue as a histochemical method Ibid 6/5 472-477
- Walmsley R 1940 The development of the patella J Anat 74 360-368
- Whillis F 1940 The development of ynovial joints J Anat 74 277-283
- William G and D S Jackson 1956 Two organic fixatives for acid mucopolysaccharides Stain Tech 31 189-191

The Ear Apparatus of the Kangaroo Rat *Dipodomys*

DOUGLAS B WEBSTER

Department of Zoology Cornell University Ithaca New York

The kangaroo rat possesses several structural and functional modifications which clearly adapt it to its desert environment. These specializations include its locomotor apparatus (Howell 32 Bartholomew and Caswell 51) its vertebral column (Hatt 32) its excretory system (Schmidt Nielsen and Schmidt Nielsen 51 52 Vimtrup and Schmidt Nielsen 52) its slow turnover of body water (Richmond et al 60) its ability to withstand elevated body temperatures (Dawson 55) and its diestrous reproductive cycle (Reynolds 58). Further specializations which may well be concerned with survival in a desert environment are the dorsal sebaceous gland complex (Quay 53 54) and the subcortical control of hind limb movement (Strauss 36) facilitating a rapid escape mechanism. The present study postulates that the ear apparatus of the kangaroo rat may represent an additional adaptation for life in an arid environment where there is little natural cover.

MATERIALS AND METHODS

Twenty five *Dipodomys merriami* and 5 *Dipodomys spectabilis* were dissected for gross study of the external middle and inner ears and histological sections of all parts of the ear apparatus were prepared (see table 1). Kaformacet formic acid and the Bouin's methods worked equally well and Peterfi's double embedding proved very satisfactory and minimized distortion of the more delicate structures. Skulls of the neotropical jerboa *Dipus* and the spring haas *Pedetes* were also examined.

In order to visualize the internal contours of the middle ear and to determine its volume quantitatively Wood's metal casts were made of the middle ear cavity of *D. merriami* (10 casts) and *D. spectabilis* (two casts). To ascertain the relationship of arteries and nerves passing

through the temporal bone and their positions relative to the inner ear a three dimensional reconstruction 40 X natural size was prepared using illustration board.

External ear

Dipodomys merriami possesses a modest sized pinna 12 mm long from intertragic notch to tip of helix with a maximum width of 9 mm. The entire anterior rim is recurved and continuous with the slightly projecting tragus (fig 4). The antihelix is a prominent ridge 8 mm proximal to the tip of the helix and is formed by the auricles sharp bend toward the concha 3 mm medial to the antihelix. From the posterior end of the subhelix the large slightly lobed antitragus extends anteriorly to terminate just medial to the base of the tragus. Thus the intertragic notch is a shallow slot between the overlapping tragus and antitragus. The concha lies flat against the skull and contains the opening to the external auditory meatus in its anterior ventral wall.

The entire pinna is covered by fine light hairs grouped more densely on the convex than on the concave surface. Along the rim of the helix are dark longer hairs which extend about 3 mm onto the concave surface of the pinna. Two rows of long light-colored hairs guard the entrance to the concha—one row on the free edge of the antitragus and the opposing row on the antihelix. The skin covering the auricular cartilage is thin and no hypodermis is present (fig 17). The epidermis averages 22 μ in thickness while the thickness of the dermis varies from 40 μ near the rim of the helix to 450 μ on the medial wall of the antitragus. The dermis is intimately attached to the auric

Present address Division of Biology California Institute of Technology Pasadena California.

TABLE 1

Histological techniques used in middle and inner ear preparations

Series	Perfused	Fixative	Decal	Clearing agent	Thickness of sections	Stain
D spec rt	+	RK ¹	FA ²	CWO ⁴	10	H & E ⁵
M 2 lt	+	RK	FA	CWO	25	H & E
M 3 lt	+	RK	FA	CWO	25	H & E
M 3 rt	+	RK	FA	CWO	25	H & E
M 7 lt	+	RK	FA	CWO	15	Mallory ⁷
M 7 rt	+	RK	FA	CWO	15	Mallory
M 15 lt	+	RK	FA	MBB	15	H & E
M 15 rt	+	RK	FA	MBB	15	Orcein
M 23 lt	+	RK	FA	MBB	15	Mallory
M 23 rt	+	RK	FA	MBB	15	Mallory
M 25 lt	—	RK	FA	MBB	10	Mallory
M 25 rt	—	RK	FA	MBB	15	H & E
M 26 lt	—	Bouin's	Bouin's ³	MBB	15	Mallory
M 26 rt	—	Bouin's	Bouin's	MBB	15	Orcein
M 27 lt	+	Bouin's	Bouin's	MBB	15	Orcein
M 27 rt	+	Bouin's	Bouin's	MBB	15	Orcein
M 36 lt	+	RK	FA	MBB	15	Mallory
M 36 rt	+	RK	FA	MBB	15	Mallory
M 38 lt	+	RK	FA	MBB	15	H & E
M 38 rt	+	RK	FA	MBB	15	Mallory

¹ Forty-eight hours of fixation in Romley's kaformacet² 8 N formic acid buffered to pH 2.2 with sodium formate—for 36 hours (Kristensen 49)³ Six months slow decalcification⁴ Cedarwood oil for 24 hours then two hours in petroleum ether⁵ One per cent celloidin in methyl benzoate for 4 days then 24 hours in benzene (Peterfi's double embedding in Carleton and Drury 57)⁶ Harris hematoxylin and alcoholic eosin⁷ Haidenbain's modification of Mallory's trichrome

ular cartilage except where muscles in tervene

The skeletal support of the external ear is formed by two cartilages a large auricular cartilage having the same general shape as the pinna and a small crescent shaped "annular" cartilage intercalated between the auricular cartilage and the rim of the bulla against which it lies When stained with orcein and Van Gieson's stain these cartilages are deep brown indicating elastic cartilage

The maximum measurements of the auricular cartilage are 15 mm in length and 9 mm in width The distal part is pinnate whereas the proximal portion is rolled into a tube with the anterior edge overlapping the posterior

The "annular" cartilage forms a semi circle with its concave edge bordering the cranio-ventral edge of the external auditory meatus opening The maximum external diameter of this cartilage is 5 mm and the internal diameter 2.5 mm Its maximum thickness is 0.5 mm making the

peripheral 0.5 mm of the external auditory meatus cartilaginous

There are 4 intrinsic muscles of the auricle The antitragicus major is a distinct muscular band lying primarily in a shallow groove along the base of the antitragus From its broad origin near the intertragic notch it curves obliquely around the base of the antitragus to insert opposite the caudal end of the antihelix

The less well defined antitragicus minor takes origin under the belly of the antitragicus major and then fans out to insert broadly near the free edge of the posterior part of the antitragus

A small intrinsic muscle termed here the auricularis is found just proximal to the intertragic notch It courses between the overlapping parts of the auricular cartilage near its base

The diffuse obliquus auricularis is found on the cranial side of the auricular cartilage It is subdivided into two parts—a narrow band opposite the antihelix and another narrow band located 2 mm dis-

tally. Most of the fibers are very short but a few extend almost to the helix.

The anterior and posterior auricular arteries which branch from the external carotid supply the external ear. The anterior auricular artery supplies the tragus and the anterior part of the helix while the posterior auricular artery supplies the remainder of the pinna. The anterior and posterior auricular veins accompany the arteries and drain independently into the posterior facial vein.

The external ear is innervated by branches of the trigeminal and facial nerves and the cervical plexus. The motor nerve to the intrinsic musculature on the lateral surface of the auricle is a branch of the temporal nerve (which is in turn a branch of the facial). The obliquus auricularis on the cranial surface of the pinna is innervated by the posterior auricular nerve (part of the facial). Sensory innervation is from the great auricular nerve of the cervical plexus and the auriculo-temporal branch of the mandibular nerve. The former accompanies the posterior auricular nerve and innervates the anti-tragus, most of the helix and most of the base of the pinna. The auriculo-temporal nerve innervates the tragus and the anterior part of the pinna. On the pinna these nerves follow the same courses as the arteries and veins.

Except for the peripheral millimeter the entire external auditory meatus is osseous. It courses obliquely medially anteriorly and ventrally to the tympanic membrane. The roof of the meatus is 4 mm long its floor measures 8 mm. Thus the membrane is obliquely oriented and forms an angle of 175° with the roof of the external auditory meatus and of 55° with the horizontal plane of the skull. The oval opening of the external auditory meatus measures 3.7 mm by 2.9 mm. The meatus then enlarges as it passes medially to the tympanic membrane which measures 5.5 mm in diameter.

Since there are no tubular glands present in the external ear one cannot speak of ceruminous glands. Large sebaceous glands 0.4 mm in height are found on the inner surface of the antitragus (fig. 18). Slightly smaller sebaceous glands (0.1 to 0.3 mm high) cover the entire

concha and extend up to the antihelix. A few very small sebaceous glands line the osseous external auditory meatus.

Middle ear

Since Howell ('32) has previously described the gross osteology of the kangaroo rat ear suffice it here to point out that the shape of the skull is distorted by the hypertrophy of the mastoid portion of the temporal bone (figs 5-8) and that within the temporal bone the middle ear is in completely divided into three portions. Both the anterior and posterior mastoid portions which are separated by a thin bony lamina, communicate with the entotympanic portion (figs 10-12).

In the present study the use of Woods metal casts and histological preparations have it possible to characterize more fully the ear apparatus. The mastoid walls and the lamina separating the anterior and posterior mastoid bullae are composed of a single layer of compact bone varying from $25\ \mu$ to $41\ \mu$ in thickness (fig. 21). The total middle ear volume is $0.49\ \text{cm}^3$ in *Dipodomys merriami* and $0.88\ \text{cm}^3$ in *D. spectabilis*. In each species the anterior mastoid comprises 49% the posterior mastoid 33% and the entotympanic 18% of the total middle ear volume. The entire cavity is lined by simple squamous mucous epithelium.

Some osteological features of the ear are observable on the medial surface of the temporal bone. Just caudal to the internal auditory meatus is the opening of the cochlear aqueduct into the subarachnoid space (fig. 9). Slightly dorsal to this foramen is the very tenuous slit-shaped aperture of the vestibular aqueduct. The shallow fossa continuous with this slit lodges the distal portion of the endolymphatic sac. A small portion of the cochlea is seen bulging medially just anterior and medial to the internal auditory meatus (fig. 9).

Tympanic membrane. The tympanic membrane is shaped like a flat cone whose base is 5.5 mm in diameter whose apex is directed medially and whose height is 1.0 mm. Except for a small flaccid part opposite the proximal end of the malleus it is firmly attached to the ectotympanic ring by a fibrous wedge-shaped ligament

The histological structure of the membrane is quite typical of mammals being composed of connective tissue fibers covered externally by an extremely thin simple squamous epithelium continuous with the epithelial lining of the external auditory meatus and covered internally by a thin simple squamous epithelium continuous with the mucous lining of the middle ear cavity. The manubrium of the malleus is embedded in the tympanic membrane and lies between the fibrous layer and the inner epithelial layer.

Auditory ossicles The gross anatomy of the kangaroo rat's auditory ossicles has previously been described (Ryder 1878; Cockerell et al 14; Howell '32). The additional observations which follow are particularly pertinent to a functional analysis of the sound transmitting apparatus.

The three ossicles together have a dry weight of 2.7 mg (malleus 1.6 mg, incus 0.9 mg and stapes 0.2 mg). The articular facets of both the malleus and the incus have complex shapes. When observed from a lateral view the incus overlaps the malleus in the dorsal part of the joint. Medially the malleus overlaps the incus.

However, when viewed from the medial aspect the relative positions are reversed. Such a complex articulation would appear to be capable of resisting shearing forces. This articulation was observed to be a true joint with a thin space between elements. The facets of both ossicles are covered with a layer of cartilage and in only one case out of the 15 observed was there any connection between these cartilaginous coverings of the malleus and incus; this was only a very small area in the lateral part of the joint. Staining with orcein showed a very fine line of dark brown fibers along each articular facet thus indicating elastic fibers. A fine connective tissue capsular ligament having no elastic fibers holds the ossicles together (fig. 19).

The joint between the incus and the stapes is an amphiplanar joint and like the malleo-incudo joint has a cartilaginous layer on each facet. Orcein staining indicated that unlike the malleo-incudo joint there were no elastic fibers along the facets; however the capsular ligament stained positively for elastic tissue. In all

15 joints observed a full distinct joint cavity was present (fig. 20). The positions of the incus and stapes indicate their relative movements. The shapes of the lenticular process head of the stapes and footplate of the stapes are not symmetrical; they are narrower posteriorly than anteriorly. The straight anterior crus of the stapes is more directly under the lenticular process of the incus than is the arc-shaped posterior crus (fig. 16). Thus it appears that most of the force from the incus is directed to the anterior crus of the stapes making the stapedia movement a rocking one.

The annular ligament holding the stapes in the fenestra ovale is composed of extremely fine short fibers which stain light blue with aniline blue and very light brown with orcein. These are probably fine collagen fibers. Their lengths vary the ligament being 28 μ wide in the posterior part and 33 μ wide in the anterior part thus allowing more movement anteriorly than posteriorly.

The posterior ligament of the incus is divided into two parts by the minute foramen in the floor of the fossa incudis. The medial part is larger and stouter extending from the medial face of the distal end of the short crus to the medial wall of the fossa incudis. The lateral part of the ligament which is a much narrower band of fibers extends from the lateral face of the distal end of the short crus to the lateral wall of the fossa incudis. Both parts of the ligament show true ligamentous structure and some of the fibers stain positively with orcein.

The anterior ligament of the malleus on the other hand is not a true ligament. Histological examination reveals that the thin lamina of the anterior process of the malleus here only 9 μ thick actually extends over a course of about 0.5 mm and is continuous with the ectotympanic element of the bulla. Fine fibers extend along each face of this lamina, but no nuclei were observed except in the thin epithelial mucous membrane covering.

Muscles The belly of the tensor tympani muscle lies within a bony canal just dorso-lateral to the cochlea which also contains the stapedia artery and the greater superficial petrosal nerve. The

muscle originates from the dorsal wall of the hypotympanic cavity about 1 mm anterior and medial to the tip of the cochlea. Its fibers converge to a tendon while still in this canal; the tendon then leaves the canal by way of the minute foramen in the medial rim of the superior tympanomastoid foramen. This foramen acts as a pulley for the tendon makes an angle greater than 90° upon leaving the canal then extends ventro-laterally for 1 mm to insert onto the muscular process of the malleus. It is innervated by a fine branch of the mandibular nerve.

The tiny stapedius muscle takes origin partially on the osseous wall of the horizontal semicircular canal and partially on the bony canal of the facial nerve. From this origin the fibers converge quickly to form a tendon which then extends 0.3 mm anteriorly to insert onto the stapes. It is innervated by a minute branch of the facial nerve.

The suspension of the ossicles by the anterior ligament of the malleus and posterior ligament of the incus is such that the center of gravity lies along the axis of rotation. In *D. merriami* the manubrial lever arm measures 2.3 mm from umbo to the axis of rotation and the incudo lever arm is 0.68 mm from the axis of rotation to the center of the lenticular process. Therefore assuming no friction a force on the umbo is amplified 3.38 times at the lenticular process and thus at the fenestra ovale. Another mechanism which also increases the effective force at the fenestra ovale involves the relative sizes of the tympanic membrane and stapedia footplate. A force on the large tympanic membrane (25.9 mm²) is resolved to the small surface area of the stapedia footplate (0.60 mm²). Since only about two-thirds of the mammalian tympanic membrane effectively acts in moving the malleus (Bekesy 41; Wever and Lawrence 54) this hydraulic effect is a ratio of 173.06 or 287.1. Combining the 3.38:1 effect of the lever system with the 287.1 force increase of the hydraulic system it is found that assuming no resistance to movement any force applied to the tympanic membrane would be magnified 97.2 times at the fenestra ovale.

Of course there is some resistance to movement that damps the sound transmitting system the amount of which is determined by friction, mass and elasticity of the component parts. Although quantitative data were not obtained several characteristics of the kangaroo rat ear tend to decrease the damping.

Factors affecting friction of the apparatus include the tonus of the intra-aural muscles, the attachments of the ossicular ligaments and the flexibility of the tympanic membrane and annular ligament. Wiggers (37) working on the guinea pig and Wever and Lawrence (54) working on the cat have shown that the primary function of the intra-aural muscles in these animals is to protect the inner ear from loud sounds by contracting and thereby lessening ossicular vibrations; this seems to be the case in most mammals (Wever and Lawrence 54). Since there is no morphological evidence to indicate that this is not the case in *Dipodomys* it can be assumed that for most acute hearing the muscles of this animal's middle ear are relaxed, placing very little tension on the ossicular system and thus producing very little friction. The two ossicular ligaments of the kangaroo rat's ear—the anterior ligament of the malleus and the posterior ligament of the incus—lie on the axis of ossicular rotation as is true in most mammals (Dahmann 30; Wever and Lawrence 54). However, most mammals also have in addition to these two ossicular ligaments a superior and a lateral ligament of the malleus (Kobayashi 55) which tend to increase the rigidity of the ossicles. Since these accessory ligaments are lacking in the kangaroo rat it follows that the rigidity of the ossicular system and hence the friction is probably less than in many mammals. There was no means of measuring the stiffness of the tympanic membrane or annular ligament; however, nothing was seen in their histological structure which would indicate excessive stiffness.

The mass of the vibrating system of the kangaroo rat ear is extremely small and the relatively large tympanic membrane probably does not add appreciably to the mass of the middle ear complex. The dry weight of the ossicles of *Dipodomys mer-*

nium is only 2.7 mg as opposed to about 10 mg in the guinea pig (Fernandez '52) and 5 mg in *Meriones* (Legoux and Wistner '55). Of course these animals are larger than *Dipodomys* but this is not relevant. The important consideration is that the ossicular system must be moved by air vibrations and that a lighter ossicular system will vibrate with weaker air pressures. The ratio of ossicular weight to body weight has no effect on the part mass plays in the damping of the middle ear.

The elasticity of the system depends on characteristics of the same structures that affect friction but in addition is affected by the volume of the middle ear cavity since a large air space permits free vibrations. As has already been stressed the kangaroo rats middle ear cavity is extremely large.

Vascularization. The vascular supply to the temporal bone and ossicles is quite complex. Most of the mastoid elements are supplied by a branch of the cervical trunk (which in turn is a branch of the subclavian artery). This branch of the cervical trunk reaches the skull at the posterior ventral surface of the posterior mastoid bulla, courses up to the ventro-caudal edge of the external auditory meatus and then follows the rim of the meatus as far as its anterior dorsal margin. Along this course it gives off 6 branches which radiate out onto the mastoid bulla (fig. 1). The part of the anterior mastoid not vascularized by the cervical trunk receives its blood supply from two small branches of the anterior

auricular artery. The ventral wall of the entotympanic bulla is vascularized by a tiny branch of the external carotid which leaves the external carotid at the same point as the posterior auricular. The external auditory meatus receives its arterial supply from a tiny branch of the posterior auricular artery; this branch penetrates the bone between the ventral rim of the external auditory meatus and the stylo-mastoid foramen and then it courses along the ventro-caudal wall of the external auditory meatus giving off many tiny twigs.

The cranial walls of the temporal bone are vascularized by branches of the stapedia artery. The more ventral portion receives 4 tiny branches as the stapedia artery courses through its canal dorso-laterally to the cochlea. The dorsal part receives minute twigs from cerebral and cerebellar dural arteries which themselves are branches of the stapedia artery. The tensor tympani and stapedius muscles also receive branches from the stapedia artery as do the auditory ossicles with the branches to the ossicles and to the stapedius muscle coming off the same stem. The branches to the ossicles reach them by way of the stapedius tendon and the posterior ligament of the incus.

Innervation. The facial nerve as it passes through the middle ear cavity is completely enclosed by a bony canal. This canal enters the middle ear cavity just dorsal to the base of the cochlea and in its lateral course runs ventro-caudally first passing just ventral to the fossa incudis and the horizontal semicircular canal. It

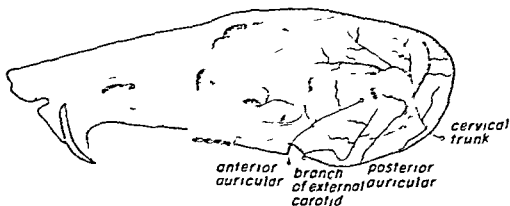


FIG. 1. Skull of *Dipodomys deserti* showing arterial supply to the mastoid bullae.

then courses immediately ventro-caudal to the wall of the external auditory meatus and finally emerges to the skull surface through the stylomastoid foramen. Along this course it gives off two branches—the fine branch to the stapedius muscle and the chorda tympani. The former leaves the posterior face of the nerve and runs medially into the base of the stapedius muscle where it spreads out and terminates. The latter the chorda tympani is so fine that it could not be observed grossly even with the aid of a $27\times$ dissecting microscope; however its route was traced through serial histological sections. It emerges from the facial canal antero-medially through a small canal (0.26 mm long, $75\ \mu$ in diameter) which opens onto the medial face of the thin bony lamina attaching Shrapnell's membrane. It passes anteriorly along this lamina between the bone and mucous membrane of the tympanic cavity. At the level of the malleoincudo joint it courses medially to the head of the malleus. It then travels anteriorly to the base of the manubrium, turns 90° ventrally and follows the posterior face of the manubrial lamina as far as the muscular process. Here it passes around the muscular process making a 180° turn and extends back up the anterior face of the manubrial lamina. Along this route the descending and ascending parts of the nerve which is $20\ \mu$ in diameter are only $85\ \mu$ apart. At the base of the manubrium it passes anteriorly along the thin lamina of the anterior process of the malleus which it pierces; it then enters a tiny canal just medial to the attachment of the anterior process of the malleus and exits from the middle ear.

Internal ear

Bony labyrinth. Much of the bony labyrinth bulges into the middle ear cavity in such a manner that the outline of the cochlea in the entotympanic cavity, the posterior and horizontal semicircular canals in the walls of the posterior mastoid and the anterior semicircular canal in the walls of the anterior mastoid portion are plainly visible (figs. 10–12).

All parts of the osseous labyrinth which are outlined in the wall of the middle ear cavity are composed of a thin layer of very

compact bone varying from $14\ \mu$ thick at the apical turn of the cochlea to $62\ \mu$ thick in the medial part of the horizontal semicircular canal. The dorsal and medial walls of the cochlea and vestibule are somewhat thicker and in histological sections one can observe here the usual three layers of bone—a dense compact endosteal bone lining the perilymphatic spaces, a layer of loose bone and then a layer of dense periosteal bone lining the cranial cavity (fig. 22). Nowhere in the kangaroo rat were isolated islands of cartilage observed in the middle layer (as described by Bast (30) in man); therefore this cannot be referred to as intrachondral bone.

The vestibule lies just medial and caudal to the ampullae of the horizontal and anterior semicircular canals (fig. 13). In the ventro-lateral wall of the vestibule is an oval opening filled by the footplate of the stapes—the fenestra ovale. Caudal to this is the very large fenestra rotunda covered by the secondary tympanic membrane. The bizarre shape of the fenestra rotunda (fig. 14) has a depressed center and medial extremity held in position by the base of the modiolus. The vestibular aqueduct measuring $97\ \mu$ by $109\ \mu$ in cross section exits from the medial dorsal part of the vestibule and travels just medial to the crus commune to the point where it opens into the subdural space just behind the ansiform lobule of the cerebellum.

The cochlear aqueduct leaves the ventral caudal part of the vestibule immediately anterior to the fenestra rotunda whence it traverses its short course to the cranial cavity. Careful examination of the cochlear part of the osseous labyrinth shows that there are $4\frac{1}{2}$ turns in the cochlea.

Membranous labyrinth. Except for specialized areas the wall of the membranous labyrinth is composed of an inner layer of extremely thin squamous epithelium and a fine outer layer of fibrous connective tissue. In the cochlear portion of the labyrinth this condition exists only in Reissner's membrane. In the vestibular part of the labyrinth the typical condition holds true in all parts except where associated with the maculae and cristae.

highly convoluted course along the cochlear nerve within the modiolus giving off many spiral arterioles en route. Each of these spiral arterioles courses along the internal wall of the scala vestibuli frequently giving off the following branches: an external branch passing just over the spiral ligament; an internal branch coursing along the inner border of the scala vestibuli and sending terminal vessels to the spiral crista, spiral ganglion and habenua perforata. There is no direct vascular supply to the organ of Corti (fig. 33).

The other two main branches of the internal auditory artery course throughout the vestibular apparatus and their exact routes could not be followed; however, a concentration of arterioles and capillaries is seen in each of the maculae and cristae.

The membranous labyrinth is drained by two principal veins: the larger one leaving

through the cochlear aqueduct and the smaller through the vestibular aqueduct. The former vein results from the joining at the base of the aqueduct of two main branches: the smaller of these branches drains the first three-quarters of the basal turn of the cochlea, the saccule and part of the utricle; the larger branch drains the rest of the cochlea, taking a spiral course along the lower inner corner of the scala tympani. The spiral veins receive smaller venules in pairs. The external venule drains the stria vascularis and spiral ligament then passes around the lower edge of the scala tympani to enter the spiral vein. The smaller internal twig drains the cochlear nerve, spiral ganglion and spiral crista (fig. 3). The kangaroo rat differs from most mammals in that there is no vein running under the zona tecta.

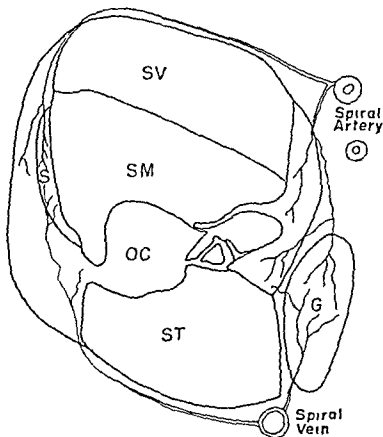


Fig. 3. Third turn of cochlea of *Dipodomys merriami* showing its vascularization in transverse section. G, spiral ganglion; OC, organ of Corti; S, stria vascularis; SM, scala media; ST, scala tympani; SV, scala vestibuli.

The second vein of the membranous labyrinth that of the vestibular aqueduct drains the three semicircular canals and most of the utricle. One branch of this vein drains the crus commune, the posterior semicircular canal and its crista and the posterior half of the horizontal semicircular canal; this branch enters the vestibular aqueduct just posterior to the endolymphatic duct. Another branch draining the cristae of the horizontal and anterior semicircular canals, most of the utricle and the anterior parts of the horizontal and anterior semicircular canals enters the vestibular aqueduct just anterior to the endolymphatic duct. These two branches course on opposite sides of the endolymphatic duct up to the base of the endolymphatic sac where the posterior branch passes medial to the endolymphatic duct to join the anterior branch, thus forming the vein of the vestibular aqueduct.

DISCUSSION

Hypertrophy of the middle ear has occurred in several convergent families of rodents and is especially prominent in some species of Heteromyidae, Dipodidae, Pedetidae and Muridae. One family of insectivores, the Macroscelididae, also possesses enlarged middle ear cavities. The species which demonstrate this convergent evolution exhibit bipedalism with ricochet al locomotion, inhabit semiarid to arid environments and are solitary nocturnal burrowing animals. Howell (32) presents a good comparison of their gross osteological features except for the Macroscelididae whose osteology is described by Keen and Grobbelaar (41) and Evans (42).

In discussing the tympano-ossicular system of *Dipodomys*, it was pointed out that a force on the tympanic membrane could (if it were a frictionless system) be magnified 97.2 times at the fenestra ovale. This amplification, called the transformer ratio, is high compared to the cat's ratio of 60.7:1 and man's of 18.3:1 (Wever and Lawrence 54). Furthermore, due to the small mass of the ossicles and the unique structure of their ligaments and articulations, the resistance to vibration is very slight. Such low damping indicates not only a very efficient sound transmitting system but also one in which resonance

phenomena would occur. Electrophysiological studies (Webster 60) have shown a very irregular spectrum of hearing indicating that resonance exists. This investigation also demonstrated that damping is increased by reducing the middle ear volume and thus indicated an auditory significance to the hypertrophied middle ear cavity.

Of those animals known to possess a hypertrophied middle ear, *Meriones* is the only genus whose inner ear has also been described (Wisner, Legoux and Petter 54; Legoux and Wisner 55). In the organ of Corti, a striking convergence is found between *Dipodomys* and *Meriones*. In both forms, there is a hypertrophy of the cells of Hensen and a large hyaline mass underlying the organ of Corti. The inner ear differs in the two forms in several respects. In the kangaroo rat, the basilar membrane divides, enclosing a hyaline mass, whereas in *Meriones* the basilar membrane apparently is situated above the hyaline mass. Furthermore, in the kangaroo rat the cells of Hensen rest directly on the innermost cells of Claudius and not on the basilar membrane as they do in *Meriones* and in most other mammals. *Meriones* also lacks the cytoplasmic processes of Hensen's cells which in the kangaroo rat support an elevated reticular lamina. Legoux and Wisner made no measurements in *Meriones* to indicate variation in the relative sizes of the parts of the organ of Corti, although the length of the basilar membrane, however, *Meriones* possesses only two and one-half turns to its cochlear duct, as contrasted to the 4 and one quarter turns found in the kangaroo rat cochlea. In general, it appears that the cytology of the kangaroo rat's inner ear is even more specialized than that of *Meriones*. It would be appropriate to investigate the organ of Corti of other mammals with hypertrophied middle ears.

Pritchard's (1876) study of the organ of Corti in man, monkey, sheep, dog, cat, rat, guinea pig, rabbit, porpoise and kangaroo reveals that the microscopic anatomy of this organ is remarkably constant in all the mammals he studied. Shambaugh (32) states that the cells of Hensen may vary in size and shape in different species but in all species they rest on the basilar

membrane. Thus the bizarre anatomy of the organ of Corti in *Dipodomys* and *Meriones* is exceptional.

What special functions the bizarre organ of Corti in *Dipodomys* may serve is conjecture. Legoux and Wisner (55) make the suggestion that the hypertrophied cells of Hensen in *Meriones* have a protective function. They feel that in the case of very intense sounds these hypertrophied cells may absorb most of the sound energy especially at low frequencies and thus protect the delicate hair cells from injury.

Such a function may be operant in *Dipodomys* whose organ of Corti also possesses large cells of Hensen and a hyaline mass associated with the zona pectinata. In addition the fact that the kangaroo rat's tectorial membrane is suspended between the elevated vestibular lip of the spiral crista and the elevated reticular lamina over Hensen's cells may be of functional significance. With the tectorial membrane suspended in this way only the apical portions of the "hairs" of the hair cells are embedded in the membrane. Such a delicate mechanism could increase the sensitivity of the organ of Corti since it is generally believed that a bending of the "hairs" is an important factor in hearing (Davis 59).

The protective function proposed by Legoux and Wisner and the increased sensitivity function proposed here are not necessarily incompatible. In the case of an intense sound the large size of the hyaline mass and cells of Hensen and Claudius (all associated with the zona pectinata) may absorb enough energy to keep the whole basilar membrane from moving far enough to damage the delicate hair cells. However in the case of an extremely weak sound the more lightly damped zona tecta may vibrate independently of the zona pectinata and move sufficiently to bend the "hairs" that are embedded in the tectorial membrane and thus trigger the nerve impulse.

SUMMARY

1 The outstanding morphological feature of the kangaroo rat middle ear is the extreme hypertrophy of the middle ear cavity.

2 The middle ear cavity averages 0.49 cm³ in *D. merriami* and 0.88 cm³ in *D. spectabilis* of which 18% is entotympanic, 33% is posterior mastoid and 49% is anterior mastoid.

3 The kangaroo rat lacks superior and lateral ligaments of the malleus. The ossicles are suspended by the anterior ligament of the malleus and posterior ligament of the incus which form the axis of rotation. This feature combined with a large tympanic membrane (5.5 mm in diameter) and light ossicles (2.7 mg) lowers the system's threshold of vibration.

4 The transformer ratio of the tympano-ossicular system is 97:2:1. This efficiency combined with a low damping of the system indicates that resonance phenomena may occur.

5 There are 4¼ turns to the cochlear duct. The organ of Corti contains several peculiarities. The zona pectinata of the basilar membrane splits—some of the fibers pass above a hyaline mass and most of them travel under this mass.

6 The cells of Claudius extend internally to the cells of Deiter forming a cup upon which the cells of Hensen rest. The cells of Hensen send large cytoplasmic processes upward which elevate the reticular lamina.

ACKNOWLEDGMENTS

The author is deeply indebted to Professor P. W. Gilbert of the Department of Zoology, Cornell University for his constant guidance during this study. This research was carried out in part at the Southwestern Research Station of the American Museum of Natural History, Portal, Arizona. It was supported by a grant from the National Science Foundation.

LITERATURE CITED

- Bartholomew G. A. Jr. and H. Caswell Jr. 1951. Locomotion in kangaroo rats and its adaptive significance. *J. Mammal.* 32: 155-169.
 Bast T. H. 1928. The utriculo-endolymphatic valve. *Anat. Rec.* 40: 61-65.
 ———. 1930. Ossification of the otic capsule in human fetuses. *Carnegie Contrib. Embryol.* (no. 121): 21: 53-82.
 Békésy G. Von. 1941. Über die Messung der Schwingungsamplitude der Gehörknöchelchen mittels einer kapazitiven Sonde. *Akust. Zeits.* 6: 1-16.

- Carleton H and R A B Drury 1957 *Histological Technique* Oxford University Press London
- Cockerell T D A L I Miller and M Printz 1914 The auditory ossicles of American rodents *Bull Am Mus Nat Hist* 33 347-378
- Dahmann H 1930 Zur Physiologie des Horens experimentelle Untersuchungen über die Mechanik der Gehörknöchelchenkette sowie über deren Verhalten auf Ton und Luftdruck. *Ztschr Hals-Nas-Ohr h k* 27 329-368
- Davis H 1959 Excitation of auditory receptors In *Handbook of Physiology* Section 1 Neurophysiology vol I H W Magoun ed American Physiological Society Washington D C
- Dawson W R 1955 The relation of oxygen consumption to temperature in desert rodents *J Mammal* 36 543-553
- Evans F G 1942 The osteology and relationship of the elephant shrews (Macroscelididae) *Bull Am Mus Nat Hist* 80 85-125
- Fernández César 1952 Dimensions of the cochlea (guinea pig) *J Acoust Soc Am* 24 519-523
- Hatt R T 1932 Vertebral columns of ricochetal rodents *Bull. Am Mus Nat Hist* 63 599-738
- Hoffman E F and T H Bast 1930 A comparative study of the utricle-endolymphatic valve in some common mammals *Anat Rec* 46 333-347
- Howell A B 1932 The saltatorial rodent *Dipodomys* The functional and comparative anatomy of its muscular and osseous systems *Proc Am. Acad Arts Sci* 67 377-536
- Keen J A and C S Grobbelaar 1941 The comparative anatomy of the tympanic bulla and auditory ossicles with a note suggesting their function *Trans Roy Soc South Africa Cape Town* 28 307-329
- Kobayashi M 1950 The articulations of the auditory ossicles and their ligaments of various species of mammalian animals Hiroshima *J Med Sci.* 4 319-349
- Kristensen H 1949 Decalcification investigation with contributions to the histological technique of the internal ear *Acta Path* 26 666-60
- Legoux J P F Petter and A Wisner 1954 Etude de l'audition chez des mammifères à bulles tympaniques hypertrophées *Mammalia* 18 262-271
- Legoux J P and A Wisner 1955 Role fonctionnel des bulles tympaniques géantes de certaines rongeurs (*Meriones*) *Acustica* 5 209-216
- Pritchard U 1876 The organ of Corti in mammals *Proc Roy Soc London* 24 346-352
- Quay W B 1953 Seasonal and sexual differences in the dorsal skin gland of the kangaroo rat (*Dipodomys*) *J Mammal* 34 1-14
- 1954 The dorsal holocrine skin gland of the kangaroo rat (*Dipodomys*) *Anat Rec* 119 161-176
- Reynolds H G 1958 The ecology of the Merriam kangaroo rat (*Dipodomys merriami* Mearns) on the grazing lands of southern Arizona *Ecol. Monog* 28 111-127
- Richmond C R T T Trujillo and D W Martin 1960 Volume and turnover of body water in *Dipodomys deserti* with tritiated water *Proc Soc Exp Biol Med* 104 9-11
- Ryder J A 1878 On the form of the stapes in *Dipodomys* *Amer Nat* 12 125
- Schmidt Nielsen B and K. Schmidt Nielsen 1951 A complete account of the water metabolism in kangaroo rats and an experimental verification *J Cell. and Comp Physiol* 38 165-181
- Schmidt Nielsen K. and B Schmidt Nielsen 1952 Water metabolism of desert mammals *Physiol Rev* 32 135-166
- Shambaugh G E 1932 Cytology of the internal ear In E V Cowdry's *Special Cytology* Paul B Hoeber Inc New York vol III pp 1335-1367
- Straus W L Jr 1936 Electrical excitation of the cerebrum of the kangaroo rat *J Mammal* 17 374-382
- Vimtrup B J and B Schmidt Nielsen 1952 The histology of the kidney of kangaroo rats *Anat. Rec* 114 515-528
- Webster D B 1960 Auditory significance of the hypertrophied mastoid bullae in *Dipodomys* (Abstract) *Ibid* 136 299
- Wever E G and M Lawrence 1954 *Physiological Acoustics* Princeton Univ Press
- Wiggers H C 1937 The functions of the intraural muscles *Am J Physiol* 120 771-780
- Wisner A J P Legoux and F Petter 1954 Etude histologique de l'oreille d'un rongeur à bulles tympaniques hypertrophées *Meriones crassus* *Mammalia* 18 371-374

membrane. Thus the bizarre anatomy of the organ of Corti in *Dipodomys* and *Meriones* is exceptional.

What special functions the bizarre organ of Corti in *Dipodomys* may serve is conjecture. Legoux and Wisner (55) make the suggestion that the hypertrophied cells of Hensen in *Meriones* have a protective function. They feel that in the case of very intense sounds these hypertrophied cells may absorb most of the sound energy especially at low frequencies and thus protect the delicate hair cells from injury.

Such a function may be operant in *Dipodomys* whose organ of Corti also possesses large cells of Hensen and a hyaline mass associated with the zona pectinata. In addition the fact that the kangaroo rat's tectorial membrane is suspended between the elevated vestibular lip of the spiral crista and the elevated reticular lamina over Hensen's cells may be of functional significance. With the tectorial membrane suspended in this way only the apical portions of the "hairs" of the hair cells are embedded in the membrane. Such a delicate mechanism could increase the sensitivity of the organ of Corti since it is generally believed that a bending of the "hairs" is an important factor in hearing (Davis 59).

The protective function proposed by Legoux and Wisner and the increased sensitivity function proposed here are not necessarily incompatible. In the case of an intense sound the large size of the hyaline mass and cells of Hensen and Claudius (all associated with the zona pectinata) may absorb enough energy to keep the whole basilar membrane from moving far enough to damage the delicate hair cells. However in the case of an extremely weak sound the more lightly damped zona tecta may vibrate independently of the zona pectinata and move sufficiently to bend the "hairs" that are embedded in the tectorial membrane and thus trigger the nerve impulse.

SUMMARY

1 The outstanding morphological feature of the kangaroo rat middle ear is the extreme hypertrophy of the middle ear cavity.

2 The middle ear cavity averages 0.49 cm³ in *D. merriami* and 0.88 cm³ in *D. spectabilis* of which 18% is entotympanic, 33% is posterior mastoid and 49% is anterior mastoid.

3 The kangaroo rat lacks superior and lateral ligaments of the malleus. The ossicles are suspended by the anterior ligament of the malleus and posterior ligament of the incus which form the axis of rotation. This feature combined with a large tympanic membrane (5.5 mm in diameter) and light ossicles (2.7 mg) lowers the system's threshold of vibration.

4 The transformer ratio of the tympano-ossicular system is 97:2:1. This efficiency combined with a low damping of the system indicates that resonance phenomena may occur.

5 There are 4¼ turns to the cochlear duct. The organ of Corti contains several peculiarities. The zona pectinata of the basilar membrane splits—some of the fibers pass above a hyaline mass and most of them travel under this mass.

6 The cells of Claudius extend internally to the cells of Deiter forming a cup upon which the cells of Hensen rest. The cells of Hensen send large cytoplasmic processes upward which elevate the reticular lamina.

ACKNOWLEDGMENTS

The author is deeply indebted to Professor P. W. Gilbert of the Department of Zoology, Cornell University for his constant guidance during this study. This research was carried out in part at the Southwestern Research Station of the American Museum of Natural History, Portal, Arizona. It was supported by a grant from the National Science Foundation.

LITERATURE CITED

- Bartholomew G. A. Jr. and H. Caswell Jr. 1951. Locomotion in kangaroo rats and its adaptive significance. *J. Mammal.* 32: 155-169.
- Bast T. H. 1928. The utricle-endolymphatic valve. *Anat. Rec.* 40: 61-65.
- 1930. Ossification of the otic capsule in human fetuses. *Carnegie Contrib. Embryol.* (no. 121) 21: 53-82.
- Békésy G. Von. 1941. Über die Messung der Schwingungsamplitude der Gehörknöchelchen mittels einer kapazitiven Sonde. *Akust. Zeits.* 6: 1-16.

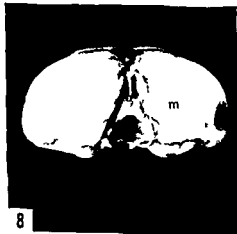


PLATE 2

EXPLANATION OF FIGURES

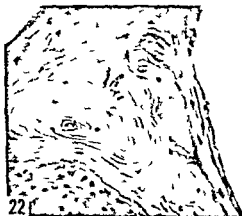
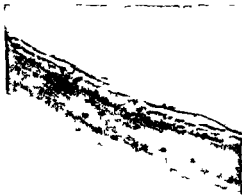
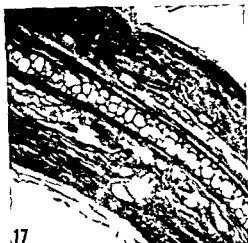
- 10 Mashed bullae of *Dipodomys merriami*, dorsal view of interior / 7.8
- 11 Posterior mashed bulla of *Dipodomys merriami*, caudal view of interior / 7.5
- 12 Endotympanic cavity of *Dipodomys merriami*, ventral view of interior c, cochlear t. tensor tympani muscle canal, s. canal = stapedial artery / 9.8
- 13 Reconstruction of the osseous labyrinth and associated nerves and vessels of *Dipodomys merriami*, lateral aspect. s. sapes
- 14 Fenestra rotunda in reconstruction of osseous labyrinth of *Dipodomys merriami*.
- 15 Valves and incus of *Dipodomys merriami*, ventro-lateral aspect. / 12.6
- 16 Sapes of *Dipodomys merriami*, ventro-medial aspect. / 20.9



PLATE 3

EXPLANATION OF FIGURES

- 17 Pinna of *Dipodomys merriami* transection $\times 110$
- 18 Sebaceous glands on antitragus of the external ear of *Dipodomys merriami* $\times 136$
- 19 Malleo-incudo joint of *Dipodomys merriami* Note the elastic fibers along the articular facets Orcein stain $\times 265$
- 20 Incudo-stapedial joint of *Dipodomys merriami* Note possible elastic fibers in the capsular ligament Orcein stain $\times 265$
- 21 Wall of anterior mastoid bulla of *Dipodomys merriami* H and E $\times 220$
- 22 Thickened portion of the cochlear wall of *Dipodomys merriami* $\times 259$



A Study of the Subgross Pulmonary Anatomy in Various Mammals^{1,2}

RICHARD F McLAUGHLIN¹ WALTER S TYLER
AND ROBERT O CANADA²

*Clinical Investigation Center U S Naval Hospital Oakland California
and Department of Anatomy School of Veterinary Medicine University
of California Davis California*

The present study is part of an investigative project designed to classify pulmonary emphysema in the human being. One phase of the study called for an animal to be used experimentally in an effort to produce emphysema. It appeared logical to select an animal possessing a lung anatomically similar to that of man. However a review of the literature showed surprisingly little precise information regarding the comparative anatomy of the lung in various species of mammals although for many years certain species differences in lungs have been recognized (Aeby 1880 Narath 01). Degrees of lobation and lobulation have been noted to be widely variable (Sisson and Grossman 56 and Hartman and Strauss 33) and a distinction has been made between animals with thick and thin pleurae (Miller 07). It has been shown that the rabbit does not possess respiratory bronchioles but that many other animals do (Loosli 38). Differences in the distribution of the bronchial artery have been reported (Miller 07) but the extent of distribution of this vessel has been the subject of disagreement. A parenchymal supply has been claimed by some (Le Fort 1858 Cudkowiec and Armstrong 51) denied by others (Miller 50). Similarly the existence of precapillary bronchial artery pulmonary artery anastomoses had been claimed by some (Ruysch 1721 Zuckerkandl 1883) but denied by others (Guil lot 1845 Miller 50).

To date little attempt has been made to define the distribution of these differences between various mammalian species or to inquire into the possible existence of added differences. Also little attempt has been made to correlate these differences with

possible attendant differences in physiology or potential pathology. Their significance however slight or marked therefore remains largely unknown. In addition the presence of these known anatomical variations has apparently had little influence on the choice of experimental animals in pulmonary studies (Tucker and Krementz 57). This is especially notable in those animal studies which have been made in substitution for studies in man since thus far no species of lung has been demonstrated to be entirely suitable for such a substitution.

The purpose of this paper is to describe the main subgross anatomical features of the lungs of various mammals to compare these features and to discuss their possible significance.

MATERIAL AND METHODS

Seven individual species of healthy young mammals were studied in the pro-

Received for publication July 1959

Supported (in part) by Contract Nonr 222(01) between the University of California (San Francisco) and the Office of Naval Research Department of the Navy. The opinions or assertions contained herein are the private ones of the authors and are not to be construed as official or necessarily as reflecting the views of the Medical Department of the Navy or the Naval Service at large.

¹Presented (in part) at the Meeting of the American College of Chest Physicians Atlantic City N J and (in part) at the Second Conference on Research in Emphysema Aspen Colorado both held in June 1959.

Present address c/o Clinical Investigation Center U S Naval Hospital Oakland 14 California

Department of Anatomy School of Veterinary Medicine University of California Davis California

Present address Captain R O Canada MC USN Commanding Officer U S Naval Hospital Jacksonville Florida

ess of which a total of 45 pairs of normal lungs was used. Most of the specimens were obtained directly from animals in the laboratory immediately following sacrifice by pentothal anesthesia and exsanguination. A few of the larger specimens however were obtained fresh from local abattoirs. The animals studied were as follows: calves (10), cows (3), lambs (5), pigs (5), dogs (5), cats (4), Rhesus monkey (1), horses (12).

The use of latex injection specimens according to the thin slice technique of Schalm and Haring (39) as modified by Julian (58) constituted the principal method of study but in addition several vinylite¹ corrosion casts were made for comparative purposes (Narat, Loeff and Narat 36). All specimens were inflated prior to injection and then via cannulae in the pulmonary artery, the left atrium and the bronchial artery were washed thoroughly with normal saline and or water to clear them of blood. No detectable difference could be noted between those specimens washed with saline and those washed with water. The average interval between sacrifice and injection was approximately one hour. Three basic colors of latex—red, blue and yellow—were used. A 4th color, green, was produced by blending blue and yellow. Generally red was used in the bronchial artery, blue in the pulmonary artery, yellow in the pulmonary vein and green in the airways. This also constituted the order of injection of these structures. Injection pressures varied from 2 to 5 pounds per square inch. Rapid solidification of the latex and fixation of tissues were accomplished by means of intratracheal injection of a 10% formalin solution mixed with small amounts of weak acetic acid and immersion of the entire specimen into vats containing a similar fluid for 24 to 48 hours. Following this the prepared lungs were quick frozen and then using an ordinary bacon slicer they were sectioned into slices approximately 3 to 4 mm in thickness. Lastly these sections were studied serially under a dissecting microscope. Since all the structures listed above were injected with different colored latex, it was quite easy to identify them. Each could be followed from the hilum to its termination or origin as the case might be.

Anastomoses between vessels e.g. the bronchial artery and pulmonary artery could be readily identified if present. Penetration of the latex into capillaries (figs 5, 6) was regularly observed and as an advantage of this technique in contrast to vinylite corrosion techniques, all injected structures could be studied in relation to intact surrounding tissues. Measurements were made with an overlying glass disc ruled with divisions 100 μ apart.

In general we found this subgross thin slice latex injection technique to be a satisfactory and comparatively uncomplicated method of study. Artefacts such as blood vessel blow outs because of their characteristic appearance were easily recognizable when present but were infrequent in occurrence.

RESULTS

A tabulation of the data obtained from these specimens has permitted them to be grouped into three distinctive subgross lung types (table 1). The cow, sheep and pig possess what has been arbitrarily designated as subgross lung type I. The monkey, dog and cat lungs have been designated in common as type II and the horse lung as type III.

Lung type I (fig. 1) is characterized by the presence of extremely well developed secondary lobules, marked interlobular septa and a thick pleura (fig. 7). The most distal airways are composed of numerous terminal bronchioles (fig. 12) leading either directly into alveolar ducts or infrequently into poorly developed respiratory bronchioles with only minimal alveolar budding taking place just proximal to the junction with the alveolar duct (fig. 11). It should be noted that each of these secondary lobules because of their extreme development constitutes in itself what might be thought of as a small individual lung. In addition the constituents of the bronchovascular tree by virtue of this marked septation have only a limited number of pathways to follow and consequently maintain a close relationship throughout.

— — —
Water soluble latex obtained from the General Latex and Chemical Corporation Cambridge, Massachusetts.

¹Acetone soluble vinylite obtained from the Bakelite Co. New York City, New York.

TABLE 1
Sub gross lung types found in 7 species of mammals

	Sub-g r type			III H r o e
	I C o w h e p p l g	II M n k e y c a t d g		
Lobulation	Extremely well developed	Absent		Imperfect development
	Thick	Thin		Thick
Arterial supply to pleura	Bronchial artery	Pulmonary artery		Bronchial artery
	O P V B R B A P A	O P V B R B A P A	O P V B R B A P A	Distal O P V B R B A P A Proximal O P V B R B A P A
General bronchovascular relationship				
Intrapulmonary termination of bronchial artery	Distal airways	Distal airways		Distal airways and alveoli
Terminal bronchioles	Present Predominant distal airway	Absent		Present
Respiratory bronchioles	Infrequently observed Extremely poor development	Present Very well developed		Present Poorly developed
Bronchial artery pulmonary artery shunts	Present Not however demonstrated in the pig	Not demonstrated		Present

TYPE I Calf, Cow, Sheep, Pig

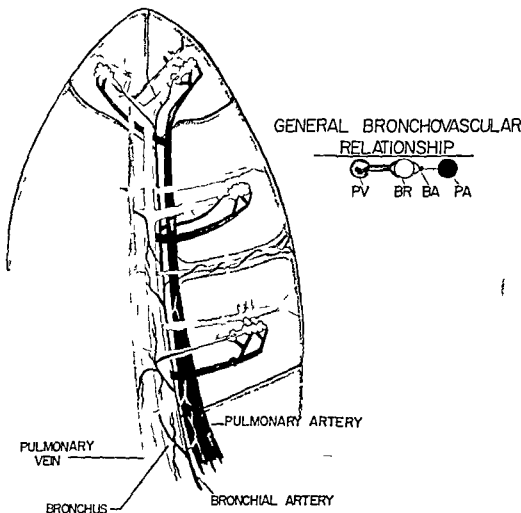


Fig 1 Diagrammatic representation of essential subgross characteristics of lung type I

their intrapulmonary course (fig 21) The bronchus is followed intimately in this lung type not only by the pulmonary artery but also by the pulmonary vein. In general the bronchus is located centrally with the pulmonary artery on one side and the pulmonary vein on the other (fig 20) The bronchial artery after leaving the aorta or the intercostal arteries proceeds to the posterior wall of the main stem bronchi. At this point branches are given directly to the hilar lymph nodes and the pleura. The bronchial artery can then be followed in its

intrapulmonary course winding about and supplying the entire wall of the bronchus (fig 20) At intervals branches are given in the form of vasa vasorum to the pulmonary artery a few also are seen to supply the pulmonary vein. Numerous other branches leave the vicinity of the bronchi and after supplying the interlobular septa progress to the pleura where they form a rich arterial network of vessels anastomosing frequently with those branches from the hilum (fig 7) The main portion of the bronchial artery then continues along the

bronchial wall and finally terminates in the distal portion of the terminal bronchiole (fig 12). The major portion of bronchial arterial blood is drained by tributaries of the pulmonary vein but in the first two to three divisions of the trachea drainage is accomplished by the azygos system as shown by Liebow (53). The remainder of the terminal bronchioles the alveolar ducts and alveoli are supplied by the pulmonary artery. Pulmonary arterial blood and bronchial arterial blood mix at the level of the terminal bronchiole in a common capillary bed but in addition a small number of bronchial arteriolar pul

monary arteriolar anastomoses (fig 25) were found to exist normally at this level.

Lung type II (fig 2) on the other hand is characterized by the absence of secondary lobules only ill-defined haphazard in traparenchymal supportive tissue strands and an extremely thin membranous pleura (fig 8). The most distal airways are composed of numerous well developed respiratory bronchioles leading into large alveolar ducts (fig 13). The monkey is an extreme example of this possessing only short large well alveolarized bronchioles which terminate in lengthy alveolar ducts (fig 4). The diameter of the

TYPE II DOG, CAT, MONKEY

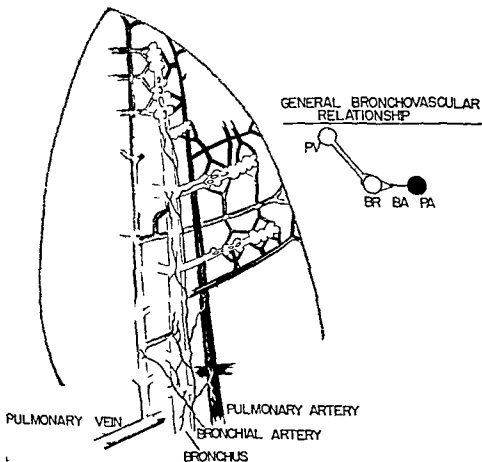


Fig 2 Diagrammatic representation of essential subgross characteristics of lung type II

the bronchial arteries in human beings. In 1951 this was reaffirmed by Cudkowicz. The opposition to this point of view has its staunchest support in the work of Miller (50). Apparently however Miller has relied heavily on the anatomy in dogs and cats and he has been criticized for using pathologic human material in his normal study (Loosli 38). Although Miller noted in 1907 that a difference in the pleural blood supply existed between animals nowhere in his published works is it found that he did a comparative study of the intrapulmonary features of various mammalian lungs other than in the dog and cat (Miller 13 '25).

The meaning of this variation in distribution of the bronchial artery as found in the horse is not clear. However this artery is known to be a nutrient vessel with a distribution primarily to the proximal airways and supportive tissues of the lung. The alveoli and respiratory bronchioles are primarily diffusing tissues. Theoretically they are capable of extracting their required oxygen either from the surrounding air (Ghoreyeb and Karsner 13) or from pulmonary arterial blood (Comroe 58). Therefore an explanation of this alveolar bronchial artery supply might be the nutritive requirement of an increased amount of supportive tissue not primarily diffusing in nature in the region of the alveolus. If this be true the possibility exists that an occlusive lesion of the bronchial arteries might cause widespread degeneration of supportive tissue similar to that seen in generalized emphysema. One would not expect such an event to occur in animals possessing lungs of types I or II.

The presence of normally occurring bronchial artery pulmonary artery anastomoses was first noted in 1721 by Ruysch and thereafter by many others. Nakamura (58), Verloop (48), Marchand, Gilroy and Watson (50), von Hayek (53) and Tobin (52) have all claimed their normal but relatively nonfunctional existence in the human being. Miller (50) is the principal antagonist of this viewpoint. In criticism of the latter's views his conclusions were based upon dog lung injection studies in which all of the vascular channels were first filled with a solution

under pressure and then were injected with various sized colored particles designed to stop at the arteriolar level. As early as 1913 Ghoreyeb and Karsner demonstrated with perfusion studies in dogs that bronchial artery flow would remain constant at a certain low level when pressure was maintained in the pulmonary artery and vein but that increases in bronchial artery flow would occur in response to a relative drop in pulmonary artery pressure. Berry, Brailsford and Daly in 1931 and Nakamura in 1958 reaffirmed this. Our own studies in which bronchial artery pulmonary artery anastomoses were demonstrated were accomplished by injecting the bronchial artery first with no pressure on the pulmonary artery or vein and then by injecting the pulmonary artery and vein afterwards. It is distinctly possible therefore that simultaneous pressures in all three vessels would have rendered the shunts inoperable and hence uninjectable. This viewpoint is further supported by Verloop's (48) demonstration of thickened bronchial artery and arteriolar muscular coats which are capable of acting as valves. In other words the anastomoses between the bronchial artery and pulmonary artery should be considered as *functional or demand shunts*.

In addition little work has been done on a comparative basis in regard to the normal existence of bronchial artery pulmonary artery anastomoses. Verloop (48, 49) found these shunts in the human being but was unable to find them in rats. Ellis, Grindlay and Edwards (52) also were unable to find them in rats. Nakamura (58) was unable to demonstrate their existence either by anatomic or physiologic methods in dogs. The possibility that the absence or presence of these shunts is species-dependent is therefore inferred. Certainly the mere fact of failing to demonstrate them in one or another species does not conclusively deny their existence in that species. It is however highly suggestive and agrees well with our own findings in which we also failed to demonstrate normally occurring bronchial artery pulmonary artery shunts in certain species, especially the dog.

In conclusion these findings suggest the need for a comparative physiology pathol-

ogy and histology of mammalian lungs. In addition a detailed interspecies survey of the incidence of generalized pulmonary emphysema in mammals would be interesting and pertinent. Also for the present great caution should be exercised in the choice of an experimental animal for pulmonary studies if they are to be applied to man. This is especially so if the dog, cat or monkey are to be used in view of their marked anatomical differences from man. Finally it is suggested that in many respects the horse lung may be anatomically more comparable to that of the human than any other presently known species.

SUMMARY

The main subgross anatomical features of the lungs of various mammals are presented. A tabulation of these features permits the lungs to be grouped into three distinctive subgross types. Type I is represented by the cow, sheep and pig; type II by the dog, cat and monkey; type III by the horse. Lobularity is extremely well developed in type I, absent in type II, imperfectly developed in type III. The pleura and interlobular septa are thick in types I and III, the pleura is extremely thin in type II and septa are absent. Arterial supply to the pleura in types I and III is provided by the bronchial artery, and in type II by the pulmonary artery. In types I, II and III the bronchial artery terminates in a capillary bed shared in common with the pulmonary artery at the level of the distal bronchiole. In type III the bronchial artery also provides blood directly to the alveolar capillary bed. True terminal bronchioles comprise the most frequent form taken by the distal airways in types I and III, although small numbers of poorly developed respiratory bronchioles are present. Well developed respiratory bronchioles on the other hand appear to be the only form taken by the distal airways in type II. In type I the pulmonary vein closely follows the course of the bronchus and the pulmonary artery from the periphery to the hilum. This may be due to the heavy interlobular connective tissue barriers present. In type III this general relationship is maintained peripherally but not centrally where the pulmonary vein follows a more independent path to the hilum as

is the case throughout the lung in type II. A small number of bronchial arteriolar pulmonary arteriolar anastomoses are seen in types I and III. None are found in type II.

The functional significance of these anatomical differences is unknown. However great care is urged in the choice of experimental animals to be used in pulmonary studies made in substitution for those in man. On the other hand the human lung and the horse lung seem to be remarkably alike in many of their respective subgross characteristics.

There is a need for understanding these differences on a basis of further study in the fields of comparative mammalian physiology, pathology and histology.

ACKNOWLEDGMENTS

The authors are grateful to Dr. Julius H. Comroe, Jr., University of California Medical Center, San Francisco; Dr. Logan M. Julian, University of California School of Veterinary Medicine, Davis; and Dr. R. M. Hood, Austin, Texas, for their suggestions and criticisms of this material.

We are also grateful to Dr. Larry Z. McFarland and Dr. Peter Manelis, Department of Anatomy, University of California, Davis; and Mr. R. T. McLaughlin, medical student, The Creighton University School of Medicine, Omaha, Nebraska, for technical assistance in the preparation of many of the specimens studied.

We are indebted to H. M. C. J. Stevenson, USN Photographic Arts Section, U. S. Naval Hospital, Oakland, Calif., for the photographs used in this study.

LITERATURE CITED

- Aeby, C. T. 1880. *Der Bronchialbaum der Säugethiere und des Menschen*. W. Engelmann, Leipzig.
- Alexander, A. F. 1938. Chronic Alveolar Emphysema in the Horse. Booklet of the Aspen Conference on Research in Emphysema, June 28.
- Berry, J. L. and I. de Burgh Daly. 1931. The relation between the pulmonary and bronchial vascular systems. *Proc. Roy. Soc., London* 109(B): 319-336.
- Berry, J. L., J. F. Brailsford and I. de Burgh Daly. 1931. The bronchial vascular system in the dog. *Ibid.* 109(B): 214-228.
- Birnbaum, G. L. 1934. Anatomy of the Bronchovascular System. Its Applications to Surgery. The Yearbook Publishers, Inc., Chicago.
- Comroe, J. 1938. Personal communication.

- Cudkowicz L and J Armstrong 1951 Observations on the normal anatomy of the bronchial arteries *Thorax* 6 343-358
- Ellis F H Jr J H Grindlay and J E Edwards 1951 The bronchial arteries I Experimental occlusion *Surgery* 30 810-826
- 1952 The bronchial arteries III Structural changes after division of the rats left pulmonary artery *Am J Path* 28 89-103
- Ghoreyeb A A and H T Karsner 1913 A study of the relation of pulmonary and bronchial circulation *J Exp Med* 18 500-506
- Guillot N 1845 Recherches anatomiques et pathologiques sur les Amas de Charbon produits pendant la vie dans les organes respiratoires Quoted by Berry Brailsford and Daly 31
- Hartman G C and W L Strauss Jr 1933 The Anatomy of the Rhesus Monkey Williams and Wilkins Co Baltimore 213
- Julian L K 1958 Personal communication
- Kennedy P C 1958 Personal communication
- Le Fort L 1808 Recherches sur l'Anatomie du poulmon chez l'homme Thèse Paris Quoted by Berry Brailsford and Daly 31
- Liebow A A 1953 The bronchopulmonary venous collateral circulation with special reference to emphysema *Am J Path* 29 251-283
- Loosli C G 1938 The structure of the respiratory portion of the mammalian lung with notes on the lining of the frog lung *Am J Anat* 62 375-425
- McLean K H 1959 The pathogenesis of pulmonary emphysema *Am J Med* 25 62-74
- Marchand P J J C Gilroy and V H Watson 1950 An anatomical study of the bronchial vascular system and its variation in disease *Thorax* 5 207-221
- Müller W S 1907 The vascular supply of the pleura pulmonalis *Am J Anat* 7 389-407
- 1913 The air spaces in the lung of the cat *J Morph* 24 459-478
- 1925 The vascular supply of the bronchial tree *Am Rev Tuberc* 12 87-94
- 1950 The Lung 2nd ed C C Thomas Springfield Ill
- Nakamura T 1958 Bronchopulmonary circulation President Lecture 22nd Annual Meeting of The Japanese Circulation Society Sendai
- Narat J K J A Loef and M Narat 1936 On the preparation of multicolored corrosion specimens *Anat Rec* 64 155-160
- Narath A 1901 Der Bronchialbaum der Säugethiere und des Menschen *Bibl Medica Stuttgart*
- Ruysch F 1721 Opera omnia I—Epistola Anatomica Problematica Sexta Amstelredami apud Janssonio-Walsbergios Quoted by Berry Brailsford and Daly 31
- Schalm W and C M Haring 1939 A method for preparing bovine udders for the study of the pathology of mastitis *J Am Vet M A* 94 372-373
- Sisson S and J D Grossman 1956 The Anatomy of the Domestic Animals 4th ed rev W B Saunders Philadelphia and London
- Tobin C E 1932 The bronchial arteries and their connections with other vessels in the human lung *Surg Gyn Obst* 95 741-750
- Tucker J L and E T Krementz 1957 Anatomical corrosion specimens II Bronchopulmonary anatomy in the dog *Anat Rec* 127 667-676
- Van Allen C M and G E Lindskog 1931 Collateral respiration in the lung *Surg Gyn Obst* 53 16-21
- Verloop M C 1948 The arteriae bronchiales and their anastomoses with the arteria pulmonalis in the human lung a mikroanatomical study *Acta Anat* 5 171-205
- 1949 On the arteriae bronchiales and their anastomosing with the arteria pulmonalis in some rodents a mikroanatomical study *Ibid* 7 1-32
- Von Hayek H 1953 Die Menschliche Lunge Gott Heidel Berlin
- Zuckerkindl E 1883 Ueber die verbindungen Zwischen den arteriellen Gefässen der menschlichen lunge Sitzungsberichte der kais Akademie der Wissenschaften in Wien Math naturwiss Klasse 8^o 171-186

PLATE 1

EXPLANATION OF FIGURE

- 4 Thin slice of monkey lung showing unusual character of distal airways. Note Remarkable early alveolarization of large bronchiole which terminates almost immediately into two large alveolar ducts. Compare with figures 11-15. Scale 100 μ /division

LUNG TYPES IN MAMMALS
 (a) hard F V L ughlin W ll S Tyl r and R bert O Canada

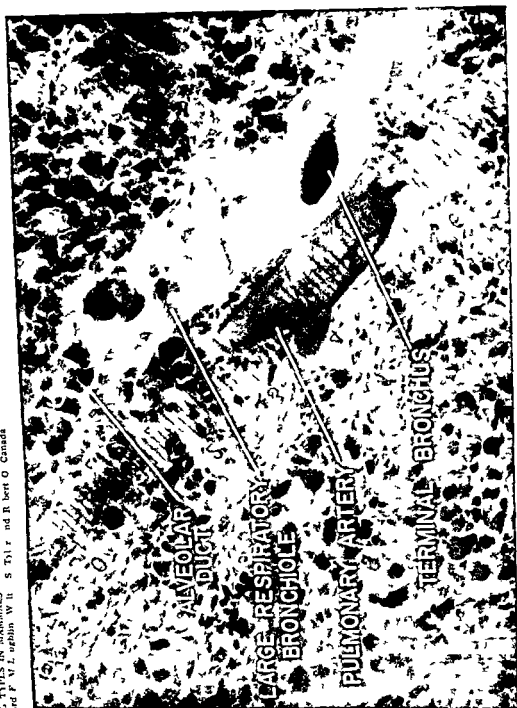


PLATE 2

EXPLANATION OF FIGURES

- 5 Thin slice of monkey lung type II Teased specimen Note blue latex from pulmonary artery filling alveolar capillary network $\times 90$
- 6 Histologic section of horse lung type III Note red latex injected in bronchial artery filling alveolar capillaries $\times 200$
- 7 Thin slice of cow lung type I Note remarkably complete development of lobules thick pleura and interlobular septa rich bronchial artery supply (red latex) to pleura interlobular septa and bronchi $\times 4$
- 8 Thin slice of dog lung type II near hilum Note thin pleura absence of lobules and limiting septa pulmonary artery (blue latex) supply and pulmonary vein (yellow latex) drainage of pleura rich bronchial artery (red latex) supply to lymph node not drained by pulmonary vein > 1
- 9 Thin slice of horse lung type III Note incomplete development of lobules thick pleura and interlobular septa extremely rich bronchial artery (red latex) supply to pleura interlobular septa and bronchi $\times 2$
- 10 Vinylite corrosion cast of horse lung type III dorsal surface Bronchial artery yellow vinylite pulmonary artery blue vinylite pulmonary vein red vinylite Note extreme development of bronchial artery supply especially pleural $\times 1/10$

Richard F. McLaughlin, Walter S. Tyler, and Robert O. Canada

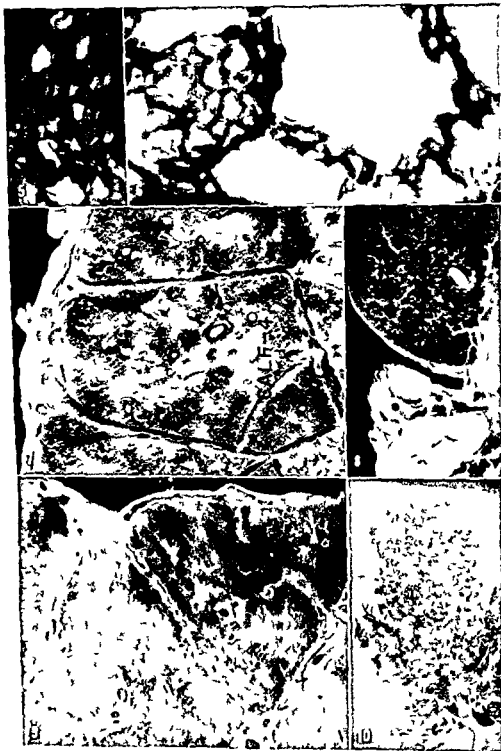


PLATE 3

EXPLANATION OF FIGURES

- 11 Thin slice of pig lung type I Poorly developed respiratory bronchiole Note scanty alveolarization of distal portion of bronchiole (left midportion of figure) Scale 100 μ /division
- 12 Thin slice of pig lung type I Terminal bronchiole Note unalveolarized distal portion of bronchiole and termination of bronchial arteriolar (red latex) supply at this level Scale 100 μ /division
- 13 Thin slice of dog lung type II Respiratory bronchiole Note extensive alveolarization of distal bronchiole prior to formation of alveolar duct termination of bronchial arteriolar (red latex) supply at this level Scale 100 μ /division
- 14 Thin slice of horse lung type III Terminal bronchiole Note unalveolarized distal bronchioles extensive bronchial artery (red latex) supply with branches directly supplying the alveolar capillary bed Scale 100 μ /division
- 15 Thin slice of horse lung type III Poorly developed respiratory bronchiole Note poor alveolarization of distal portion of bronchiole Scale 100 μ /division
- 16 Vinylite corrosion cast of horse lung type III Truncated specimen Note the closeness with which the pulmonary artery (blue vinylite) is followed by the bronchial artery (yellow vinylite) extreme degree of proximal and distal bronchial artery development $\times 1$
- 17 Thin slice of horse lung type III Bronchial artery red latex pulmonary artery blue latex Note the presence of direct bronchial artery supply to the alveolar capillary bed Scale 100 μ division
- 18 Thin slice of horse lung type III Colors as in figure 17 Note the presence of direct bronchial artery supply to the alveolar capillary bed Scale 100 μ /division

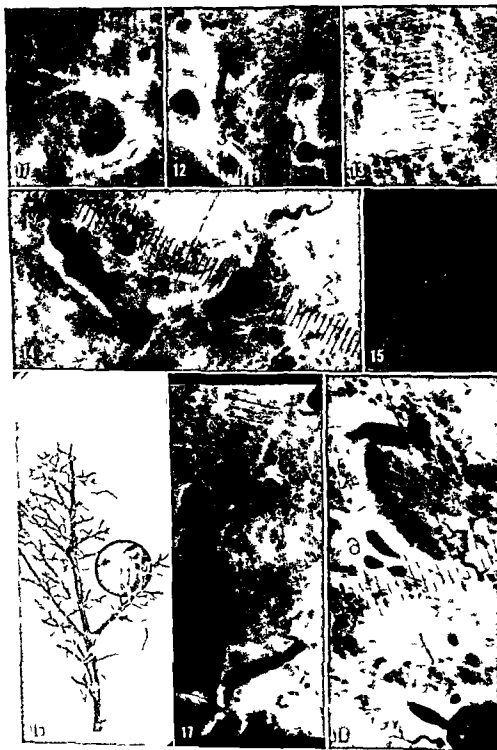
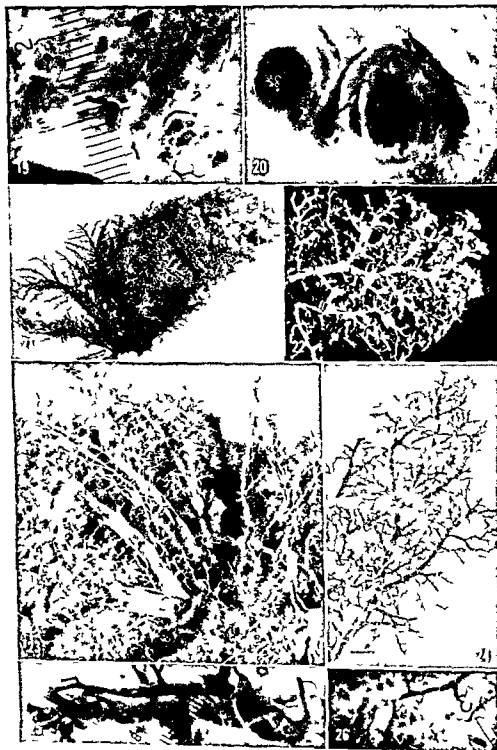


PLATE 4

EXPLANATION OF FIGURES

- 19 Thin slice of horse lung type III Bronchial artery red latex pulmonary artery blue latex Note the presence of bronchial artery supply meeting directly with pulmonary artery supply in alveolar capillaries Scale 100 μ /division
- 20 Thin slice of calf lung type I Glycerin cleared specimen Bronchial artery red latex pulmonary vein yellow latex Note general bronchovascular relationships with the pulmonary artery to the left the bronchus in the center and the pulmonary vein to the right pulmonary vein drainage of bronchial wall Scale 100 μ /division
- 21 Vinylite corrosion cast of calf lung Pulmonary artery blue vinylite pulmonary vein red vinylite Note the close relationship and common course of the pulmonary artery and vein both distally and proximally \times 1/6
- 22 Vinylite corrosion cast of dog lung type II Pulmonary artery blue vinylite pulmonary vein yellow vinylite Note the independent course of the pulmonary vein and pulmonary artery in comparison with the common course seen in type I \times 3
- 23 Vinylite corrosion cast of horse lung type III Bronchial artery yellow vinylite pulmonary artery blue vinylite pulmonary vein red vinylite Note central independence of pulmonary vein from pulmonary artery extensive general bronchial artery supply bronchial artery supply to pulmonary vein \times 1/6
- 24 Vinylite corrosion cast of horse lung type III Trimmed specimen Colors as in figure 23 Note close relationship of pulmonary artery and vein distally pulmonary vein draws away from pulmonary artery centrally following an independent course to the hilum extensive distal bronchial artery distribution \times 2
- 25 Thin slice of lamb lung type I Teased specimen Bronchial artery red latex pulmonary artery blue latex pulmonary vein yellow latex bronchiole green latex Note pulmonary artery top with splotches of red latex bronchial artery winding along bronchiole anastomosis of bronchial arteriole with pulmonary arteriole top left (specimen broken at site of anastomosis in teasing process) bronchial artery injected first accounting for splotches of red latex in pulmonary artery pulmonary artery injected secondly accounting for splotches of blue in bronchial artery by means of retrograde flow Scale 100 μ division
- 26 Thin slice of horse lung type III Colors as in figure 25 Note anastomosis of pulmonary arteriole with bronchial arteriole Scale 100 μ /division



Studies on Adrenal Transplantation

I HOMOLOGOUS AND AUTOGENOUS TRANSPLANTS

GERALD P. BODEY¹, OLGA MIODUSZEWSKA² AND GEORGE O. GEY
Finney Howell Cancer Research Laboratory Department of Surgery
The Johns Hopkins University School of Medicine
Baltimore Maryland

While attempting transplantation of rat adrenal tissue maintained *in vitro* for over 20 years into adrenalectomized rats our interest was aroused in studying the functional capacity of autogenous and homologous transplants maintained *in vitro* for varying periods of time. Although numerous attempts at autografts and homografts of rat adrenals have been made few reports concerning tissue culture transplants are available.

Lux et al (38a, 36b) attempted homologous transplantation after growing fragments of the adrenal in media containing the host's serum. Martinovitch (55) has successfully transplanted adrenal cortex maintained in organ culture but only when the tissue was taken from rats 4 to 5 days old.

The following experiments were devised to test whether the adrenal gland when removed from a rat and grown in tissue culture for 7 to 48 days can successfully survive and maintain function when grafted back into the same rat. Whole adrenal transplants and some homologous transplants of tissue maintained *in vitro* from 10 to 77 days were also attempted. Also the effects of ACTH on these cells in tissue culture was studied.

METHODS AND MATERIALS

The animals used in these experiments were from a colony of hooded rats inbred for 19 years. The animals were pen mated and every effort made to prevent litter mating.*

Whole adrenal transplants. Eleven rats of both sexes 25 to 44 days old served as hosts and donors. Both adrenals were removed on the day of transplantation and placed *in toto* in balanced salt solution. One gland from each animal was trans-

planted into the groin of one of the other animals along with some blood charcoal as a marker. An incision was made over the right femoral fossa and the whole gland coated with the carbon marker was inserted. The animals were maintained on a regular diet with no saline supplements.

Autogenous transplants. This group consisted of 15 animals of both sexes 37 to 75 days old. One adrenal was removed and cut into 32 to 36 fragments about 1.5 mm in diameter. Special care was taken to include the capsule but the medulla was eliminated. The tissue was explanted into two tubes coated with reconstituted collagen (Ehrmann and Gey 56) and incubated in roller drums at 37°C. The medium consisted of Gey's balanced salt solution, Eagle's basal medium (without glutamine) and human placental serum (4:3:3) with the addition of penicillin (100 units per ml) and streptomycin (50 units per ml). The cultures were treated three to 6 times per week depending upon the rapidity of pH drop. At a later date (7 days in three cases, 8 to 10 days in 6 cases, 13 days in three cases and 48 days in three cases) the remaining adrenal was removed and the tissue culture fragments from the same animal were inoculated into the right femoral fossa. This was done by making a small incision and inserting a pipette through the subcutaneous tissue to the femoral fossa. These animals were

¹ Henry Strong Denison Fellow 1958-59, 1959-60.

² Rockefeller Foundation Fellow 1958-59.

*We are indebted to Dr. Eleanor Delfs for supplying these pen-bred rats. These rats were the only ones available which in any way resembled those used in earlier studies of adrenal tissue cultures in this laboratory.

maintained on a regular diet with 0.9% saline supplements *ad libitum* for 4 to 21 days

Homologous transplants This group consisted of 10 animals of both sexes 40 to 48 days old. One adrenal was removed and placed in tissue culture as above. At a later date (10 days in two cases, 28 days in 4 cases and 79 days in 4 cases) the second adrenal was removed and the tissue culture fragments were inoculated as above. The animals were paired in such a fashion that each pair exchanged adrenal tissue. These animals were maintained on a regular diet with saline supplements up to three weeks.

ACTH treated cultures About 90 cultures (including some of the above) were treated as described above. In addition ACTH¹ 1/125 or 1/250 IU per ml of medium was added to one half of the cultures so that the tissue from one half of the animals was subjected to ACTH, the remaining half serving as a control. If necessary the tissue cultures were transferred every two to three weeks.

RESULTS

Whole adrenal transplants

Of the group of 11 rats only three lived longer than two weeks. Autopsy of those animals which died showed necrotic adrenal tissue in the right femoral fossa with no normal adrenal tissue. Microscopic sections were not made of this necrotic material. The following animals survived this procedure.

Rat 1249 Four months after transplantation the groin was explored. In the right femoral fossa a purplish hypertrophied adrenal gland was found having a good blood supply via an artery derived from the femoral artery. The adrenal graft was removed and the incision sutured. The animal was maintained on a regular diet and expired two weeks later. Autopsy revealed no adrenal tissue remaining either in the groin or adjacent to the kidneys.

Rat 1250 Four months after transplantation the right femoral fossa of this rat was explored. A typical appearing adrenal gland was found with a good blood supply from the femoral artery. Two weeks

after removal of this graft the animal died. On autopsy no adrenal tissue was found anywhere in this animal.

Rat 1251 Nine months following transplantation this animal was sacrificed. An hypertrophied adrenal was found in the right femoral fossa. No other adrenal tissue was discovered.

In all three cases the graft appeared like a typical adrenal adenoma. However the central portion contained no cells and no medullary tissue could be located in these grafts. (See fig 1)

Autogenous transplants

The three rats whose adrenal tissue had remained *in vitro* for only 7 days remained healthy. Two months after transplantation the right femoral fossae of these animals were explored and the purplish nodules of adrenal tissue were removed. All three animals died within 23 days after the removal of the adrenal transplants.

Of the 6 animals whose adrenal had been maintained *in vitro* for 8 to 10 days two died within 21 days. Two of the animals died 5 to 6 months after transplantation. Examination of the graft sites revealed several nodules of healthy looking tissue. It was not possible to ascertain whether these rats died from adrenal insufficiency or from some other cause. However these grafts must have functioned up to the time of their demise for the rats to have survived for that length of time. The remaining two rats were explored 7 months after transplantation. Several small nodules of purplish adrenal tissue with a good blood supply from the femoral vessels were found. One animal died 23 days after removal of its grafts. The other was sacrificed and re-explored and several more nodules were found in the groin but none adjacent to the kidneys.

The three rats whose adrenal tissue remained *in vitro* for 13 days and the three rats whose tissue remained *in vitro* for 48 days all died within 20 days of transplantation. Tissue was removed from some of these animals for microscopic examination. Generally the nodules appear small and diffusely distributed in the femoral fossa.

Microscopic sections of the autogenous transplants which were successful all appeared very similar. There were several nodules of varying sizes. In some animals there was a definite tendency for the tissue to form an organ structure (fig 2) in others the tissue was diffuse with no attempt at organ formation (fig 3). Two types of cells were present: one was a small foamy cell with small nuclei, probably glomerulosa, and the other was a larger cell with eosinophilic cytoplasm and intensely stained nuclei resembling fasciculata. There was no inflammatory response to this tissue.

It is interesting to note that the tissue taken from autogenous transplants which failed to maintain the animal appeared healthy on microscopic examination and very similar to those described above. There was no inflammatory response to these cells either.

It appears from the information at present that this tissue is capable of surviving when transplanted autogenously. However, the grafts maintained the life of the animals in 100% of the cases if transplanted within 7 days, in 67% of the cases if transplanted within 8 to 10 days and in no cases by 13 to 48 days. Some transformation apparently occurs whereby the tissue cultured cells lose their functional capacity when maintained *in vitro* longer than two weeks.

Homologous transplants

In this series in every case except one the rats died within 25 days after transplantation. In some cases the tissue was removed on autopsy for microscopic evaluation. Rat 8MB was sacrificed 50 days after transplantation and a small nodule was found in the right femoral fossa. Microscopic examination showed a large hemorrhagic center with necrosis and lymphocytic infiltration but no living adrenal tissue. No other adrenal tissue was found but an accessory gland may have been overlooked.

The microscopic sections of 4 of the grafts showed healthy appearing adrenal tissue similar to the zona glomerulosa and fasciculata. There was some inflammatory reaction at the periphery of these

grafts (fig 4). It is possible that if tissue maintained *in vitro* less than 7 days had been homotransplanted better results might have been obtained.

ACTH treated cultures

Growth of the untreated control cultures began on the third day and at this time three types of cells could be identified. Most numerous were small round cells containing a few refractive granules and a large nucleus. These cells grew separately surrounding the explants, the darkest most granular of these probably represented degenerating forms. The second type of cell was a rather infrequent large polygonal cell forming epithelioid cell spreads. The nucleus was relatively small and the cytoplasm contained numerous small refractive granules. The third cell type was the fibroblasts which started their growth from the capsule but after a few days spread radially around whole fragments.

The spread of the epithelioid sheets ceased after a few days. The fragments were then surrounded with fibroblasts mixed with the first cell type which often lost their granules and appeared as rounded elements with clear cytoplasm. After 14 to 18 days in culture the whole collagen slant was covered with this mixed fibroblastic and round cell population. Around the periphery of the colonies there appeared numerous large polygonal cells with small nuclei occasionally containing a few refractive vacuoles in their cytoplasm. Heavily granular cells were also present but few in number. If transferred the tissue grew more slowly and finally the fibroblasts predominated.

The cell cultures grown in the presence of ACTH differed from the above. The growth began at the same time but consisted of epithelioid sheets composed of large polygonal cells with very granular cytoplasm. Small round cells were also present but they were not as numerous. After a few days of active spread the outgrowth decelerated. Starting from the 8th to 10th day of growth the morphology of the cultures changed slightly. Large cells forming epithelioid sheets gradually lost their numerous granules so that after two weeks the cytoplasm became almost clear.

Stained preparations showed few vacuoles persistent in the cortical cells

In addition to the changes in morphological characteristics of the adrenal cells the rate of fibroblastic growth varied in these cultures. This difference was most striking in the first 4 to 5 days when the fibroblastic outgrowth was quite active in the control cultures but was very slight or completely unobservable in those tubes treated with ACTH. After this initial period the difference diminished gradually and the spread of fibroblasts increased in the cultures treated with ACTH. A group of cultures grown in the absence of ACTH for 4 to 6 weeks were then treated with ACTH. Their morphology changed markedly and granulation of the cytoplasm appeared in the cells which previously had clear or only slightly granular cytoplasm. The transplantability of the ACTH cultures was no different from the controls in this small series.

DISCUSSION

There have been numerous contradictory statements made regarding cultivation and transplantation of the adrenal gland. Marunovitch (55) stated that to cultivate the adrenal it must be explanted complete and should not be taken from rats more than 4 to 5 days old. He states that the temperature of 37 C is unsuitable for culture of the adrenal cortex. Schaberg (55b, 57) however has reported successful cultivation of fragments of adrenal from 5-day-old rats maintained on coagulated plasma medium at 37 C. We have succeeded in culturing adrenal fragments from 37 to 75-day-old rats on reconstituted rat tail collagen at 37 C for as long as 79 days.

Schaberg found that after 5 days in culture the fragments became encapsulated and the cellular structure varied from a majority of fibroblasts to a majority of epithelial cells. After 10 to 12 days the central portion showed extensive degeneration. This degeneration occurred mainly in the fascicular layer and typical fascicular structures were no longer present. Cultures of the fasciculata alone showed very little activity and in two weeks only fibroblasts remained. A portion of fasciculata from hooded adult rats has been maintained in our laboratory for over 20 years

and still contains cells resembling glomerulosa and fasciculata. Schaberg noted that regeneration occurred only when the capsule and adjacent zone were present and that there is differentiation of cells resembling glomerulosa and fasciculata.

Schaberg has reported that cells maintained in the presence of 1/5 IU per ml of ACTH for three days showed decreased nucleus to cytoplasm ratio. The amount of cytoplasm increased and contained vacuoles. We have found similar results with the use of ACTH. He further demonstrated that the same effect could be obtained if the adrenal was cultured adjacent to the pituitary.

Numerous attempts at autogenous transplants have been made with varying results. Pencharz et al (31) reported 5 out of 12 successful adrenal transplants to the ovary in the rat. Wyman and Tums (32) found 95% of abdominal transplants successful in rats adrenal ectomized at 45 to 120 days. Everett (49) reported 10 out of 11 successful grafts in non adrenalectomized rats and 13 out of 17 successful in hemi adrenalectomized rats. The grafts were transplanted beneath the renal capsule and were removed 21 to 45 days later. Kroc (42) attempted transplantation to the pinna of one third to one-half of an adrenal in 104 rats aged 43 days to 9 months. He found 50% successful grafts in males without supplementary salt and 33% success with salt supplements. Of the females 7% of the grafts were successful in animals without salt supplements and 36% with salt supplements. He found that a loss of 14% or more of body weight after adrenalectomy indicated that the rat would not survive.

Williams (47) attempted autogenous transplants to the ears of one-year-old albino rats with one adrenal left intact. He placed the capsule in one ear and the enucleated portion in the other ear. One week later the second adrenal was removed. Within three months 12 of the 28 animals died. The graft comprising the enucleated portion never survived after 17 days. Of those surviving after three months all died when the ear containing the capsular graft was removed.

Blodinger et al (26) using whole or partial grafts to the kidney spleen

omentum and rectus muscle of 14 dogs reported total failure. Coupland (57) transplanted the adrenal medulla and inner cortical cells in the anterior chamber of the eye in partially adrenalectomized rabbits. He reported 79 out of 80 graft survivals but 88% of those who subsequently had the remaining adrenal removed died. He concluded that for a graft to succeed the second adrenal should not be removed for 7 to 28 days after transplantation. Jaffe (27) reported 84% successful grafts of adrenal fragments to the abdominal wall in guinea pigs with the second adrenal being removed several weeks later.

Parkes (55) reported 88% successful rat adrenal autotransplants which had previously been frozen to -79°C . These were intrarenal transplants and all animals were autopsied 6 weeks later. Franksson et al (56) attempted autogenous transplants in 5 humans suffering from carcinoma of the breast and two with Cushing's disease. Three of these grafts had been frozen to -80°C . They were transplanted to the sartorius muscle and all 7 were successful grafts.

There has been a great variation in the success of homologous transplants. Ingle et al (38) reported that "close similarity in the genetic constitution of donor and host is essential for the regeneration and function of homeografts of the adrenal gland." They found 48 of 56 successful grafts in an inbred rat strain and no successes in 26 unrelated animals. Geiringer (54) reported 100% successful transplantations in a strain of rats brother-sister mated for 40 years. He felt that the sex of the animal was not critical. Wyman and Tum Suden (37) found successful grafts in 71% of female rats and only 20% in male rats. They concluded that the sex of the donor made no difference but the sex of the recipient was important.

Pomerat et al (44) transplanted the adrenal cortex of newborn rats to the brain of 100 gm rats from whom they removed one adrenal at the time of transplantation and the second two weeks later. Fifty per cent of the grafts survived more than 30 days after the second adrenalectomy but only 25% showed excellent growth. Turner (39) transplanted ad-

renal cortex from rats one to 32 days old into the anterior chamber of the eye of 60 to 186 days-old non adrenalectomized rats. He reported 51% recovery in 96 animals with bilateral transplants and 64% of 39 with unilateral transplants. He recovered about 90% of grafts in adrenalectomized hosts but did not determine whether these were functioning.

Egdahl et al (57) placed adrenal grafts in millipore chambers and inserted them intraperitoneally in two normal dogs. They found that after two weeks 95% of the cells were dead. Using bilaterally adrenalectomized rabbits they discovered 90% of the cells dead after two weeks. Poor (58) transplanted 14-day fetal adrenal cortex into the cheek pouch of three month-old hamsters and 22 days later the animals were adrenalectomized. Four of the 6 grafts were successful and the remaining hamsters died when the grafts were removed.

Bailey and Keele (36) and Beer and Oppenheimer (34) reported successful homotransplants in humans but these results appear doubtful. Goldzieher and Barishaw (37) successfully transplanted hyperplastic adrenal tissue. On autopsy the patient's own adrenals were replaced by scar tissue but the graft appear healthy.

On numerous occasions H. S. N. Greene (60) has reported the successful homotransplantation of human adrenal tissue. The following information is given with his approval. A man suffering from Addison's disease received into the rectus muscle an adrenal transplant from a three month fetus. All therapy was discontinued and he remained symptomless. Nine months later the surgeon inadvertently removed the whole transplant when taking a biopsy and the patient's symptoms promptly reappeared.

Parkes reported 50% successful homotransplants in the rat after freezing the graft to -79°C . Joshi and Blumenthal (58) compared the results of frozen and non frozen homografts. The frozen grafts showed a diminished lymphocytic and connective tissue reaction. They concluded that the better survival of frozen grafts was probably due to a diminished elaboration of some injurious substance produced by host donor incompatibilities.

Stained preparations showed few vacuoles persistent in the cortical cells

In addition to the changes in morphological characteristics of the adrenal cells the rate of fibroblastic growth varied in these cultures. This difference was most striking in the first 4 to 5 days when the fibroblastic outgrowth was quite active in the control cultures but was very slight or completely unobservable in those tubes treated with ACTH. After this initial period the difference diminished gradually and the spread of fibroblasts increased in the cultures treated with ACTH. A group of cultures grown in the absence of ACTH for 4 to 6 weeks were then treated with ACTH. Their morphology changed markedly and granulation of the cytoplasm appeared in the cells which previously had clear or only slightly granular cytoplasm. The transplantability of the ACTH cultures was no different from the controls in this small series.

DISCUSSION

There have been numerous contradictory statements made regarding cultivation and transplantation of the adrenal gland. Martinovitch (55) stated that to cultivate the adrenal it must be explanted complete and should not be taken from rats more than 4 to 5 days old. He states that the temperature of 37 C is unsuitable for culture of the adrenal cortex. Schaberg (55b, 57) however has reported successful cultivation of fragments of adrenal from 5-day-old rats maintained on coagulated plasma medium at 37 C. We have succeeded in culturing adrenal fragments from 37 to 75-day-old rats on reconstituted rat tail collagen at 37 C for as long as 79 days.

Schaberg found that after 5 days in culture the fragments became encapsulated and the cellular structure varied from a majority of fibroblasts to a majority of epithelial cells. After 10 to 12 days the central portion showed extensive degeneration. This degeneration occurred mainly in the fascicular layer and typical fascicular structures were no longer present. Cultures of the fasciculata alone showed very little activity and in two weeks only fibroblasts remained. A portion of fasciculata from hooded adult rats has been maintained in our laboratory for over 20 years

and still contains cells resembling glomerulosa and fasciculata. Schaberg noted that regeneration occurred only when the capsule and adjacent zone were present and that there is differentiation of cells resembling glomerulosa and fasciculata.

Schaberg has reported that cells maintained in the presence of 1/5 IU per ml of ACTH for three days showed decreased nucleus to cytoplasm ratio. The amount of cytoplasm increased and contained vacuoles. We have found similar results with the use of ACTH. He further demonstrated that the same effect could be obtained if the adrenal was cultured adjacent to the pituitary.

Numerous attempts at autogenous transplants have been made with varying results. Pencharz et al (31) reported 5 out of 12 successful adrenal transplants to the ovary in the rat. Wyman and Tum Suden (32) found 95% of abdominal transplants successful in rats adrenal ectomized at 45 to 120 days. Everett (49) reported 10 out of 11 successful grafts in non adrenalectomized rats and 13 out of 17 successful in hemi adrenalectomized rats. The grafts were transplanted beneath the renal capsule and were removed 21 to 45 days later. Kroc (42) attempted transplantation to the pinna of one third to one half of an adrenal in 104 rats aged 43 days to 9 months. He found 50% successful grafts in males without supplementary salt and 33% success with salt supplements. Of the females 7% of the grafts were successful in animals without salt supplements and 36% with salt supplements. He found that a loss of 14% or more of body weight after adrenalectomy indicated that the rat would not survive.

Williams (47) attempted autogenous transplants to the ears of one year-old albino rats with one adrenal left intact. He placed the capsule in one ear and the enucleated portion in the other ear. One week later the second adrenal was removed. Within three months 12 of the 28 animals died. The graft comprising the enucleated portion never survived after 17 days. Of those surviving after three months all died when the ear containing the capsular graft was removed.

Bloeding et al (26) using whole or partial grafts to the kidney spleen

Schaberg (55b) reported 7 successes out of 13 transplants of 5-day-old rat adrenal maintained *in vitro* for three weeks when transplanted to young adult rats. Whereas in the cultures few fasciculata cells were present the grafts consisted almost entirely of fasciculata.

Martinovitch (55, 56, 57) grew whole adrenals from 4 to 5-day-old rats on watch glasses at 32-33°C for three weeks to three months. He then grafted this tissue into the anterior chamber of the eye of two- to 7-week-old rats adrenalectomized up to 7 days prior to transplantation. He concluded that grafted explants behaved similarly to normal transplants but that they regenerate better and live longer. The genetic relationship between the grafted tissue and the host animal did not seem to have a marked effect on the regenerative capacity. Explants kept *in vitro* longer than 7 weeks showed steady decline of regenerative power. After three months *in vitro* there was no regenerative power and ACTH administered to the host had no effect. He concluded "Apparently a stage in the aging process of the cell is reached *in vitro* when no appropriate stimulus can induce its further division."

To our knowledge no one has previously attempted to transplant adrenal tissue back into the same animal after culture *in vitro*. It is interesting to note that *in vitro* cultivation for one week has no effect upon successful autotransplantation but that after two weeks there are no successes even though this tissue appears perfectly healthy. The animals die from a lack of function of this tissue rather than from its active destruction by the host. One might conclude that the tissue loses its ability to respond to ACTH but in a few instances ACTH was used in the medium without any change in the transplantability even though these cells demonstrated the characteristic morphological effects of ACTH stimulation. Furthermore the tissue *in vitro* was capable of responding to ACTH after being maintained in its absence for 4 to 6 weeks. A most likely possibility is that these cells *in vitro* are unable to maintain certain enzymatic processes responsible for the production of adrenal steroids.

SUMMARY AND CONCLUSIONS

1 It is possible to maintain adrenal cultures *in vitro* at 37°C for at least 80 days.

2 Whole adrenal homotransplants are 27% successful in 6-week-old adrenalectomized rats. The medulla however does not survive.

3 Adrenal fragments maintained *in vitro* up to 7 days and then autogenously transplanted are 100% successful. Tissue maintained *in vitro* for longer periods gradually loses its functional capacity until at two weeks *in vitro* the tissue is no longer able to maintain the adrenalectomized host.

4 Homologous transplants maintained *in vitro* for 10 to 19 days prior to grafting were uniformly unsuccessful.

5 Adrenal tissue *in vitro* demonstrates a characteristic response to ACTH stimulation.

ACKNOWLEDGMENTS

The authors are indebted to Dr. Eleanor Delfs for supplying the rats used in these experiments to Dr. Carlo Bruni for interpretation of some of the microscopic sections and to Parke Davis and Company for supplying ACTH.

LITERATURE CITED

- Bailey H. and K. D. Keele 1936 Addison's disease treated by adrenal grafting. *Proc. Roy. Med.* 29: 42-44.
- Beer E. and B. S. Oppenheimer 1934 Transplantation of the adrenal cortex for Addison's disease. *Ann. Surg.* 100: 689-697.
- Bernstein D. E. 1930 Autotransplantation of adrenal gland in the spleen and mesentery of rats. *Proc. Soc. Exp. Biol.* 73: 175-176.
- Blodinger I. H. E. Klebanoff and H. Laurens 1926 Suprarenal transplantation in the dog. *Am. J. Physiol.* 76: 151-157.
- Coupland R. E. 1937 Factors affecting the survival of the adrenal medulla and associated cortical cells in the anterior chamber of the rabbit's eye. *J. Endocrinol.* 15: 162-170.
- Darcy D. A. 1952 Survival of adrenal gland homografts in the rabbit's skin. *Nature* 170: 805.
- Dempster W. J. 1935 The transplanted adrenal gland. *Brit. J. Surg.* 42: 540-552.
- Egdahl R. H., F. D. Roller and R. L. Varco 1937 Survival and function of adrenal cortex and skin in millipore chambers. *Transpl. Bull.* 4: 146-147.
- Ehrmann R. L. and G. O. Gey 1936 The growth of cells on a transparent gel of reconstituted rat tail collagen. *J. Natl. Cancer Inst.* 26: 1375.

- Everett N B 1949 Autoplastic and homoplastic transplants of the rat adrenal cortex and medulla to the kidney *Anat Rec* 103 335-348
- Franksson C G Birke G Moberger and L O Plantin 1956 Storage and autotransplantation of human adrenal tissue *Acta Chir Scand* 111 113-123
- Gezinger E 1954 *Endocrines Transpl Bull* 1 137-140
- Goldzieher M A and S B Barishaw 1937 Transplantation of adrenal tissue in Addison's disease *Endocrinology* 21 394-400
- Greene H S N 1960 Personal communication
- Halsted W S 1909 Auto- and isograft transplantation of the parathyroid glandules *J Exp Med* 11 175-199
- Higgins G M and D J Ingle 1938 Functional homeoplastic grafts of the adrenal gland of newborn rats *Anat Rec* 70 145-154
- Ingle D J and G M Higgins 1937 Transplantation of regeneration of the adrenal gland in the rat preliminary report *Proc Mayo Clin* 12 204
- Ingle D J G M Higgins and H W Nilson 1938 Homeoplastic transplantation of adrenal glands in rats of inbred strain *Am J Physiol* 121 650-656
- Jaffe H L 1927 On the transplantation of the guinea pig suprarenal and the functioning of the grafts *J Exp Med* 45 587-594
- Joshi R A and H T Blumenthal 1958 Alteration of homotransplantability of rat adrenal and aorta by dehydration freezing *Lab Invest* 19-29
- Kroc P L 1942 Rat ear as a site for adrenal cortical grafts and subsequent ear adrenalectomy *Endocrinology* 30 150-157
- Lux L G M Higgins and F C Mann 1938a Homeotransplantation of the guinea pig and rabbit adrenal grown in vitro *Anat Rec* 67 353-365
- 1938b Functional homeografts of the rat adrenal gland grown in vitro *Ibid* 70 29-44
- Martinovitch P N 1955 Infantile rat adrenal transplanted into the anterior eye chamber of adrenalectomized hosts after cultivation in vitro *J Exp Zool* 129 99-120
- 1956 Explantation and transplantation of various infantile rat endocrine glands *Transpl Bull* 3 33-39
- 1957 The future of tissue culture in relation to morphology Discussion *J Nat Cancer Inst* 19 651-652
- Parkes A S 1955 Viability of adrenocortical tissue transplanted after freezing and thawing *Proc Roy Soc Ser B* 144 314-327
- Pencharz R I J M D Olmsted and G Giragos sintz 1931 The survival of rats after total and partial adrenalectomy and adrenal transplantation *Physiol Zool* 4 501-514
- Pomerat C M C G Breckenridge and L Gordon 1944 Homoplastic adrenal grafts to the cerebral cortex of the rat *Endocrinology* 34 60-68
- Poor E 1958 Functional adrenocortical homotransplants in the golden hamster *Proc Soc Exp Biol Med* 97 535-539
- Schaberg A 1955a *Endocrines Transpl Bull* 2 145-146
- 1955b Regeneration of the adrenal cortex in vitro *Anat Rec* 122 205-222
- 1957 The influence of ACTH and the anterior lobe of the hypophysis on the adrenal cortex in vitro *Proc Koninkl Nederl Akademe van Wetenschappen C60* 463-470
- Stone H B J C Owings and G O Gey 1933 Living grafts of endocrine glands *Calif West Med* 38 409 39 10
- Turner C D 1939 Homotransplantation of suprarenal glands from prepubertal rats into the eyes of adult hosts *Anat Rec* 73 145-162
- Williams R G 1945 The characteristics and behavior of living cells in autogenous grafts of adrenal cortex in rabbits *Am J Anat* 53-80
- 1947 Studies of adrenal cortex regeneration of the transplanted gland and the vitality of autogenous grafts *Ibid* 81 197-232
- Wyman L C and C Tum Suden 1932 Studies on suprarenal insufficiency XI The Growth of transplanted cortical tissue in the rat *Am J Physiol* 101 662-667
- 1937 Factors determining and limiting the growth of transplanted suprarenal cortical tissue *Endocrinology* 21 523-528
- Wyman L C H A Eddy P L Griffin R Whitney and D I Patt 1937 Relation of number of transplants to total volume of regenerating adrenocortical tissue *Proc Soc Exp Biol Med* 36 249-251

PLATE

PLATE 1

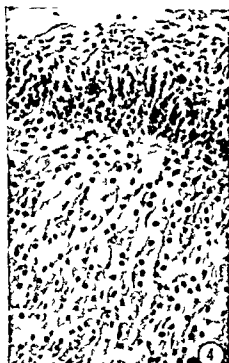
EXPLANATION OF FIGURES

- 1 A successful whole adrenal transplant This section shows a well-encapsulated mass of adrenal tissue. Distinct cords of moderately granulated and vesicular adrenal cortical cells are present. There is no inflammatory reaction. $\times 300$
- 2 A successful autogenous transplants This section shows an encapsulated adrenal mass. The cells are similar to those in figure 1 but there are fewer cells with large vacuoles. Again no inflammatory reaction is present. $\times 300$
- 3 Successful autogenous transplants with adrenal tissue spread out diffusely rather than organized into large nodules. This section shows essentially unencapsulated irregular adrenal cell masses. No inflammatory response is present. $\times 300$
- 4 Unsuccessful homologous transplant The tissue is encapsulated and the cells are well preserved. There is a great amount of peripheral inflammatory reaction. $\times 300$

ADRENAL TRANSPLANTATION

Gerald P Bodey Olga Miodu zew k and George O Cey

PLATE



(Araldite Ciba Ltd) or in a mixture of methyl and butyl methacrylates

Thick sections from suitably oriented blocks were studied in the phase microscope and contiguous thin sections were studied in an RCA 2E electron microscope following staining with potassium permanganate by the method of Lawn (60) or with saturated lead acetate (Watson 58). Staining was unnecessary in the case of permanganate fixed material. Methacrylate sections were mounted on collodion covered grids and covered with a second layer of collodion after staining (Watson 57).

Retinal fixation by fixatives containing OsO_4 proved rather erratic both with respect to results obtained in different specimens and in different blocks from the same specimen. These difficulties apparently result from the erratic penetration of the vitreous humor by the fixative. The impression was obtained that the fixative tended to form a channel and that a variable coating of mucopolysaccharide remaining on the retina resulted in local inequalities of rates of fixative penetration. While potassium permanganate fixation seemed somewhat better than osmic fixation with regard to penetration it too gave somewhat erratic results. However all the fixatives employed gave excellent preservation when this was evaluated by light microscopy.

RESULTS

In material deemed to be properly fixed by osmic-chrome fixation (fig. 1) vertical sections of the retina showed groups of spherical cross sections of ganglion cell axons and vertically infiltrating glial processes. These glial elements fully occupy the surface of the retina at its interface with the vitreous humor. In poorly fixed material the most striking change was a loss of integrity of many glial cell membranes resulting in a false impression that the axons of the ganglion cells lay in syncytial glial cytoplasm.

The glial cell processes which occupy the inner retinal surface vary in their appearance (figs. 1, 2, 3). In some areas particularly near the optic papilla the cytoplasm possessed relatively few mitochondria and was rather clear except for the presence of fibrous material. This

material was unevenly distributed within the cells and in general appeared to increase in concentration as a cell process approached the vitreous humor. In other areas the cell processes possessed more mitochondria, moderate amounts of fibrous material and had in addition numerous small circular profiles and dense particles (fig. 2). Sometimes desmosomes were observed between glial cells (fig. 2). Inasmuch as the full extent of any individual glial cell in this area could only be determined by serial sectioning and since this was not carried out it is not clear whether this variability of appearance is due to the presence of more than one variety of glial cell among cells forming the inner retinal surface or to an uneven distribution of organelles within the cells. Well preserved mitochondria in neurites adjacent to glial processes with few mitochondria suggest that mitochondria are not being destroyed by poor fixation. The generally distinctive appearance of glial cell processes provided a means of identifying glial cells and facilitated the tracing of their processes through fields of axon cross sections. The circular profiles in the glial cells probably represent cross sections of an agranular reticulum and gave an impression of a vesicular cytoplasm.

The glial cell processes of the optic fiber layer were not tightly packed and appreciable extra-cellular spaces were evident (fig. 2). In addition the retinal surface on the vitreous humor as constituted by contiguous glial cells was not sharply demarcated inasmuch as the loose packing of the cells frequently permitted extensions of the vitreous chamber volume between the cells (fig. 3). A basement membrane was observed to be interposed between the vitreous chamber and the retinal cells (figs. 1, 2, 3, 7) and occasionally this was also folded into the crevasses between glial cells. In addition points of invagination of the surface of the glial cells on the vitreous chamber were observed (fig. 2) and the basement membrane was folded into these invaginations.

The glial processes extended about the axons of the ganglion cells but this infiltration appeared to be random. It was the rule rather than the exception that

axons frequently abutted directly upon one another without being separated by glial cell membranes. Thus in figure 3 a complete ring of contiguous axons can be discerned. On the other hand while axons were commonly in contact they were never distant from glial cells and in certain areas most of the axons in a given section possessed some surface contact with a glial cell (fig 4). It is not clear however whether a given pair of contiguous axons remain approximated for considerable distances. Attempts to cut sections along the length of the axons did not answer this question because undulation of the axons (fig 2) did not permit following extensive lengths.

Occasionally individual axons were enveloped by glial cells in a manner suggesting restriction of axon to axon contact (figs 5-7) although it is not certain that this isolation would continue for the full length of the fibers. When methods of fixation become more reliable and a systematic exploration of the optic fiber layer becomes possible it may well be that in certain areas of the retina such restriction of axon to axon contiguity may be more common than in others. However it is already clear that in most regions axon to axon contiguity is quite common and probably usual.

Some efforts have been made to determine the distribution of frequency in axon

diameter classes in the fiber layer. As previously noted the axons seen in cross sections tended to occur in groupings (fig 1). A number of such groups were photographed at magnifications of 2000 diameters and photographic enlargements were made at magnifications of 8000 diameters. All the axons in each of three groups from a temporal area not far from the optic papilla were measured with the results seen in table 1. The axon diameters ranged from 0.2-3.0 μ with the most frequent class being the 0.4-0.5 μ class. The general distribution was skewed. These results should in no way be interpreted as representing average fiber diameter distributions of the monkey retina. While they might ultimately prove to be representative they were obtained from one restricted area of one animal and are presented as a sample of the probable ranges to be encountered in a definitive investigation.

DISCUSSION

As Horstmann and Meves (59) have pointed out in investigations of neurite glial cell relationships in the central nervous system a serious obstacle is the difficulty of distinguishing dendritic axonal and fine glial processes. However in the area of the internal limiting membrane of the monkey retina the predominant neurites are axons and the predominant glial species possess a distinctive fibrous cyto-

TABLE 1
Diameter of ganglion cell axons

Range	Fid			Sum
	A	B	C	
* 0.2-0.3	18	27	18	63
0.4-0.5	112	123	105	340
0.6-0.7	62	69	60	191
0.8-0.9	31	51	50	132
1.0-1.1	43	33	35	111
1.2-1.3	23	8	19	50
1.4-1.5	7	8	9	24
1.6-1.7	5	5	8	18
1.8-1.9	3	1	3	7
2.0-2.1	2	2	3	7
2.2-2.3	2	1	2	5
2.4-2.5	0	0	1	1
2.6-2.7	1	2	4	7
2.8-2.9	0	0	0	0
3.0-3.1	1	0	0	1
	310	330	317	957

plasm That fibrous astrocytes are the predominant species of retinal glial cell has been an early interpretation (Marchesani 27) Polyak (41) lists the ectodermal glia of the monkey retina as Müller cells fibrous astrocytes protoplasmic astrocytes and mixed (slightly fibrous) astrocytes The presence in the primate retina of oligodendroglia he regards as unproven and doubtful In view of the variance in fiber concentration of the glial cells encountered in this investigation and in view of the fact that these glial cells of varying appearance are obviously all involved in the composition of the internal limiting membrane (described by Polyak as consisting of "the juxtaposed vitreal ends of Muller's fibers") it would appear that either the cell of Muller is a species of astrocyte whose cytoplasm may display a variable fibrous content or that more than one variety of glial cell participates in the inner retinal surface Some of the glial cells whose processes constitute the internal limiting membrane were observed to have their nuclei at the level of the optic nerve fibers (fig 6) This might constitute evidence that more than one glial species contribute to the inner retinal surface inasmuch as Polyak (41) states that the typical location of the nuclei of the glial cell of Muller is at the level of the bipolar cell nuclei (Polyak's layer 6c) However he also notes that they may rarely occur in other levels including the ganglion cell and optic nerve fiber levels Sjostrand (58) in a study of the receptor bipolar synaptic area of the guinea pig has called attention to the presence in the Muller cells of distinctive particulate material The cytoplasm of the Muller cells of the guinea pig as seen in Sjostrand's electron micrographs strongly resemble the particulate and reticular glial cytoplasm described above Finally the more fibrous glial cells of the internal limiting membrane of the monkey strongly resemble fibrous astrocytes of other areas of the central nervous system as demonstrated in the electron micrograph (58)

There is some ambiguity in the use of the term "internal limiting membrane" in the literature on the retina (41) employs this term for the internal limiting membrane of the vertical cell

cells of Muller but recognizes the existence of an extra retinal "hyaloid membrane" interposed between the vitreous humor and the Muller cells He mentions however that certain investigators are using the term for an extracellular entity Wolter (59) in a study of the glial cell varieties of the human retina employs the term "internal limiting membrane" to include both the Muller cell processes and an included homogenous material Finally investigators of the ciliary body (Pappas and Smelser 58) seem to employ the term for an extracellular membrane the basement membrane As the above investigation shows there is a basement membrane interposed between the cellular surface of the retina and the vitreous chamber As superficial extensions of the vitreous chamber penetrate between the surface processes of the glial cells the basement membrane is likewise infolded and lines these crevasses Moreover the basement membrane may line invaginations of the glial cells of the retinal surface Since the mucopolysaccharide of the vitreous humor and basement membranes in general are periodic acid Schiff positive these observations tend to account for a dense PAS positive band delimiting the inner retinal surface The interdigitation of basement membranes and of fibrous cell processes suffices to account for the distinctive membrane like appearance seen in the light microscope In the mouse (unpublished observations) the embryonic optic vesicle is completely enclosed in a basement membrane before the formation of the lens and this arrangement persists in the adult where the basement membrane of the inner retina proves to be continuous with that of the ciliary body iris and pigment epithelium This is probably the case in the primate retina

If the penetration of extensions of the vitreous body between the cells of the retinal surface results in a greater adhesion of the retina to the vitreous body then this situation may provide a clue in the etiology of retinal detachment subsequent to movements of

the vitreous body relationships of new cells early in postnatal life have been re-

viewed by Schmitt (58) In the well known examples of medullated peripheral and central neurites and non medullated peripheral neurites sheathing cell membrane (or membrane derivatives) separate individual neurites so that the neural processes are physically isolated from one another However with the continued application of electron microscopy to nervous tissue a number of examples of contiguous neurites have come to light In the spinal cord of the lamprey Schultz et al (56) found fields of neurite fibers with a relative paucity of glial elements In the olfactory nerves of mammals Gasser (58) and De Lorenzo (57) found that the axons were collectively enveloped in fascicles containing numerous axons Except at the periphery of the fascicle most of the axons were contiguous with and completely surrounded by other axons Similarly in the case of the unmedullated components of the frog optic nerve Maturana (60) found that these axons were collectively enveloped in glial elements in a manner similar to that in the olfactory nerves In insects Hess (58) and Gray (60) have reported instances of contiguous axons in the cockroach and locust respectively Finally in the retina of the mouse contiguity of some portions of the receptors has been reported (Cohen 60)

In the case of the axons of the fiber layer of the monkey it is well known that these are normally unmyelinated and that they become myelinated in the optic nerve (Polyak 41) Preliminary observations with the electron microscope have confirmed the absence of unmedullated fibers in the monkey optic nerve

Since fibers may be contiguous in the retina that become separated when they acquire their myelin sheaths in the optic nerve it is probable that myelin is not required for insulation between neighboring fibers but that it serves some function necessary for accelerating the rate of conduction

Contiguity of axons suggests a potentiality for interaction Interactions of experimentally contiguous non medullated nerves have been studied by Jasper and Monnier (38) Katz and Schmitt (40) and Arvanitaki (42) Rosenbluth (41) has made similar studies on medullated

nerves Arvanitaki coined the term *epihaptic transmission* to describe the induction of a propagated transmission in one neurite by a propagated transmission in a contiguous neuritic element While there is little doubt that the experimental evidence suggests neuritic interactions in terms of inhibitions and facilitations *epihaptic firing* of neurites has generally required prior facilitation by chemical or electric means and generally may not occur in physiological situations On the other hand the unmedullated nerves (crab) used in some of the mentioned investigations may well have possessed Schwann sheaths and accordingly in instances of true neuritic contiguity may not have been put to the test Maturana has pointed out (60) that the linear extent of contiguity of axons is also of importance in considering whether they interact Moreover as he further suggests the retinal location of the ganglion cells from which two axons have arisen may be of some significance in considering problems of signal interference The tendency observed for the axons in the fiber layer to occur in clusters might suggest that these are functional units of some sort Indeed a reconstruction analysis of these clusters after serial sectioning might reveal a tendency for particular glial cells to belong to particular clusters This might represent a subtle form of collective envelopment Polyak (41) notes that there is indeed a tendency for fibers emerging from a minute territory of the retina to preserve their relative position with respect to other fibers However he also notes that there is often an exchange of fibers with immediately adjacent bundles Interactions between fibers derived from minute retinal territories may not be of great importance particularly if the information being conveyed by the signals is of a general sort (e.g. brightness) rather than of an epicritic quality One might expect that axons of the small ganglion cells in the foveal information path might require more shielding These axons which constitute the so-called papillomacular bundle may contain more examples of instances where the fibers are physically separate from one another

Where fibers are contiguous the distances between osmiophilic lines were of the order of 150–200 Å and the osmic fixed retina conforms to the rest of the central nervous system in its apparent paucity of extra cellular space about neuritic elements.

Axons of less than one micron diameter were indicated by the early electron microscope report of Fernandez Moran (53) and subsequently confirmed by the work of Gasser (58), De Lorenzo (57), Horstmann and Meves (59) and Maturana (60) among others.

Maturana (60) found in the frog optic nerve an unmyelinated axon diameter range of 0.15–0.6 μ with a peak at 0.2–0.3 μ and a myelinated axon diameter range of 0.7–5 μ with most axons below 1.5 μ . It would appear from the preliminary measurements of the pre-myelinated axons of the monkey retinal fiber layer that the diameter range is also largely below 1.5 μ but with a peak at 0.5 μ .

It has been suggested that the oligodendroglia are responsible for myelination (Del Rio-Hortega cited by Penfield 32). Polyak (41) believes that oligodendroglia are probably absent from the primate retina. Accordingly an opportunity may be afforded to settle the controversy over which glial cell seen in electron microscope preparations corresponds to the oligodendroglial cell of the light microscopist (see Luse 60). The primate retina would provide examples of the spectrum of appearances of astrocytes. These are also found in the optic nerve. Accordingly any new and distinctive glial cell appearing in the optic nerve would presumptively tend to be associated with the process of myelination and accordingly be a likely choice for the oligodendroglial cell.

SUMMARY

The optic fiber layer and internal limiting membrane of the Rhesus monkey were studied with the electron microscope. The primary purpose of the investigation was to ascertain the relationships to one another and to glial cells of the axons of the retinal ganglion cells prior to the acquisition of their myelin sheaths. In addition the general cytoarchitecture of the internal limiting membrane was of interest.

The retina was seen to be separated from the vitreous humor by a basement membrane. This membrane together with vitreous humor "space" penetrated to a moderate extent between the glial cells occupying the inner retinal surface and into invaginations of retinal glial cells. It is conceivable that some degree of adhesiveness of vitreous humor and retina might result from these arrangements.

The glial cells constituting the internal limiting membrane all possessed a generally fibrous cytoplasm such as to suggest their classification as fibrous astrocytes. In certain areas agranular reticulum and dense particles were also noteworthy cytoplasmic features. The degree of fibrosity of the cells varied considerably both in different regions of individual cells and between cells. Since these cells occupy the inner surface position of the retina the classical position assigned to the glial cell of Muller it is likely that either the glial cell of Muller is a fibrous astrocyte of variable appearance or that more than one glial species contribute to the inner retinal surface.

Axons of the fiber layer occurred in groups within which axons very frequently were contiguous with neighboring axons. However the linear extent over which contiguity was maintained could not be ascertained. On the other hand axons were usually not distant from infiltrating glial processes. Some few samplings of groups within which axon diameters were measured gave a skewed distribution with most of the axons being less than one micron in diameter and with a peak at 0.5 μ .

Some of the implications of these findings for retinal morphology and physiology are discussed.

LITERATURE CITED

- Arvanitaki A. 1942. Effects evoked in an axon by the electrical activity of a contiguous one. *J. Neurophys.* 5: 89–108.
 Cohen A. I. 1960. The ultrastructure of the rods of the mouse retina. *Am. J. Anat.* 107: 23–48.
 ———. 1961. Some preliminary electron microscopic observation of the outer receptor segments of the retina of the Macaca fascicularis. In: *The Structure of the Eye*. Academic Press, New York, pp. 151–158.
 Dalton A. J. and M. D. Felix. 1955. A study of the Golgi substance and ergastoplasm in a

- series of mammalian cell types. In *Fine Structure of Cells*. Interscience New York pp 274-293
- De Lorenzo A. J. 1957 Electron microscopic observations of the olfactory mucosa and olfactory nerve. *J Biophys Biochem Cytol* 3: 839-850
- Fernandez Moran H. 1953 Observations on the structure of submicroscopic nerve fibres. *Exp Cell Res* 4: 481-482
- Gasser H. S. 1958 Comparison of the structure as revealed with the electron microscope and the physiology of the unmyelinated fibers in the skin nerves and in the olfactory nerves. *Ibid Supp* 5: 3-17
- Gray E. G. 1960 The fine structure of the insect ear. *Phil Trans Roy Soc B* 243: 74-94
- Hess A. 1958 The fine structure of nerve cells and fibers neuroglia and sheaths of the ganglion chain in the cockroach (*Periplaneta americana*). *J Biophys Biochem Cytol* 4: 731-742
- Horstman E. and H. Meves. 1959 Die feine struktur des molekularen rindengraves und ihre physiologische bedeutung. *Z. Zellforsch.* 49: 596-604
- Jasper H. H. and A. M. Monnier. 1938 Transmission of excitation between excised non myelinated nerves. An artificial synapse. *J Cell and Comp Physiol.* 11: 259-277
- Katz, B. and O. H. Schmitt. 1940 Electric interaction between two adjacent nerve fibers. *J Physiol.* 97: 471-488
- Lawn A. M. 1960 The use of potassium permanganate as an electron dense stain for sections of tissue embedded in epoxy resin. *J Biophys Biochem. Cytol.* 19: 197-198
- Luft J. H. 1956 Permanganate A new fixative for electron microscopy. *Ibid* 2: 799-802
- Luse S. 1958 Ultrastructure of reactive and neoplastic astrocytes. *Lab Invest* 17: 401-417
- . 1960 The ultrastructure of normal and abnormal oligodendroglia. *Anat Rec* 138: 461-472
- Marchesani O. 1927 Die drei gliarten in der retina und in sehnerven. *Zentralbl f d Ges Ophthalm* 17: 428
- Maturana H. R. 1960 The fine anatomy of the optic nerve of anurans—An electron microscope study. *J Biophys Biochem Cytol* 7: 107-120
- Palade G. E. 1952 A study of fixation for electron microscopy. *J Exp Med* 95: 285-298
- Pappas G. D. and G. K. Smelser. 1958 Studies on the ciliary epithelium and the zonule. *Am J Ophth* 46: 299-318
- Penfield W. 1932 Neuroglia. Normal and pathological. In *Cytology and Cellular Pathology of the Nervous System*. Penfield ed Hoeber New York pp 423-479
- Polyak, S. L. 1941 The Retina. U of Chicago Press Chicago
- Rosenblueth A. 1941 The stimulation of myelinated axons by nerve impulses in adjacent myelinated axons. *Am. J Physiol* 132: 119-128
- Schmitt F. O. 1958 Axon-satellite cell relationships in peripheral nerve fibers. *Exp Cell Res., Suppl.* 5: 33-57
- Schultz R. E. C. Berkowitz and D. C. Pease. 1956 The electron microscopy of the lamprey spinal cord. *J Morph.* 98: 251-273
- Sjostrand F. S. 1958 Ultrastructure of retinal rod synapses of the guinea pig eye as revealed by three-dimensional reconstructions from serial sections. *J Ultrastructure* 2: 122-170
- Watson M. L. 1957 Reduction of heating artifacts in thin sections examined in the electron microscope. *J Biophys Biochem. Cytol.* 3: 1017-1022
- . 1958 Staining of tissue sections for electron microscopy with heavy metals. *Ibid* 4: 475-478
- Wolter J. R. 1959 Glia of the human retina. *Am J Ophthalmol* 48: 370-393
- Yamada E., K. Tokuyasu and S. Iwaki. 1958 The fine structure of retina studied with electron microscope. III. Human retina. *J Kurume Med Assn.* 21: 1979-2027

PLATE 1

EXPLANATION OF FIGURE

- 1 A low power electron micrograph of the internal limiting membrane and optic fiber layer $\times 4650$. Between the glial cells (G) and the vitreous humor (V) lies a basement membrane (B). A glial nucleus (N) and a portion of a ganglion cell (GA) are also evident. Note the variation in fibrosity of the glial cells.

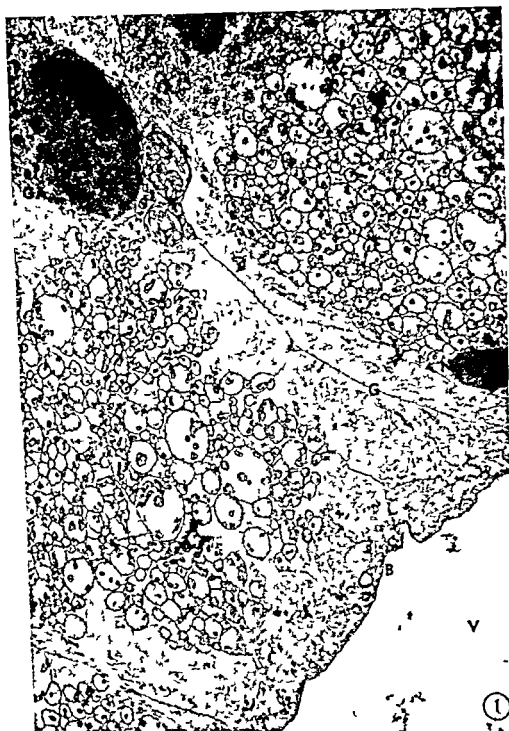


PLATE 2

EXPLANATION OF FIGURE

- 2 A macular area of the internal limiting membrane and optic fiber layer showing circular profiles (V) and particulate (P) elements in the cytoplasm of the surface glial cells in addition to some fibrous cytoplasmic material. A desmosome (D) is present between two glial cells and large extracellular spaces (S) as well as smaller spaces (arrows) are not rare. A basement membrane (B) separates the cells from the vitreous chamber and extends into invaginations of glial cell membrane. Undulating axons (A) are seen in a limited extent of contiguity. $\times 19,300$



PLATE 3

EXPLANATION OF FIGURE

- 3 A view of the internal limiting membrane at an area where fibrous material is characteristic of the cytoplasm of the glial cells $\times 11,900$. Note the penetration of vitreous humor (V) and basement membrane (B) between the loosely interdigitating surface portions of the glial cells (G). Note also the random manner in which the axon (A) area is infiltrated by glial processes. In addition to the fibrous material in the cytoplasm of the glial cells note the paucity of mitochondria as contrasted with axon cross sections.



PLATE 4

EXPLANATION OF FIGURE

- 4 A view of cross sections of axons of ganglion cells in the fiber layer $\times 66680$. Note the fibrous components in the cytoplasm of the glial cells (G). A ring of contiguous axons including axons A, B, and C is presented to illustrate interweaving of axons and glial processes. The glial cells of Muller run vertically in the retina while the axons run horizontally.

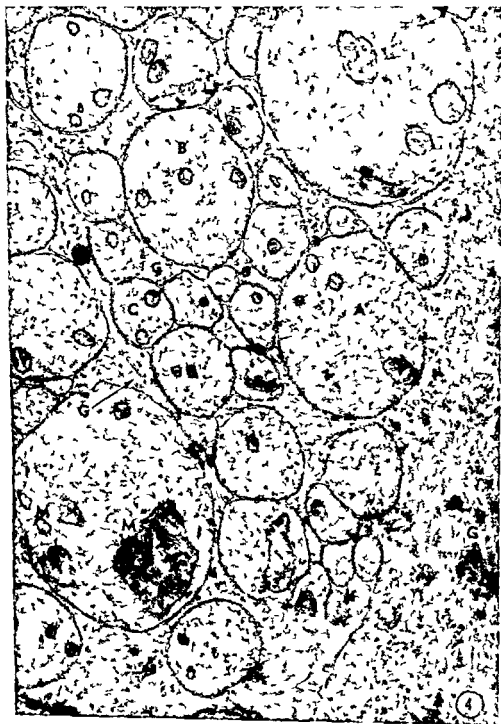


PLATE 5

EXPLANATION OF FIGURES

- 5 An example of an axon (A) of a ganglion cell which is apparently isolated through envelopment by a glial cell (G). This was rarely encountered. A retinal capillary (C) with its typically thick basement membrane is also in evidence. / 25,300
- 6 Evidence of the location of some of the nuclei (N) of the glial cells whose processes (G) infiltrate the ganglion cell axons in the optic fiber layer. 18,000



PLATE 6

EXPLANATION OF FIGURE

- " A view of permanganate fixed retina 12 000 Most of the mitochondria are somewhat swollen. Note however the example of three axons which appear to be physically separated from one another with connecting mesaxons (MA). The surface basement membrane (B) is also evident.



The Ultrastructure of Human Cardiac Muscle and its Associated Tissue Space¹

CHARLES G. BATTIG AND FRANK N. LOW

*Department of Anatomy Louisiana State University School of Medicine
New Orleans, Louisiana*

Investigation of the ultrastructure of sectioned cardiac muscle was initiated by Kisch, Grey and Kelsch (48) on tissue obtained from a child shortly after death. This pioneer work was followed by that of Weinstein (54) who used more refined techniques to examine cardiac tissue from the cat, dog, guinea pig, frog, snake, turtle and chicken as well as human tissue. During the next few years the subject was studied with increasing technical proficiency with notable contributions by Lindner (summarized in 57) on dog, frog and guinea pig; by Moore and Ruska (57) on dog, rat and mouse; and by Fawcett and Selby (58) on turtle atrium. Specialized topics were investigated by Hibbs (54) who described cardiac muscle histogenesis in the chick and by van Breeman (53) and Sjostrand and Andersson (51) who examined the intercalated disc. The fine structure of the contractile mechanism of striated muscle has been studied chiefly in skeletal muscle (Huxley and Hanson, 60) but is essentially the same in the heart. The non-contractile elements emphasized in Bennett's review (60) may likewise be interpreted for cardiac muscle. The ultrastructural norms established by Lindner (57) and others provided a necessary background for expansion into related basic sciences as illustrated by the correlated pathological and physiological studies of Poche (57a, 57b, 58a, 58b, 59, 60).

The literature now offers several reviews of cardiac ultrastructure and closely related topics. The work of the Dusseldorf group more active than any other is successively summarized with comprehensive bibliographies by Lindner (57), Poche (58b) and Meessen (59). A small volume on the ultrastructure of the cardiovascular system in general by Kisch (57) recently

appeared in English translation (60). Two articles in Bourne (60) on contractile and non-contractile elements (cited above) are supplemented by a chapter on the intercalated disc by Sjostrand and Andersson. Cedergren (60). A current Russian concept of ultrastructure in striated muscle may be found in Studitsky's "Experimental Surgery of Muscles" (59) which presents a scholarly account of the subject. In Studitsky's critique there are copious references to the published work of the western world but it appears that very little original work on cardiac ultrastructure has been done in eastern Europe. The investigation of Khristolyubova (58) on frog ventricle is the only one that has come to our attention.

An improved means of study is provided by polyester embedments (Ryter and Kellenberger, 58). The thermostable nature of these embedments permits the attainment of a significantly improved level of image resolution and clarity. In addition the insolubility of the polyester matrix in organic solvents permits the use of such solvents for clearing mounted sections and as vehicles for the usual heavy metal stains (Low, 61a, b). The possibility of better preparations and the routine availability of human biopsy material from open heart surgery prompted the present investigation. This paper accordingly describes the electron microscopy of human heart tissue with special emphasis on ultrastructural characteristics not previously demonstrated or extensively analyzed.

MATERIAL AND METHODS

Small biopsy specimens of grossly normal right auricular appendage or right

Aided by grant H1663 from the United States Public Health Service.
Cardiovascular Trainee (USPHS HT-133)

ventricular wall were obtained from 7 patients during open heart operations. The specimens were flooded with buffered OsO₄ (Palade '52) and cut into strips approximately 1 mm by 5 mm. Each strip was attached to a small square of dental wax with glass pins and immersed in fresh fixer at approximately 0°C. The muscle strips were thereby maintained under gentle linear tension during fixation and the original orientation and length preserved. Less than 15 seconds elapsed between the surgical removal of the tissue and its initial flooding with osmic acid. Following fixation for 2 to 2½ hours the muscle strips were cut into smaller blocks of known orientation and embedded in Vestopal W (Ryder and Kellenberger '58). Sectioning was done on a Porter Blum microtome using small angle glass knives. Sections were mounted on copper grids covered with formvar or carbon formvar membranes. A number of grids were heat cleared (Low '61a). Others were cleared and stained by immersion in a mixture of equal parts of acetone and ether containing 0.1% PTA, 0.5% PTA or 0.05% Thorium nitrate by weight (Low '61a). A few grids were stained with aqueous lead hydroxide (Watson '58) or 1% PTA. The particular procedure used for each of the illustrations is given within its own caption. The micrographs were taken on an RCA EML-1B electron microscope.

OBSERVATIONS

The tissue space and the connective tissues

Figures 1 and 2 show the major stromal components of the tissue space and their relationships to muscle cells. A large proportion of the tissue space often appears empty (figs 1, 2, 5). Capillaries, unmyelinated nerves and two cell types distinctive but unidentified are frequently found together in close proximity (fig 2). One of the unidentified cell types is characterized by the absence of a boundary membrane (see page 208 for explanation of terminology) and the presence of long thin sheets of cytoplasm (figs 1-5). The other cell type is found in cross section, possesses scant cytoplasm, lies next to a capillary and is enclosed in a boundary membrane (fig 2). Abundant bundles of

unit fibers, elastic fibers and microfibrils are frequently present and pass through the tissue section in many directions (figs 1, 4, 8).

The capillary structure of human cardiac muscle corresponds to established ultrastructural patterns seen in other forms (Moore and Ruska '57; Bennett, Luft and Hampton '59). A dense granular boundary membrane surrounds the outer plasma membrane. It measures approximately 200-250 Å in thickness and is separated from the plasma membrane by a zone of lesser density measuring about the same. Desmosomal junctions are observed at lines of contact of adjacent endothelial cells (figs 3, 4, 5). The nucleus displays the usual granular structure and is surrounded by a double nuclear membrane (fig 5). Numerous small vesicles are seen in various stages of formation along both the inner and outer walls of the capillaries (figs 3, 4, 5). These vesicles are also present free in the cytoplasm of the endothelial cells (figs 3, 4). The density of the wall of the vesicles is similar to that of the plasma membrane and that of the contents resembles the boundary membrane.

Small cytoplasmic extensions are frequently seen in close contact with the capillaries (figs 1, 2, 3). Such cytoplasm is surrounded by its own distinct plasma and boundary membranes and appears oval in section. No points of communication with the cytoplasm of the capillary endothelial cells have been observed, but at points of contiguity the two boundary membranes appear fused. As yet even though many sections have been examined the nuclei assumed to be associated with these islands of cytoplasm have not been observed in continuity with them.

Another cell type found in close association with many capillaries appears spindle shaped in section (figs 1, 2, 4). The oblong nucleus is large and may possess an irregular margin (fig 4). A thin rim of cytoplasm surrounds the nucleus except at the nuclear poles. Here the cytoplasm is more abundant and contains numerous

Furnished through the courtesy of Dr. H. M. Albert, Department of Surgery, Louisiana State University School of Medicine, New Orleans, Louisiana.

large vacuoles of irregular size and shape (figs 1-4). In some sections many dense inclusion bodies are seen in association with these vacuoles (fig 2). Vesicles are usually not present along the plasma membrane. The abundant cytoplasm at the nuclear poles abruptly attenuates into long thin extensions which border adjacent capillaries or extend between muscle cells. At their points of greatest attenuation these cytoplasmic extensions appear almost as thin as double membrane systems (fig 2, arrows). Here they measure only 300-400 Å across, thereby being unresolvable in light microscopy. At times these cytoplasmic extensions are seen with out their corresponding cell bodies (figs 3-5). This cell type is unique in being the only one found in human cardiac muscle that does not possess a boundary membrane. In some sections however a bias cut creates the illusion of such a membrane (fig 4, arrows).

The second cell type is characterized by constant close association with a capillary, a large round nucleus and a very thin rim of cytoplasm (fig 2). The densely granular nucleus possesses nucleoli and the usual double membrane. Its contour usually has a single thin cleft at one point along its periphery (fig 2). Both a plasma membrane and a boundary membrane are present. The scant cytoplasm contains small vesicles which appear to arise from the plasma membrane. Much larger cytoplasmic vacuoles are also present but neither myofibrils nor myofilaments are demonstrable. Although many sections have been examined no cytoplasmic extensions have been observed. In particular no cytoplasmic communication has ever been observed between these cells and the isolated islands of cytoplasm lying next to the capillaries, as described above. This cell type has not been observed in the absence of a capillary.

Unmyelinated nerves are frequently seen in close association with the capillaries (figs 1-2 & 6). They conform to the classical pattern described by Gasser (55). The nerves are composed of typical Schwann cells and neuraxons (fig 6). The plasma membrane of the Schwann cell may be followed and seen to form indentations in which are contained the individual neuraxons. In places the double infold-

ing of the plasma membrane forms a mesaxon. The neuraxons are surrounded by separate distinct plasma membranes. A boundary membrane surrounds the entire nerve but does not dip down into the indentations containing the neuraxons (fig 6).

Unit fibers of collagen seem to be randomly dispersed throughout the tissue space and do not bear any constant relationship to other structures (figs 1-4 & 8). In these preparations a dense outer wall gives them a tubular appearance in cross-section. The diameter averages approximately 210 Å. The elastic fibers are less numerous (figs 1-3 & 5-8). They consist of a homogeneous matrix surrounded by a dense outer shell and possess an irregular branching structure (fig 8). Microfibrils (Low 61b,c) appear as thin sometimes granular filaments of about 80 Å diameter (figs 5-8). Although they are randomly distributed they are in close association with the elastic fibers. At times they appear to be matted within the elastic fiber network (fig 8). Another conspicuous localization occurs along the boundary membranes surrounding the cellular components of the tissue space. Although the boundary membrane is conventionally regarded as a somewhat unorganized granular layer adjacent to the plasma membrane, many micrographs suggest that it is composed of a multitude of matted microfibrils (figs 3-4 & 5-8).

Muscle fibers

Figures 9 and 17 illustrate the typical electron morphology of cardiac muscle cells seen in longitudinal section at low power. The myofibrils are crowded to the edge of the cell in the region of the nucleus. The relatively large amount of non-fibrillar cytoplasm at the nuclear poles contains mitochondria, groups of lipid droplets, dense bodies (dichte Körper) and the Golgi zone, all of which will be described later. The nuclei of human cardiac muscle tend to be oval in shape but may often possess irregular processes especially at the poles. At irregular intervals about the periphery of the nucleus nuclear pores are found in the double membrane (figs 15-16). In some sections the outer component of the nuclear membrane can be seen to separate from the nucleus and to

form a component of the sarcoplasmic reticulum (fig 17) Immediately beneath the inner component of the nuclear membrane there is often recognizable a dense zone of 200-400 Å thickness It is characterized by an accumulation of markedly dense granules These granules are denser than those observed within the accumulations of chromatin in the remainder of the nucleus (figs 15 16) In low power micrographs the true nuclear membrane is not evident and the "membrane of the nucleus appears to be delineated by this dense zone (figs 9 16 17) One or more nucleoli may be found in some nuclei They are oval round or serpentine and are composed of a compact accumulation of very dense granules At times small vacuoles or areas of decreased density are present within the nucleoli (fig 9)

In longitudinal section the myofibrils are grouped into myofibrils which run chiefly parallel to the long axis of the muscle cell (figs 9 11 12 17) Both primary and secondary myofibrils are identifiable (figs 11 12) The larger primary myofibrils measure 120-150 Å in diameter and are separated from each other by intervals of 160 Å The smaller secondary filaments are located in the linear spaces between the primary filaments and measure approximately 50 Å The primary and secondary filaments are connected to each other at discrete points along their length by cross bridges The characteristic Z I A M and H bands of striated muscle of other forms are also present in human cardiac muscle fibers (figs 11 12 17) In relaxed muscle the A band appears most prominent (fig 11) The M band is characterized by increased granularity and thickness of the myofibrils In the I band the myofibrils become thinner and tend to lose their discrete individual structure (figs 11 12) This less orderly arrangement in the I band gives the impression of a network of filaments Individual myofibrils however can be traced from A band through the I band and across the Z band (fig 11 arrows)

Although borders of myofibrils are typically ill-defined in cross section the constituent myofibrils are evident (fig 13) The filaments are often seen passing

through the cross section in various directions indicating that not all myofibrils of an individual muscle cell are in perfect parallel array At times spiral arrangements of myofibrils have been observed (fig 14) High power fields (fig 13) demonstrate the now familiar hexagonal array of myofibrils in cross section (Huxley and Hanson 60) The primary filaments have a tubular appearance and suggest the presence of rod like bodies in their walls The secondary filaments are symmetrically located in the spaces between adjacent primary filaments No internal structure has been observed

Groups of lipid droplets are usually present in the cytoplasm opposite one or both nuclear poles (figs 9 16 17) The groups tend to be oval Some of these seem to be surrounded by a single dense membrane and others not At times the membrane appears to have ruptured releasing the internal lipid droplets (fig 18) The droplets forming a single lipid mass vary in size and density The smaller droplets are the most dense the largest droplets are the least dense Most of the droplets appear distributed towards the periphery of the surrounding membrane This configuration gives the appearance of a central vacuole to many of the lipid masses (fig 18)

Groups of vacuoles representing the Golgi zone are usually found in close association with the lipid masses next to the nuclear pole (figs 15 16) The vacuoles are characteristically located in close proximity to the nuclear membrane No other structures are observed to separate these vacuoles from the nuclear membrane In a few sections collections of these vacuoles have been observed at several discrete points about the periphery of the nucleus (fig 17) suggesting that the Golgi zone occurs at locations other than the nuclear poles The number of vacuoles comprising a group varies but usually 40 to 100 vacuoles can be counted The size and shape of the constituent vacuoles vary considerably however most vacuoles appear oval and range from 250-1250 Å in section The vacuoles have a single limiting membrane no character

istic structure or material has been identified within the vacuoles.

The mitochondria (sarcosomes) of human cardiac muscle are found in the sarcoplasm at the nuclear poles in rows between the myofibrils and at the periphery of the cell. At the nuclear poles they are intermixed with the groups of lipid droplets and are located distal to the Golgi zone and dense bodies (figs 9, 16). In this location no characteristic pattern of distribution has been observed. The mitochondria lying between the myofibrils are arranged in long chains and often appear to be compressed into oblong shapes (fig 9). Other mitochondria appear round, oval or tear shaped in section. The internal cristae exhibit no one characteristic pattern. Some cristae have a complex branching pattern (figs 15, 16) while others have a more uniform lamellar structure (figs 12, 16). The cristae exhibit the usual double membrane structure. No attempt has been made to determine statistically the relative distribution of mitochondria in the ventricle and atrium. However, a subjective impression of a greater number of mitochondria per unit area of ventricular heart muscle has been noted in our sections.

Groups of dark bodies (dichte Körper, Poche 58b) are characteristically found within the sarcoplasm usually lying between the Golgi zone and the bordering mitochondria at the nuclear poles (figs 15, 16). These dense bodies are rather uniformly oval in shape and measure 1250–4000 Å along the long axis. They possess a granular matrix and may appear to have internal lamellae (fig 15). Their appearance is quite distinct from that of the mitochondria (fig 15). In some sections they are observed to lie in a somewhat semicircular distribution about the Golgi zone. Their number is not constant but usually 6 to 8 are seen in section.

Surrounding the muscle cell are the plasma membrane and the boundary membrane (figs 7, 9). These two membranes have been referred to jointly as the exomembrane (Lundner & Poche 58b). The boundary membrane appears identical to the corresponding membranes which surround capillaries, unmyelinated nerves

and the unidentified cells. The boundary membrane of human cardiac muscle cells (perimembrane) measures between 200–250 Å. It is separated from the plasma membrane by a zone of lesser density measuring about the same. The plasma membrane can often be seen to dip down into the sarcoplasm and contact the Z band of a myofibril (fig 17). Numerous vesicles are frequently observed in various stages of formation along the plasma membrane (fig 7). These vesicles show no organized internal structure and appear morphologically similar to those seen within the cytoplasm of capillaries.

Intercalated discs (Sjostrand and Andersson Cedergren 60) are clearly identifiable in human cardiac muscle (figs 10, 17). The disc is a double membrane system formed by the infolding of the plasma membranes (sarcolemmae) of two contiguous muscle cells. The perimembrane (boundary membrane) does not fold in with the plasma membranes (fig 10). The space between the membranes is of decreased density except in the S^r regions (fig 10 arrow). Here there is an increased accumulation of dense granular material in the sarcoplasm. These granules form one or more lamellae parallel to the plasma membranes. In addition a series of thin fibrils run perpendicularly across this space and join the plasma membranes of the two cells. Although the intercalated discs often pass irregularly through the tissue section the classical staircase pattern is observed (Sjostrand and Andersson Cedergren 60). In some sections a disc can be completely traced from one cell border to the next.

Small aggregations of protoplasm for which there is no descriptive term at present in general use are randomly scattered throughout the cytoplasm (ITM in figs 7, 12, 14, 15). These masses although possessing variable form and highly irregular contours are clearly structural in their organization. The purely descriptive term "irregular tubulo-membranous component (ITM)" has been chosen to designate this system of formed elements (Battig and Clevenger 61). The basic structural organization of ITM is well illustrated in places where the cytoplasm lacks a high concentration of other visible structures

(figs 7-12) ITM membranes are about 30 Å thick or less and the tubular element possesses a near minimum diameter of about 100 Å. The latter may be understood to constitute the basic form or stem of the ITM. Sacculations and branchings along the course of the stem are often so numerous that the basic form of the ITM is rendered obscure. These swellings and branchings are also responsible for its highly irregular contours. Wherever RNP granules (Palade '55) are present they are associated with ITM. However, most of the ITM possess variable densities that are considerably less than the very high density of the RNP granules.

DISCUSSION

The ultrastructure of human cardiac muscle revealed by the newer techniques is essentially a confirmation of earlier work on human (Poche '58) and animal tissue (Weinstein '54, Lindner '57, Fawcett and Selby '58 and others). However, some new features have been demonstrated and others merit interpretation in accord with our rapidly growing knowledge of ultrahistology.

The finer structure of the contractile elements corresponds well to the pattern characteristic of cross striated muscle (Huxley and Hanson '60). All established features of ultrastructure including both kinds of protein filaments (primary and secondary) are recognizable in human tissue. There is no reason to believe that the molecular basis of contraction in human cardiac muscle differs in any way from that of cross striated muscle in general. Although of less fundamental interest, the spiral course and profound directional changes of the individual myofibrils within a single myofibril are conspicuous. This is especially notable since the tissue was fixed and dehydrated under conditions that prevented gross positional changes.

The non-contractile formed elements of human cardiac muscle resemble those described by Bennett ('60) for skeletal muscle in general. The ultrastructure of the nucleus itself is undistinguished. However, the dark band of granules sometimes observed just inside the nuclear membrane is striking in many prepara-

tions. This has not attracted the attention of other investigators although it is noticeable in an illustration of frog heart by Lindner ('57, fig. 4) and conspicuous in a myo-epithelial cell illustrated by Meessen ('59, fig. 7). This band in light microscopy could be mistaken for the nuclear membrane and give rise to erroneous ideas about its thickness.

The sarcoplasmic reticulum is characteristic and may safely be interpreted along the lines recently indicated by Bennett ('60). It is heavy and conspicuous wherever observed and conforms to the patterns described by Porter and Palade ('57) in the rat and by Lindner ('57) in the dog. Its proximity to the sarcolemma and the Z-bands was emphasized by Peachey and Porter ('59) who interpreted it as an intracellular conduction system that facilitated rapid contraction in cross striated muscle. However, the spiral pattern of attachment to the nucleus reported by Moore and Ruska ('57) was not observed in our preparations.

The sarcosomes correspond well to those illustrated by Poche ('58b) in human heart and Lindner ('58) in the dog. The resemblance between certain of the dense bodies (figs 15-16) and mitochondria was noticed by Lindner ('57) who called them "cytosome B." Poche ('58b) referred to them simply as dense bodies (*dichte Körper*) and observed them close to the Golgi zone. Very similar structures that are also very difficult to distinguish from small mitochondria are common in blood monocytes (Low and Freeman '58, pp. 78-85) and in other cell types. Palade and Farquhar ('60) have demonstrated the segregation of ferritin by certain dense bodies in the visceral epithelial cells of the renal glomerulus of nephrotic rats. However, the much larger size of these bodies and their lack of internal lamellae distinguish them from the *dichte Körper* of human cardiac muscle.

The Golgi zone has been recognized in cardiac muscle by several authors (Lindner '57, Fawcett and Selby '58 and others) but has usually been interpreted to lie at one or both of the nuclear poles. In our preparations the larger and more conspicuous representatives of the Golgi

zone are indeed at the nuclear poles. However, except for the total size of the aggregate, there is no difference between these and smaller groups of membranous vacuoles scattered randomly around the nuclear circumference. As many as 7 separate aggregates around a single nucleus have been observed (fig. 17).

The groups of lipid droplets so conspicuous in our preparations (figs. 9, 16, 18) have received considerable attention from others. They are the "cytosome C" of Lindner (57). Poche (58b) adopted this designation and identified them as lipofuchsin (Poche 57b). He believed that although present in normal muscle they increased in atrophic muscle. In hypertrophy they arose chiefly from dense bodies (dichte Körper) and in atrophy from degenerating mitochondria. This general opinion has been supported by others (Meessen 59; see discussion at end of his paper). These groups of lipid droplets are morphologically indistinguishable from aggregations of pigment elsewhere in the body as, for example, in Leydig cells of the human testis (Fawcett and Burgos 56). These authors point out that this form of lipochrome or ceroid is very common in most cells of steroid-producing endocrine glands.

The irregular tubulo-membranous component (ITM) has received very little critical attention although it is conspicuously recognizable in many of the cytological electron micrographs published during the past few years. In general, the frequency of striking demonstration has developed in direct proportion to improvements in specimen quality. At low magnifications the ITM appears as an essentially amorphous mass of coagulated material that hardly merits description. However, good microscope resolution at higher magnifications brings out a structural organization that commands attention. Whenever mentioned it has usually been described as granular (Fawcett and Selby 58; Bennett 60). It cannot be denied that this interpretation is appropriate in view of its close association with RNP granules, a relationship that has been clearly demonstrated in whole cells (Palade 55) and in fractionated preparations (Palade and Siekevitz 56; Siekevitz

and Palade 58, 60). On the other hand, observations made in this laboratory (Battig and Clevenger 61) indicate that a "granular" interpretation is not well suited to the ubiquity and protean characteristics of ITM. The term "irregular tubulo-membranous component" was chosen not only to describe its appearance as presented in this paper but also to be applicable to a much more extensive system of protoplasmic formed elements. In the hyaloplasm of human cardiac muscle its "basic" structural organization is well exemplified (figs. 7, 12, 14, 15).

The ultrastructure of the intercalated disc has been exhaustively analyzed (Sjostrand and Andersson Cedergren 60) and our own observations are essentially a confirmation of previously recognized patterns. In human cardiac muscle as in all forms examined by others, both of the cells involved retain their structural distinctness (Meessen 59; Kisch 60 and fig. 10 of this paper). However, the lamination of the S regions and other parts of the disc in man is less complex than in the guinea pig and mouse (Sjostrand and Andersson Cedergren 60) although more complex than in the turtle (Fawcett and Selby 58) and frog. The basic structure of the disc is formed by a double membrane with clear interspace (fig. 10). This was designated mesomembrane by Lindner (57) who distinguished it from the exomembrane covering the free surface of the cell. The exomembrane is also double (fig. 10) but in a very different way. Both meso- and exomembranes contain expressions of the sarcolemma (plasma membrane) of the muscle cell (Bennett 60). In each intercalated disc the sarcolemmata of two muscle cells are represented, each cell contributing one lamina to the mesomembrane. On the free surface of the cell the sarcolemma called protomembrane by Lindner (57), Poche (58b) and others forms the inner, dense member of the exomembrane. Here the inner surface of the sarcolemma is studded with numerous vesicles of pinocytosis (fig. 7), the caveolae intracellulares of Yamada (55). The outer member of the exomembrane, Lindner's perimembrane, is not a part of the muscle cell. It is stromal rather than parenchymal and

is best considered along with the other formed elements of the tissue space.

Gersh and Catchpole (49) and Gersh (52) working with the PAS technique and the light microscope demonstrated a system of Hotchkiss positive membranes that formed the limits of the connective tissue space. These were located basal to epithelia and also enclosed certain formed elements (blood vessels, muscle, nerve, fat cells). These structures are usually called basement membranes but the term *boundary membrane* has also been used (Low 61b). The latter name was chosen because the boundaries of the tissue space are determined by this membrane system externally by the membrane basal to epithelia and internally by the membranes surrounding the above mentioned structures. The tissue space proper exists within the physical limits thus defined and contains numerous formed elements (connective tissue fibers and cells) that conspicuously lack any membranous ensheathment.

The above concept is applicable to tissue space and connective tissues in general and has been used in this paper to describe the stromal tissues of the human heart. Since no surface epithelium is present the external boundary membrane is of course not involved. Internal boundary membranes however surround muscle fibers (figs. 2, 7-9, 10), capillaries (figs. 1-5) and unmyelinated nerves (figs. 1, 2, 1, 6). The tissue space itself contains connective tissue fibers (figs. 1, 3-5, 8) and certain cells (figs. 1-5) all of which exist free and uncovered in a structureless matrix. The electron microscopic appearance of these stromal formed elements is interpreted below in somewhat greater detail.

Human cardiac capillaries possess typical ultrastructure. According to the classification of Bennett, Luft and Hampton (59) they belong in type A1, which indicates that there is a continuous boundary membrane, no fenestrations or pores in the endothelial cytoplasm and an incomplete pericapillary cellular investment. Their vesicles correspond to those described by Moore and Ruska (57). These workers assigned the function of cytoplasmic (transmission by cell) to these vesicles. More recently this type of trans-

port was demonstrated by Farquhar and Palade (60) in the glomerular capillaries of the rat kidney.

The unmyelinated nerves of human cardiac muscle present no new features. The classic pattern described by Gasser (55) prevails with typical Schwann cell relationships that are now recognized to be characteristic of nervous tissue in general (Robertson 58). The investing boundary membrane is also typical. Concerning the ultrastructure of the myoneural junction no new evidence is offered here. However the work of Robertson (58) on reptilian material and the recent review of Couéroux (60) indicate that the investing boundary membranes of nerve and muscle fiber are definitely present although combined at the synaptic gutter where nerve and muscle are in most intimate contact.

The small cytoplasmic extensions observed close to capillaries have no structural characteristics which might help identify them. But they do possess a conspicuous boundary membrane which often blends with that of the neighboring endothelium. The round unidentified cells also have a boundary membrane. Although cytoplasmic continuity between the extensions and the round cells has not been observed the presence of a boundary membrane about both makes them clearly distinguishable from the spindle shaped cells. In the absence of more conclusive evidence it is tempting to identify the membrane-ensheathed round cells and extensions as Rouget cells of primarily myoid identity. The spindle shaped cells could then be undifferentiated mesenchymal cells or fibroblasts and any unclad cytoplasmic extensions would belong to them. It appears that the presence or absence of an investing boundary membrane may provide a useful criterion for identifying cell types at the level of ultrastructure.

Karrer's study of the loose connective tissue in the bronchiolar tunica propria of the mouse (58) described patterns of fibrillar organization that may be applied without essential change to our preparations. Unit collagen fibers exist in aggregates of varying size all the way from large ones forming the collagen fibers of light microscopy (fig. 1) through all intermediate sizes (figs. 4, 5, 6, 8) to isolated filers

an arrangement typical of loose connective tissues in general. Also characteristic is the occasional but inconstant demonstration of axial periodicity in longitudinal section (fig 6 upper left) and the 'hol low' appearance in cross section (fig 4). These fibers have been interpreted as solid (homogeneous) by some and hollow by others (discussed by Karrer 58). Rhodin and Dalhamn (55) state that the indication of an "outer limiting membrane is vague in longitudinal sections but more pronounced in transverse ones. This is probably the most acceptable interpretation of unit fiber structure as seen in sectioned embedded tissue.

Elastic fibers in loose connective tissue tend to be very irregular in their form and spatial disposition (Karrer 58, Rhodin and Dalhamn 55) and those of the human heart also follow this pattern (figs 1, 3, 5, 8). The generally homogeneous matrix and the somewhat darker margin both vary considerably in density. The matrix in particular may vary from light gray in some areas to nearly black in others. The very irregular contours of the fibers cut in section is particularly conspicuous.

A smaller filamentous element of connective tissue has been observed by numerous authors (Jakus 54, Robertson 56a, Karrer 58). These became so conspicuous in human lung tissue embedded in Vestopal W that a special descriptive name *microfibrils* was assigned to them (Low 61b). In human cardiac tissue they have their greatest concentrations about elastic fibers. In many places they are associated with boundary membranes to such an extent that the membranes themselves seem to be made up largely of matted microfibrils. Occasional microfibrils may be seen among unit collagen fibers or free in the tissue space. These last two locations however suggest random scattering rather than an association of functional significance.

The tissue space of human cardiac muscle thus contains three types of connective tissue fibers in addition to the mesenchymal cells (fibroblasts). The remainder of the formed elements are all separated from the tissue space by identical ensheathing boundary membranes. These structures include the capillaries, nerves, and Rouget

(?) cells representing the stromal tissues and the cardiac muscle cells as the parenchyma. The complex of relationships involving parenchyma, stroma, tissue space and the connective tissues are at the level of ultrastructure fundamentally the same in the heart as they are elsewhere in the body.

ACKNOWLEDGMENTS

Grateful acknowledgment is made to Dr C M Goss for the freedom to proceed at discretion during this investigation to Mr M P Clevenger for technical assistance to Mr R E Druce for maintenance of the electron microscope and to Mrs B Arseneaux for the typing of this manuscript.

LITERATURE CITED

- Battig C G and M R Clevenger 1961 An irregular tubulo-membranous component (ITM) of protoplasm. *Anat Rec* 139:328.
- Bennett S H 1960 The structure of striated muscle as seen by the electron microscope. In: *Structure and Function of Muscle*. G H Bourne, ed. Academic Press, New York. 1:137-181.
- Bennett S H, J H Luft and J C Hampton 1959 Morphological classifications of vertebrate blood capillaries. *Am J Physiol* 196:381-390.
- Bourne G H 1960 *The Structure and Function of Muscle*. Vol 1. Structure. Academic Press, New York.
- Couteaux R 1960 Motor end plate structure. In: *Structure and Function of Muscle*. G H Bourne, ed. Academic Press, N Y. 1:337-380.
- Farquhar M G and G F Palade 1960 Segregation of ferritin in glomerular protein absorption droplets. *J Biophys Biochem Cytol* 7:297-304.
- Fawcett D W and M H Burgos 1956 Observations on the cytomorphosis of the germinal and interstitial cells of the human testis. *Ciba Foundation Colloquia on Ageing* 2:86-99.
- Fawcett D W and C C Selby 1958 Observations on the fine structure of the turtle atrium. *J Biophys Biochem Cytol* 4:63-72.
- Gasser H S 1935 Properties of dorsal root unmyelinated fibers on the two sides of the ganglion. *J Gen Physiol* 38:709-728.
- Gersh I 1952 Ground substance and the plasticity of connective tissues. In: *The Harvey Lectures 1949-50*. C C Thomas, Springfield. pp 211-241.
- Gersh I and H R Catchpole 1949 The organization of ground substance and basement membrane and its significance in tissue injury, disease and growth. *Am J Anat* 85:47-522.
- Hibbs R G 1956 *Electron microscopy of developing cardiac muscle in chick embryos*. *Ibid* 99:17-51.
- Huxley H E and J Hanson 1960 The molecular basis of contraction in cross striated muscle.

- cles In Structure and Function of Muscle G H Bourne ed Academic Press New York 1 183-227
- Jakus M 1954 Studies on the cornea I The fine structure of the rat cornea Am J Ophthal 38 40-53
- Khristolyubova N B 1958 Study of the structure of heart muscle with the electron microscope Rep Acad Sci USSR 119 168-170 (in Russian)
- Kisch B 1957 Der Ultramikroskopische Bau von Herz und Kapillaren Verlag von Dr Dietrich Steinkopf Darmstadt
- 1960 Electron Microscopy of the Cardiovascular System Charles C Thomas Springfield Ill
- Kisch B E. Grey and J J Kelsch 1948 Electron histology of the heart Exp Med Surg 6 346-365
- Low F N 1961a Methods of clearing tissue sections embedded in Vestopal W The proceedings of the European Regional Conference on Electron Microscopy Delft 1960 in press
- 1961b The extracellular portion of the human blood air barrier and its relation to tissue space Anat Rec 139 105-124
- 1961c Microfibrils a small extracellular component of connective tissue Anat Rec 139 250
- Low F N and J A Freeman 1958 Electron Microscopic Atlas of Normal and Leukemic Human Blood The Blakiston Division McGraw Hill Book Company Inc New York
- Meessen H 1959 Die submikroskopische Morphologie des Herzmuskels In I Symposium an der medizinischen Universitätsklinik Münster (Westf) Georg Thieme Verlag Stuttgart pp 1-21
- Moore D H and H Ruska 1957a Electron microscope study of mammalian cardiac muscle cells J Biophys Biochem Cytol 3 261-268
- 1957b The fine structure of capillaries and small arteries Ibid 3 457-462
- Palade G E 1952 A study of fixation for electron microscopy J Exp Med 95 285-298
- 1955 A small particulate component of the cytoplasm J Biophys Biochem Cytol 1 59-68
- Palade G E and P Siekevitz 1956 Pancreatic microsomes An integrated morphological and biochemical study J Biophys Biochem Cytol 2 671-690
- Peachey L D and K R Porter 1959 Intracellular impulse conduction in muscle cells Science 129 721-722
- Pease D C 1960 The basement membrane substratum of histological order and complexity Fourth Int Conf on Electron Microscopy Berlin 1958 II 139-148
- Poche R 1957a Das submikroskopische Bild der Herzmuskelveränderungen nach Überdosierung von Schilddrüsenhormon Beitr Pathol Anat Allg Pathol 118 40-40
- 1957b Elektronenmikroskopische Untersuchungen des Lipofuchsin im Herzmuskel des Menschen. Zentralbl Allg Pathol Pathol Anat. 96 (abstract)
- 1958a Submikroskopischer Beitrag zur Pathologie des Herzmuskels Verhand D Gesell Pathol Gustav Fischer Verlag Stuttgart pp 35-55
- 1958b Submikroskopische Beiträge zur Pathologie der Herzmuskelzelle bei Phosphorvergiftung Hypertrophie Atrophie und Kaliummangel Virchows Arch 331 162-178
- 1959 Elektronenmikroskopische Untersuchungen zur Morphologie des Herzmuskels vom Siebenschläfer während des aktiven und des lethargischen Zustandes Z Zellforsch 50 332-360
- 1960 Experimentelle Pathologie des Herzmuskels Fourth International Conference on Electron Microscopy Berlin 1958 Springer Verlag Berlin II 308-315
- Porter K R and G E Palade 1957 Studies on the endoplasmic reticulum III Its form and distribution in striated muscle cells J Biophys Biochem Cytol 3 260-300
- Rhodin J and T Dalhamn 1956 Electron microscopy of collagen and elastin in lamina propria of the tracheal mucosa of rat Exp Cell Res 9 371-375
- Robertson J D 1956a Some features of the ultrastructure of reptilian skeletal muscle J Biophys Biochem Cytol 2 369-380
- 1956b The ultrastructure of a reptilian myoneural junction Ibid 2 381-391
- 1958 Structural alterations in nerve fibers produced by hypotonic and hypertonic solutions Ibid 4 349-364
- Ryter A and E Kellenberger 1958 Linéolons au polyester pour l'ultramicrotomie J Ultrastruct Rec 2 200-214
- Siekevitz P and G E Palade 1958 A cytochemical study on the pancreas of the guinea pig II Functional variations in the enzymatic activity of microsomes J Biophys Biochem Cytol 4 401-410
- 1960 A cytochemical study on the pancreas of the guinea pig VI Release of enzymes and ribonucleic acid from ribonucleoprotein particles Ibid 7 631-644
- Sjöstrand F and E Andersson 1954 Electron microscopy of the intercalated discs of cardiac muscle tissue Experimentia 10 360-370
- Sjöstrand F A and E Andersson Cedergren 1960 Intercalated discs of heart muscle In Structure and Function of Muscle G H Bourne ed Academic Press New York 1 421-445
- Studitsky A N 1959 Experimental surgery of muscles Academy of Science Moscow USSR (in Russian)
- van Breeman L 1953 Intercalated discs in heart muscle studied with the electron microscope Anat Rec 117 49-63
- Watson M L 1958 Staining of tissue sections for electron microscopy with heavy metals II Application of solutions containing lead and barium J Biophys Biochem Cytol 4 727-729
- Weinstein H J 1954 An electron microscope study of cardiac muscle Exp Cell Res 130-146
- Yamada E 1955 The fine structure of the gall bladder epithelium of the mouse J Biophys Biochem Cytol 1 441-458

PLATES

- cles. In *Structure and Function of Muscle* G. H. Bourne ed. Academic Press New York 1 183-227
- Jakus M. 1954 Studies on the cornea. I. The fine structure of the rat cornea. *Am J Ophthalmol* 38 40-53
- Khrizoljubova N. B. 1958 Study of the structure of heart muscle with the electron microscope. *Rep Acad Sci USSR* 119 168-170 (in Russian)
- Kisch B. 1957 *Der Ultramikroskopische Bau von Herz und Kapillaren*. Verlag von Dr. Dietrich Steinkopf Darmstadt
- 1960 *Electron Microscopy of the Cardiovascular System*. Charles C. Thomas Springfield Ill
- Kisch B. E. Grey and J. J. Kelsch. 1948 *Electron histology of the heart*. *Exp Med Surg* 6 346-365
- Low F. N. 1961a Methods of clearing tissue sections embedded in Vestopal W. The proceedings of the European Regional Conference on Electron Microscopy Delft 1960 in press
- 1961b The extracellular portion of the human blood air barrier and its relation to tissue space. *Anat Rec* 139 105-124
- 1961c Microfibrils: a small extracellular component of connective tissue. *Anat Rec* 139 250
- Low F. N. and J. A. Freeman. 1958 *Electron Microscopic Atlas of Normal and Leukemic Human Blood*. The Blakiston Division McGraw-Hill Book Company Inc. New York
- Meessen H. 1959 Die submikroskopische Morphologie des Herzmuskels. In: I. Symposium an der medizinischen Universitätsklinik Münster (Westf.). Georg Thieme Verlag Stuttgart pp 1-21
- Moore D. H. and H. Ruska. 1957a Electron microscope study of mammalian cardiac muscle cells. *J Biophys Biochem Cytol* 3 261-268
- 1957b The fine structure of capillaries and small arteries. *Ibid* 3 457-462
- Palade G. E. 1952 A study of fixation for electron microscopy. *J Exp Med* 95 285-298
- 1955 A small particulate component of the cytoplasm. *J Biophys Biochem Cytol* 1 59-68
- Palade G. E. and P. Siekeitz. 1956 Pancreatic microsomes: An integrated morphological and biochemical study. *J Biophys Biochem Cytol* 2 671-690
- Peachey L. D. and K. R. Porter. 1959 Intracellular impulse conduction in muscle cells. *Science* 109 721-722
- Pease D. C. 1960 The basement membrane substratum of histological order and complexity. Fourth Int Conf on Electron Microscopy Berlin 1958 II 139-158
- Poche R. 1957a Das submikroskopische Bild der Herzmuskelveränderungen nach Überdosierung von Schilddrüsenhormon. *Bull Pathol Anat Allg Pathol* 118 407-40
- 1957b Elektronenmikroskopische Untersuchungen des Lipofuchsin im Herzmuskel des Menschen. *Zentralbl Allg Pathol Pathol Anat* 96 (abstract)
- 1958a Submikroskopischer Beitrag zur Pathologie des Herzmuskels. *Verhand D Gesell Pathol* Gustav Fischer Verlag Stuttgart pp 35-53
- 1958b Submikroskopische Beiträge zur Pathologie der Herzmuskelzelle bei Phosphorvergiftung. Hypertrophie, Atrophie und Kalkumangel. *Virchow's Arch* 331 163-18
- 1959 Elektronenmikroskopische Untersuchungen zur Morphologie des Herzmuskels vom Siebenschläfer während des aktiven und des lethargischen Zustandes. *Z Zellforsch* 50 332-360
- 1960 Experimentelle Pathologie des Herzmuskels. Fourth International Conference on Electron Microscopy Berlin 1958 Springer Verlag Berlin II 308-315
- Porter K. R. and G. E. Palade. 1957 Studies on the endoplasmic reticulum. III. Its form and distribution in striated muscle cells. *J Biophys Biochem Cytol* 3 269-300
- Rhodin J. and T. Dalhamn. 1956 Electron microscopy of collagen and elastin in lamina propria of the tracheal mucosa of rat. *Exp Cell Res* 9 371-375
- Robertson J. D. 1956a Some features of the ultrastructure of reptilian skeletal muscle. *J Biophys Biochem Cytol* 2 369-380
- 1956b The ultrastructure of a reptilian myoneuronal junction. *Ibid* 2 381-391
- 1958 Structural alterations in nerve fibers produced by hypotonic and hypertonic solutions. *Ibid* 4 349-364
- Ryter A. and E. Kellenberger. 1958 Linclions au polyester pour l'ultramicrotomie. *J Ultrastruct Rec* 2 200-214
- Stekewitz P. and G. E. Palade. 1958 A cytochemical study on the pancreas of the guinea pig. II. Functional variations in the enzymatic activity of microsomes. *J Biophys Biochem Cytol* 4 401-410
- 1960 A cytochemical study on the pancreas of the guinea pig. VI. Release of enzymes and ribonucleic acid from ribonucleoprotein particles. *Ibid* 7 631-644
- Sjöstrand F. and E. Andersson. 1954 Electron microscopy of the intercalated discs of cardiac muscle tissue. *Experientia* 10 360-370
- Sjöstrand F. A. and E. Andersson-Cedergrén. 1960 Intercalated discs of heart muscle. In: *Structure and Function of Muscle*. G. H. Bourne ed. Academic Press New York 1 421-445
- Studitsky A. N. 1959 Experimental surgery of muscles. *Academy of Science Moscow USSR* (in Russian)
- van Breeman V. L. 1953 Intercalated discs in heart muscle studied with the electron microscope. *Anat Rec* 117 49-63
- Watson M. L. 1958 Staining of tissue sections for electron microscopy with heavy metals. II. Application of solutions containing lead and barium. *J Biophys Biochem Cytol* 4 727-729
- Weinstein H. J. 1954 An electron microscope study of cardiac muscle. *Exp Cell Res* 130-146
- Yam da F. 1955 The fine structure of the gall bladder epithelium of the mouse. *J Biophys Biochem Cytol* 1 445-458

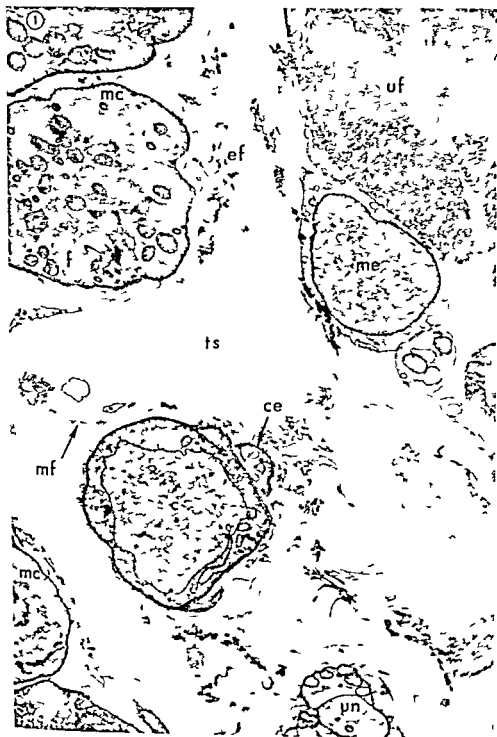


PLATE 2

EXPLANATION OF FIGURE

- 2 Four structural elements of the tissue space frequently found in close association to a muscle cell (mc) are the capillary (c) unmyelinated nerve (un) unidentified round cell (rc) and mesenchymal cell (me). The mesenchymal cell contains an aggregation of osmophilic bodies (ob) as well as many large vacuoles. The long attenuated cytoplasmic extension of the mesenchymal cell is striking (arrows). The unidentified round cell is characterized by a thin perinuclear rim of cytoplasm and a single cleft (cl) in the nuclear outline. A distinct boundary membrane surrounds the para capillary cytoplasmic extension (ce). Note also the identical appearance of the boundary membrane (bm) surrounding the capillary and the muscle cell. Grid immersed in equal parts of acetone and ether containing 0.5% PTA by weight for 45 minutes. $\times 13,000$



PLATE 3

EXPLANATION OF FIGURES

- 3 The capillary contains a portion of a blood cell (bc). Desmosomal junctions (dj) are prominent. Many vesicles of pinocytosis (p) are present in various stages of formation along the plasma membrane of this capillary. The boundary membrane (bm) appears to be composed of a mass of matted microfilaments rather than granules. Other microfilaments (mf) are dispersed randomly throughout the tissue space (ts) or surround elastic fibers (ef). Isolated cytoplasmic extensions (ce) lie adjacent to the capillary. The mesenchymal cell (mc) can be identified by the characteristics described in figure 2. Grid immersed in equal parts of acetone and ether containing 0.1 PTA by weight for 45 minutes. 16000.
- 4 Boundary membranes surround the capillary (c), unmyelinated nerve (un), and muscle cell (mc). A bias cut of the plasma membrane of the mesenchymal cell (mc) creates the illusion of a boundary membrane (arrows). Numerous microfilaments (mf) and unit fibers (uf) pass through this section. Some of the unit fibers which are in almost perfect cross section appear tubular. Grid immersed in equal parts of acetone and ether containing 0.5 PTA by weight for one hour. $\times 17000$.

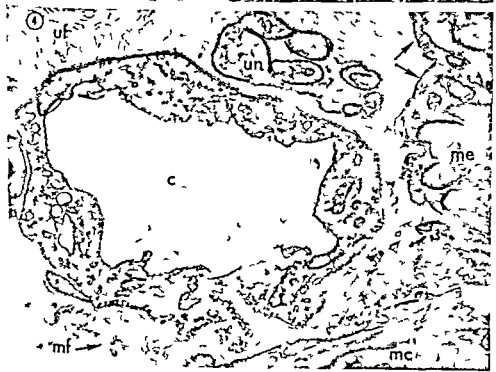
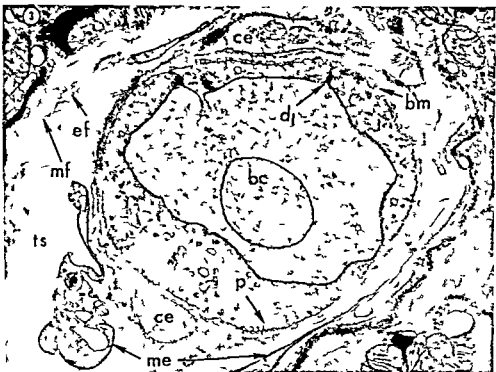


PLATE 4

EXPLANATION OF FIGURES

- 5 Three capillaries (c) are seen here in cross-section. Adjacent to one capillary is a cytoplasmic extension which lacks a boundary membrane (arrow). According to the interpretation in the text it therefore belongs to either a mesenchymal cell or fibroblast. In contrast the cytoplasmic extension between the two remaining capillaries is ensheathed by a boundary membrane which circumstance suggests its identity as a Rouget cell. Unit fibers of collagen (uf), elastic fibers (ef) and microfibrils (mf) are identifiable in the tissue space of this unstained specimen. Grid immersed in equal parts of acetone and ether overnight followed by 250 C for $\frac{1}{2}$ hour $\times 14\ 000$
- 6 This cross-section of an unmyelinated nerve displays the typical identifications of the Schwann cell (sc), plasma membrane (pm) in which are contained the individual neuraxons (na). A mesaxon (ma) is formed by the double infolding of the plasma membrane. The boundary membrane (bm) surrounds the entire nerve but does not dip down into the indentations. Grid immersed in equal parts of acetone and ether overnight then 200 C for $\frac{1}{2}$ hour followed by immersion in equal parts of acetone and ether containing 0.1% PTA for $\frac{1}{2}$ hour $\times 20\ 000$

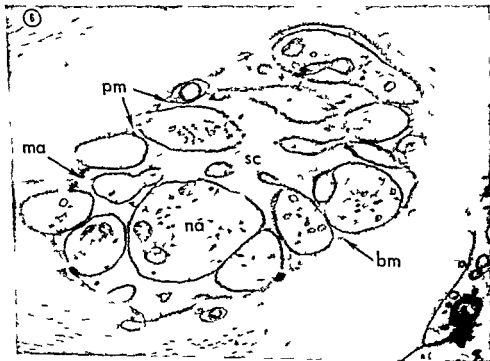
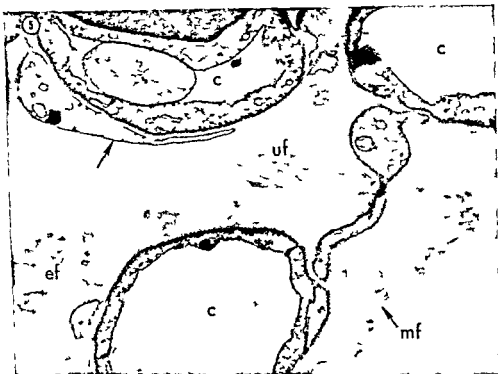


PLATE 5

EXPLANATION OF FIGURES

- 7 Two closely adjacent muscle cells are separated by a narrow tissue space (ts) measuring 400 Å. The boundary membranes (bm) and plasma membranes (pm) appear quite dense in this thick section. The thickness of the section also displays to advantage the irregular tubulo-membranous component (itm) of the cytoplasm and its typical variations in density. The ITM has a distinct saccular structure which can be contrasted in appearance with the vesicles of pinocytosis (p). In some areas (arrows) the ITM appears to form chains. Grid immersed in equal parts of acetone and ether containing 0.1% PTA by weight for 3½ hours. $\times 73,000$
- 8 Typical features of unit fibers (uf) elastic fibers (ef) and microfibrils (mf) are illustrated by this micrograph. The unit fibers pass obliquely through the section. Elastic fibers consist of a homogeneous matrix surrounded by a dense shell. The filamentous microfibrils exhibit a linear granularity and are seen enmeshed in the elastic fibers. In this section a matted layer of microfibrils appears to contribute to the boundary membrane of an adjacent cell (arrow). Two hundred fifty degrees centigrade for one hour followed by flotation of the grid on a 1% aqueous solution of ITA for one hour. $\times 43,000$

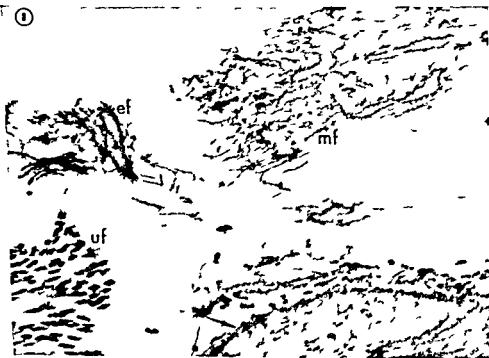
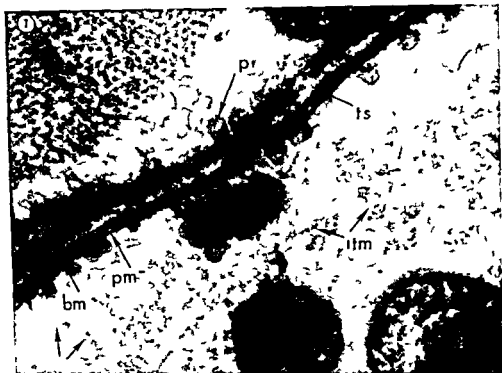


PLATE 6

EXPLANATION OF FIGURES

- 9 This low power micrograph shows two adjacent muscle cells in longitudinal section. The entire width of the lower cell is included. Many structural elements are represented in this micrograph: nucleus (n), nucleolus (nu), lipid (l), Golgi zone (g), mitochondria (m) and myofibrils (mb). The centrally located nucleus may contain one or more nucleoli of varied shapes. The groups of lipid may be single or multiple and may be present at one or both nuclear poles. The mitochondria lying between adjacent myofibrils are crowded into long chains (arrow). Two hundred fifty degrees centigrade for $\frac{1}{2}$ hour $\times 5100$
- 10 An intercalated disc runs horizontally across the field. The boundary membrane (bm) does not fold in with the plasma membranes (sarcolemmæ) which form the disc. Typical S-regions (S) are present along the course of the disc. At one S region (arrow) there is a transverse bridging of the disc by small filaments. The lamellar branching nature of the mitochondrial cristæ membranes is striking as they pass diagonally through this section. Grid floated on 1% aqueous lead hydroxide for 50 minutes
33 000

HUMAN CARDIAC MUSCLE
Charles G. Bating and Frank N. Low

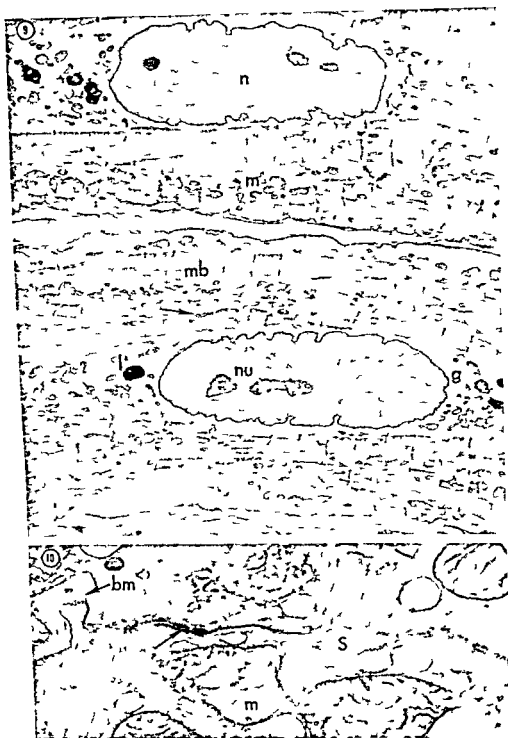


PLATE 7

EXPLANATION OF FIGURES

- 11 These sarcomeres are partially but not totally contracted as shown by the narrow I bands (I). At the single arrow both primary and secondary myofilaments are visible. At the double arrows there is continuity of the myofilament through the Z-band. In the space between these two myofibrils are mitochondria and small vesicles of sarcoplasmic reticulum. Grid immersed in equal parts of acetone and ether for $\frac{1}{2}$ hour followed by immersion in equal parts of acetone and ether containing 0.1% PTA by weight for 6 hours $\times 30\,000$.
- 12 In the A band (A) the myofilaments (f) possess a tubular appearance and are easily followed. However in the I band they become lacy in appearance and the orderly array is not maintained. The ITM component is prominent in this micrograph (itm) and is clearly distinguishable from the much larger sarcoplasmic reticulum (sr). The tubular and saccular phases of the ITM are well represented. Two hundred fifty degrees centigrade for $\frac{1}{2}$ hour then grid immersed in equal parts of acetone and ether for 26 $\frac{1}{2}$ hours followed by immersion in equal parts of acetone and ether containing 0.1% PTA by weight for $\frac{1}{2}$ hour $\times 43\,000$.

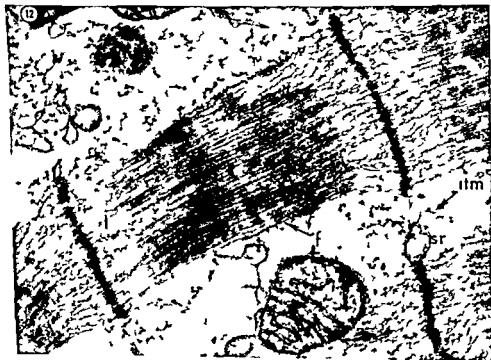


PLATE 8

EXPLANATION OF FIGURES

- 13 The primary myofilaments (pf) appear tubular in cross section and possess an outer granular shell. In some areas the secondary myofilaments (sf) are also identifiable. However their internal structure is not evident. A mitochondrion (m) lies at the junction of these myofibrils. Grid floated on an aqueous solution containing 1% PTA by weight for 65 minutes followed by 250 C for 30 minutes. $\times 87,000$
- 14 These myofibrils exhibit no uniform orientation as they pass through the section. Two adjacent spiral arrays of myofibrils show the primary myofilaments in cross section as well as in longitudinal spiral section. Secondary myofilaments (sf) can also be identified in cross section. The ITM component (itm) here displays its tubular branching structure. Its form contrasts sharply with that of the sarcoplasmic reticulum (sr). Grid immersed in equal parts of acetone and ether for one hour followed by immersion in equal parts of acetone and ether containing 0.05% Thorium nitrate by weight for one hour. $\times 40,000$

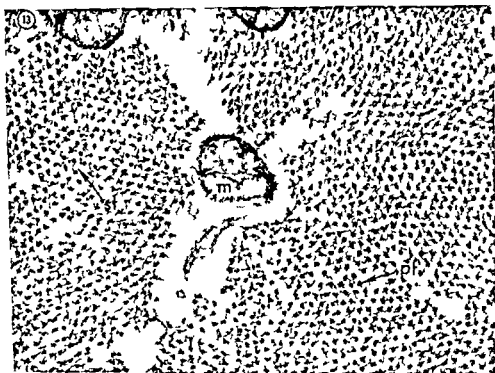


PLATE 9

EXPLANATION OF FIGURES

- 15 Dense bodies (dk) are usually in close association with the Golgi zone (g) at a nuclear pole (np). The bodies are densely granular and several exhibit internal lamellae (ll). Typical mitochondria (m) are present and appear quite distinct from the dense bodies. The cytoplasmic ITM component (itm) is somewhat filamentous in this preparation and is noticeably less dense than the RNP granules. An aggregation of particularly dense granules along the inner surface of the nuclear membrane creates the impression of a secondary membrane (arrow). Two hundred fifty degrees centigrade for $\frac{1}{4}$ hour followed by fixation on a 1% aqueous solution of lead hydroxide for one hour.
x 42 000
- 16 The Golgi zone (g) consists of an aggregation of small membrane lined vacuoles of varied sizes. Typically located at a nuclear pole it is closely associated with mitochondria (m), lipid droplets (l) and small granular dense bodies (dk). The mitochondria in this field illustrate the typical non uniformity of internal structure seen in human heart muscle. Some possess elaborately branching cristae while others possess cristae arranged in parallel array (arrows). Two hundred fifty degrees centigrade for $\frac{1}{2}$ hour.
17 000

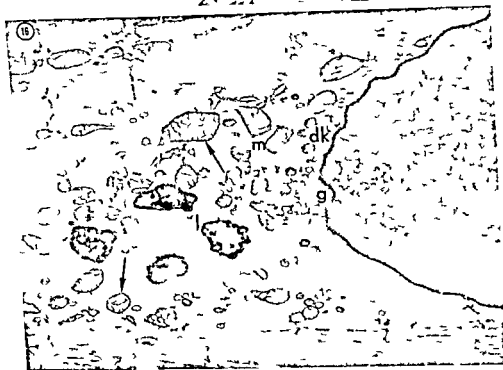
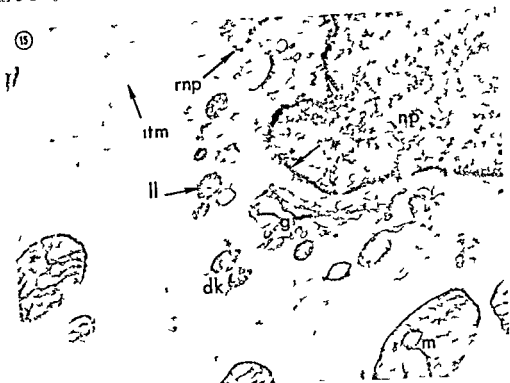
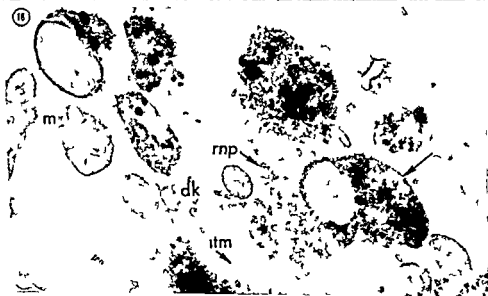


PLATE 10

EXPLANATION OF FIGURES

- 17 This large central muscle cell nucleus (n) is surrounded by several groups of vacuoles (v) resembling Golgi zones. At one point (arrow) the outer component of the nuclear membrane extends out into the cytoplasm as sarcoplasmic reticulum. An intercalated disc (id) is present in an adjacent cell. Two hundred fifty degrees centigrade for $\frac{1}{2}$ hour $\times 3000$.
- 18 These groups of lipid droplets contain droplets of two main densities superimposed on a dense granular component. A membrane (arrow) surrounds some lipid masses. Other masses appear somewhat dispersed and lack a corresponding membrane. Note the dense bodies (dk) and mitochondria (m). The close association of the RNP granules and the irregular tubulo-membranous component (itm) as well as their conspicuously different densities is well exemplified by this micrograph. Two hundred fifty degrees centigrade for $\frac{1}{2}$ hour $\times 37000$.



Use of Colchicine for the Measurement of Mitotic Rate in the Intestinal Epithelium

CATHERINE E. STEVENS HOOPER

Department of Anatomy McGill University Montreal Canada

Colchicine has been used as an investigative tool in problems concerning cell proliferation since the early 1930's. The earliest and some of the most comprehensive studies on the qualitative and quantitative effect of this drug in causing the arrest in metaphase of cells undergoing division were made by P. Dustin Sr (36), Brues (36), Ludford (36) and Bucher (39) who showed that at certain dose levels and within a certain period of time colchicine acted only to arrest in metaphase and did not interfere with the normal rate of entry of cells into mitosis. Following these early investigations colchicine was used principally to emphasize sites of normal cell division or the action of hormones and other compounds on mitotic activity. More recently interest has been revived in use of the drug in quantitative studies. It has been employed in attempts to measure the rate of proliferation of the intestinal epithelium of rats (Leblond and Stevens 48) and cats (McMinn 54) and also of the epidermis (Storey 49), alveolar cells of the lung (Bertalanffy and Leblond 53) and the epithelium lining the urinary bladder of rats (Vulpe 54).

The work to be reported in this paper is an examination of the action of colchicine and its suitability as an agent in the quantitative estimation of the mitotic rate using the intestinal epithelium of rats as the test tissue.

The epithelium of the intestinal crypts was selected because of its high mitotic activity. Thus significant increases in the number of arrested metaphases may be expected to appear within a relatively short period of colchicine treatment. A short experimental period also has the advantage that the effect of the drug is less likely to wear off during the experiment.

Furthermore the tendency of arrested metaphases to degenerate and eventually to disappear in mammalian tissues of high mitotic activity may be avoided. The desirability of a rapid and complete action of the drug prompted an investigation of its effects in the tissue soon after injection and of the best route of administration. The effects of single and repeated doses of colchicine were compared as to their efficiency in maintaining the effect of the drug. The results were analyzed to determine whether colchicine could be used to measure the normal mitotic rate in the intestinal epithelium and also to calculate the duration of the stages of mitosis.

MATERIALS AND METHODS

Colchicine

U.S.P. Colchicine (Inland Alkaloid Co. Tipton, Indiana) was purified on a chromatographic column according to the method of Ashley and Harris (44). About half the original weight of material was recovered; the crystals having a very pale yellow color as compared with the stronger shade of the starting material. The melting point of the original colchicine was about 150°C following chromatography; it rose to 153°C. A comparison of the action of both samples in arresting metaphase in the ileal crypts of rats 4 hours after the injection of 0.1 mg per 100 gm of body weight showed no significant difference (original colchicine mean number of metaphases per crypt in three rats 27.5; "purified" colchicine mean number of metaphases per crypt in 4 rats 26.7). In all subsequent experiments the "purified"

fied" colchicine was used as a solution in distilled water made up immediately before injection

Animals and histological procedures

Healthy rats of Sherman stock fed on Purina Fox Chow were used when their body weight reached approximately 260 gm (range 216-308)

Each group consisted of 4-11 rats and all experiments were conducted in the morning to minimize any possible effects of diurnal variation on mitotic activity. Control uninjected animals were sacrificed at approximately the same time as the experimental animals

While the animals were under chloroform anesthesia about 1 cm of the ileum proximal to the caecum was removed as rapidly as possible and placed in Susa fluid. After 5-6 hours fixation the Susa was replaced with 4% formalin overnight. For each animal three non-consecutive longitudinal 4 μ paraffin sections were mounted and stained with Harris hematoxylin and eosin

Counting technique

Areas of the sections were selected for counting in which the crypts were cut approximately throughout their length and also appeared fairly straight and close together i.e. regions where the mucosa was not stretched. At 800 \times magnification all stages of mitosis and all interphase nuclei of the epithelial cells lining the crypts were counted except when less than half the nucleus was included in the section. This meant in practice that nuclear fragments that were too small to be identified with certainty were left out of the counts

The stages of mitosis were identified as follows

Prophase The change from an interphase to a prophase nucleus is usually shown by an increase in nuclear diameter. The chromatin instead of being rather finely dispersed in the nuclear sap with some accumulations around the nucleolus and nuclear membrane collects in slightly larger clumps which are more definitely concentrated on the nucleolus and nuclear membrane. The background staining of the nucleus presumably provided by very

finely dispersed chromatin becomes much weaker in early prophase as if the stainable material had become attached to the chromatin clumps. Thus the prophase nucleus stands out from the interphase ones by reason of the greater contrast in staining intensity of the sap and chromatin clumps. These changes increase in degree until they become very obvious and at the same time the nuclei begin to move apically towards the crypt lumen. This stage passes gradually into mid prophase in which the nucleus is still large although tending to become smaller. The chromatin becomes more definitely arranged into strands rather than in clumps. Late prophase is a brief stage in which the short thick and often spiral chromosomes are scattered fairly uniformly about the nucleus. The nucleus becomes much smaller at the end of this stage and the nuclear membrane is only faintly seen. The nucleolus may or may not be visible. By the end of prophase the mitotic nuclei are located above the row of interphase nuclei

Metaphase is very well defined as the stage in which the chromosomes lie closely clumped at the equatorial plate. In polar view they appear as an irregular circle often having a paler center and in equatorial view as a short oblong. Colchicine metaphases differ widely. Some are like normal ones or more closely clumped. In others the chromatin mass may be broken into two or as many as 7 or 8 irregular pieces. Generally in the most disrupted metaphases the pieces are scattered further apart than in metaphases which are only fragmented into two or three parts. Colchicine metaphases may show signs of dissolution and pyknosis. The chromatin material appears as dark staining droplets, the cytoplasm becomes increasingly eosinophilic and may also eventually round up in droplet form. These signs of cell death were rarely seen in the intestinal epithelium of normal control animals

Anaphase was judged to extend from the first signs of separation of the metaphase plate into two parts until the chromatin of the daughter nuclei had reached the poles and the first sign of formation of separate cell membranes was seen. The reappearance of the nuclear membrane

was not used as a criterion as it is difficult to detect

Telophase Early telophase was defined as the stage in which the chromosomes of the daughter nuclei are present as one intensely staining clump. This stage merged with mid telophase when the chromatin mass became larger as the chromosomes seemed to lengthen and lie twisted and tangled together. This loosening proceeded until a small oval or somewhat oblong nucleus was formed crisscrossed with strands of chromatin and having a faintly stained nuclear membrane. This passed gradually into the last stage or late telophase in which the nuclear appearance returned gradually to the normal. The nuclei became rounder and sank towards the basement membrane; the chromatin is more dispersed and the nucleolus and nuclear membrane more evident.

An average of about 1200 cells was counted per animal although the range was between 933 and 1698 cells. The results are expressed as nuclei in division per cent of total nuclei and Student's "t" test was used to determine the significance of differences between pairs of mean values.

EXPERIMENTS

Experiment I Previous experience had shown that a dose of 0.1 mg of colchicine per 100 gm of body weight was successful in causing arrest of metaphases in rats. The changes in mitotic activity were examined in groups of male rats sacrificed 1 1/2, 2 1/2 and 3 hours after subcutaneous injection of colchicine in this dose. All groups were sacrificed between 9:00 A.M. and 1:30 P.M. including one group of control uninjected rats sacrificed at 9:30-10:00 A.M. and another at 12:30-1:00 P.M. The mitotic arrest in female rats was examined in groups sacrificed 1 1/2 and 3 hours after subcutaneous injection of a similar dose of colchicine and in control uninjected rats sacrificed in mid morning. The results are shown in table 1.

Experiment II The effect of 0.1 mg colchicine per 100 gm of body weight was compared in three groups of female rats which received the drug by subcutaneous or intraperitoneal injection or via the femoral vein (under ether anesthesia). The animals were sacrificed 1/2 hour and

3 hours after injection and portions of the ileum removed for measurement of mitotic activity. Two control uninjected groups were also sacrificed. The results are shown in table 2.

Experiment III The possibility that the administration of several small doses of colchicine might have a more consistent effect than a single dose in arresting metaphase was investigated. One group of male rats received a single subcutaneous injection of 0.1 mg of colchicine per 100 gm of body weight. Another group received 1/6th of this dose by subcutaneous injection every 1/2 hour for 6 injections. The animals were sacrificed three hours after the first injection. The experiment was repeated using female rats sacrificed 1 1/2 hours after a single dose or 1 1/2 hours after the first of three injections of 1/6th of the standard dose. The mitotic activity was measured in the ileal crypts of these groups and in control uninjected male and female rats and is reported in table 3.

RESULTS AND INTERPRETATION

If one could select the properties desired in a drug colchicine would possess the following characteristics. Firstly the drug would have no effect on the initiation of mitosis or its duration prior to the precise point at which arrest is effected. Secondly the drug would act on all cells immediately following injection. Thirdly the effect would continue evenly for several times the duration of metaphase so that for statistical reasons a large enough number of arrested divisions would be accumulated. (For practical reasons the duration of the experiment must be less than the intermitotic time of the tissue so that there is no shortage of cells available for mitosis.) Under these circumstances what would be the changes in the mitotic counts in the tissue following the administration of colchicine? Let us imagine a tissue in which 10% of cells are normally seen in division at any one time. Let the duration of mitosis be 50 minutes: prophase 20 minutes, metaphase 10 minutes, anaphase 5 minutes, telophase 15 minutes and colchicine act to prevent cells from passing from metaphase to anaphase. Then the distribution of cell divisions in the tissue will be as follows:

		Prophase	% Metaphase		% Anaphase	% Telophase
			Normal	Blocked		
0 time		4	2	0	1	3
5 mins	colchicine	4	2	1	0	3
10 mins	colchicine	4	2	2	0	2
15 mins	colchicine	4	2	3	0	1
20 mins	colchicine	4	2	4	0	0
40 mins	colchicine	4	2	8	0	0

Once colchicine has begun to act the per cent metaphase in the tissue should increase by 2% (normal % metaphase) every 10 minutes (normal metaphase duration). Anaphases will begin to disappear coincidentally with the arrest of metaphases. The telophases should decrease by 3% (normal % telophase) within 15 minutes (normal telophase duration) after the anaphases disappear. As the cells in one stage of mitosis do not all enter that stage at precisely the same moment there would be for example a gradual disappearance of telophase which would be complete after 20 minutes of colchicine treatment in this scheme.

Let us now examine the results of experiment I in which the effect of colchicine on the crypt mitoses was measured from one hour to three hours after subcutaneous injection. The results are shown in table 1. Figure 1 also shows the mean values for percentage metaphase plotted as the ordinate against duration of treatment as the abscissa. Taking the results from the male rats first the following conclusions may be drawn.

1. Comparison of the percentage distribution of the stages of mitosis in the two control uninjected groups should show whether there is any diurnal variation in mitotic activity during the morning. The per cent prophase in the control rats killed late in the morning is on the borderline of being significantly higher than in the group killed around 9:00-9:30 A.M. ($0.02 < P < 0.05$). There is no significant difference between the percentage of cells in the other stages of mitosis. These figures indicate that there has been no major fluctuation in mitotic activity in the crypt epithelium during the morning. The increase in per cent prophase towards the end of the morning may indicate the beginning of a rise in mitotic activity in

the early afternoon but this period was not included in our experiments.

2. The percentage of cells in prophase in the colchicine injected groups is not significantly different from that in the control groups. In the $1\frac{1}{2}$ hour colchicine group the per cent prophase is on the borderline of being significantly higher than the early morning control group ($0.02 < P < 0.05$) and the later morning control group ($0.05 < P < 0.1$) largely due to a slightly but not significantly higher percentage of early prophase. It is possible that if colchicine had simultaneously stimulated and speeded prophase or inhibited and slowed this stage the percentage appearing in the tissue would be unchanged as compared with normal control animals. However such alterations in the normal course of prophase would be expected to cause initially some change in the ratios of early, middle and late prophase. As no significant disturbance of the percentage of any of the stages of prophase was seen it may be concluded that one of the requirements of colchicine action has been fulfilled in that it did not cause any change in the normal rate of initiation of prophase nor its duration.

3. The percentage of metaphase in all groups of colchicine injected rats is significantly higher than in the control groups. The difference between the control and the one hour group has a P value of < 0.0001 to < 0.01 and for all the other groups $P < 0.001$. Thus the effect of colchicine in arresting metaphase is seen from one to three hours after injection. Whether the effect is complete throughout this period of time will be shown by the rate of accumulation of blocked metaphases and the presence or absence of anaphases and telophases.

The results in table 1 show that the mean percentage of metaphase does increase progressively with increasing

TABLE 1
Effect of varying periods of colchicine treatment on mitosis

Colchicine treatment	No. of rats	Mean % nuclei in mitosis \pm standard error													
		Prophase			Metaphase			Anaphase	Telophase						
		Early	Mid	Late	Total	Total	Prokaryotic		Early	Mid	Late	Total			
hours															
0 ¹	5	3.80 ± 0.42	0.40 ± 0.10	0.37 ± 0.06	4.71 ± 0.49	0.03 ± 0.15	0.0	0.46 ± 0.06	1.24 ± 0.09	1.13 ± 0.09	0.43 ± 0.13	1.24 ± 0.09	1.13 ± 0.09	2.80 ± 0.25	
0 ²	5	4.47 ± 0.47	0.24 ± 0.15	0.23 ± 0.10	5.14 ± 0.44	1.59 ± 0.26	0.01	0.35 ± 0.02	1.44 ± 0.26	1.29 ± 0.14	0.53 ± 0.06	1.44 ± 0.26	1.29 ± 0.14	3.19 ± 0.38	
1	6	4.67 ± 0.58	0.34 ± 0.08	0.35 ± 0.07	5.26 ± 0.68	6.39 ± 1.21	0.01	0	0.18 ± 0.07	0.53 ± 0.13	0	0.18 ± 0.07	0.53 ± 0.13	0.69 ± 0.19	
1½	5	5.81 ± 0.32	0.43 ± 0.02	0.35 ± 0.05	6.29 ± 0.34	8.64 ± 0.99	0.38	0	0.09 ± 0.05	0.03 ± 0.07	0.02 ± 0.05	0.09 ± 0.05	0.03 ± 0.07	0.14 ± 0.07	
2	5	4.65 ± 0.24	0.32 ± 0.03	0.39 ± 0.12	5.41 ± 0.16	9.15 ± 0.71	0.05	0	0.05	0.03	0	0.05	0.03	0.08	
2½	5	4.68 ± 0.31	0.41 ± 0.09	0.16 ± 0.03	5.29 ± 0.48	12.47 ± 0.80	0.16	0	0.02	0	0	0	0	0	
3	5	4.84 ± 0.59	0.61 ± 0.26	0.43 ± 0.09	5.89 ± 0.63	13.2 ± 0.66	0.23	0	0	0	0	0	0	0	
0	9 ¹	4.21 ± 0.34	0.61 ± 0.09	0.32 ± 0.09	4.95 ± 0.53	1.20 ± 0.13	0.0	0.19 ± 0.04	0.03 ± 0.13	1.78 ± 0.14	0.34 ± 0.04	0.03 ± 0.13	1.78 ± 0.14	3.06 ± 0.22	
1½	11 ²	4.30 ± 0.37	0.41 ± 0.06	0.26 ± 0.05	4.93 ± 0.39	5.18 ± 0.38	0.05	0	0.07 ± 0.03	0.27 ± 0.05	0	0.07 ± 0.03	0.27 ± 0.05	0.34 ± 0.06	
3	7 ²	4.75 ± 0.44	0.37 ± 0.05	0.27 ± 0.05	5.40 ± 0.44	11.02 ± 0.93	0.0	0.02	0	0.11 ± 0.08	0	0	0.11 ± 0.08	0.11 ± 0.08	

¹ Control uninjected rats sacrificed 9:30-10:00 A.M.

² Control uninjected rats sacrificed 12:30-1:00 P.M.

³ The animals of the last three groups were female the others were male rats

length of colchicine treatment. The difference between the one and $1\frac{1}{2}$ hour groups is not statistically significant nor is the difference between the $2\frac{1}{2}$ and 3 hour groups but between all the other groups $P < 0.02$. In figure 1 an imaginary line drawn through the successive values for mean per cent metaphase indicates a fairly constant rate of accumulation of blocked metaphases although it may fall toward the longer periods of colchicine treatment. (This relationship is treated mathematically in the Discussion.)

One possible cause of a decreased rate of accumulation may be the loss of arrested metaphases by pyknosis, degeneration and disintegration. Examination of the counts shows that the number of pyknotic and degenerating metaphases increased progressively with greater length of colchicine treatment. However as the percentage of pyknotic metaphases in the crypt remained below 0.4% this could account for only a very small decrease in the metaphase number.

If there were a decrease in the tissue concentration of colchicine with the passage of time after injection so that some of the mitoses were not permanently held in metaphase some anaphases and telophases would appear in the tissue. However examination of the counts showed that by one hour after injection of colchicine all anaphases and early telophases had disappeared from the tissue. The mean value for total telophase was one fifth that of the control groups which showed a significant decrease ($P < 0.001$). By $1\frac{1}{2}$ hours after injection telophase was further decreased ($P = 0.02$). In animals receiving colchicine for longer periods of time very few or no telophases were seen. Such few as were rarely found were in the late stage and were probably cells having an unusually long telophase rather than cells which had escaped the colchicine blockade.

The conclusion may be drawn that there is an accumulation of arrested metaphases for one to three hours following colchicine administration without escape of the cells from the influence of the drug or appreciable loss by degeneration.

One of the characteristics desirable in colchicine is that of effective action immediately following injection. Such a result did not seem too likely following subcutaneous administration of the drug. Experiment II was conducted to discover how soon after subcutaneous injection an effect of colchicine could be shown and whether the intraperitoneal or intravenous routes were more suitable to our needs. Table 2 shows the mean percentage of crypt epithelial cells in various stages of mitosis $\frac{1}{2}$ hour and 3 hours after injection of colchicine by one of these three routes into groups of rats. The drug did not cause any significant change in the percentage of cells in prophase in any of the groups as compared with the value found in control uninjected animals and thus did not interfere with the initiation or duration of prophase. One half hour following subcutaneous injection of colchicine no difference from control values was observed in the percentage of any of the stages of mitosis and thus the treatment had failed to cause metaphase arrest during this period. Following intra

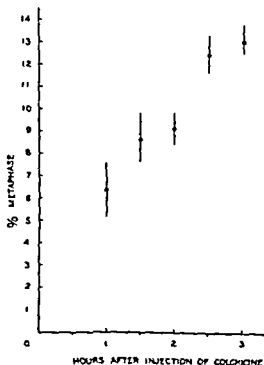


Fig. 1 Each dot indicates the mean of the percentage metaphase in one group of animals. The vertical lines on either side of the dot indicate the standard error of the mean.

TABLE 2
Effect of subcutaneous intraperitoneal and intravenous administration of colchicine on mitosis

Colchicine treatment	No of rats	Mean \bar{x} nuclei in mitosis \pm standard error										
		Prophase			Metaphase			Anaphase			Telophase	
		Early	Mid	Late	Total	Pyknotic	Total	Early	Mid	Late	Total	
hours												
0	4	4.09 ± 0.79	0.44 ± 0.05	0.50 ± 0.15	5.03 ± 0.79		1.42 ± 0.15	0.31 ± 0.04	0.81 ± 0.13	1.94 ± 0.22	3.08 ± 0.27	
1½ sub- cutaneous	5	4.05 ± 0.45	0.31 ± 0.12	0.26 ± 0.05	4.63 ± 0.44		1.06 ± 0.09	0.12 ± 0.04	0.80 ± 0.19	1.25 ± 0.31	2.17 ± 0.22	
1½ intra peritoneal	5	3.55 ± 0.62	0.38 ± 0.07	0.32 ± 0.07	4.26 ± 0.62		2.20 ± 0.29	0 0.04	0.17 ± 0.06	1.14 ± 0.31	1.43 ± 0.27	
1½ intra venous	6	4.49 ± 0.24	0.28 ± 0.05	0.27 ± 0.01	4.81 ± 0.23		4.15 ± 0.11	0 0.01	0.07 ± 0.04	1.14 ± 0.11	1.21 ± 0.11	
0	5	4.30 ± 0.20	0.37 ± 0.14	0.26 ± 0.08	4.89 ± 0.29		1.02 ± 0.18	0.37 ± 0.08	1.03 ± 0.19	1.65 ± 0.18	3.05 ± 0.37	
3 sub- cutaneous	7	4.75 ± 0.44	0.37 ± 0.05	0.27 ± 0.05	5.40 ± 0.44		11.02 ± 0.93	0 0	0 0	0.11 ± 0.08	0.11 ± 0.08	
3 intra peritoneal	6	4.26 ± 0.57	0.12 ± 0.06	0.29 ± 0.09	4.98 ± 0.65		11.27 ± 1.24	0.87 ± 0.36	0 0	0.01 0	0.01 0	
3 intra venous	6	3.78 ± 0.43	0.30 ± 0.07	0.11 ± 0.05	4.22 ± 0.51		10.12 ± 1.19	0.43 ± 0.30	0 0	0 0	0 0	

peritoneal injection of colchicine the percentage of metaphases present in the tissues (2.20 ± 0.29 SE) was again not significantly different from that of the control group (1.42 ± 0.15 SE). However there may have been some metaphase arrest in these animals. Firstly the per cent metaphase is significantly higher ($0.001 < P < 0.01$) than that of the subcutaneous injection group (which showed less animal variation than the control group). Secondly there were no anaphases or early telophases present and the percentage of the later stages of telophase was significantly reduced. In rats sacrificed half an hour after intravenous administration of colchicine there was no doubt that metaphase arrest had occurred. The per cent metaphase (4.15 ± 0.11 SE) was significantly higher than the control and other colchicine injected groups there were no anaphases or early telophases and the later stages of telophase were much reduced in number. Therefore it seems probable that intravenous colchicine fulfilled our original requirement that the drug be effective immediately following injection.

Despite the more rapid onset of the action of intravenously administered colchicine at the end of a three hour period of treatment there was no significant difference between the % metaphase in rats given by any of the three routes of injection. There was no reappearance of anaphases or telophases nor difference in the pyknotic metaphases. One explanation of the lack of difference may lie in the relatively long period of treatment. Since the duration of metaphase is probably 10–15 minutes (see later discussion) in three hours 12–15 metaphase periods would elapse. Thus the expected difference in per cent metaphases due to the failure of subcutaneous or intraperitoneal colchicine to block one or two sets of metaphases immediately after injection may be overlaid by the animal variation or other unknown factors.

Another requirement of colchicine was that it should act evenly over the experimental period. It was thought that it might be easier to maintain an effective concentration over a period of time if several doses of the drug were given rather

than a single one. Table 3 shows the effect of a single dose of colchicine at 1½ and 3 hours after injection and the effect of giving one sixth of this dose every half hour and killing the rats 1½ hours (three injections) and three hours (6 injections) after the initial injection. It is apparent that by 1½ hours the divided dose had arrested some mitoses since there were about twice as many metaphases as in the control rats. However the blockade could not have been complete since there were still considerable numbers of early to late telophases present. The single dose of colchicine caused the appearance of nearly 4 times as many metaphases as in control rats and only a few of the late telophase stages were seen. In other words there has been metaphase arrest for most of the experimental period. However, it is interesting that when the experiment was carried to three hours the blockade by the divided dose is just as effective as that caused by the single dose. There is no significant difference between the percentage of metaphase blocked by either means. One would expect that even if colchicine became fully effective from 1½ hours onward in the divided dose experiment by three hours the accumulated metaphases would still be about 30 % less than in the single dose experiment whereas the difference is less than 10%. There are slightly more pyknotic metaphases in the single dose three hour group though this hardly seems enough to indicate a significant loss by this means. An unlikely possibility is that the tissues of female rats such as used in the 1½ hour experiment react differently to a divided dose than the tissues of male rats which were employed in the three hour experiment. In any event it was concluded that no advantages were attained by giving a divided rather than a single subcutaneous injection.

DISCUSSION

Time of onset of colchicine action

Although histological examination has shown that most sites of mitotic activity in the animal body are affected by colchicine there is little precise information available on the rate of penetration of colchicine into the tissues and the time of onset of its mitotic blockade. The early effects of

TABLE 3
Effect of single and divided doses of colchicine on mitosis

Colchicine treatment	No. of rats	Mean % nuclei in mitosis is \pm standard error										
		Prophase a			Metaphase		Anaphase	Telophase				
		Early	Mid	Late	Total	Pyknotic		Early	Mid	Late	Total	
0	4	4.09 ± 0.79	0.44 ± 0.05	0.50 ± 0.15	5.03 ± 0.79	1.42 ± 0.15	0	0.13 ± 0.05	0.31 ± 0.04	0.81 ± 0.13	1.94 ± 0.22	3.08 ± 0.27
1½ hr. 1 inj	5	3.66 ± 0.45	0.31 ± 0.08	0.26 ± 0.06	4.24 ± 0.44	5.59 ± 0.28	0.06	0	0	0	0.37 ± 0.10	0.37 ± 0.10
1½ hr. 3 inj	6	3.98 ± 0.57	0.48 ± 0.14	0.37 ± 0.02	4.84 ± 0.58	2.83 ± 0.15	0.05	0	0.32 ± 0.02	0.36 ± 0.17	0.94 ± 0.22	1.33 ± 0.02
0	5 ^a	4.47 ± 0.47	0.24 ± 0.15	0.23 ± 0.16	5.14 ± 0.44	1.59 ± 0.26	0.02	0.35 ± 0.03	0.53 ± 0.06	1.44 ± 0.26	1.29 ± 0.38	3.19 ± 0.38
3 hr. 1 inj	5 ^a	4.84 ± 0.59	0.64 ± 0.26	0.43 ± 0.09	5.89 ± 0.63	13.2 ± 0.66	0.23 ± 0.07	0	0	0	0	0
3 hr. 0 inj	5 ^a	5.78 ± 0.82	0.49 ± 0.07	0.33 ± 0.07	6.62 ± 0.76	12.2 ± 1.52	0.09 ± 0.03	0	0	0	0.01	0.01

^a 0.1 mg colchicine/100 gm body weight one s.c. injection

^b One-sixth of 0.1 mg colchicine/100 gm body weight every half hour for three injections

^c One-sixth of 0.1 mg colchicine/100 gm body weight every half hour for 6 injections

^d Female rats

colchicine in regenerating liver of partially hepatectomized rats were examined by Brues and Jackson (37). The drug was given by subcutaneous injection at a time when mitotic activity was beginning and the effects were seen at once or within one hour. In our own work the effect of intravenously administered colchicine was seen in the intestinal crypt half an hour after injection. A simple calculation indicates that the action of the drug probably started almost immediately after injection. Since nearly three times as many metaphases were present in the injected animals as in the control group (of which one set of metaphases may have been present at the time of injection) at least two metaphase durations must have elapsed during the 30 minutes of treatment. As these figures agree with other estimates of the duration of metaphase (see later discussion) it is fairly certain that colchicine starts to act immediately following intravenous injection.

The extent of the delay in onset of colchicine action following subcutaneous injection may also be calculated. If metaphases continued to accumulate at the same rate following intravenous injection there should have been 85% in the crypts one hour after injection. The figure observed after this interval of colchicine treatment was 63% or 77% of the theoretical value. Thus the delay period was about 23% of one hour or about 15 minutes. In the experiment in which animals were sacrificed half an hour after subcutaneous injection of colchicine no arrest was seen. Thus the delay in onset of colchicine action following subcutaneous injection may vary from 15 minutes to half an hour and represents about one or two metaphase durations.

The rate of accumulation of arrested metaphases following subcutaneous injection of colchicine is indicated by the slope of the curve of number of arrested metaphases plotted against the time elapsed since injection. If metaphase arrest began immediately after injection the number of mitoses present at zero time should be included in the curve. As there is a delay in the onset of action of subcutaneously administered colchicine this point should be left out of the calculations. Alternatively the starting point and the 1/2 hour

subcutaneous value should be moved over on the graph by a distance equivalent to the delay or for greater ease of plotting simply reduced by 23%. A method for finding the line of best fit to a series of points was applied to the colchicine figure alone and to the colchicine figures plus the corrected zero time and 1/2 hour points (Lewis and Lewis 17). In the first plot the calculated rate of accumulation of metaphases is 3.38% per hour, by the second 4.13% per hour the difference in these two rates being well within the error of the method. The fact that these points may be fitted to a straight line and that there was no evidence of change in the rate of initiation or duration of prophase nor escape of arrested metaphases indicates that there was an even rate of accumulation of metaphases from the time of onset of colchicine action lasting for three hours after injection.

Duration of colchicine effect

These conditions of colchicine action in the gastro-intestinal epithelium of rats may not last for much longer than three hours after injection. In some unpublished work on the action of colchicine in mitotic activity of mucus containing cells in the gastric mucosa it was observed that the number of pyknotic metaphases was small up to three hours after injection but nearly half the metaphases showed some pyknotic change by 4 hours. The percentage of cells in prophase also decreased during this time possibly indicating some inhibition or perhaps speeding of this stage. Thus the colchicine results would not be reliable in the gastric epithelium later than 4 hours after injection. Leblond and Stevens (48) estimated the mitotic activity in the ileal epithelium of rats sacrificed 6 hours after injection of colchicine. In this case also nearly half the metaphases were severely degenerated and there was a reduced proportion of prophases. However all the tissues of the body are not equally sensitive to the deleterious effects of colchicine. For example Storey (51) observed no change in the percentage of cells in prophase nor any significant degree of pyknosis of arrested metaphases in the Malpighian layer of the plantar epidermis of rats 6 hours after

injection of colchicine Brues (36) examined the mitotic activity in the regenerating liver of partially hepatectomized rats using colchicine injected every 8 hours. Comparison of the numbers of arrested mitoses indicates that all dividing cells are arrested in metaphase without inhibition or stimulation throughout this remarkably long period of time. Thus the conditions for the use of colchicine as a quantitative tool must be examined separately for each tissue.

Mitotic rate

Since it has been concluded that under certain conditions colchicine causes the arrest in metaphase of all cells entering division in the normal course of cell formation in the intestinal epithelium of rats, these results may be used to calculate the mitotic rate in the epithelium. The mitotic rate will be equal to the rate of accumulation of blocked metaphases. The mitotic rate can also be expressed as the time required for a given percentage of cells to undergo mitosis. In the intestinal epithelium the new cells formed by mitosis are used for the renewal of the epithelium; cell formation is counterbalanced by cell loss. Crypt cells move into the villus epithelium and are eventually lost from the tips of the villi. Thus there is no over all increase in cell population size so that the mitotic rate is equal to the rate of cell loss and also to the rate of cell renewal. Thus the mitotic rate may be expressed as the theoretical length of time required for 100% of the cells to divide or be renewed, which is called the "turnover time" of the epithelium. If 3.38% of cells divide and are renewed in one hour, 100% of the cells will be renewed in 29.6 hours. Similarly it may be calculated that if 4.13% of cells divide and are renewed in one hour, the turnover time is 24.2 hours in the crypts of the rat's ileum.

These figures may be compared with the estimate made by Leblond and Stevens that the turnover time of the crypt plus villus epithelium of the rat ileum was equal to 34 hours. Since crypt cells make up about half the cell population of the ileal epithelium, the turnover time in the crypts would be about half that of the whole epithelium, namely 17 hours. Widner, Storer and Lushbaugh (51) esti-

mated the intermitotic time (same as our turnover time) in the crypts of the rat jejunum as 33.5 hours, which is also in good agreement with our results.

It is of interest to compare these results with those of radioautographic studies in which labeled substances have been incorporated into dividing crypt nuclei. As epithelial cells divide fairly close to the mouths of the crypts, the time for the first labeled cells to migrate to the tips of the villi approximates the renewal time of the villus epithelium rather than that of the whole epithelium. Thus Leblond, Stevens and Bogoroch (48) noted that nuclei labeled with P^{32} had migrated about half way up the villus epithelium of rat ileum and duodenum by 24 hours after injection. The renewal time of the villus epithelium is therefore probably about 48 hours. Walker and Leblond (58) obtained radioautographs of intestinal epithelium labeled with adenine C^{14} in mice. They observed that in the duodenum labeled cells had already reached the tips of some villi at 24 hours after injection, whereas in the ileum cell migration was slower. The renewal time of the villus epithelium was therefore about 24 hours in the duodenum and was accomplished within 72 hours in the ileum. Also in mice renewal of the jejunal epithelium requires about three days, as shown by experiments with tritium labeled thymidine (Leblond and Messier 58). Presumably the renewal time of the crypts was roughly of the same duration. The results of the various techniques all indicate that the renewal of the small intestine epithelium of rats and mice is accomplished in about 2-3 days, with some regional differences.

Duration of mitosis

The colchicine results may also be used to calculate the duration of the stages of mitosis. The calculations are made in the following manner:

$$\frac{\text{Duration of stage } x = \frac{\text{nuclei at stage } x \text{ in normal tissue}}{\text{nuclei in metaphase of } t \text{ minutes colchicine}} \times t \text{ minutes of colchicine treatment}}$$

We will first consider metaphase since this stage is very sharply defined. Calculations using the two curves previously de-

scribed give values of 19.2 and 21.75 minutes respectively for the duration of metaphase. Storey (49) also using colchicine, obtained a value of 11 minutes in rat planar epidermis. Observations on tissue culture of chick mesenchymal cells by Levi (16-17) gave figures of 8-11 minutes while Lewis and Lewis (17) found that 20 minutes was the average duration. All of these results are in reasonably good agreement.

Widner Storer and Lushbaugh (51) estimated mitotic duration in rat tissues as the time for mitoses to disappear following administration of a dose of x-rays which prevented the appearance of new mitoses. These authors give a value of 27 minutes for the duration of stages that probably correspond to our stages beginning of late prophase to the end of anaphase. The sum of the durations of these stages from our figures is 29-34 minutes. McMinn (54) used 5 hours of colchicine treatment in the investigation of the mitotic activity of the small intestinal epithelium of cats. For stages which may correspond to our stages beginning of mid prophase to end of mid telophase the calculated duration was 75 minutes. The corresponding value from our results in the rat is 63 minutes.

It is not possible to compare the duration of early prophase and late telophase with estimates made by other workers because the limits of these stages are too difficult to define. Our own results indicate that the stage we recognize as the whole of prophase lasts about 1-1½ hours. Evidence from other sources indicated that this may be only a fraction of the time required for a cell to double its content of deoxyribonucleic acid in preparation for division.

Stages of telophase were recognizable whose duration was calculated to be 43-53 minutes. If the effect of colchicine were to arrest all the metaphases present in the tissue and any further cells entering metaphase the anaphases and telophases present at the time of injection should have become completed and become interphase nuclei within a time interval which was equal to the anaphase plus telophase duration (50-60 minutes). We have already estimated that there is roughly a 15-

minute delay before subcutaneously injected colchicine begins to arrest division and this period should be included in the expected time for anaphases and telophases to disappear making it 65-75 minutes. In actual fact the percentage of telophase either lasts a little longer than calculated or does so in the circumstances of colchicine treatment or the delay in onset of colchicine action is slightly longer than calculated.

Suggestions for future studies

The foregoing experiments have reaffirmed the validity of the colchicine technique as a method for the quantitative estimation of the mitotic rate in the intestinal epithelium of the rat. The author is confident that this method may be used with equal success in other tissues and in other species. However in each instance the proper conditions for experimentation must be established. Animal species vary in their sensitivity to colchicine and the rate of penetration of the drug; the viability of the affected cells and their normal life span may alter the results. The more obvious problems of variation in mitotic activity during the day and the sex cycle must also be considered.

In most instances a little educated guesswork can contrive a pilot experiment which comes fairly close to the desired result. For example the approximate dose may be gleaned from the literature on colchicine and one would expect that a tissue with an extremely active mitotic rate would respond best to intravenously injected colchicine and a short treatment period whereas subcutaneous injection and a longer experiment might benefit in a tissue with a slow mitotic rate. The sections may first be examined for the presence of anaphases and telophases. If these are present the dose is too small or the treatment too short. If the pilot experiment is successful in causing significant metaphase arrest without escape or obvious degeneration of the cells one must then compare the counts of prophases with that of the control group. If the number of prophases is depressed by colchicine the dose must be reduced. If there is little or no difference in the number of prophases i.e. little or no change in the initial

ation and duration of prophase one may then devise experiments to determine the exact dose and best route of administration. In these trials counts of metaphase and intermitotic nuclei will suffice. However the numbers of prophases should be checked in the group finally chosen. If it appears that there is no alteration of the normal mitotic rate except to cause arrest then the effect of the drug should be measured soon after injection (half an hour) and at several times afterwards. This will show if there is a period of steady increment in the number of arrested metaphases and the extent of any initial delay. If possible the animals should be sacrificed at times after injection that are several times the duration of metaphase. All stages of mitosis should be included in the count. All being well when the results are plotted as a graph at least the first portion should describe a straight line. The calculations of the mitotic rate of the tissue may be made from the slope of this line or from points towards the middle of it with corrections for delay in onset of action if necessary.

SUMMARY

The effect of colchicine on mitosis in the intestinal epithelium of rats was investigated to determine the suitability of this drug for the quantitative estimation of the mitotic rate. Under certain precise experimental conditions injected colchicine causes the arrest at metaphase of all cells undergoing mitosis. Mitosis is neither stimulated nor inhibited neither hastened nor prolonged. There is little delay in action of the drug after injection nor escape from its effects for at least three hours. Consequently the proportion of nuclei in metaphase counted in tissue sections at certain times after colchicine injection may be used to calculate the mitotic rate. In our experiments satisfactory conditions were obtained when Sherman stock albino rats were injected subcutaneously with 0.1 mg of purified colchicine in aqueous solution and the animals sacrificed two to three hours later. Counts of the numbers of mitoses and intermitotic nuclei were used to calculate the duration of mitosis and its stages. The turnover time of the epithelium of the crypts of Lieberkühn of

the intestine was calculated to be 24-29 hours.

It is felt that the colchicine technique outlined in this article may be used with equal success for the measurement of the mitotic rate of other tissues and in other species.

ACKNOWLEDGMENT

This work was done with the support of a Block Term Grant from the National Research Council of Canada to Dr C P Leblond.

LITERATURE CITED

- Ashley J N and J O Harris 1944 Purification of colchicine by chromatography *J Chem Soc* 677
- Askovitz S I 1955 Mean rates of change and least squares—interpretations and rapid graphic methods *J Appl Physiol* 8 347-542
- Bertalanffy F D 1954 Histology and histophysiology of the alveolar lung tissue Ph.D Thesis McGill University
- Bertalanffy F D and C P Leblond 1953 The continuous renewal of the two types of alveolar cells in the lung of the rat *Anat Rec* 115 515-542
- Brues A M 1936 The effect of colchicine on regenerating liver *J Physiol* 86 63P (Proc)
- Brues A M and E B Jackson 1937 Nuclear abnormalities resulting from inhibition of mitosis by colchicine and other substances *Am J Cancer* 30 504-511
- Bucher O 1939 Zur Kenntnis der Mitose VI Der Einfluss von Colchicin und Trypavlatin auf den Wachstumsrhythmus und auf die Zellteilung in Fibrocytenkulturen *Z. F. Zellforsch Mikr Anat (Abt A)* 29 283-322
- Dustin A P 1936 La colchicine reactif de l'immence carboxinétique *Arch Portug Sc Biol* 5 39-43
- Leblond C P and B Messier 1958 Renewal of chief cells and goblet cells in the small intestine as shown by radioautography after injection of thymidine-H³ into mice *Anat Rec* 122 247-259
- Leblond C P and C E Stevens 1948 The constant renewal of the intestinal epithelium in the albino rat *Ibid* 100 357-378
- Leblond C P, C E Stevens and R Bogacz 1948 Histological localization of newly formed desoxyribonucleic acid *Science* 103 531-533
- Levi C 1916-17 Il ritmo e le modalità della mitosi nelle cellule vivente coltivate "in vitro" *Arch Ital Anat Embiol* 15 243-244
- Lewis W H, and M R Lewis 1917 The duration of the various phases of mitosis in the mesenchyme cells of tissue cultures *Anat Rec* 13 359-367
- Ludford R J 1936 The action of toxic substances upon the division of normal and malignant cells in vitro and in vivo *Arch Exp Zellforsch* 18 411-441
- McMinn R M H 1954 The rate of renewal of intestinal epithelium in the cat *J Anat.* 88 527-532

- Patterson D D 1939 *Statistical Technique in Agricultural Research* McGraw Hill
- Storey W F 1949 Renewal time of the epidermis in the white rat MSc Thesis McGill University
- Storey W F and C P Leblond 1951 Measurement of the rate of proliferation of epidermis and associated structures *Ann New York Acad Sci* 53 Art 3 537-545
- Vulpé M 1954 The renewal of the epithelium of the urinary bladder MSc Thesis McGill University
- Walker B E and C P Leblond 1958 Sites of nucleic acid synthesis in the mouse visualized by radioautography after administration of C^{14} labelled adenine and thymidine *Exp Cell Res* 14 510-531
- Widner W R J B Storer and C C Lushbaugh 1951 The use of X ray nitrogen mustard to determine the mitotic and intermitotic times in normal and malignant rat tissues *Cancer Res* 11 877-884

A Study of the Arterial Variations in the Limbs, with Special Reference to Symmetry of Vascular Patterns

J A KEEN

Department of Anatomy University of Cape Town
Cape Town South Africa

The descriptions of the arterial trunks of the limbs and of the arrangement of their main branches found in anatomy textbooks represent the patterns encountered in a majority of subjects and such patterns are then accepted as the "normal" or average arrangement. Variations of these arterial patterns or so-called "abnormalities" have received considerable attention in anatomical literature. The terms "abnormal" "abnormality" are recognized to be unsuitable ones but have become sanctioned by use. An "abnormality" does not in any way imply an inferior or less effective blood supply of the region but is simply a variation or departure from the "normal". Studies of variations of arterial arrangements are usually based on the analysis of a large number of dissected right and left limbs but the authors seldom consider the question of bilateral symmetry in individual cases. When a departure from the normal pattern is met with in one limb it is often assumed that the particular variation is likely to be present also on the other side. In other words a certain symmetry is accepted *a priori* because we believe that the right and left limbs of an embryo tend to develop as mirror images of each other. However the present study will show that this assumption is far from justified. In fact the opposite tends to be the case: an arterial anomaly in one limb is more often than not absent in the other and rare anomalies are unlikely to be present bilaterally.

METHODS AND MATERIAL

Methods A scheme was devised for recording the arrangement of the arteries in the limbs: one for the upper limb and another for the lower limb, the right and left sides of each subject being recorded

together on the same sheet. The following points of information were noted: (a) The diameters of the arterial trunks and of their main branches. (b) The points of origin of the main branches along the parent trunk. (c) The levels of the various bifurcations with reference to recognized anatomical levels: e.g. radio-humeral joint, lower border of popliteus, medial tubercle of the calcaneum. Special notes were made of any abnormalities.

The measurements were made with a pair of sliding calipers. When measuring the diameters of arteries the conical enlargements at the point of origin of branches must be avoided (Adachi '28). Large arterial trunks in dissecting room subjects may be flattened out; this must be corrected because otherwise the measurements of the diameters would be too large. When recording the point of origin of a branch the distance along the parent trunk is measured from the beginning of the trunk to the distal angle of the branch. The distal angle is more acute and offers a definite point for the caliper tip while the proximal angle is more open and less well defined (Adachi '28). A branch which leaves the parent trunk at its commencement would be recorded as arising at 0 mm. When determining the distance between two branches at their origin, Adachi recommends measuring the distance from the distal angle of one branch to the distal angle of the other for the same reason.

Material The material for the investigation were dissecting room cadavers after the students had completed the dissection of the limbs. It is preferable to make the recordings while the limbs are still attached to the trunk when the levels at which the axillary and femoral arteries

commence are more easily determined. The data were entered on the recording sheets right and left sides being done simultaneously or one immediately after the other. The aim was to obtain a sufficient number of complete recordings of the arterial patterns in the 4 limbs of individual subjects.

The investigation was begun in South Africa where I obtained data from 90 subjects. The majority came from the Durban medical school, a certain number from the Pretoria and Cape Town medical schools, and I wish to thank Professor T. Muller of the University of Pretoria and Professor L. H. Wells of the University of Cape Town for permission to use material from their departments. The majority of these subjects were Bantu, but a certain number of Cape Coloured are included.

During an 18 months stay in Geneva I continued to collect data at Swiss anatomical institutes, a total of 56 European subjects. I wish to express my gratitude to the heads of these various anatomy departments for permission to use this material. Professor J. A. Baumann of Geneva, Professor A. Faller of Fribourg, Professor E. Hintzsche of Bern, Professor G. Tondury of Zurich, Professor G. Winkler of Lausanne and Professor G. Wolf Heidegger of Basel.

The age and sex of the individuals were entered on the recording sheets, but no differential groupings were made on those grounds. In all countries the dissecting room subjects are elderly persons and tend to be largely male. Increased tortuosity with lengthening of some arteries as well as increased diameters in some regions are pathological features seen in old people. These were allowed for when making length or diameter measurements, such as arteriosclerotic changes do not affect the fundamental pattern in each individual. Among the total number of 146, the data for the 4 limbs were available in 136 subjects, in 6 subjects I had the data for the upper limbs only, and in 4 subjects only for the lower limbs.

Racial differences. Adachi (28) established certain racial differences in the arteries of the limbs as between the Japanese and the European. In the present

investigation no cadavers of Asiatic origin were included among the dissecting room material, and thus the racial differences noted by Adachi could be ignored. Further, the impression gained from Adachi's publications was that racial differences are not very important. Whenever a particular abnormality in the present series was investigated, and its percentage frequency was compared with that given by Adachi, the difference was usually of such a nature that it could not be considered as being statistically significant.

However, racial differences, if any, as between Negro and European must be taken into account here, because the material is very mixed racially, viz. a preponderance of Bantu and Cape Coloured subjects (90) with a considerable proportion of European subjects (56). Several publications by American authors discuss racial differences in the arterial patterns of the limbs, as between the American White and American Negro. Charles (31) made a study of the types of origin of the profunda brachii artery in the two groups (300 dissections) and came to the conclusion that racial differences were slight. Trotter (30) investigated the branchings of the axillary artery in Whites and in American Negroes based on 384 dissections. No racial differences were found in the male series, slight differences in the female series (10 White, 27 Negro females). The numbers in the latter series were so small that the differences noted are not significant statistically. In another study by Trotter (40) the level of termination of the popliteal artery was investigated in a series of dissections (123 White, 169 Negroes). The differences between the two racial groups were not significant statistically.

De Garis and Swartley (28) studied the axillary artery in White and Negro stocks based on 512 dissections (129 White, 127 Negro subjects). The term "Negro" included all subjects classed socially as such, but many were admittedly hybrid. The authors recognized 23 different patterns of the axillary artery and of its branchings, a method which complicated the analysis enormously. The tables show that there is more diversity of patterns in "Negroes" than in the White group. Actually

is only applied in the case of the authors patterns A and B the difference here being an independent origin of the lateral thoracic as against an origin in common with the acromio-thoracic. In the other 21 subgroups the differences were not significant statistically. Among the individuals classed as Negro there was a high degree of hybridity and the analysis can not claim to be a satisfactory one as between European and Negro stocks. The authors themselves suggest that a high degree of hybridity may be associated with the greater frequency of variations.

On the whole it is probable that racial differences are minimal in respect of the limb artery patterns. Variations follow much the same lines in European and Negro stocks. Thus for the purposes of this study I decided to leave aside any question of racial differences more particularly because the investigation is primarily concerned with establishing the existence or non-existence of right and left sided symmetry in the arrangement of the limb arteries.

ARTERIAL VARIATIONS IN THE UPPER LIMB

I The axillary artery and its branches

The acromio-thoracic artery is an extraordinarily constant branch and without exception emerges opposite the upper border of the pectoralis minor (Adachi 28). In my scheme of recording I have preferred to define the acromio-thoracic artery in terms of its point of origin along the axillary artery. The mean distance of origin measured from the outer border of the first rib was 2.6 cm. The superior thoracic, the lateral thoracic and the anterior circumflex humeral arteries are extremely variable and inconstant and should be left out of any statistical study. The anterior circumflex humeral arises in common with the posterior circumflex humeral artery in about 30% (Adachi 28); the present series showed a common trunk for the two circumflex humeral arteries in approximately the same proportion of cases.

Subscapular artery The important variations in the arrangement of the branches of the axillary artery revolve around the

point of origin of the subscapular artery. If the subscapular arises from the third part of the axillary at a mean distance of 4.7 cm from the acromio-thoracic (calculated in the present series) and more or less on a level with the circumflex humeral arteries this is looked upon as the normal. When the subscapular arises much nearer to or perhaps on a level with the acromio-thoracic this is spoken of as a "high origin" of the subscapular. For purposes of a statistical study in the present series it was necessary to make an arbitrary definition of "high origin." Thus whenever the subscapular artery arose at a point 10 mm or less from the acromio-thoracic the variation was called a "high origin."

On this basis "high origin" of the subscapular occurred 82 times in 284 dissections that is $29\% \pm 2.7\%$. Included are two instances where the acromio-thoracic and the subscapular had a common trunk and one instance where the two arteries arose at the same level. Coulouma and Bastien (34) described one case (104 dissections) where the subscapular arose at a point above the acromio-thoracic. Huelke (59) divides "high origin" of the subscapular into two categories: (a) an origin of the subscapular from the second part of the axillary i.e. from the part lying deep to the tendon of the pectoralis minor; this occurred in 15% (178 dissections); (b) An origin from the first part of the axillary 0.6%. In the latter variation the trunks of the subscapular and of the continuation of the axillary can be of the same thickness. Under these conditions the author speaks of a "high division" of the main trunk into a brachial and "deep brachial" arteries; the second and third parts of the axillary being then considered to be absent.

Posterior circumflex humeral artery A common trunk for the subscapular and posterior circumflex humeral arteries is another frequent "abnormality." It occurred 88 times in 284 dissections i.e. $31\% \pm 2.7\%$. There was no correlation between this abnormality and the "high origin" of the subscapular. A common trunk was observed 05 times in the case of subscapular arteries arising at a low level and 23 times in the case of subscap

ulars with a "high origin" If the lesser frequency of the "high origin" is taken into consideration this shows a very similar frequency distribution as between the two types of subscapular artery Huelke (59) states that the posterior circumflex humeral artery arises as an independent branch from the third part of the axillary in 80% (178 dissections) and in 20% from the subscapular The frequency of this particular anomaly appears higher in the present series $31\% \pm 2.7\%$ against $20\% \pm 3.0\%$ The percentage difference is $11\% \pm 4.0\%$ The actual difference is less than three times the standard error and therefore cannot be considered as being statistically significant

Another important and rare variation of the posterior circumflex humeral artery is the origin of this vessel from the axillary at a low level The artery then travels below the tendons of the latissimus dorsi and teres major muscles and ascends behind these tendons to join the circumflex nerve The abnormality occurred 8 times in 284 dissections i.e. 2.8% Skopakoff (59) found this abnormal course of the posterior circumflex humeral artery three times in 610 dissections (0.5%) Coulouma and Bastien (34) saw the same abnormality three times in 104 dissections (2.9%) The existence of an anastomosis between the posterior circumflex humeral and the profunda brachii arteries behind the tendons of the teres major and latissimus dorsi allows several patterns of these vessels to arise (Adachi 28)

II Arteries of the arm

Profunda brachii This artery is extremely variable It is often represented by more than one trunk which follow the radial nerve In 26% (284 dissections) the profunda brachii arose from the terminal part of the axillary artery that is the origin was from the main arterial trunk at a level above the lower border of the teres major tendon In 6% the profunda brachii arose as a branch of the posterior circumflex humeral or of the subscapular in the case of a common trunk for these two vessels A third abnormality of the profunda brachii is its origin from the posterior circumflex humeral after this artery has penetrated into the quadrangu-

lar space and a subsequent downward course behind the teres major tendon 19 times in the present series of dissections (7%)

Charles (31) lists 7 types of origin of the profunda brachii artery The profunda brachii appeared as a single vessel arising from the upper part of the brachial artery in only 55% of the cases (300 dissections) The ulnar collateral and supratrochlear branches are so variable that they do not lend themselves to a statistical study

The "superficial brachial artery" The brachial artery normally runs deep to the median nerve When a large arterial trunk runs superficial to the nerve this is the "arteria brachialis superficialis" (Adachi 28) It may replace the main trunk or it may be accompanied by an equally important less important or more important trunk running parallel and deep to the median nerve in the normal position In these cases the superficially placed vessel may continue as the radial or more rarely as the ulnar artery Adachi further subdivides the "arteria brachialis superficialis" into superior media and inferior according to its point of origin from the main arterial trunk

The point of origin may be from the axillary most frequently it is from the upper part of the brachial but a "superficial brachial artery" may also arise from the lower part of the brachial artery nearer the elbow Adachi gives further subdivisions which concern its relationship to the ulnar nerve In the analysis of my dissections I have limited myself to three types (a) Those "superficial brachial arteries" which continue into the cubital fossa and then bifurcate as usual (b) the "superficial brachial artery" continues as the radial called "high origin" of the radial artery (c) the "superficial brachial artery" continues as the ulnar called "high origin" of the ulnar artery Both radial and ulnar arteries run a superficial course in the forearm in such cases

In the present series (284 dissections) the "superficial brachial artery" including those which continued as superficially placed radial and ulnar arteries was found 35 times (12.3%) A few of these need a special description In a left upper limb I found a comparatively small branch (2

mm diameter) which arose from the upper part of the brachial (5 mm diameter) passed superficial to the median nerve and then rejoined the main trunk a short distance above the bifurcation in the cubital fossa. This is an example of so-called *Inselbildung* (Adachi 28). The median nerve ran through this arterial "island" or ring. The case was not included among the "superficial brachial arteries" because the main brachial artery had the usual course with a bifurcation at the normal level nevertheless it is related to this type of abnormality.

One "superficial brachial artery" arose in the axilla from the third part of the right axillary artery a little more than 2 cm distal to the origin of the acromio-thoracic. At this level the main arterial trunk bifurcated into (1) a superficial brachial artery (6 mm diameter) which crossed superficial to the medial root of the median nerve (2) a deeper trunk (5 mm diameter) which passed deep to the medial root of the nerve and gave rise to the subscapular the two circumflex humeral arteries and the profunda brachii. Another dissection of a right arm showed a superficial brachial artery arising from the upper part of the brachial. Actually it was a bifurcation because two trunks of equal diameters (3 mm) continued downwards one superficial and the other deep to the median nerve. The "superficial brachial artery" descended in the superficial fascia and in front of the bicipital aponeurosis it bifurcated into radial and ulnar arteries both vessels running downwards in the forearm superficial to the muscles. The more deeply placed trunk of the brachial artery supplied the interosseous arteries the recurrensts and muscular branches. Such instances have the characteristics of the three types defined above a superficial brachial artery with a bifurcation as well as radial and ulnar arteries with "high origins".

Another example of *"Inselbildung"* was found in a right arm. A large "superficial brachial artery" (6 mm diameter) left the upper part of the brachial artery while a small parallel artery (2 mm diameter) ran downwards deep to the median nerve. At the level of the radio-humeral joint the two vessels united again to form a single

trunk. This artery bifurcated as usual in the cubital fossa at a normal level below the radio-humeral joint. When all the instances of superficial brachial artery were considered together and sorted into the three types the results were as follows: 10 instances belonged to type (a) i.e. 3.6% 17 instances of type (b) i.e. 5.9% 8 instances of type (c) i.e. 2.8%. Thus in the present series of dissections "high origin" of the radial was the commonest type next the "superficial brachial artery" with a normal bifurcation the least common type being "high origin" of the ulnar.

The "superficial brachial artery" has received considerable attention in the literature on arterial variations. Müller (39) believes that the superficial brachial artery is an atavistic condition since a main brachial artery crossing superficial to the median nerve is said to be the usual arrangement in the primates. Singer (33) believes that the "superficial brachial artery" is a persisting embryonic vessel its continuation in the forearm being a superficially running median artery. The "superficial brachial artery" has anastomoses with the radial and ulnar arteries if these persist the result is a "high origin" of either of these vessels.

Skopakoff (59) gives the percentage frequency of all types of "superficial brachial artery" as 19.7% (610 dissections). The author includes several instances of comparatively small branches of the brachial which ran superficial to the median nerve and resolved themselves into muscular branches without a downward continuation. This probably explains the higher percentage frequency as compared with that found in the present series. In Poirier's text book of anatomy the "superficial brachial artery" is discussed. In 100 dissections the brachial artery crossed superficial to the median nerve 6 times. "High origin" of the ulnar artery was found 20 times in 440 dissections. "High origin" of the radial according to Poirier is rarer.

III Arteries of the forearm and palm of the hand

Some of the abnormalities of the forearm arteries have already been dealt with under the headings of "high origin" of the

radial and ulnar arteries. In the scheme for recording the arteries the level of the bifurcation of the brachial artery was related to the level of the radio humeral joint which is easily felt. In order to avoid any errors Adachi (28) advises an incision to open the articular capsule. The bifurcation in the cubital fossa is always a little lower and the average distance below the joint level was 16 mm calculated over a large number in this series. The variations in the level of the bifurcation were comparatively slight and seemed of no particular significance. The diameters of the radial and ulnar arteries were entered on the recording sheet the ulnar being practically always the stronger artery. At the wrist level the relationship is usually the reverse since the radial gives off few branches in the forearm while the ulnar has given off the interosseous vessels and many muscular branches. When the ulnar passes into the palm of the hand various kinds of superficial palmar arch result according to the type of anastomosis.

Superficial palmar arch. Adachi (28) gives three types of superficial palmar arch: (a) The "ulnar type" in which the contribution by the radial artery is absent or minimal; (b) the "radio-ulnar" type; (c) the "mediano-ulnar" type in which a median artery is sufficiently strong to reach the palm of the hand and to take part in the formation of the arch. According to Adachi the ulnar type is the most frequent (59%) next the radio-ulnar (32%) and the mediano-ulnar type the least common (9%).

The differentiation between the ulnar and radio-ulnar types is obviously a difficult one as it depends on the observer's estimate as to what constitutes a minimal contribution by the radial artery. If only very obvious superficial palmar branches of the radial running superficial to the muscles are looked for then the "ulnar type" is undoubtedly the most frequent. Poirier states that the variations in the superficial palmar arch are so numerous that it is difficult to establish a type. Further the importance of the superficial palmar arch varies inversely with that of the deep palmar arch. The radio-ulnar type may be divided into subgroups according to the course taken by the superficial pal-

mar branch of the radial either superficial to or through the muscles of the thenar eminence or the radial contribution may be an anastomotic branch coming from the princeps pollicis or radialis indicis (sometimes called the *deep radio-ulnar* type). A very rare type of superficial palmar arch is a large median artery which anastomoses with the radial the ulnar contribution being suppressed or very small. In the present series of dissections there was one instance of this in a left arm it may be called the "*mediano radial*" type. However in many cases of mediano-ulnar type the radial artery also has a share. In the right and left hands of the same individuals there was a general tendency towards symmetry where the ulnar and radio ulnar types were concerned although slight differences were not uncommon (noted 19 times).

Strong median artery. The median artery is an important vessel in the embryonic circulation of the forearm. The continuation of the main "axis artery" is at first the anterior interosseous. When the latter recedes it is replaced by the more superficially placed median artery. The median artery in turn becomes replaced by the radial and ulnar arteries (Starck 55). A strong median artery which reaches into the palm and takes part in the formation of the superficial palmar arch is an important anomaly and represents the persistence of an embryonic vessel. This anomaly was noted 27 times in 284 dissections that is 9.5%. The median artery in its forearm course sometimes perforates the median nerve this was seen three times among my dissections. In one individual on both sides on the right side the median artery pierced the median nerve twice on the left side only once. The third instance was on the right side only. Adachi (28) also mentions this feature.

Arteria antebrachialis dorsalis superficialis. Under this heading Adachi describes a rare abnormality which was seen 8 times in 698 dissections (1.1%). It may be called the "superficial radial artery" to distinguish it from "high origin" of that vessel. The radial artery gives off a powerful branch at varying levels in the forearm. This branch is often thicker than

the continuing trunk. It travels dorsally across the surface of the brachio-radialis muscle and runs downwards in the superficial fascia over the thumb tendons but ends like the normal radial artery by piercing the first interosseous space. The continuing smaller trunk of the radial takes a normal course to the wrist then deep to the thumb tendons and usually ends in the posterior carpal arch.

In the present series of 284 dissections a "superficial radial artery" was seen three times (1%). In one individual the whole radial artery became superficial about the middle of the forearm and then travelled in the manner described as far as the first interosseous space which it pierced in the usual way the abnormality was present on both sides. This anomaly must not be confused with "high origin" of the radial where the course of the artery is superficial in the upper part of the forearm but the artery becomes deep once the wrist is reached. In the above instance of bilateral "superficial radial artery" the brachial arteries on both sides had a normal course deep to the median nerve with bifurcations in the cubital fossa at the usual level. The third instance of "superficial radial artery" was on the right side only the abnormal radial artery (4 mm diameter) left the trunk of the radial a little more than halfway down the forearm and ran a course in the superficial fascia to the first interosseous space which it traversed as usual. The much smaller deeper trunk of the radial had a normal course to the wrist then deep to the thumb tendons and ended in the posterior carpal arch.

In this general survey of arterial variations it has obviously been impossible to deal with all the deviations from the average arrangement. Table 1 presents a selected list of the important arterial variations in the upper limb and these have been grouped in such a way as to show their frequency distribution on the right side, left side or on both sides in individual subjects.

ARTERIAL VARIATIONS IN THE LOWER LIMB

1 The femoral artery and its branches

The three main branches of the femoral artery profunda femoris medial circum-

flex and lateral circumflex must be considered as independent units which can arise in all kinds of combinations and variations of points of origin. Adachi looks upon the circumflex arteries as the two main branches of the femoral the profunda femoris being a subsidiary vessel linked with the circumflex arteries. The two circumflex arteries may arise by a common trunk with the profunda femoris as a continuation this is Adachi's truncus profundo-circumflexus perfectus the type usually described as the "normal" arrangement. The profunda femoris may be associated with the lateral circumflex called truncus profundo-circumflexus lateralis. It may be associated with the medial circumflex truncus profundo-circumflexus medialis. The level of origin of the profunda femoris along the femoral artery is of considerable interest. When the profunda femoris gives off both circumflex arteries (truncus profundo-circumflexus perfectus) it arises nearer the inguinal ligament than in the case of a truncus profundo-circumflexus lateralis or medialis. In my dissections the mean distance of origin of the truncus profundo-circumflexus perfectus was 38 mm. Adachi gives the distance as 31-40 mm in the majority of cases.

A more practical subdivision of the femoral artery patterns is that suggested by Poirier who gives 4 types. (1) The profunda femoris gives rise to both circumflex arteries corresponding to Adachi's truncus profundo-circumflexus perfectus. (2) The medial circumflex artery arises from the femoral corresponding to Adachi's truncus profundo-circumflexus lateralis. (3) The lateral circumflex arises from the femoral corresponding to the truncus profundo-circumflexus medialis. (4) Both medial and lateral circumflex arteries arise from the femoral. Poirier's method of classifying these variations is more in line with the usual anatomical description of the vessels and will be used for the analysis of my material.

The percentage distribution of these 4 types in the present series of 280 dissections (140 subjects) was as follows: type 1 118 times or 42% type 2 87 times or 31% type 3 56 times or 20% type 4 19 times or 7%. Poirier found type 1 the so-called "normal" much more

TABLE 1

Showing the frequency distribution of 12 variations of the arterial patterns in the two upper limbs of 142 subjects (284 dissections)

Variations	Right side only	Left side only	Both sides	Percentage frequency
1 Subscapular artery arising from third part of axillary	11	29	81	71
2 "High origin" of subscapular artery (p 247)	29	11	21	29
3 Common trunk for subscapular and posterior circumflex humeral arteries	14	22	26	31
4 Post circumflex humeral passes below teres major and ascends behind teres major (p 248)	2	2	2	28
5 Profunda brachii arising from third part of axillary	20	17	18	26
6 Profunda brachii arising from post. circumflex humeral	3	6	4	6
7 Prof brachii from post circumflex humeral and passes behind teres major (p 248)	8	5	3	7
8 "Superficial brachial artery" including all types (p 248)	19	6	5	12.3
9 "High origin" of radial artery (p 248)	10	3	2	5.9
10 "High origin" of ulnar artery (p 248)	3	3	1	2.8
11 Strong median artery reaching palm of hand (p 250)	5	6	8	9.5
12 Superficial radial artery" (p 250)	1		1	1

often i.e. 124 times in 200 dissections (62%) but this author includes 26 instances where the medial circumflex arose from the femoral at the same level as the profunda femoris in my series these were counted as type 2. Senior (24) states that the "normal" pattern occurs in approximately 50% of cases in the other 50% the medial and lateral circumflex or both arise from the femoral. A fairly rare abnormality is the absence of a medial circumflex the vessel is replaced by the first perforating or by an enlarged obturator artery 7 times or 2.5%. For purposes of the general classification these were counted among type 1 provided the lateral circumflex came from the profunda femoris.

Adachi gives a table of the percentage distribution of the various femoral artery

patterns in 7 series of observations 4 European series two Japanese and one American series which included Negroes. The percentage distribution of the 4 types of femoral artery patterns in the present series closely corresponds to the American series of White and Negro (Lipschutz) which appears in column 1 of Adachi's table (vol II p 152). The percentage differences in the 7 series are considerable and often significant statistically. Apart from possible racial differences it is clear that a certain arbitrariness in the interpretation of these patterns has played a role. E.g. the lateral circumflex may present itself as two branches called by Senior (24) art circumflexa lateralis and art circumflexa descendens one of the branches may arise from the femoral the other from the profunda femoris. The levels of origin of

the circumflex arteries further complicate the analysis and can lead to differences in interpretation

When the circumflex arteries branches of the femoral their levels of origin are usually above the origin of the profunda femoris the medial circumflex arising nearer the inguinal ligament than the lateral circumflex. Exceptions are not uncommon the medial circumflex arose at the same level as the profunda femoris in three instances and in three other dissections its level of origin was a little below that of the profunda. The lateral circumflex arose at a lower level much more often in 18 dissections it was found to leave the femoral artery at the same level as the profunda and there were 9 instances where its level of origin was below that of the profunda. The origins of the superficial branches of the femoral artery and the arrangement of the perforating arteries are so variable that they do not lend themselves to a statistical study

II The popliteal artery and its branches

Variations in the pattern of the popliteal artery revolve around the "high division" of that trunk and the resulting differences in the arrangement of the terminal branches the posterior tibial anterior tibial and peroneal arteries. According to Adachi any terminal division of the popliteal artery which takes place at a level above the middle of the posterior surface of the popliteus muscle must be considered as a "high division". Actually the majority of "high divisions" take place at a level a little above the upper border of the popliteus muscle. Three types of "high division" of the popliteal artery are recognized (a) The popliteal artery splits into two branches a lateral branch which continues into the anterior tibial and a medial one which becomes the common stem for the posterior tibial and peroneal arteries (b) The splitting of the popliteal artery is the same as in type (a) but the anterior tibial gives off the peroneal artery (c) The popliteal artery splits into two branches above the upper border of the popliteus an anterior branch travels downwards in front of the popliteus between the muscle and the tibia and continues as the anterior tibial

the posterior branch becomes the posterior tibial which gives off the peroneal as usual

An abnormality of the popliteal artery which is allied to "high division" is the formation of an elongated arterial "island" on the posterior surface of the popliteus muscle (Adachi). A thin vessel leaves the popliteal near the upper border of the popliteus muscle runs downwards parallel to the popliteal artery and joins the posterior tibial artery a little below the bifurcation or it may unite with the vessels at the bifurcation or with the anterior tibial artery. One instance of such "Inselbildung" was found in the present series in a right leg. The thin artery (1 mm diameter) was 43 mm long it left the popliteal artery at the upper border of the popliteus ran downwards close to the popliteal artery and fused with the posterior tibial 8 mm below the bifurcation. "Inselbildung" has already been mentioned in connection with the superficial brachial artery. In the case of the popliteal it is a form of "high division" in which the normal bifurcation at the lower border of the popliteus has become predominant and the thin artery represents the remains of a posterior tibial artery which arose at a higher level.

"High division" of the popliteal artery was found 14 times in 280 limbs (5%). Of these 14 instances 10 belonged to type (a) with the vessels running behind the popliteus and the peroneal artery coming from the posterior tibial three belonged to type (b) with the peroneal artery arising from the anterior tibial in these the branchings occurred opposite the lower border of the popliteus muscle. One instance of type (c) with the high division well above the upper border of the popliteus and the anterior tibial artery passing in front of the popliteus between the muscle and the tibia. In three subjects "high division" was noted on both sides in one of these the peroneal artery came from the posterior tibial on the left side (type a) and from the anterior tibial on the right side (type b). In the remaining 8 instances "high division" of the popliteal artery was present on one side and not on the other. The frequency of occurrence of "high division" of the popliteal given in anatomical literature is as follows. Poirier found "high division" 10 times in 227 cases

(4.4%) Trotter (40) gives the incidence as about 5%. Adachi gives 2.8% for the Japanese (770 limbs). These percentage differences are not significant statistically.

An embryological study by Senior ('29) provides a clear explanation of the way in which this abnormality of the popliteal artery can arise. In the embryo before the 14 mm stage the "axis" artery of the lower limb is the art. ischiadica. At the knee joint level the "axis" artery becomes the popliteal which at this stage runs in front of the popliteus ("deep popliteal" artery) and then continues as the anterior tibial. At the 14-mm stage the art. ischiadica is being supplemented by the femoral artery. Two longitudinal arteries which traverse the leg in the embryo, the future posterior tibial and peroneal arteries, arise from the axial vessel at the upper border of the popliteus. A gradual proximo-distal union of the posterior tibial and peroneal arteries occurs and is well advanced in embryos of 20 mm. This union forms the part of the definitive popliteal artery that lies behind the popliteus muscle. A communicating branch from either at the lower border of the popliteus enlarges to become the definitive anterior tibial while the "deep popliteal" artery gradually disappears.

Another variant of the popliteal artery pattern is the so-called "trifurcation" (Adachi) where all three terminal branches arise together at the level of the lower border of the popliteus muscle. The three arteries may arise from the termination of the popliteal at exactly the same level or the peroneal may branch off a few millimeters lower down. As long as the point of origin of the peroneal artery is 5 mm or less from the main bifurcation Adachi still classes the case as belonging to this variation. Trifurcation of the popliteal artery was seen 12 times in my series (4.3%).

III Arteries of the leg and foot

Peroneal artery The peroneal artery except in the case of trifurcation and in some instances of "high division" leaves the posterior tibial at a mean distance of 2.7 cm below the level of the bifurcation at the lower border of the popliteus, the maximum distance noted as an origin below the bifurcation was 59 mm. Trotter

(40) gives the average level of origin of the peroneal artery as 2.5 cm below the commencement of the posterior tibial. The mean length of the posterior tibial artery above the origin of the peroneal the *truncus tibio-peroneus* of French anatomists is given by Adachi as 26-30 mm.

The peroneal artery is the key to the variations in the patterns of the leg arteries. Stieda (16) considers that the peroneal artery is the main continuation of the popliteal artery, the anterior tibial and posterior tibial being side branches; this view provides an easy explanation of the variations. If one or other or both side branches are weak or absent they are reinforced or replaced by the peroneal artery at the ankle level. In the case of the anterior tibial and *dorsalis pedis* by a strong perforating branch, and in the case of the posterior tibial by a strong communicating branch. Rarely a strong peroneal artery may take on the functions of both anterior and posterior tibial arteries at the ankle joint level. One instance of this was found in a left leg. When noting these abnormalities on the recording scheme small perforating or communicating branches were not considered, only vessels of 2 mm diameter or more which obviously either reinforced a weak artery or replaced it entirely.

A strong peroneal artery which replaced or reinforced the terminal piece of the anterior tibial continuing as the *dorsalis pedis* was found 14 times in the present series of dissections (5%). Huber (41) found 6 cases in 200 dissections (3%) where the *dorsalis pedis* artery began as a continuation of the perforating branch of the peroneal artery. There were 7 instances where the peroneal artery replaced or reinforced the posterior tibial (2.5%). Among these were two subjects in which the posterior tibial artery was absent on both sides. In each case the vessel was replaced by a strong peroneal artery which turned medially at the ankle joint level and then assumed the functions of a posterior tibial artery.

Arteries of the foot Variations of the arteries of the foot revolve around the predominance of the arteries of the *dorsum* and of the sole. The *dorsalis pedis* is so variable in its course and in the distribu-

tion of its branches that it is useless for purposes of statistical analysis. Adachi describes and illustrates no less than 17 different patterns. Huber (41) made a very careful study of the arterial network on the dorsum of the foot and confirms the enormous variability of the arterial arrangements in this region. Although this author recognized a basic arterial pattern on the dorsum of the foot the variations within this pattern were so numerous that the "textbook picture" was present in detail in only 5.5% of the 200 feet dissected. 4 main types were defined with 7 other subgroups differing in varying degrees from the main types.

As regards the termination of the posterior tibial artery a note was made on the recording scheme as to the level of its bifurcation into lateral and medial plantar arteries. This corresponded to that of the medial tubercle of the calcaneum in most cases, occasionally a little above or a little below that level. Adachi gives 7 types of bifurcation of the posterior tibial artery but the variations refer to differing anatomical relationships between the two plantar arteries and the corresponding nerves. Adachi's illustrations all show the bifurcation at about the same level as that of the medial tubercle of the calcaneum.

Comparison between lateral and medial plantar arteries. The relative importance of the two plantar arteries is judged by the eye which is a more accurate method than measuring with the calipers in fractions of a millimeter (Adachi). In my series the lateral plantar artery was noted as the more important in all the dissections except in 4 instances where the two plantar arteries are described as equal in importance. Adachi found the medial plantar artery the stronger vessel 6 times in 223 feet. Dubreuil-Chambardel (55) made a study of persisting superficial plantar arches which he found 5 times in 101 dissections. The medial plantar arteries were obviously strong vessels in those instances but the author does not state whether the medial plantar arteries were actually the stronger vessels as compared with the lateral plantar ones.

The plantar arch. The relative importance of the lateral plantar and of the dorsalis pedis in the formation of the arch

were noted in each dissection. Again a visual impression of the two vessels was relied upon rather than caliper measurements and three possibilities exist: (a) The dorsalis pedis predominates, (b) the lateral plantar is larger than the dorsalis pedis and makes the more important contribution to the arch, (c) the two vessels are equal in importance. In the present 280 dissections the dorsalis pedis was noted as the more important artery 134 times (48%) the lateral plantar artery was judged the more important vessel 48 times (17%) the two vessels were noted as equal 98 times (35%).

Table 2 presents a selected list of the important arterial variations in the lower limb. As in the case of the upper limb these have been grouped so as to show their frequency distribution on the right side, left side or on both sides in individual subjects.

SYMMETRY OF ARTERIAL VARIATIONS IN THE LIMBS

Anatomical literature. In the many accounts of arterial variations little attention is paid to the question as to whether a variation which exists in one limb is likely to be present in the corresponding other limb or not. In *Poirer's text book of Human Anatomy* variations of the limb arteries are fully discussed. Some tables show the distribution of variations on the right and left sides but not with reference to individual cases. It appears that asymmetry of such variations is assumed. Dubreuil-Chambardel (55) describes 5 instances of superficial plantar arches in 101 human dissections. The findings were in the right and left feet of 5 different individuals and not one of them presented the abnormality on both sides. Asymmetry seems to be the rule with rare abnormalities.

Skopakoff (59) in his important and careful studies on the branchings of the axillary artery and on the "superficial brachial artery" nowhere considers bilateral symmetry although the distribution of the various anomalies in right and left limbs is analyzed. The same applies to Huelke (59). Pierson (25) describes 7 arterial anomalies of the human leg and foot. Of the 7 only one was present on

TABLE 2

Showing the frequency distribution of 12 variations of the arterial patterns in the two lower limbs of 140 subjects (280 dissections)

Variations	Right side only	Left side only	Both sides	Percentage frequency
1 Both circumflex arteries arising from profunda femoris	27	23	34	42
2 Medial circumflex arising from femoral artery	17	26	22	31
3 Lateral circumflex arising from femoral artery	22	20	7	20
4 Both circumflex arteries arising from femoral artery	10	7	1	7
5 Absent medial circumflex artery	2	1	2	2.5
6 "High division" of popliteal artery (p 253)	3	5	3	5
7 Trifurcation of popliteal artery (p 254)	5	5	1	4.3
8 Peroneal artery replaces dorsalis pedis (p 254)	8	4	1	5
9 Peroneal artery replaces posterior tibial artery (p 254)		3	2	2.5
Formation of plantar arch				
10 Dorsalis pedis is the more important artery	20	18	48	48
11 Lateral plantar is the more important artery	14	10	12	17
12 Dorsalis pedis and lateral plantar are equal in size	14	20	32	35

both sides of the same subject all the others on one or other side. Trotter (30) in a study on the branchings of the axillary artery based on 384 dissections states that in approximately half the cases the arrangements resemble each other on the right and left sides in the other half not. A greater frequency of variations on the right side is noted in a table. Schwyzer and others (35) describe three diverse patterns of the "superficial brachial artery" all were one sided anomalies.

Finerty (47) records a case of persisting ischiatic artery which was present on the right side in a male Negro the left side being normal. According to the author this very rare abnormality has been recorded 16 times in the literature. However it is not stated whether a strong ischiatic artery taking the place of the

femoral has ever been observed on both sides in an individual. Adachi found one instance of a right sided arteria ischiadica in a Chinese subject the left side being normal. In the present series there was one instance of "arteria ischiadica". In the left lower limb of a female Bantu a large inferior gluteal artery (5 mm diameter) continued into the popliteal artery the latter was joined by a branch from the femoral (2 mm diameter). The right side showed no abnormality.

De Garis and Swartley (28) refer to symmetry according to individual records. In one group (113 subjects) the patterns were similar on the right and left sides in 66 dissimilar in 47. Statistically there is no significant difference and it meant roughly that similarity and dissimilarity occur equally frequently. The authors con-

clude that there is a tendency towards symmetry to this extent that a given variation occurring on one side is a little more likely also to occur on the other side. This conclusion is not justified on the figures given. Huber (41) discusses bilateral symmetry. Among the 100 cadavers dissected there were only 4 in which both feet gave arterial pictures which were exactly alike when all the details were considered. These facts according to the author give a wrong impression of the degree of bilateral similarity. In 65 of the 100 cadavers both feet gave pictures which fell into the same main group, thus showing a definite tendency towards bilateral symmetry. Hilty (55) in a dissertation on the termination of the long saphenous vein (52 cadavers, 104 dissections) refers to certain arterial anomalies in two limbs: the profunda femoris and in two others the medial circumflex crossed superficial to the femoral vein just above the termination of the long saphenous vein. In each instance the abnormality was one-sided.

Adachi's monumental research into the arterial system of the Japanese was primarily concerned with establishing the different patterns, variations in origin of the branches from the main trunks, the frequency distribution of variations according to the sides of the body according to sex, racial differences etc. In the case of some arterial variations Adachi analyzes their unilateral or bilateral occurrence in individual subjects. Eg. in such a series of 187 subjects a strong median artery was seen: right side only in 7 subjects, left side only in 9 subjects, on both sides in 8 subjects. Thus 16 subjects in the series showed asymmetry and 8 subjects showed bilateral presence of the abnormality or symmetry. In another individual series of 345 subjects "high division" of the popliteal artery was seen: right side only in 7 subjects, left side only in 6 subjects, on both sides in two subjects. In both series there is a considerable preponderance of subjects with unilateral presence of the arterial abnormality, that is a tendency towards asymmetry. In the first example the numbers are hardly significant statistically, but in the second example the difference is highly

significant and cannot be due to fortuitous sampling.

Results in the present series. The right sided, left sided or bilateral distribution of arterial variations in individual cases are shown in tables 1 and 2 (pp. 252 and 256). Variation 1 (table 1) is the "normal" arrangement of the subscapular artery; this was observed in 71% of the dissections bilaterally in 81 subjects and either right or left side only in 40 subjects. Thus a symmetrical or bilateral occurrence is more common than an asymmetrical or unilateral one. This will obviously be the case with all the "normal" patterns. "Abnormal" patterns or variations (nos. 2-12, table 1) on the other hand show a tendency towards asymmetry. This becomes clear when the totals of columns 1 and 2 (table 1) are added together and compared with the total of column 3, leaving out variation 1 which is the "normal". The totals for columns 1 and 2 are 195 against 91 for column 3. In other words the 11 variations (nos. 2-12) taken together were encountered on both sides 91 times and on one side only 195 times, that is more than twice as frequently. These figures are highly significant statistically and cannot be due to random sampling.

The figures appearing in table 2 may be analyzed in the same way. Variation 1 appears in most text books as the "normal" in this series of dissections it was seen 118 times (42%). The pattern shows no tendency towards symmetry (in 50 subjects unilateral, in 34 subjects bilateral) and can therefore be treated as a variation. On the other hand variations 10, 11 and 12 show a tendency towards symmetry and are very evenly distributed; they really are subdivisions of the "normal" pattern. For this reason I have added the totals of variations 1-9 only, giving for columns 1 and 2 a figure of 188 against 73 for column 3. This again shows a highly significant tendency for variations to occur unilaterally rather than bilaterally. With some variations eg. variation 12 of table 1 and variation 5 of table 2 the tendency is not obvious, but as the number of observations is so small the distribution here is almost certainly fortuitous and due to random sampling.

Right sided preponderance Three of the variations in table 1 viz 'high origin of the subscapular (variation 2) the superficial brachial artery' (variation 8) and 'high origin of the radial (variation 9) show a significant tendency to occur more frequently on the right side than on the left. This has been found by other observers. Eg Trotter (30) noted the greater frequency of arterial variations on the right side in general. Adachi showed that the "superficial brachial artery" and 'high origin of the radial artery occurred much more frequently on the right side than on the left. In 187 cadavers dissected on both sides a "superficial brachial artery" occurred 22 times on both sides 33 times on the right side only and 15 times on the left side only a difference between the right and left sides which is undoubtedly significant.

The right sided preponderance of "high origin" of the subscapular artery has not been mentioned by other observers in the literature at my disposal. As both 'high origin' of the subscapular and the superficial brachial artery show this greater right sided frequency some correlation appeared possible. Counting the 5 subjects where the superficial brachial artery" occurred bilaterally that gave 24 instances of this abnormality on the right side. Of these 14 were found in upper limbs which presented a "normal origin of the subscapular (variation 1) and 10 in upper limbs with a "high origin" of the subscapular (variation 2). Considering that variation 1 represents 71% of the total and variation 2 represents 29% the distribution suggests some positive correlation but certainly not of a high degree.

DISCUSSION

Numerous radiographic studies of the arterial patterns in the limbs of new born infants and full term fetuses (Belou 34) clearly reveal the adult arrangement of the arteries at or near full term. Therefore the factors which produce departures from the so-called "normal" patterns must be active either at the fetal or at the embryonic stage. The early embryonic circulation consists of capillary networks in each region. By the enlargement of certain channels across this pre-existing vascular

network the large arteries are formed. According to Broman (21) the arteries of the upper limb are formed at the end of the second month and have a pattern which corresponds to that of the adult. In the case of the lower limb the adult pattern is completed somewhat later that is during the third month.

Seniors embryological studies (24 '29) confirm that the adult patterns are laid down at an early developmental stage. e.g., at the 13 mm stage there exists a rete femoralis or capillary network in the thigh and a primary arterial trunk or "axis" artery which runs along the dorsal surface of the thigh and leg. At the 14 mm stage a large direct channel through the rete femoralis has made its appearance and this represents the femoral artery. In the 19 mm stage the axis artery (ischiatric artery inferior gluteal) has become plexiform in appearance and the posterior aspect of the adductor magnus is supplied through another enlarged channel in the rete femoralis which becomes the profunda femoris and either the first or second perforating. When in rare cases the ischiatic artery persists as a large channel continuous with the popliteal artery and the femoral artery is reduced in caliber such an anomaly is almost certainly a genetic mutation. In view of the early developmental establishment of the adult patterns it is probable that all arterial variations are of genetic origin and it has been shown that these genetic factors act more often in an independent manner in right and left limbs and less often bilaterally.

A study of the arterial variations in the limbs of a pair of identical twins would be of great interest. For instance if an important arterial variation were found in one limb of a twin its symmetrical presence in the corresponding limb of the other twin of the pair would show that this particular variation had a genetic origin. Here a difficulty arises as some authors maintain that the symmetry in uniovular twins is of the mirror image character ("reverse symmetry") while others state that the ordinary symmetry arrangements are the rule.

Weber (23) was able to study two pairs of uniovular twins both at the fetal stage

The relationship of a coronary artery and vein on the anterior aspect of the two hearts showed "reverse" symmetry. The same applied to the arrangement of the cerebral sulci, a deviation of the confluence of the sinuses in the skull and the appearance of certain papillae in the tongue. Weber concluded by stating that the existence of "reverse" symmetry must be taken as proof that a pair of identical twins are truly monozygotic. *A priori* an arterial abnormality of genetic origin, say in the right arm of one of a pair of identical twins, could be expected to be found in the left arm of the other twin provided they are really uniovular. Other writers do not agree. Ludwig (22) who studied hair lines, papillary ridge patterns, etc. in twins, came to the conclusion that mirror image or "reverse" symmetry is rare and that normal symmetry arrangements are more common.

There is no question that the distribution of arterial abnormalities is more often unilateral than bilateral and that these variations seem to arise independently in either right or left limbs. Nevertheless the frequency distribution on either right or left sides or sometimes on both sides is not completely haphazard. If the bilateral distribution of the variations as against their right or left sided distribution is studied by the χ^2 test, it becomes clear that a bilateral appearance is more frequent than can be explained as a fortuitous occurrence on the right or left side or sometimes right and left sides in an individual. This applies to all the variations except no. 10 in table 1 and nos. 3, 4, 7 and 8 in table 2. Thus if each variation is considered as a genetic mutation, such mutations do not occur entirely haphazardly in either right or left limbs but appear on both sides significantly more often than can be explained as a purely chance phenomenon. In other words the genetic influence that produces the variation does not act entirely independently on the right and left sides but has a certain tendency towards symmetry.

In the causation of arterial variations locally operating factors might perhaps be invoked such as the position assumed by the fetus in utero, early movements of the limbs, unusual muscular development.

Such explanations would be quite speculative in the present state of our knowledge. The right sided preponderance of the "high origin" of the subscapular of the "superficial brachial artery" and of the "high origin" of the radial (variations 2, 8, 9 in table 1) remain unexplained.

SUMMARY AND CONCLUSIONS

The arterial patterns of the upper and lower limbs were investigated in 146 subjects. The diameters of the principal arterial trunks, the points of origin of the main branches along those trunks and their relative sizes were noted on specially designed recording sheets. There were separate recording sheets for the upper and lower limbs but each sheet contained the information relating to the right and left sides of an individual. A note was made of any abnormalities encountered.

A general survey is given of the different arterial patterns in the upper limb with a review of the literature on the subject. The variations are discussed under the following headings:

I *The axillary artery and its branches* in which section a special importance is attached to the "high origin" of the subscapular artery and the variations in the origin and course of the posterior circumflex humeral artery.

II *Arteries of the arm with special emphasis on the "superficial brachial artery"* and its allied "high origin" of the radial and ulnar arteries.

III *Arteries of the forearm and palm of the hand* in which section the varieties of the superficial palmar arch are discussed also the strong median artery and the rare abnormality of the superficially running radial artery at the wrist level. In table 1 the arterial variations of the upper limb are listed their frequency distribution in the right and left limbs or on both sides in individual subjects are noted and their percentage frequency is given.

Similarly there is a general survey of the arterial variations in the lower limb under the headings:

I *The femoral artery and its branches*. 4 different patterns are recognized the so-called "normal" arrangement being in reality one of the variations.

II *The popliteal artery and its branches* with special emphasis on the "high division" of the popliteal artery. The resulting variations in the origin and course of the main branches are discussed and the embryological explanation of this abnormality is given.

In section III *Arteries of the leg and foot* there is a special emphasis on the role of the peroneal artery in explaining the different patterns. As regards the arteries of the foot a note was made of the relative sizes of the dorsalis pedis and of the lateral plantar arteries in the formation of the plantar arch. The percentage frequency of the three resulting types was established as these presented themselves in this series of dissections. Table 2 lists the arterial variations encountered in the lower limbs gives their right sided left sided or bilateral distribution in individual subjects as well as the percentage frequency of the variations in the whole series.

In the anatomical literature asymmetry of arterial variations that is their unilateral occurrence appears to be generally assumed especially in respect of rare abnormalities. When the figures showing the number of times of unilateral appearance in tables 1 and 2 are added these are more than twice the number of those indicating a bilateral appearance. Thus there is a strong tendency towards asymmetry in respect of arterial variations in the limbs. In general an arterial variation may not be expected to be present on both sides except in approximately one out of three cases. As regards unusual abnormalities the literature seems to show that it is only in exceptional instances that a bilateral or symmetrical occurrence can be expected.

Three of the variations listed for the upper limb showed a significant right sided preponderance. The adult arterial patterns are laid down at an early developmental stage. In view of this it is concluded that all arterial variations must be looked upon as genetic mutations and that locally operating factors do not play any role. A study of the frequency distribution on both sides as against on the right or left sides shows that arterial variations appear bilaterally more often than can be explained on purely fortuitous grounds.

Although the genetic influence manifests itself more often independently in the two limbs nevertheless there is some tendency towards symmetry.

LITERATURE CITED

- Adachi B 1928 *Das Arteriensystem der Japaner* Kyoto vol I pp 8 205 208 210 280 309 315 322 357 358 365 368 389 vol II pp 137 147 152 154 197 200 204 206 227 242 262 269
- Belou P 1934 *Atlas estereoscopico de anatomia de las arterias* El Ateneo Buenos Aires
- Broman I 1921 *Grundriss der Entwicklungsgeschichte des Menschen* J F Bergmann München p 237
- Charles C M and others 1931 The origin of the deep brachial artery in American White and in American Negro Males *Anat Rec* 50 299-302
- Coujouma P and P Bastien 1934 *Résultats de 104 observations sur la disposition des branches de l'axillaire* C R Assoc Anat 29 193-199
- De Garis C F and W B Swartley 1928 The axillary artery in white and negro stocks *Am J Anat* 41 353-397
- Dubreuil-Chambardel L 1905 *De l'arcade plantaire superficielle* C R Assoc Anat 3 79-86
- Finerty J C 1947 Persistent ischiatic artery *Anat Rec* 98 587-595
- Hilty H 1955 *Die makroskopische Gefässvariabilität im Mundungsgebiet der Vena saphena magna des Menschen* Dissertation der Medizinischen Facultät der Universität Bern
- Huber J F 1941 The arterial network supplying the dorsum of the foot *Anat Rec* 80 373-391
- Huelke D F 1959 Variation in the origins of the branches of the axillary artery *Ibid* 135 33-41
- Ludwig E 1922 *Über den Haarstrich einiger Zwillinge* *Anat Anz* 55 1-11
- Müller R A 1939 Observations upon the arrangement of the axillary artery and the brachial plexus *Am J Anat* 64 143-163
- Pierson H H 1925 Seven arterial anomalies of the human leg and foot *Anat Rec* 30 139-145
- Poirier P *Traité d'Anatomie Humaine* L Baillière & Co Paris vol II pp 734 756 822 833
- Schwytzer A G and C F de Garis 1935 Three diverse patterns of the arteria brachialis superficialis in Man *Anat Rec* 63 400-416
- Senior H D 1924 The description of the larger direct or indirect muscular branches of the human femoral artery a morphogenetic study *Am J Anat* 33 243-265
- 1929 Abnormal branching of the popliteal artery *Ibid* 44 111-120
- Singer E 1933 Embryological patterns persisting in the arteries of the arm *Anat Rec* 55 403-416
- Skopakoff C 1959 *Über die Variabilität der Ab- und Verzweigung der A. brachialis superficialis* *Anat Anz* 106 356-368

- 1959 Über die Variabilität der Abzweigung der Hauptäste der Aa axillaris et brachialis Ibid 107 294-304
- Starck D 1955 Embryologie Georg Thieme Stuttgart p 529
- Stieda L 1916 Die Varietäten der Arterien der Extremitäten des Menschen Anat Anz 49 535-549
- Trotter M and others 1930 The origins of branches of the axillary artery in Whites and in American Negroes Anat Rec 46 133-137
- Trotter M 1940 The level of termination of the popliteal artery in the White and the Negro Am J Anthropol 27 109-118
- Weber A 1923 Recherches anatomiques sur les jumeaux humains univitellins (monozygotes) C R Assoc Anat 18 519-526

Localization of Acid Phosphatase, Nonspecific Esterases and β -D Galactosidase in Parotid and Submaxillary Glands of Domestic and Laboratory Animals¹

HOWARD H. CHAUNCEY AND GIULIANO QUINTARELLI
Department of Research Tufts University School of Dental Medicine
Boston Massachusetts

Due to the accessibility of pure saliva, mammalian salivary glands provide a unique opportunity for the study of secretory cell metabolism. Secretion rate studies (Coats et al. 56 Kay 58) biochemical analysis of the secreted fluids (Coats and Wright 57 McDougall 48 Reid and Huffman 49) and histological staining techniques (Hauser 37 Jacoby and Leeson 59 Silver 54 Stormont 32 Zeigler 29) have been employed in an attempt to establish functional relationships between the different glands of a single species or the same gland in several different species.

While biochemical analysis of salivary fluids is a valuable tool for determining overall glandular function it discloses little information concerning tissue activity at the cellular level. Furthermore histological examination of tissues using conventional dyes and stains only permits discernment of morphological similarities or nuances. Thus there is a paucity of information concerning the metabolic activity of the various histological components of mammalian salivary glands. Histochemical techniques when employed in conjunction with the aforementioned procedures present a promising means for studying cellular metabolism. A series of investigations therefore was undertaken to determine the enzymatic reactivity of the major salivary glands from several species of mammals. It is the opinion of the authors that studies of this type will prove of aid in understanding the metabolism of the various secretory cells comprising these glands. In addition the determination of a normal hydrolytic enzyme "pattern" may also serve as a basis for

evaluating the effect of local and systemic disease on the salivary glands.

The current publication on the localization of acid phosphatase nonspecific esterases and beta D-galactosidase in cow sheep hog rat rabbit and dog salivary glands is part of a series of articles dealing with the comparative histochemistry and biochemistry of mammalian salivary glands. Observations noted in the study of enzyme reactivity of the parotid and submaxillary glands of humans and the meta chromatic reactivity of the submaxillary gland in 7 species of mammals have been previously detailed (Chauncey and Quintarelli 59 Quintarelli and Chauncey 60).

METHODS AND MATERIALS

Collection and fixation of tissues
Specimens of parotid and submaxillary glands were obtained from freshly slaughtered cow sheep and hog. Tissue from the rat rabbit and dog were obtained immediately after sacrifice. All tissues were cut into blocks approximately 2-3 mm thick and fixed for 18-24 hours at 4 C in chloral hydrate formaldehyde (CHF) solution. The blocks were then washed in running tapwater for two hours embedded in gelatine (Fishman and Baker 56) and replaced in the fixative solution for 2-3 days. The specimens were cut from the surrounding gelatine retaining only a minimum coating around each tissue and washed for 30 minutes. Sections 10-15 μ

This work was supported by grant D-402 of the National Institutes of Health United States Public Health Service.

Present address: University of Rome School of Medicine and Surgery Rome Italy

thick were prepared on a freezing microtome and placed in appropriate substrate solutions

Histochemical techniques Acid phosphatase activity was localized employing the post-coupling method of Rutenburg and Seligman (55). A 25 mg/100 ml solution of the substrate sodium 6 benzoyl 2 naphthyl phosphate was prepared in 0.1 M acetate buffer pH 5.0. Diffusion of the tissue phosphatase into the incubating fluid was prevented by adding 2.0 gm of sodium chloride to each 100 ml of substrate solution. Representative sections of parotid and submaxillary gland from each animal were incubated at 37°C for periods ranging from 30 minutes to 2½ hours. With this substrate 30 minutes was the optimum incubation time for permitting an evaluation of the comparative activity of the glands from the different species. Tissues which exhibited a moderate to intense reaction during this time were too heavily colored if the incubation was lengthened while tissues which exhibited only weak or no activity during the first 30 minutes were not greatly enhanced by increasing the length of incubation.

After incubation the sections were washed for several minutes in distilled water and placed in a freshly prepared cold (4°C) solution of diazotized O dianisidine (1 mg/ml) which had been alkalinized with sodium bicarbonate. The action between the diazonium salt and the enzymatically liberated 6 benzoyl 2 naphthol was usually complete after one minute. Sites of activity were visualized by the purple azo dye formed. The sections were then rewashed in distilled water and mounted on glass slides.

Nonspecific esterase activity was demonstrated using a modified Gomori method (52). The substrate employed was naphthyl AS acetate. Eight tenths milliliter of a 1% stock solution (half and half propylene glycol and acetone) was dissolved in 12 ml of propylene glycol. Thirty seven milliliters of distilled water, 5.0 ml of 0.2 M phosphate buffer (pH 6.6) and 20 mg of diazotized O amino azotoluene* were added successively. After shaking to ensure complete mixing the solution was filtered through Whatman no. 1 paper to remove the larger undissolved particles of the Gar-

net GBC salt. Tissue sections were incubated for 30-60 minutes at 37°C. A 60 minute incubation period provided an optimal color density for evaluating the comparative esterase activity of the various species employed. Therefore the reaction herein described was the result of a standard 60 minute incubation period. Reaction sites were visualized by a red purple dye while nonreactive areas were colored yellow. Following incubation the sections were washed in distilled water and mounted.

Beta D galactosidase activity was localized using the post coupling technique described by Cohen et al (52). The substrate (6 bromo-2 naphthyl β D galactopyranoside) was prepared by dissolving 15 mg in 10 ml of methanol. Complete dissolution of the salt was insured by adding 15 ml of boiling water. Twenty milliliters of 0.1 M acetate buffer (pH 5.0) was added to adjust the pH to the desired level. Five and eight tenths grams of NaCl was then placed in the volumetric flask and the mixture was diluted with distilled water to produce a final volume of 100 ml. Specimens of fixed salivary gland tissue were incubated at 37°C for 18 hours. Following removal of the test sections, aliquots of the incubating solution were tested for the presence of free 6 bromo 2 naphthol. By making the substrate hypertonic with sodium chloride it was possible to incubate for 18 hours without having a significant amount of free hydrolysis products or free enzyme in the incubating solution. Enzymatically liberated 6 bromo 2 naphthol was visualized by coupling with diazotized O dianisidine utilizing the procedure described for acid phosphatase.

RESULTS

Acid phosphatase

Parotid glands From among the three species of domestic animals tested only the bovine parotid gland exhibited acid phosphatase activity (fig 1). Acinar and duct cells were moderately reactive showing a homogeneous red violet stain which was granular in character. Rat parotid gland acini and ducts exhibited marked activity.

* Brentamine fast blue B Imperial Chemical Industries Ltd Manchester England

* Brentamine garnet GBC Imperial Chemical Industries Ltd Manchester England

(fig 2) The same components in the rabbit (fig 3) were moderately reactive. No noticeable difference in reaction intensity was observed among the intralobular interlobular or excretory duct types or between acini and duct epithelium. In contrast the acinar cells in the canine tissue (fig 4) were only weakly reactive while the entire duct system of the dog was markedly stained, being quite similar in reactivity to rat and rabbit tissue.

Submaxillary glands A high degree of variability was noted in submaxillary gland tissue. This was in part due to basic histological differences occurring in the glands of the various animals studied. Cow, sheep, hog and dog submaxillary tissue contains mucous acini, a characteristic found in most higher mammals. Although certain structures bear a morphological resemblance to mucous cells, the same glands in rodents seem to be devoid of mucous bearing components. For this reason these cells have been called "mucoid" or "special" serous cells. Recently Jacoby and Leeson (59) have confirmed that these elements are actually tubules which contain secretion granules. Following the example set by previous authors, this component will be referred to as secretory tubules.

Cow and sheep submaxillary glands were weakly positive (figs 5, 6). No activity could be demonstrated in hog glands. Only the ducts of the bovine tissue stained while in the sheep gland the ducts and demilunes were colored. However, the color intensity of the latter cells was extremely weak.

Rat secretory tubules were unreactive except for the basement membrane of these cells which was lightly stained (fig 7). This presented a noticeable contrast to the acinar and duct cells which were markedly reactive. Rabbit secretory tubules (fig 8) were moderately reactive and could not be distinguished from the serous acini which had a similar intensity of color. In the dog (fig 9) the serous demilunes were moderately colored while the mucous acini were unstained.

The ducts of the three laboratory animals were reactive, intensity of staining increasing in the order: dog, rabbit and rat. In each animal the intralobular inter-

lobular and excretory ducts were equally colored.

Nonspecific esterases

Parotid glands Activity in the cow and sheep parotid was generally confined to the ducts (intralobular, interlobular and excretory) with a very light scattering of dye granules present in the acini (figs 10, 11). Thus the shape and histological characteristics of only the ducts could be discerned. The difference in reaction between ducts and acini in the bovine tissue was heightened by the high degree of reactivity exhibited by the ducts' basement membrane. Contrary to the above findings, the acinar epithelium of porcine gland was markedly reactive while the duct cells were only weakly positive (fig 12).

Parotid gland duct cells showed a strong esterase reaction in rat, rabbit and dog. The reaction in rodent tissue was concentrated primarily in the basal portion of these cells (figs 13, 14) while in the dog (fig 15) the deposition of granules was evenly dispersed throughout the duct cytoplasm. Serous acini of all three animals were moderately stained and provided a homogenous background for the more heavily colored ducts.

Submaxillary glands Cow mucous acini appear to be positive even though their principal content is mucinogen. The demilunes previously revealed to be serous structures (Quintarelli and Chauncey 59) were intensely stained and had clearly visible basal membranes. The mucous cells, although exhibiting a lesser degree of staining, were definitely colored. Dye granules were present in all epithelial components—demilunes, mucous acini and duct cells. The latter showed only weak activity as evidenced by the presence of a light scattering of colored granules (fig 16). Sheep gland (fig 17) also exhibited an intense reaction, but in this animal the activity was confined to the ducts. Demilunes and mucous cells were at best only weakly positive. In the hog submaxillary gland (fig 18) the serous demilunes surrounding the mucous acini were intensely stained. Ducts were moderately colored and evidenced a fair number of granules.

Examination of the esterase activity in the submaxillary tissue of the laboratory

animals revealed a definite variation in the reactivity pattern among the three species. Ducts and secretory tubules in the rat were quite strongly stained especially in the basal portion of the cytoplasm. Acinar cells showed a moderate reaction (fig 19). Serous acini and secretory tubules in the rabbit exhibited a moderate degree of activity both being slightly less intense than the ducts (fig 20). In the dog the serous demilunes and basement membrane of the mucous acini were only slightly reactive (fig 21). Intralobular interlobular and excretory ducts were markedly positive. All duct types contained an even dispersion of stained material.

Beta D-galactosidase

Parotid glands Of the three domestic species only cow parotid gland exhibited β -D-galactosidase activity (fig 22). The acini and intralobular ducts were moderately reactive and were homogeneously stained making it difficult to distinguish between these two components. Interlobular and excretory ducts appeared nonreactive.

All cellular components of the rat parotid were unreactive. Activity in rabbit tissue was weak, acini and ducts exhibiting a light homogeneous stain (fig 23). Dog parotid gland was more reactive than the rodent tissues, the duct being moderately stained and clearly visible against the background of weakly staining serous acini (fig 24).

Submaxillary glands All duct cells in the submaxillary glands of the cow, sheep and hog were moderately colored (figs 25, 26, 27). In the cow and sheep the demilunes were also reactive but to a lesser degree than the ducts. Mucous acini in these two animals were unstained. Mucous cells in porcine gland were weakly colored with the stain generally being seen in the demilunes and ducts.

Serous acini and ducts in the rat submaxillary were weakly responsive while the secretory tubules were unstained (fig 28). Sections of rabbit gland were also weakly stained, the color density being homogeneous throughout. Ducts could be discerned but it was not possible to distinguish between the serous acini and the

secretory tubules (fig 29). The serous demilunes in dog gland were weakly stained while the ducts showed moderate activity (fig 30).

DISCUSSION

Classification of mammalian salivary glands is generally based on the presence or absence of mucin-containing cells. Glands are thus divided into serous, mucous and mixed types. The parotid glands of the 7 species studied in the present and two prior investigations (Chauncey and Quintarelli '59, Quintarelli and Chauncey '60) are all considered to be strictly serous glands. The submaxillary gland in 5 of these species—dog, cow, sheep, hog and human—is a mixed gland (table 1). From among these 5 mammals only the human gland contains both serous alveoli as well as mucous alveoli with serous demilunes. In the 4 other species the serous cells are found only in the form of demilunes. Rat and rabbit submaxillary gland are devoid of mucous-bearing elements (a characteristic shared by several other rodents—mouse, hedgehog, muskrat, gopher and guinea pig). The submaxillary glands of these rodents except for the guinea pig have secretory "granular" tubules which contain "secretory granules" but differ cytologically from the acinar cells present in the parotid and submaxillary glands of these and other species (Stormont '32) (table 1).

The discovery of an active enzyme (amylase) in the secretions emanating from salivary glands which contain serous elements resulted in the assumption that all serous acinar components are zymogenic. The terminology serozymogenic and serous have thus been used synonymously.

TABLE 1
Serous and mucous components of mammalian submaxillary glands

	Serous acini	Serous demilunes	Mucous acini	Secretory tubules
Rat	+	+	—	—
Rabbit	+	+	—	—
Dog	+	+	+	+
Cow	+	+	+	+
Sheep	+	+	+	+
Hog	+	+	+	+
Human	+	+	+	+

+ Present — absent

even in those animals where it has not been possible to demonstrate amylase activity either in the saliva or salivary glands (table 2)

The term serozymogenic thus may well be a misnomer especially if one considers the enzyme content of sheep parotid gland. In this animal it has not been possible to demonstrate the presence of salivary amylase (Scheunert and Trautmann '21 Schwarz and Rasp '28). Furthermore the present investigation indicates that sheep serous acini are devoid of demonstrable acid phosphatase and beta D galactosidase and exhibit only slight esterase activity (table 3)

The morphological plan and cytological appearance of the salivary glands from the various species of mammals studied may seem similar in many respects. However these similarities should not be interpreted as indicating functional similarity. Comparison of parotid and submaxillary gland enzymatic activity of the three domestic animals studied in the present investigation (tables 3 and 4) shows that the enzyme activity patterns of these animals are quite different. Perhaps the best indicator of functional difference is the amount of saliva secreted by the various animals. It has been estimated that the cow secretes about 56 liters of mixed saliva

TABLE 2
Amylase activity of mammalian saliva

	Parotid fluid	Submaxillary fluid	"Mixed" saliva
Rat (Coats et al. '56 Schwarz and Rasp '28)	+	+	+
Rabbit (Schwarz and Rasp '28)	?	?	+
Dog (Gomori '52 Roseboom and Patton '29)	?	+	+
Sheep (Scheunert and Trautmann '21 Schwarz and Rasp '28)	—	—	—
Cow (Palmer '16)	?	?	+
Hog (Schwarz and Stemmetzger '23)	+	?	+
Human (Schneyer '46)	+	+	+

+ Presence demonstrated — not demonstrated ? presence not definitely established

TABLE 3
Parotid gland

	Acid phosphatase	Alkaline phosphatase	β-D-Galactosidase
Cow			
Acini	2	1	2
Ducts			
Intralobular	2	2½	0
Interlobular	2	2½	0
Excretory	2	2½	0
Sheep			
Acini	0	1	0
Ducts			
Intralobular	0	2½	0
Interlobular	0	2½	0
Excretory	0	2½	0
Hog			
Acini	0	2½	0
Ducts			
Intralobular	0	1½	0
Interlobular	0	1½	0
Excretory	0	0	0

Reactivity 4 intense 3-3½ marked 2-2½ moderate 1-1½ weak ½ or less (qual), 0 negative

TABLE 4
Submaxillary gland

	Acid phosphatase	Nonspecific esterase	β -D- galactosidase
Cow			
Demilunes	0	4	1
Ducts			
Intralobular	1	1	2
Interlobular	1	1	2
Excretory	1	1	2
Mucous cells	0	2	0
Sheep			
Demilunes	1	1	1½
Ducts			
Intralobular	1½	4	2½
Interlobular	1½	4	2½
Excretory	1½	4	2½
Mucous cells	0	0	0
Hog			
Demilunes	0	4	2
Ducts			
Intralobular	0	2	2
Interlobular	0	2	2
Excretory	0	2	2
Mucous cells	0	0	1

per day while the sheep secretes about 4 liters per day (Dukes 55). The daily output for man is estimated to be 1.5 liters (Dukes 55). Differences in glandular output cannot be attributed solely to size but must imply functional differences. This assumption is supported by the finding that the parotid secretion in ruminants is almost continuous (Duke 55) being at most only slightly affected by chemical (Dukes 55, Kay 58) and psychic stimuli (Scheunert, Krzywanek and Zimmerman '29). This continuous parotid flow is necessary to ensure an adequate amount of fluid buffers and phosphate for the proper function of the first three stomach compartments. On the other hand, the parotid gland of man does not secrete continuously and a copious flow can be elicited by the application of gustatory, olfactory and psychic stimuli (Chauncey and Shannon '60, Schneyer et al. '56).

Although little is known about the biological function of acid phosphatase, nonspecific esterases and β -D-galactosidase, evaluation of tissue reactivity allows the investigator to establish an "activity pattern" for the various cytological components being studied. By comparing dif-

ferences in cellular "activity patterns" both between the different major salivary glands of a single species and the same gland among several species, it may be possible to establish certain functional and cytological relationships.

Some evidence has been obtained indicating that acid phosphatase is related to nucleoprotein metabolism in nerve cells (Bodian and Mellors '45). In addition, Junqueira et al. ('49) have noted a sexual dimorphism in the acid phosphatase activity of mice submaxillary gland, greater activity being observed in glands of males. Similarly, Lacassagne ('40a, b) and Jacoby and Leeson ('59) have noted that the secretory tubules in male mice and rats were larger than in females. They contend that this might be the result of the influence of sexual hormones on these glands, producing an action similar to that observed in the prostate gland (Gutman and Gutman '39). This contention of an interrelationship between male sexual organs and salivary gland phosphatase activity is supported by the observation that the parotid saliva acid phosphomonoesterase activity is increased in persons having prostatic

carcinoma (Hoerman Chauncey and Herold 59)

Noback and Montagna (49) in a study of the histochemistry of mammalian pancreas and salivary glands observed that the cytoplasm of rat parotid acinar and duct cells was weakly positive for acid phosphatase. In the submaxillary gland the cytoplasm of the ducts and serozymogenic cells was moderately reactive while that of the secretory tubules was at most only faintly reactive. Hill and Bourne (54) investigating the histochemistry of salivary gland duct cells noted that the cytoplasm of both ducts and acini in the rabbit parotid gland gave a positive reaction the activity of the ducts being somewhat less than that found in the acini. However they were unable to demonstrate this enzyme in the rat parotid gland. The submaxillary glands of both rat and rabbit were positive. The ducts in both species were said to exhibit less activity than the serous acini.

In the current investigation the acid phosphatase reactivity of duct and acinar epithelium of rodent (rat and rabbit) parotid glands did not differ appreciably (table 5). In contrast the acini in the canine tissue were less active than the

ducts. The submaxillary glands of the three species presented a more variable picture. This was in part due to cytological differences between the glands of rodents and the glands of the dog which contain mucous cells. In the submaxillary gland of all three species the ducts stained more intensely than the acini (table 6). The mucous cells of dog gland were negative as were rat secretory tubules. Rabbit secretory tubules were moderately positive.

The heightened esterase reactivity of salivary gland duct cells has been noted previously. Burstone (56) observed that the duct cells in the rat parotid gland were quite active in contrast with the acini which were only slightly reactive. He further noted that the submaxillary gland did not appear as reactive as the parotid. Ducts were both positive and negative. At best the "mucoid" cells or secretory tubules were lightly stained while acinar cells never demonstrated activity.

Hill and Bourne (54) had similar results with rat tissue. These latter authors found that rabbit parotid reacted in the same manner as rat tissue. On the other hand rabbit submaxillary gland was strongly positive the deeply staining red granules being concentrated in duct cells.

TABLE 5
Parotid gland

	ph	Acid phosphatase	Non specific esterase	β -D. galactosidase
Rat				
Acini		3	2½	0
Ducts				
Intralobular		3	3½	0
Interlobular		3	3½	0
Excretory		3	3½	0
Rabbit				
Acini		2½	2	1½
Ducts				
Intralobular		2½	4	1½
Interlobular		2½	4	1½
Excretory		2½	4	1½
Dog				
Acini		1½	2	1
Ducts				
Intralobular		3	3	2½
Interlobular		3	3	2½
Excretory		3	4	2½
Reactivity 4 intense 3-3½ marked 2-2½ moderate 1-1½ weak ½ occasional 0 negative				

TABLE 6
Submaxillary gland

	Acid phosphatase	Nonspecific esterase	β -D- galactosidase
Rat			
Serous acini	3	2	1½
Secretory tubules	0	4	0
Ducts			
Intralobular	3½	4	1½
Interlobular	3½	4	1½
Excretory	3½	—	1½
Rabbit			
Serous acini	2	2½	1½
Secretory tubules	2	2½	1½
Ducts			
Intralobular	3	3	1½
Interlobular	3	3	1½
Excretory	3	3	1½
Dog			
Demilunes	2	½	1½
Ducts			
Intralobular	2½	3	2½
Interlobular	2½	3	2½
Excretory	2½	3	2½
Mucous cells	0	½	0

The present investigation confirms these prior findings of intense duct reactivity. However, the parotid gland serous cells of all three species were moderately reactive (table 5). Rodent submaxillary glands were also heavily stained (table 6). Of particular interest was the finding that rat secretory tubules reacted with the same intensity as the duct cells while rabbit secretory tubules were less reactive than duct cells containing approximately the same degree of coloration as the serous cells. In the dog submaxillary the reaction was generally confined to the ducts. Mucous cells and demilunes exhibited only occasional activity.

Beta D galactosidase activity has been found in homogenates of rat and dog salivary glands (Cohen et al. 52). Rutenburg and Seligman (55) in a histochemical study of the enzyme in rat tissues observed that the serous acini and ducts in rat submaxillary gland were quite active. The secretory tubules were only lightly stained except for the basal aspect of these cells which exhibited a dark blue color. In the current investigation parotid tissue showed a marked species difference (table 5). Rat glands were nonreactive, rabbit glands were weakly reactive, duct and

acinar epithelium having the same color intensity. However, in dog glands the ducts were moderately reactive and the acini showed only weak activity. The submaxillary gland cytological components in both rodents were only weakly positive except for rat secretory tubules which were colorless. The ducts of the dog gland were moderately stained while demilunes were weakly colored and mucous cells were unstained (table 6).

The results obtained in the present investigation thus both confirm and contradict the findings of previous workers. The disparities may result from differences in the type of substrate and/or method of tissue fixation or both. Noback and Montagna (47), Junqueira et al. (49) and Hull and Bourne (54) used sodium beta glycerophosphate for the demonstration of acid phosphatase activity. This method used extensively in the past is subject to numerous artifactual errors such as non enzymatic staining and enzyme diffusion and has generally been superseded by techniques employing substituted naphthols as the substrate.

Naphthyl AS-acetate, the esterase substrate used in the present study, was also employed in the investigations of Burstone

(56) and Hill and Bourne (54) Our findings of activity in components which in prior studies were reported to be negative or only weakly positive may be due to differences in fixation techniques Unfortunately Hill and Bourne (54) do not describe the methods whereby their tissues were prepared Burstone (56) used freezing and in vacuo paraffin embedding with subsequent deparaffinization in petroleum ether and acetone While this latter procedure may produce enzyme inactivation or loss due to the deparaffinization process Burstone (58) upon comparing the effect of freeze drying and formalin fixation noted that formalin fixed liver showed suppression of several esterase activity bands On the other hand Baker Hew and Fishman (58) have shown that with "Chloral Formalin" fixative (CHF) it is possible to fix tissue for extremely long periods and still maintain a high degree of enzyme activity Our results would thus tend to confirm the excellent preservative qualities of this fixation technique

In conclusion it can be stated marked differences in glandular function appear to exist even between the glands of phylogenetically related species Rat and rabbit salivary glands exhibit different enzyme activity patterns In addition there is little similarity between sheep and cow glands The current state of knowledge concerning the action of salivary gland acid phosphatase nonspecific esterases and beta D galactosidase does not permit correlation of the present histochemical observations with the biochemical findings obtained by prior workers (Coats and Wright 57 McDougall 48 Reid and Huffman 49) However the present investigation does serve to point out that certain cytological components of salivary glands of different species of mammals which appear similar when conventional histological dyes are used actually are biochemically and functionally different

SUMMARY

Cow sheep hog rat rabbit and dog parotid and submaxillary glands were examined for acid phosphatase nonspecific esterases and beta D galactosidase activity

Acid phosphatase activity was demonstrable in the following tissues cow rat

rabbit and dog parotid glands cow sheep rat rabbit and dog submaxillary glands Nonspecific esterase were present in both glands for all 6 species Beta D galactosidase activity was observed in cow rabbit and dog parotid glands while the submaxillary gland for all 6 animals was observed to be reactive

Enzyme activity was generally confined to the cytoplasm of serous cells and ducts Nuclei connective tissue adipose tissue and blood vessels usually exhibited little or no activity Mucous cells were generally unreactive except for bovine cells—moderate esterase activity hog mucous cells—weak beta D galactosidase activity and dog mucous cells—occasional esterase activity In all instances the colored material present was concentrated in the basal area of the mucous cells and may have been the result of diffusion of enzyme or free naphthol from the adjacent demilunes

The different cytological components in the parotid and submaxillary gland demonstrated varying degrees of enzyme reactivity among the 6 animals studied In addition these components exhibited specific "enzyme activity patterns" which were different for each species

LITERATURE CITED

- Baker J R H H Hew and W H Fishman 1958 The use of a chloral hydrate formaldehyde fixative solution in enzyme histochemistry *J Histochem Cytochem* 6 244-250
 Bodian D and R C Mellors 1945 The regenerative cycle of motoneurons with special reference to phosphatase activity *J Exp Med* 81 469-487
 Burstone M S 1956 Esterase of the salivary glands *J Histochem Cytochem* 4 130-139
 ——— 1958 The relationship between fixation and techniques for the histochemical localization of hydrolytic enzymes *Ibid* 6 322-339
 Chauncey H H and G Quintarelli 1959 Histochemical localization of hydrolytic enzymes in human salivary glands *J Dent Res* 38 961-968
 Chauncey H H and I L Shannon 1960 Parotid gland secretion rate as method for measuring response to gustatory stimuli in humans *Proc Soc Exp Biol Med* 103 459-463
 Coats D A D A Denton J R Goding and R D Wright 1956 Secretion by the parotid gland of the sheep *J Physiol* 131 13-31
 Coats D A and R D Wright 1957 Secretion by the parotid gland of the sheep The relationship between salivary flow and composition *Ibid* 135 611-622

TABLE 6
Submaxillary gland

	Acid phosphatase	Nonspecific esterase	β D- galactosidase
Rat			
Serous acini	3	2	1½
Secretory tubules	0	4	0
Ducts			
Intralobular	3½	4	1½
Interlobular	3½	4	1½
Excretory	3½	—	1½
Rabbit			
Serous acini	2	2½	1½
Secretory tubules	2	2½	1½
Ducts			
Intralobular	3	3	1½
Interlobular	3	3	1½
Excretory	3	3	1½
Dog			
Demilunes	2	½	1½
Ducts			
Intralobular	2½	3	2½
Interlobular	2½	3	2½
Excretory	2½	3	2½
Mucous cells	0	½	0

The present investigation confirms these prior findings of intense duct reactivity. However the parotid gland serous cells of all three species were moderately reactive (table 5). Rodent submaxillary glands were also heavily stained (table 6). Of particular interest was the finding that rat secretory tubules reacted with the same intensity as the duct cells while rabbit secretory tubules were less reactive than duct cells containing approximately the same degree of coloration as the serous cells. In the dog submaxillary the reaction was generally confined to the ducts. Mucous cells and demilunes exhibited only occasional activity.

Beta D galactosidase activity has been found in homogenates of rat and dog salivary glands (Cohen et al. 52). Rutenburg and Seligman (55) in a histochemical study of the enzyme in rat tissues observed that the serous acini and ducts in rat submaxillary gland were quite active. The secretory tubules were only lightly stained except for the basal aspect of these cells which exhibited a dark blue color. In the current investigation parotid tissue showed a marked species difference (table 5). Rat glands were nonreactive, rabbit glands were weakly reactive, duct and

acinar epithelium having the same color intensity, however. In dog glands the ducts were moderately reactive and the acini showed only weak activity. The submaxillary gland cytological components in both rodents were only weakly positive except for rat secretory tubules which were colorless. The ducts of the dog gland were moderately stained while demilunes were weakly colored and mucous cells were unstained (table 6).

The results obtained in the present investigation thus both confirm and contradict the findings of previous workers. The disparities may result from differences in the type of substrate and/or method of tissue fixation or both. Noback and Montagna (47), Junqueira et al. (49) and Hill and Bourne (54) used sodium beta glycerophosphate for the demonstration of acid phosphatase activity. This method used extensively in the past is subject to numerous artifactual errors such as non-enzymatic staining and enzyme diffusion and has generally been superseded by techniques employing substituted naphthols as the substrate.

Naphthyl AS acetate, the esterase substrate used in the present study, was also employed in the investigations of Burstone

PLATES

PLATE 1

EXPLANATION OF FIGURES

Figs 1 through 9 Acid phosphatase fixation in chloral hydrate formaldehyde Substrate 6-benzoyl 2-naphthyl phosphate $\times 200$

- 1 Bovine parotid gland Acinar and duct cells are moderately reactive
- 2 Rat parotid gland Acinar and duct cells exhibit marked activity Greatest activity is present in basal area of the duct cells Nuclei appear to be nonreactive
- 3 Rabbit parotid gland Moderate acid phosphatase activity is present in the acinar and interlobular duct cells Epithelial cells lining the intercalated ducts appears to be highly reactive Connective tissue and fat cells are nonreactive



PLATE 2

EXPLANATION OF FIGURES

- 4 Dog parotid gland Acinar cells exhibit weak activity Ducts are markedly stained
- 5 Bovine submaxillary gland Only the ducts cells are stained Serous and mucous cells are negative
- 6 Sheep submaxillary gland Mucous cells negative Serous cells weakly stained Ducts cells slightly more reactive than demilunes

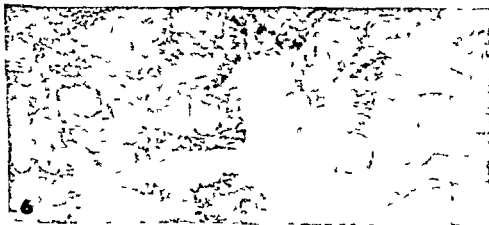
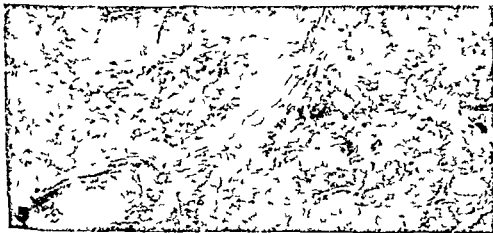


PLATE 6

EXPLANATION OF FIGURES

- 16 Bovine submaxillary gland. Demilunes are intensely stained. Mucous cells are also colored. Ducts show weak activity as evidenced by the presence of a light scattering of colored granules.
- 17 Sheep submaxillary gland. Ducts exhibit an intense reaction. Demilunes and mucous cells are only weakly positive.
- 18 Porcine submaxillary gland. Serous demilunes are intensely stained. Ducts are moderately colored and contain a fair number of granules. Mucous cells are negative.

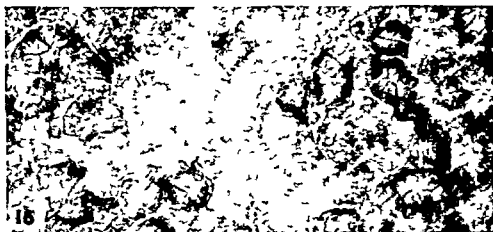


PLATE 7

EXPLANATION OF FIGURES

- 19 Rat submaxillary gland Intense reactivity of secretory tubules and intralobular ducts is noted Dye appears to be concentrated in basal portion of these cells Acinar cells show a moderate degree of activity
- 20 Rabbit submaxillary gland Serous acini and secretory tubules exhibit moderate activity both being less heavily colored than the ducts
- 21 Dog submaxillary gland Weak esterase activity present in demilunes and basement membrane of mucous acini Ducts are markedly reactive



PLATE 8

EXPLANATION OF FIGURES

Figs 22 through 30 Beta D galactosidase fixation in chloral hydrate formaldehyde Substrate 6-bromo-2 naphthyl β D galactopyranoside $\times 200$

- 22 Bovine parotid glands Acinar cells and intralobular ducts are moderately reactive Homogenous reaction causes difficulty in identifying the various components
- 23 Rabbit parotid gland Acinar and duct cells show a weak staining which is similar in intensity for both components
- 24 Dog parotid gland Ducts stain moderately and stand out against the background of weakly staining acinar cells

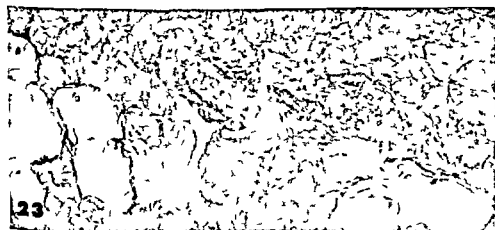


PLATE 9

EXPLANATION OF FIGURES

- 25 Bovine submaxillary gland Mucous cells are nonreactive demilunes weakly positive
Ducts exhibit moderate coloration
- 26 Sheep submaxillary gland Duct cells are moderately reactive Demilunes show a weak
stain while the mucous acini appear to be negative
- 27 Porcine submaxillary gland Mucous cells appear slightly reactive Demilunes and
ducts exhibit a moderate amount of color

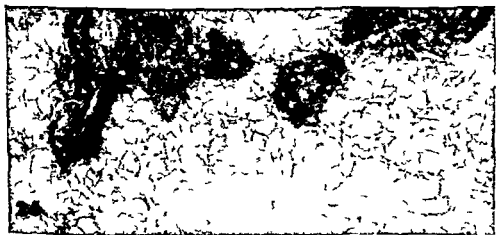
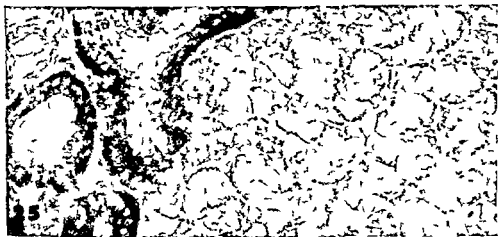
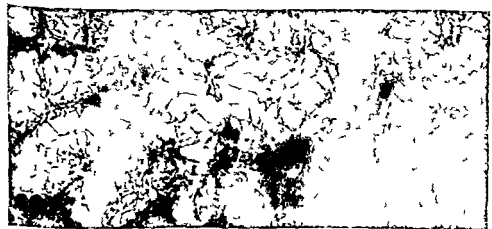
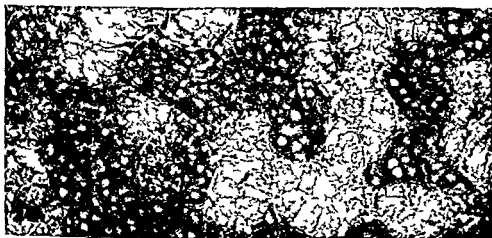


PLATE 10

EXPLANATION OF FIGURES

- 28 Rat submaxillary gland Acinar and duct cells show a weak to moderate response Secretory tubules are unstained
- 29 Rabbit submaxillary gland Homogenous weak to moderate stain Ducts can be identified but it is not possible to distinguish between acinar cells and secretory tubules
- 30 Dog submaxillary gland Ducts show moderate activity Demilunes exhibit a weak stain while the mucous cells appear to be nonreactive



The Composition of the Anal Glands of *Dasypus novemcinctus*¹

JULIAN F HAYNES AND ALLEN C ENDERS
Department of Biology Rice University Houston Texas

The nine banded armadillo (*Dasypus novemcinctus*) is monestrus (Hamlett 32) and apparently ovulates spontaneously (Talmage and Buchanan 54) The vagina is separated from the exterior by an extensive urogenital sinus and cornification does not occur at any stage of the reproductive cycle (Enders and Buchanan 59) The inaccessibility of the vagina and lack of prominent cycle make the use of vaginal smears in this animal of limited value Furthermore no changes in the external genitalia of sufficient magnitude to serve as an index of the reproductive cycle have been observed It has long been known that mammalian cutaneous glands serve definite functions in marking territory and locating trails and appear to play a part in the reproductive cycles of many mammals (Bourliere 54) Recently Bruce (60) has shown that in mice the scent of a strange male can disrupt an estrus pregnancy and Parkes (60) has emphasized that sense of smell may be more important than it had previously been considered to be

The armadillo possesses a pair of highly developed anal glands (Owen 36) which produce a characteristic odor Although the development and histology of the integument of the nine banded armadillo have been examined (Wilson 14) and a histological study has also been given (Cooper 30) the integumentary derivatives which form the anal gland secretory have not been studied It was the principal purpose of this investigation to study the structure of this complex and to determine whether there is evidence of variation in secretion in relation to the reproductive cycle

MATERIAL AND METHODS

A total of 20 armadillos from all stages of the reproductive cycle were killed by

abrupt vertebral fracture and their anal glands removed fixed dehydrated double imbedded in celloidin and paraffin and sectioned The histology of the glands was studied using 10 μ serial sections stained with hematoxylin and eosin and representative sections from other glands stained either with Ehrlich's hematoxylin chromotrope 2R orange G and fast green or with Weigert's hematoxylin and fast green Whole mounts of several glands were prepared by staining the intact gland with paracarmine dehydrating and clearing in cedar oil and then dissecting away the outer connective tissue capsule Glycogen was demonstrated by the application of the periodic acid Schiff test to sections from glands fixed in Carnoy's or Rossman's fluids and controlled by digestion in a 1% malt diastase solution at pH 6 Cytoplasmic basophilia was observed using Zenker's fixed material stained with eosin methyl green blue at pH 5.2 For the demonstration of lipids pieces of the glands were fixed in buffered formalin and sections were colored with Sudan black B phospholipids were revealed by the Elftman method (Elftman 57)

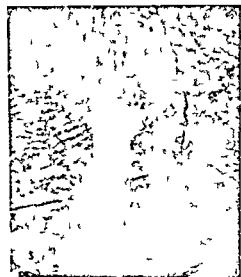
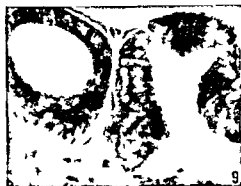
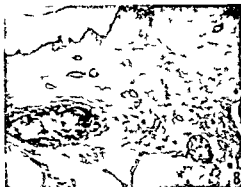
To induce pregnancy pregnant mares serum (Equine) was administered to 5 animals for a period of three days in doses ranging from 10 to 500 IU Subsequently a single injection of 250 IU of chorionic gonadotropin (Arnitin S) was administered The animals were killed after an interval of 24 hours Examination of the ovaries yielded a complete ovulation had occurred

The anal glands of periparturient animals were 1-2.5 cm in shape and size. The glands of the United States were 9113 from the

PLATE 2

EXPLANATION OF FIGURES

- 5 Sebaceous gland The dark (osmophilic) material is lipid Flemmings tetrachrome $\times 110$
- 6 PAS-positive substances in an anal gland of a non-experimental female Note the absence of demonstrable glycogen and presence (especially in the upper left corner) of a PAS positive luminal fringe Periodic acid Schiff $\times 435$
- 7 Glycogen in the apocrine gland of an animal in which ovulation was induced The position of the glycogen against the cell membranes is a diffusion artifact Periodic acid Schiff $\times 435$
- 8 Glycogen in sebaceous glands Glycogen is abundant in a duct (left of picture) A small amount is also present in the peripheral cells of a lobule (lower right corner) Periodic acid Schiff $\times 10$
- 9 Cytoplasmic basophilia in columnar cells of the apocrine glands Note that between the juxtanuclear and apical regions there is interposed a non basophilic region Eosin methylene blue $\times 435$
- 10 An electron micrograph through part of a region of basophilia of apocrine gland cells note the orderly arrangement of endoplasmic reticulum with associated RNP particles in the cell at the upper left G Golgi zone S secretion droplet M cell membrane Buffered osmium tetroxide sucrose \times about 15 000



On the Fine Structure of the Parotid Gland of Mouse and Rat¹

HAROLD F. PARKS

Department of Anatomy University of Rochester
School of Medicine and Dentistry
Rochester New York

The parotid gland of the mouse has never been the subject of extensive cytological investigation possibly because in routine histological preparations it seems to have no unusual features or because it is not as conveniently accessible as other glandular organs. However the mouse parotid has been found to be more amenable to good electron microscopic fixation than other salivary glands with which the writer has had experience and has been used in our laboratory for experimentation and for basic cytological studies. It was therefore felt that a detailed description of the secretory portion of the organ would not be unduly supererogatory.

Chievitz (1885) briefly describes the development of the gland. Oppel (00) comments briefly on a tendency for acinous cells to be binucleate or have giant nuclei and refers to an early histological description by Asp (1873) reporting that only one kind of secreting cell was found in the gland. Schultze (11) studied the gland at the cytological level describing intercellular secretory canals in the acini and concluding that mitochondria in the striated ducts transform into secretion granules. More recently the mouse parotid has been the subject of a brief histological description by Fekete (41) and has been touched upon in a few histochemical studies (Noback and Montagna 47, Martin 53, Hill and Bourne 54 and Shklar et al. 58).

The recent publication of an electron microscopic study of the rat's parotid gland by Scott and Pease (59) furnishes an opportunity to compare the parotid glands of two closely related species and also affords occasion for the writer to record very briefly some independent observations on the parotid gland of the rat.

MATERIALS AND METHODS

This description is based on observations made on the parotid glands of approximately 100 mice and 40 rats. For electron microscopy parotid tissue taken from nembutal or urethane anesthetized animals was fixed in cold (0-5 C) modified Palade's fixative containing 0.22 M sucrose (cf. Caulfield 57) and buffered to pH 7.4, dehydrated in ethyl alcohol and imbedded in butyl methacrylate catalyzed with 1-1.5% benzoyl peroxide and polymerized at 50 C. Sections were cut with a Porter Blum microtome using glass knives stained for 20-30 minutes with lead hydroxide (Watson 58) sandwiched with formvar (Watson 57) and examined with a Siemens Elmiskop Ia operated at 60 kv using 50 μ objective apertures. Polystyrene latex spherules² were sometimes used as a focusing aid. For light microscopy the glands were fixed in Regaud's or formaldehyde-calcium solutions imbedded in paraffin, sectioned at 3-5 μ and stained with phosphotungstic acid hematoxylin, acid hematein (Baker 46), toluidine blue or with the PAS reaction controlled by malt diastase digestion and counterstained with hematoxylin.

OBSERVATIONS

Mouse gland histological structure

The mouse's parotid gland possesses the three secretory segments typical of most major salivary glands: acini, intercalated ducts, and striated ducts. The acini are similar to pancreatic acini; the cells are pyramidal in shape, contain chromophilic material in their basal parts, often are

¹This work was supported by research grant D-689 from the N.I.D.R., U.S. Public Health Service.

²Courtesy of Dow Chemical Company.

binucleate or have an unusually large nucleus and are packed with secretion granules in their apical parts. A majority of the granules stain blue with phosphotungstic acid hematoxylin while the other granules remain unstained. The unstained granules are usually large refractile and homogeneous while the blue staining granules show a great variability in size and often appear ring shaped in optical section. There is a tendency for individual cells to contain only one kind of granule but in some cells the granule types are mixed in varying proportions. A majority of granules show a positive reaction to PAS that is not abolished by diastase digestion while the remaining granules are PAS-negative. The PAS-positive granules exhibit the same morphological characteristics as blue staining granules described in connection with phosphotungstic acid hematoxylin and are therefore presumably identical.

The acini appear on superficial examination to be solid masses of cells but intercellular canals are numerous and a central or main acinous lumen one or two μ in diameter (usually no larger than intercellular canals) can occasionally be found. The central lumen despite its small diameter may have as many as 5 cells bordering it in a single sectional plane.

Intercalated ducts are small tubules about 10 μ in diameter with a 3 μ lumen lined by a single layer of low cuboidal cells. Proximally i.e. near the acini these cells resemble miniature acinous cells in having basophilic basal cytoplasm and apical secretion granules. Most of the secretion granules stain blue with phosphotungstic acid hematoxylin but a few remain unstained. With PAS red staining granules are very prominent but it is not possible to ascertain from our material whether PAS-negative granules are also present. Distally the intercalated ducts have a slightly larger lumen (5 μ) and the cells are devoid of secretion granules. The distal segment is usually short and occasionally absent. None of the secretion antecedents in acini or intercalated ducts is stained by acid hematein.

Intralobular striated ducts are 30–40 μ in diameter with an 8 to 10- μ lumen

The columnar epithelium lining these ducts is characterized by radial striations in the basal cytoplasm of the cells. The striate appearance is due in part to the presence of radially arranged mitochondria however fine PAS positive striations are also demonstrable in the bases of cells in sections in which mitochondria are not stained thus showing that mitochondria are not solely responsible for the striate appearance. Although the term striated duct is commonly used to designate an intralobular segment of the duct system in salivary glands it should be noted that interlobular ducts of this gland also have basal striations.

Phosphotungstic acid hematoxylin and acid hematein often but not invariably stain a number of granules in the apical cytoplasm in striated duct cells. It is difficult to decide with these "mitochondrial" stains whether stained granules are mitochondria or secretion antecedents. The only conspicuous PAS positive granules in these cells show no preferred pattern of localization and fail to resist diastase digestion these therefore probably represent glycogen deposits. The lumina of ducts often contain a homogeneous PAS positive material which is presumably a secretion product of acinous and intercalated-duct cells. None of the secretion antecedents in the gland stains metachromatically with toluidine blue.

Mouse gland electron microscopic structure

1 *The acinous cell and its histological relationships* The acinous cell of the parotid gland resembles that of the exocrine pancreas in the general appearance of its nucleus, endoplasmic reticulum and Golgi apparatus. Its secretion antecedents however exhibit marked differences from the dense homogeneous pancreatic zymogen granules. Three morphological types of secretion antecedent have been observed. (1) The most numerous type of secretion granule (fig. 2) is usually inhomogeneous in texture consisting of a dense peripheral substance surrounding a less-dense central portion that occasionally contains one or more masses of dense material similar to that of the periphery of the granule.

This appearance probably represents a fixation artifact in figure 7 a number of granules are seen one of which is "typical" (i.e. inhomogeneous) and another homogeneously dense while others appear to be almost uniformly dense but show a subtle difference in texture between peripheral and central parts. This series of appearances suggests that the secretion granule is a rather dense homogeneous structure that imbibes water and swells during fixation (2). A less frequently occurring secretion granule is relatively homogeneous in texture and low in density. These granules are rather unstable and tend to coalesce during fixation forming large irregularly shaped masses (fig 3). It will be noted that both types of secretion granules are contained within a membrane similar to the plasma membrane of the cell (3). The least frequently observed secretion antecedent takes the form of a small mass of cytoplasm that is demarcated and partially separated from the rest of the cell's cytoplasm by a group of tiny membranous vesicles arranged so as to enclose a spherical inclusion and appearing in section as a circular or oval array (fig 4). The cytoplasm immediately surrounding such a group of vesicles is often of a density greater than that of the cytoplasm inside the group of vesicles. Secretion antecedents of this kind are destined to be extruded from the cell as cytoplasmic blebs.

The nucleus of the acinous cell exhibits no remarkable features. As in the nuclei of most cells the nuclear sap contains a dispersion of granules similar to the ribonucleoprotein granules of the cytoplasm while the nucleoli appear to be dense aggregations of somewhat smaller granules (fig 6). The nuclear membrane is a two-layered structure containing fenestrations through which the nucleoplasm communicates with cytoplasm. The outer layer of the nuclear membrane which is often studded with ribonucleoprotein particles does not always run a course parallel with the inner nuclear membrane but occasionally forms plications that project out into the cytoplasm. These projections are sometimes seen to be continuous with the endoplasmic reticulum of the cytoplasm (cf Watson 55).

The endoplasmic reticulum takes the form of flattened membranous vesicles that are commonly known as cisternae (Palade and Porter 54). The most conspicuous morphological feature of these membranous structures is the presence of ribonucleoprotein (RNP) particles on their outer surfaces. On cisternae that have been sectioned in a plane perpendicular to their broad surface no pattern of distribution of RNP granules is apparent but broad surface views show the granules to be arranged in circular or spiral groups usually containing 5 to 10 granules (cf Palade 55). Cisternae tend to be arranged parallel to one another in the base of acinous cells (fig 9) but are more randomly distributed elsewhere in the cell (figs 2 3 4 8). It should be mentioned that all the RNP particles in the cytoplasm are not attached to the membranes of the endoplasmic reticulum many particles lie free in the cytoplasm (figs 5 9).

The Golgi bodies several of which may be present in a cell resemble the endoplasmic reticulum in being membranous structures but differ from it in being devoid of RNP granules (figs 6 10). Two morphological components are distinguishable for purposes of description small spherical membranous vesicles 300-600 Å in diameter and lamellae which are larger flattened membranous vesicles of variable length and width and about 200-300 Å in thickness. The lamellae tend to occur in compact groups stacked parallel to one another while the vesicles are randomly distributed in the vicinity of the lamellae. Spheroidal bodies interpreted to be immature secretion granules are almost invariably seen in close relation to the Golgi bodies (figs 6 10) and it is obvious from some electron micrographs that these granules arise by a swelling and enspherulation of the Golgi lamellae.

A miscellaneous group of cytoplasmic inclusions remains to be mentioned without detailed description. Mitochondria the structure of which is too well known to require description appear in most cases to be randomly disposed in the cytoplasm but have frequently been seen to lie in close proximity with long axis parallel to the basal or lateral cell membrane. Membranous spherules containing a num

ber of much smaller vesicles a kind of inclusion first described in nerve cells (Palay and Palade '55) and later described in numerous cell types are seen rarely in adult glands but are numerous in the glands of very young animals. Finally a type of inclusion that probably represents a degenerative body consists of a membranous enclosure 1μ or less in diameter containing membranous formations (fig 6) some of which are myelin like (fig 10). Some degenerative bodies are homogeneous or vacuolated masses of material containing no internal membranous formation.

The surface of the acinous cell usually but not always sends microvillous extensions into the lumina i.e. the central lumen of the acinus and the intercellular canaliculi (figs 7 and 8). In one group of mice of unknown strain the lumina contained virus like bodies similar in appearance to the leukemia virus described by de Harven and Friend ('59). These bodies could often be seen budding off from the surfaces of microvilli. In some cases they were so numerous as to occlude the lumen completely.

Acinous cells appear to be firmly attached to one another in the vicinity of the lumina. This is apparent in histological preparations in which the basal parts of cells often shrink apart while the apical parts remain attached around the lumen. In electron micrographs numerous desmosomes are seen near lumina (fig 7). The cytoplasm immediately adjacent to the cell membranes of two apposed cells in the vicinity of a lumen often exhibits a marked increase in density (fig 8). The dense material is revealed in some micrographs to be fibrillar in character and the fibrils are sometimes seen terminating at the cell membrane where it is modified to form half a desmosome. In more basal parts of the lateral surfaces of cells where desmosomes are seldom seen interdigitation and interfoliation of cytoplasmic processes occur and occasionally profiles are seen which indicate that villous processes from one cell are fitted into appropriately shaped excavations in a neighboring cell (fig 6). The basal surface of the acinous cell is sometimes smooth but often has infoldings or leaf like processes much like those of

the lateral surface of the cell. Occasionally a group of small vesicles is seen in the cytoplasm next to an infolding where their position suggests that they arose by invagination and pinching off of the plasma membrane (fig 5).

The plasma membrane at the base of the cell is covered with a thin layer of amorphous material that is commonly called the basement membrane" (fig 9). This "membrane" which appears to be a somewhat condensed layer of connective tissue ground substance it not reflected between cells for any appreciable distance at intercellular boundaries but bridges the gap between cells to become continuous with the basement membrane of neighboring acinous cells. Thus the basement membrane might be said to form a barrier or a landmark separating the acinus from extra acinous structures. Outside the basement membrane the main tissue elements to which the acinus is related histologically are nervous and vascular.

The nerves appear to consist mainly of postganglionic autonomic fibers myelinated axons having been seen only near the hilum of the gland or in connective tissue septa dividing it into major subdivisions. At the level of striated ducts the nerves appear to run in fascicles of about 30 fibers accompanied by numerous longitudinally disposed collagenous fibrils in addition to their Schwann-cell investments the whole being surrounded by a thin sheet of cytoplasm from a connective tissue cell whose relation to the nerve fascicle is analogous with that of an endothelial cell to the capillary lumen. At the inter acinous level (fig 9) the nerve fascicles are smaller have fewer fibers and are devoid of connective tissue elements. Here some nerve fibers are often only partially invested by Schwann-cell cytoplasm and their uncovered parts are separated from the acini only by connective tissue ground substance. Although the definitive relationship between nerve fiber and acinous cell is usually achieved by the axons penetrating the basement membrane of the acinus and passing between secretory cells to form a terminal expansion characterized by its content of numerous tiny membranous vesicles (cf Scott and Pease '59) it is not uncommon to see axons contain

ing large numbers of these vesicles while coursing through the interacinous connective tissue space (fig 9) This observation is reminiscent of the varicosities that are seen in the classical light microscopic preparations designed to show nerve fibers and endings in salivary glands (Arnstein 1895 Boeke 31)

Capillaries are intimately related to the acini (fig 9) there appears to be nothing separating acinous cell from endothelial cell except a small amount of connective tissue ground substance including the basement membranes of the two cells The endothelial cells are characterized by the presence of numerous membranous vesicles and flask like invaginations of the cell membrane at both luminal and basal surfaces (cf Palade 60 Moore and Puska 57) In some places there appear to be fenestrations in the endothelial cell about 50 mμ in diameter these are occasionally seen to have a single membrane stretched across them suggesting the possibility that failure to see membranes across all fenestrations is due to imperfect fixation

Inside the basement membrane enclosing the acinus the acinous cells are associated with three kinds of "intra acinous" cellular elements the endings of nerve cells myoepithelial cells and a third type for which there is no special name The nerve endings have been described above Myoepithelial cell cytoplasmic processes (figs 1 5) resemble the cytoplasm of typical smooth muscle cells showing faint longitudinal striations and having at places along their plasma membrane flask like invaginations or "pinocytotic vesicles" however the striations are not so conspicuous nor the pinocytotic vesicles so numerous as in typical smooth muscle Since an occasional section through the nucleus seems to show more than two cytoplasmic processes radiating from it the impression has been gained that the cells are stellate or spider shaped The third type of cell occurring inside the basement membrane of the acinus is perhaps best characterized at the present stage of the writer's knowledge in negative terms it is non-secretory non nervous and non muscular Its cytoplasm contains a few mitochondria a few membranous vesicles and some more or less evenly scattered ribonucleoprotein par-

ticles that are not attached to membranous structures The overall paucity of cytoplasmic inclusions gives the impression that the cytoplasm is of unusually low density No precise account of the shape of this cell can be given It appears to be stellate having numerous tenuous cytoplasmic processes that lie adjacent to or between the bases of acinous cells and thus in some sections can be difficult to distinguish from processes of nerve cells or smooth muscle cells The cell body containing the nucleus appears to be located at the periphery of the acinus either between the bases of neighboring acinous cells or between acinous cell and basement membrane

2 The *intercalated ducts* constitute a relatively small portion of the mass of the gland and therefore are not frequently encountered in sections The epithelial cells lining the lumen in the part of the duct near the acini are similar to acinous cells in that they contain secretion granules and have a relatively large amount of endoplasmic reticulum (figs 11 12) The chief qualitative difference between the two cell types is in the character of their secretion granules Whereas the great majority of secretion granules in acinous cells are in homogeneous in fixed sectioned material the granules in intercalated duct cells are homogeneous There are apparently two kinds of granules some light and some dense The granules like those of acinous cells are separated from the surrounding ground cytoplasm by a membrane resembling the plasma membrane of the cell The luminal surfaces of duct cells send short microvillous projections of cytoplasm into the lumen No nerve endings have been seen in relation to intercalated duct cells but the two other non secretory cellular elements of the acinus are present as parts of the intercalated ducts The tenuous cytoplasmic processes of cells characterized by a low-density "empty" cytoplasm lie between the basal parts of epithelial cells as they do in the acini Myoepithelial cell processes often appear to be longitudinally disposed along the basal surface of the duct the overall shape of these cells i.e. whether they are fusiform or stellate cannot be ascertained from the material studied The distal segments of the intercalated ducts appear to be much

ber of much smaller vesicles a kind of inclusion first described in nerve cells (Palay and Palade 55) and later described in numerous cell types are seen rarely in adult glands but are numerous in the glands of very young animals. Finally a type of inclusion that probably represents a degenerative body consists of a membranous enclosure 1μ or less in diameter containing membranous formations (fig 6) some of which are myelin like (fig 10). Some degenerative bodies are homogeneous or vacuolated masses of material containing no internal membranous formation.

The surface of the acinous cell usually but not always sends microvillous extensions into the lumina i.e. the central lumen of the acinus and the intercellular canaliculi (figs 7 and 8). In one group of mice of unknown strain the lumina contained virus like bodies similar in appearance to the leukemia virus described by de Harven and Friend (59). These bodies could often be seen budding off from the surfaces of microvilli. In some cases they were so numerous as to occlude the lumen completely.

Acinous cells appear to be firmly attached to one another in the vicinity of the lumina. This is apparent in histological preparations in which the basal parts of cells often shrink apart while the apical parts remain attached around the lumen. In electron micrographs numerous desmosomes are seen near lumina (fig 7). The cytoplasm immediately adjacent to the cell membranes of two apposed cells in the vicinity of a lumen often exhibits a marked increase in density (fig 8). The dense material is revealed in some micrographs to be fibrillar in character and the fibrils are sometimes seen terminating at the cell membrane where it is modified to form half a desmosome. In more basal parts of the lateral surfaces of cells where desmosomes are seldom seen interdigitation and interfoliation of cytoplasmic processes occur and occasionally profiles are seen which indicate that villous processes from one cell are fitted into appropriately shaped excavations in a neighboring cell (fig 6). The basal surface of the acinous cell is sometimes smooth but often has infoldings or leaf like processes much like those of

the lateral surface of the cell. Occasionally a group of small vesicles is seen in the cytoplasm next to an infolding where their position suggests that they arose by invagination and pinching off of the plasma membrane (fig 5).

The plasma membrane at the base of the cell is covered with a thin layer of amorphous material that is commonly called the "basement membrane" (fig 9). This "membrane" which appears to be a somewhat condensed layer of connective tissue ground substance it not reflected between cells for any appreciable distance at intercellular boundaries but bridges the gap between cells to become continuous with the basement membrane of neighboring acinous cells. Thus the basement membrane might be said to form a barrier or a landmark separating the acinus from extra acinous structures. Outside the basement membrane the main tissue elements to which the acinus is related histologically are nervous and vascular.

The nerves appear to consist mainly of postganglionic autonomic fibers myelinated axons having been seen only near the hilum of the gland or in connective tissue septa dividing it into major subdivisions. At the level of striated ducts the nerves appear to run in fascicles of about 30 fibers accompanied by numerous longitudinally disposed collagenous fibrils in addition to their Schwann-cell investments the whole being surrounded by a thin sheet of cytoplasm from a connective tissue cell whose relation to the nerve fascicle is analogous with that of an endothelial cell to the capillary lumen. At the inter-acinous level (fig 9) the nerve fascicles are smaller have fewer fibers and are devoid of connective tissue elements. Here some nerve fibers are often only partially invested by Schwann-cell cytoplasm and their uncovered parts are separated from the acini only by connective tissue ground substance. Although the definitive relationship between nerve fiber and acinous cell is usually achieved by the axon penetrating the basement membrane of the acinus and passing between secretory cells to form a terminal expansion characterized by its content of numerous tiny membranous vesicles (cf Scott and Pease 59) it is not uncommon to see axons contain

the desmosomes consist largely of a finely fibrillar substance and appear denser than the ground cytoplasm. The most apically situated desmosomes, which are approximately $\frac{1}{2} \mu$ from the luminal surface, tend to be associated with more copious amounts of the dense cytoplasmic material than are lower desmosomes. This condition probably accounts for the appearance of "terminal bars" in histological preparations. It also gives the false impression in some sections that a "diaphragm" of the dense material remniscent of the terminal web of the intestinal epithelial cell (Palay and Karlin '59) is passing across the upper part of a cell (cf figs 14-18). It is possible that the most apically situated desmosomes are really sections through a single elongate desmosomal formation that extends entirely around the cell at a level about $\frac{1}{2} \mu$ below its luminal surface (cf Palay and Karlin '59).

A basement membrane similar to that surrounding acini is present at the bases of duct cells (figs 15-16). Despite the light microscopic observation that a PAS positive substance can sometimes be seen as thin basal striations, electron micrographs do not show any evidence that basement membrane or any other connective tissue element passes up between the cell processes. It therefore seems likely that the PAS positive element in the histological preparation is the cell membrane itself.

The relationship of striated ducts to blood capillaries is essentially the same as that of the acini (fig 13). No nerve endings have been seen in relation to striated duct cells.

It will be recalled that the epithelium of the striated ducts in salivary glands often appears pseudostratified rather than simple, i.e. one layer of cells in thickness (see fig 12). In fact it is generally true of glands deriving from surfaces lined with stratified squamous epithelium that the duct has either a pseudostratified or two-layered epithelium while the secretory elements have a single layer of glandular epithelium, the basal layer of cells having merged with or transformed into myoepithelial cells. These considerations suggest the question in what form is the myoepithelial cell represented (if indeed it is represented at all) in the striated ducts? Cer-

tainly there are no obvious myoepithelial cells here of the sort that invest sweat gland tubules. The basal nucleus in figure 12 appears too large to be a muscle cell nucleus. However, one very occasionally sees cells in the striated ducts which resemble the external shape of smooth muscle fibers to the extent that sections through the nucleus show very little cytoplasm surrounding it and longitudinal sections through the cytoplasm indicate a slender tapering shape (fig 19). The cytoplasm of these cells is denser than that of the regular epithelial cells, but it shows none of the frank characteristics of smooth muscle such as longitudinal striations or "pinocytotic" vesicles at the cell membrane. It seems possible that these cells represent a transitional form between epithelial cells and muscle cells, but the information available at present will permit only the most casual speculation on this point.

Brief note on parotid gland of rat

Histological examination of the rat's parotid gland shows it to be very similar in structural organization to that of the mouse. The secretion granules of a relatively small number of cells are stained intensely blue by phosphotungstic acid hematoxylin or black by acid hematein, but the granules in the great majority of cells show no affinity for these stains. Conversely, the secretion granules in all but a few of the cells are PAS positive while those of the remaining cells are not. Inter-calated ducts like those in the mouse parotid have two segments. The cells of the proximal segment contain secretion granules which are not stained by phosphotungstic acid hematoxylin or acid hematein but stain more brilliantly with PAS than the acinous cell granules. All PAS positive granules in acini and ducts resist digestion with malt diastase. Fine granular deposits of a PAS-positive substance are present in widely variable amount in the striated duct cells. These granules are removed by malt diastase digestion and are presumed to represent glycogen. None of the secretion antecedents in the gland stains metachromatically with toluidine blue.

The rat's parotid gland has been described in detail at the electron microscopic level by Scott and Pease ('59). Inasmuch

as the writer's observations are generally in accord with theirs only a few isolated points are noted here wherein the writer's interpretations amplify or vary with theirs (1) A strong impression was gained that secretion granules take origin in the Golgi apparatus of the acinous cell. This was demonstrated to the author's satisfaction in the gland of an animal whose tissues were taken for examination one hour after an injection of pilocarpine hydrochloride (2) Non granular secretion antecedents of the type illustrated in figure 4 are occasionally seen in acinous cells of the rat parotid as well as in the mouse (3) Myoepithelial cells were found to be present in relation to the acini and intercalated ducts of the parotid glands of Wistar rats (4) Scott and Pease find that endoplasmic reticulum and Golgi material are present only in minimal quantities in intercalated duct cells. The writer fully concurs with this description as it applies to the distal nonsecretory segment of the duct but finds these organelles to be relatively plentiful in the proximal secretory segment.

DISCUSSION

The acinus of the parotid gland is not properly described by any of the adjectives usually applied to salivary glands. Except for the presence of a few mucous acini in the parotids of some species the mammalian parotid glands are described as "serous glands" in the major reviews (Oppel '00; Zimmermann '27; Stormont '32). In routine histological sections and in some cytological preparations the mouse parotid displays all the characteristics associated with serous glands but since the term "serous" implies a secretion devoid of mucous elements (Stormont '32) it does not suitably describe a gland containing PAS positive secretion antecedents. The mouse parotid is not unusual in this respect; however, Junqueira and Hirsch ('56) report PAS positive secretion granules in the parotids of 18 species. Also since no enzyme has yet been demonstrated in the secretion of the mouse parotid to the author's knowledge the term "serozymogenic" seems to be inapplicable on two scores. The secretion granules of the mouse parotid do not stain metachromatically with toluidine blue after formalin bichromate

fixation and thus appear not to resemble many secretion granules that are frankly mucous or Bensley's "tropochrome granules" (Stormont '32).

The parotid acinus of the mouse is not a homogeneous secretory unit but contains three different types of secretion antecedent. The most numerous type which is stained by PAS and phosphotungstic acid hematoxylin exhibits a characteristic fixation artifact at the electron microscopic level in which a layer of dense material at the periphery of the granule surrounds a relatively empty central part that may contain an irregularly shaped mass of dense material. This artifact is manifested in light microscopic preparations by the ringlike appearance of many secretion granules and thus shows that the dense component of the fixed granule is responsible for its tinctorial affinities. A less frequently encountered granule is homogeneous and low in density in electron micrographs and is in all probability the secretion antecedent that is negative to the stains listed above. In electron microscopic structure and density this granule resembles the majority of granules in the rat parotid but differs from them histochemically in being PAS negative. The least frequently encountered secretion antecedent is not a granule but a quantum of cytoplasm. The details of the extrusion of these various secretion antecedents will be reported in a future publication.

Apart from the peculiarities of its secretion antecedents the parotid acinous cell presents no major differences from acinous cells in the well-described mouse pancreas (e.g. Sjostrand and Hanzon '51a,b) or the rat parotid (Scott and Pease '59). Therefore beyond reiterating that secretion granules become recognizable morphological entities in relation to the Golgi apparatus rather than in the endoplasmic reticulum (as is the case in the guinea pig pancreas; Palade '56) no further discussion will be devoted to these important organelles. A detailed morphological study of the endoplasmic reticulum and its relationship to nucleus and Golgi apparatus will be reported in a separate paper.

It is pointed out in the description above that the intercalated duct of the mouse parotid consists of two segments: the prox-

imal segment being composed of secretory cells and the distal part of undifferentiated cuboidal epithelial cells. It is interesting in this connection that Ellenberger (11) in a general description of parotid glands speaks of an "Alveolengang lined with glandular epithelium and having basket (myoepithelial) cells as well as the acini interposed between acini and intercalated ducts. This account is somewhat paralleled in Pischinger's (24) observation of secretion granules in intercalated ducts of the human submaxillary gland. The presence of secretory cells within intercalated ducts is evidently not a general or universal condition among salivary glands; however Stormont (32) cites several authors who found an abrupt change from secretory to non secretory cells at the junction of intercalated duct with acinus.

Electron micrographs show that striated duct cells of the mouse parotid contain granules and vesicles in their apical cytoplasm. These are interpreted to be secretion antecedents. It is possible that the granules are stained by phosphotungstic acid hematoxylin and acid hematein but one cannot always be sure with light microscopy whether these stains are staining mitochondria or secretion granules. It is the writer's impression that the secretion antecedents in these cells are PAS negative.

The unusual features of striated duct epithelium are its large content of radially arranged mitochondria and the peculiar shape of its cells: the basal cytoplasm of which is divided into numerous leaf-like or cylindrical processes. The latter condition of course increases greatly the area of basal cell membrane and mitochondria are so situated that any given area of basal cell membrane is closely related to a mitochondrion. Since mitochondria are the energy factories of the cell it seems likely that mitochondria furnish the energy for a large amount of transfer of materials (water and/or ions) across the cell membrane in a preferred direction. A similar significance for striated duct mitochondria was postulated by Heidenhain (11). As to the shape of striated duct cells Zirmmermann (32) demonstrated as much of their complicated morphology as could be seen with a light microscope by macerating glands and sepa-

rating individual cells. This study has merely shown that the various cell processes have numerous secondary appendages too small to be seen with light microscopy. It seems indeed that one of the functions of electron microscopy is to redirect attention to the discoveries of the ancients that have gradually been dropped from text book accounts.

It will perhaps be noticed that while this description of the bases of striated duct cells in mice has emphasized the presence of large processes of irregular shape and their intermingling with parts of other cells the account of Scott and Pease (59) in rats has emphasized an intercellular relationship characterized by a more or less regular serpentine configuration of the interlocked surfaces of two adjacent cells. It is the writer's impression that the latter type of intercellular relationship occurs in more distal parts of the striated ducts (including interlobular ducts) while the former type obtains in more proximal parts of the duct.

Myoepithelial cells are present around the acini and intercalated ducts of the mouse parotid but are not abundant. Furthermore the cytological characteristics that help to identify smooth muscle are often inconspicuous as in the case of myofilaments or even absent in parts of the cell as is the case with pinocytotic vesicles associated with the cell membrane. Scott and Pease (59) comment on this latter point in connection with the myoepithelial cells in rat submaxillary and sublingual glands. It seems probable that the apparent absence of myoid elements in their parotid gland material was due to the fact that their work was done before the advent of staining with lead hydroxide. In addition to being difficult to find with the electron microscope some other negative attributes of the myoid cells in the mouse and rat parotid are apparent from light microscope studies. It has been observed by the author that phosphotungstic acid hematoxylin stains myoepithelial cells proximally in certain cutaneous glands of the dog (Parks II unpublished study). In the cytological preparations of mouse and rat parotids stained with phosphotungstic acid hematoxylin however the smooth muscle cells of blood vessels

stained a deep blue color but myoepithelial cells were unstained. Also Silver (54) reports that myoepithelial cells in the sheep are demonstrated by an alkaline phosphatase reaction but published accounts of alkaline phosphatase tests on the parotid of mouse and rat do not mention a positive reaction in myoepithelial cells (Noback and Montagna 47 Hill and Bourne 54). Silver (54) also remarks that myoid cells in the cow's parotid do not give a positive reaction. From these divergent results it is apparent that differences exist among myoepithelial cells.

It will be recalled that an apparently undifferentiated non secretory non nervous non muscular cell type is described in the acini and intercalated ducts of the mouse parotid. Beyond reminding the reader that this cell apparently has a shape similar to that of myoepithelial cells and may therefore represent a transitional stage between epithelial cell and muscular cell further speculation would be idle.

The innervation of the mouse parotid seems to be essentially the same as that in the rat i.e. there are nerve endings on the acini but none on the ducts (cf. Scott and Pease 59). Nerve processes are in our experience most often seen between acinous cells in the mouse but structures that appear to be nerve endings filled with "synaptic vesicles" are frequently seen at the base of acinous cells in the rat. Scott and Pease found these latter structures so plentiful as to suggest a one to one ratio of fibers to cells. This apparent abundance of nerve fibers especially at the base of cells may possibly be explained in terms of the observations of histologists on salivary gland nerve fibers stained with methylene blue and the Golgi method (see Arnstein 1895 and Bocke 31). In some of their preparations a single nerve fiber running at the periphery of an acinus is related to more than one cell and some times to more than one acinus and may show numerous varicosities along its course. It is not improbable that each varicosity represents an aggregation of "synaptic" vesicles within the axis cylinder. If such were the case a relatively small number of nerve fibers could innervate a large number of acinous cells and sections taken through the tissue

would give the impression that a large number of nerve fibers were present in the tissue. That aggregations of synaptic vesicles can occur at sites other than nerve endings is obvious from figure 9. On the other hand if we are to believe all that the classical histologists show us we must believe that there is a profusion of nerve endings between striated duct cells (Arnstein 1895). In this study however a careful search was made for intra epithelial nerve endings and none was found. If indeed there are no nerve endings in direct contact with duct epithelium the possibility again presents itself that the aggregations of "synaptic vesicles" occurring in the course of nerve fibers (fig. 9) are sources for the release of acetyl choline or whatever the chemical stimulating substance for duct secretory activity may be. The electro physiological work of Lundberg (58) indicates that striated duct cells are capable of reacting to nervous stimuli.

The virus like bodies illustrated in figure 7 (and also present in figures 3 and 4) are clearly different from the salivary gland viruses of Luse and Smith (58) in point of both morphology and relationship to cells. However these viruses resemble the leukemia virus of DeHarven and Friend (59) in size (these are about 1100 Å in diameter theirs averaged 870 Å) in behavior (both form by "budding" from the plasma membrane of a cell) and in internal morphology (both sometimes show a third membrane between the inner and outer shell).

Comparison of mouse and rat parotid glands. Both glands are essentially similar in point of gross anatomical relations, vascular relations, distribution of nerves and myoepithelial cells, intercellular relationships of epithelial cells and the general organization of the various specialized cellular elements constituting a gland and its duct structure. A conspicuous qualitative difference between the two glands is found in the secretory granules of their acini and intercalated ducts. Phosphotungstic acid hematoxylin stains the great majority of secretion granules in the mouse parotid acinus, the majority of granules in the rat parotid are negative in this respect. On the other hand the great majority of granules in both glands are

PAS positive. The minority of granules in the rat gland that stain with phosphotungstic acid hematoxylin are also stained by acid hematein (and thus resemble pancreatic zymogen granules in terms of their behavior toward these two dyes). However the granules in the mouse parotid gland that stain with phosphotungstic acid hematoxylin are not stained with acid hematein (and thus fail to resemble pancreatic zymogen granules tinctorially). Apparently the only common feature of the acini in the two glands is that a large fraction of their secretion contains polysaccharide (mucoid) substances. The intercalated ducts of both species contain secretion granules that are PAS positive but only those in the mouse are stained by phosphotungstic acid hematoxylin and none in either species is stained by acid hematein.

SUMMARY

Cytological features and certain histological relationships in the mouse parotid gland are described in detail at light and electron microscopic levels. A brief note on the rat parotid is added to relate the author's electron microscopic observations on this organ with those of Scott and Pease (59) and to permit comparison of the glands in mouse and rat. The acini of these glands are not homogeneous secreting units but have three recognizably different secretion antecedents. The least numerous secretion antecedent is a small quantum of cytoplasm demarcated and partially separated from the ambient cytoplasm by a sheet like formation of small membranous vesicles so arranged as to enclose a sphere. The other two types are granules which are distinguishable in terms of staining affinities and submicroscopic structure. The intercalated ducts in both species have two segments: a proximal secretory part with granules similar in staining properties to those in their respective related acini and a distal nonsecretory part. Epithelial cells invest acini and intercalated ducts in both species. Striated duct cells are shown to have secretion antecedents in their apices and to have bases exceedingly complicated in shape. Parotid glands in mouse and rat are basically similar but differ in the struc-

tural and tinctorial characteristics of the secretion granules in acini and intercalated ducts.

LITERATURE CITED

- Arnstein C 1895 Zur Morphologie der sekretorischen Nervendapparate. *Anat Anz* 10: 410-419.
- Asp G 1873 Bidrag till spottkörtlarnes mikroskopiska anatomi. Akad Abhandl. Helsingfors 128S.
- Baker J R 1946 The histochemical recognition of lipine. *Quart J Micro Sci.* 87: 441-471.
- Boeke J 1931 Cytology and Cellular Pathology of the Nervous System vol 1 W Penfield ed. New York pp 241-309.
- Caulfield J 1957 Effects of varying the vehicle for OsO₄ in tissue fixation. *J Biophys Biochem Cytol* 3: 827-829.
- Chiewitz J H 1885 Beiträge zur Entwicklungsgeschichte der Speicheldrüsen. *Arch Anat Physiol* 9: 401-436.
- DeHarven E and C Friend 1959 Further electron microscope studies of a mouse leukemia induced by cell free filtrates. *J Biophys Biochem Cytol* 7: 747-751.
- Ellenberger W 1911 Handbuch der Vergleichenden mikroskopischen Anatomie der Haustiere vol III Berlin.
- Fawcett D W 1958 Frontiers in Cytology S Palay ed. New Haven.
- Fekete E 1941 Biology of the Laboratory Mouse. G D Snell ed. Philadelphia.
- Heidenhain M 1911 Plasma und Zelle. Part 2. Jena.
- Hill C R and G H Bourne 1954 The histochemistry and cytology of the salivary gland duct cells. *Acta Anat* 20: 116-128.
- Junqueira L C U and G C Hirsch 1956 Cell secretion: a study of pancreas and salivary glands. *Internat Rev Cytol* 5: 323-364.
- Lundberg A 1958 Electrophysiology of salivary glands. *Physiol Rev* 38: 21-39.
- Luse S A and M G Smith 1958 Electron microscopy of salivary gland viruses. *J Exp Med* 107: 623-632.
- Martin B F 1953 "Lipase" in gland duct epithelium and in mucus secreting cells. *Nature* 172: 1049-1049.
- Moore Dan H and H Ruka 1957 The fine structure of capillaries and small arteries. *J Biophys Biochem Cytol* 3: 457-462.
- Noback C and W Montagna 1947 Histochemical studies of the basophilia lipase and phosphatases in mammalian pancreas and salivary gland. *J Anat* 81: 343-367.
- Oppel Albert 1900 Lehrbuch der Vergleichenden Mikroskopie. *Anat. Anz* der Wurbeltiere Vol III Jena.
- Palade G C 1955 A small particulate component of the secretory apparatus. *J Biophys Biochem Cytol* 1: 5-6.
- 1956 Intracellular granules in the exocrine cells of the pancreas. *Proc Natl Acad Sci* 42: 417-421.
- 1960 The fine structure of the cross section of the endothelial cells of the pancreas. *Anat Rec* 136: 254.

- Palade G E and A R Porter 1951 Studies on the endoplasmic reticulum I The identification in cells *in situ* J Exp Med 100 641-656
- Palay S and L Karlin 1959 An electron microscopic study of the intestinal villus J Biophys Biochem Cytol 5 363-381
- Palay S L and G Palade 1955 The fine structure of neurons Ibid 1 69-88
- Pischinger A 1924 Beiträge zur Kenntnis der Speicheldrüsen besondere der Glandula sublingualis und submaxillaris des Menschen Z Mikr Anat Forschung 1 437-489
- Porter K R and C Bruni 1960 Fine structural changes in rat liver cells associated with glycogenesis and glycogenolysis Anat Rec 136 260-261
- Schultze O 1911 Über die Genese der Granula in den Drüsenzellen Anat Anz 38 257-260
- Scott B L and D C Pease 1959 Electron microscopy of the salivary and lacrimal glands of the rat Am J Anat 104 115-140
- Shklar G I Glickman and S Turcay 1958 A histochemical study of the salivary glands in normal and cortisone injected white mice J Dent Res 37 119-121
- Silver I A 1954 Myoepithelial cells in the mammary and parotid glands J Physiol Lond 125 BPDP (Proceedings of Physiological Society)
- Sjöstrand F S and V Hanzon 1951a Membrane structures of cytoplasm and mitochondria in exocrine cells of mouse pancreas as revealed by high resolution electron microscopy Exp Cell Res 7 393-414
- 1951b Ultrastructure of Golgi apparatus of exocrine cells of mouse pancreas Ibid 7 415-429
- Stormont D L 1932 The salivary glands In Special Cytology vol I E V Cowdry ed New York pp 153-190
- Watson M L 1955 The nuclear envelope Its structure and relation to cytoplasmic membranes J Biophys Biochem Cytol 1 257-270
- 1957 Reduction of heating artifacts in thin sections examined in the electron microscope Ibid 3 1017-1022
- 1958 Staining of tissue sections for electron microscopy with heavy metals II Application of solutions containing lead and barium Ibid 4 727-730
- Zimmermann A W 1927 Die Speicheldrüsen der Mundhöhle und die Bauchspeicheldrüse In Handbuch der Mikroskopischen Anatomie des Menschen vol 5 part 1 W von Möllendorff ed Berlin pp 61-211

PLATE 1

EXPLANATION OF FIGURES

Note All illustrations are electron micrographs of sections of mouse parotid gland stained with lead hydroxide

- 1 Tangential section of acinus showing a tenuous segment of myoepithelial cell passing vertically through the micrograph. "Inocytotic vesicles" and longitudinal striations are not as plentiful or conspicuous as in the smooth muscle fibers of blood vessel walls. Portions of acinous cell are seen on each side of the myoid cell segment $\times 28,000$
- 2 The secretion granule in the center of the micrograph exemplifies the most numerous type in acini of the mouse parotid. It is inhomogeneous being characterized by a peripheral layer of dense substance surrounding a less dense center which occasionally contains a mass of dense material similar to that at the periphery. The granule is enclosed by a membrane not visibly different from the plasma membrane of the cell $\times 21,000$
- 3 This micrograph shows a less frequently encountered type of secretion granule of the parotid acinus. The granules which are homogeneous and low in density are less stable than those shown in figure 2 despite their enclosing membrane and tend to coalesce during fixation to form larger structures. In the upper left corner an intercellular secretory canal is seen. It contains a few virus like bodies (cf fig 7) $\times 12,000$
- 4 In the center of the micrograph is the least numerous type of secretion antecedent of the parotid acinus. It is a small spheroidal mass of cytoplasm which is demarcated from the surrounding cytoplasm by a group of tiny membranous vesicles. These structures are ultimately extruded into the lumen as cytoplasmic blebs. The mantle of cytoplasm immediately surrounding the secretion antecedent is free of endoplasmic reticulum and other cytoplasmic inclusions. Below and to the right of the secretion antecedent is an intercellular secretory canal that shows some microvilli cut in cross section and some virus like bodies $\times 22,000$

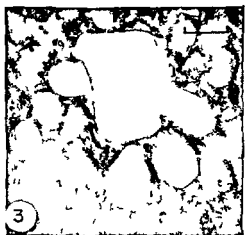


PLATE 2

EXPLANATION OF FIGURES

- 5 Oblique section through a segment of myoepithelial cell at the periphery of an acinus. In this example longitudinal striations and pinocytotic vesicles are more noticeable than in figure 1. Above and below the myoid cell are parts of an acinous cell (or acinous cells). The basal membrane of the upper portion of acinous cell exhibits infoldings (arrows) one of which appears to be pinching off small vesicles into the cytoplasm (dotted arrow). The bracketed portion of a cell at the right cannot be identified in the section. It might be a process from a nerve cell or another myoepithelial cell. $\times 28,000$.
- 6 Tangential section of an acinus passing through the bases of several cells. This micrograph illustrates the interrelationship of the lateral surfaces of the basal parts of acinous cells which is characterized by a rather intricate interdigitation and interfoliation of short cytoplasmic processes and by a paucity of desmosomes (one desmosome is seen in the lower right corner). The nucleus in the upper left corner contains a nucleolus which appears to consist of a dense aggregation of granules somewhat smaller than those dispersed throughout the nucleoplasm. Immediately beneath this nucleus is a "degenerative" body containing a membranous formation. Five small Golgi bodies are present in the field. $\times 7500$.

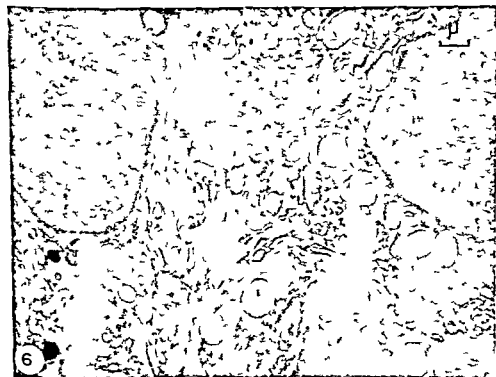
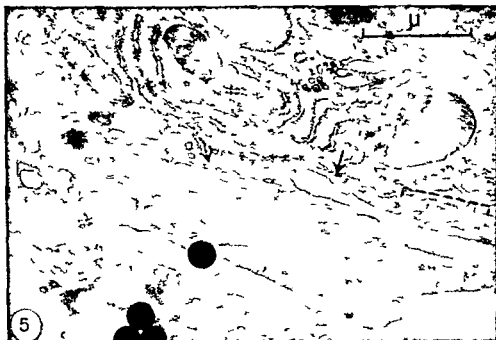


PLATE 3

EXPLANATION OF FIGURES

- 7 Section of an acinus passing through the main lumen (above) and lumen of intercellular canal (below) Both lumina contain virus like particles which are double shelled bodies that appear to form by budding from the surface of acinous cells Two desmosomes are seen on the apposed cell membranes passing between the two lumina The typical inhomogeneous appearance of the secretion granule in the upper right probably represents a fixation artifact resulting from imbibition of water by homogeneous granules of the kind seen in the lower part of the field $\times 28\ 000$
- 8 Longitudinal section through an intracellular secretory canal showing numerous microvilli in lumen An increase in the density of the cytoplasm immediately bordering these canals is often seen at sites where parts of two adjacent cells are apposed The greater density is due to the presence of a fine fibrillar substance which is probably related to desmosomes in the vicinity $\times 18\ 000$

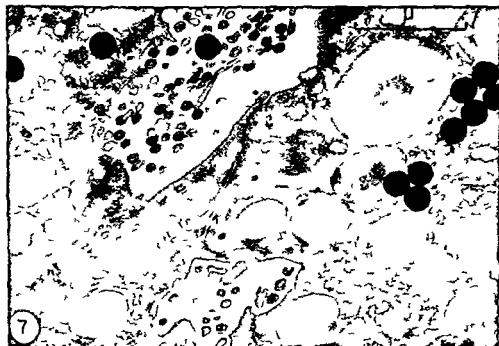


PLATE 4

EXPLANATION OF FIGURES

- 9 Section through the base of an acinous cell a capillary and some unmyelinated nerve fibers. The cisternae of the endoplasmic reticulum show a more or less parallel arrangement in the base of the acinous cell. The endothelial cell cytoplasm contains a large number of membranous vesicles and exhibits flask like invaginations of the plasma membrane at basal and luminal surfaces. It cannot be determined whether the layer of cytoplasm applied to the upper side of the capillary represents an overlapping part of an endothelial cell or a part of a connective tissue cell. Many of the nerve fibers contain "synaptic" vesicles. A condensation of connective tissue ground substance called the "basement membrane" is seen on the surfaces of acinous cell endothelial cells and the outer surface of the nerve fiber—Schwann cell complex. $\times 20\,000$
- 10 Golgi apparatus of an acinous cell. The Golgi material consists of elongate flattened membranous lamellae and small spherical vesicles. Secretion granules appear to arise by swelling of the lamellae. In the lower left corner a nucleus is seen. In the upper right is a "degenerative" body containing a myelinic formation. $\times 30\,000$

FINE STRUCTURE OF PAROTID GLAND
Harold F. Paas

PLATE 5

EXPLANATION OF FIGURES

- 11 Junction of acinus with intercalated duct. The intercalated duct (two cells at lower left) has light and dark secretion granules all homogeneous. Three intercellular canals are seen in the acinus (arrows). Two membranous bodies are seen in the duct lumen at the left; these are probably remnants of cytoplasmic blebs extruded by the acinous cells (cf fig 4) $\times 9000$
- 12 Low power view of intercalated duct showing light and dark secretion granules and copious amounts of endoplasmic reticulum. The cell at the lower left was identified as a myoepithelial cell in a higher powered micrograph of this field $\times 4500$
- 13 Low power view of a striated duct showing acinous elements at the periphery of the micrograph and a capillary at the top. The rectangles indicate the fields shown in figures 14 and 15 $\times 1700$



PLATE 6

EXPLANATION OF FIGURES

- 14 Apical portion of striated duct cell (higher magnification of field indicated in figure 13) The duct lumen is on the right side of the micrograph. Granular and vesicular secretion antecedents are present in the apical cytoplasm. The section passes through two centrosomes (arrows). The base of this cell is seen in figure 15. $\times 16,000$
- 15 Basal portion of striated duct cell (higher magnification of field indicated in figure 13) The basement membrane is seen at the left side of the micrograph. The infoldings of the basal cell membrane do not fold back directly on themselves but arch over a piece of cytoplasm belonging to another cell. In this picture the cell containing the nucleus at the right sends 5 cytoplasmic processes down to the basement membrane; the spaces between these processes are occupied by cytoplasmic processes from neighboring duct cells. The tenuous basal cytoplasmic processes of these cells are largely filled with mitochondria. The smallest black granules in the cytoplasm are ribonucleoprotein particles; the larger granules are believed to represent glycogen. $\times 16,000$

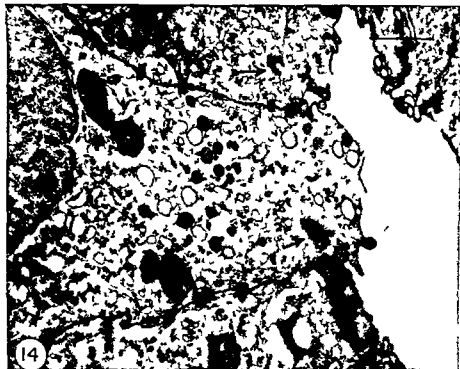
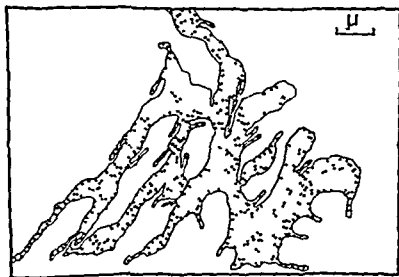


PLATE 7

EXPLANATION OF FIGURES

- 16 Tangential section of striated duct passing somewhat obliquely through striated duct cell near the level of the nucleus. The overlay traces the outline of the cell containing the nucleus. At supra nuclear levels a cross section of a cell appears hexagonal in outline. In the level shown the near-cross sectional outline of the cell is more complicated being characterized by numerous tenuous lateral cytoplasmic extensions. $\times 0000$
- 17 Tangential section of striated duct passing somewhat obliquely through basal cytoplasm of duct cells. The plane of this section is approximately perpendicular to that shown in figure 15. At this level the profuse intermingling of cytoplasmic processes produces a complicated picture. The profile of a single mass of protoplasm is traced on the overlay. $\times 9000$



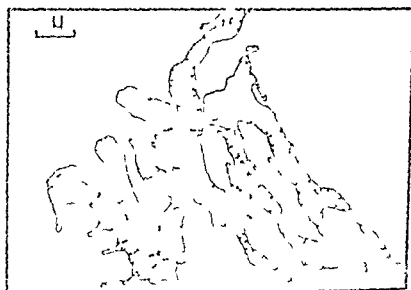
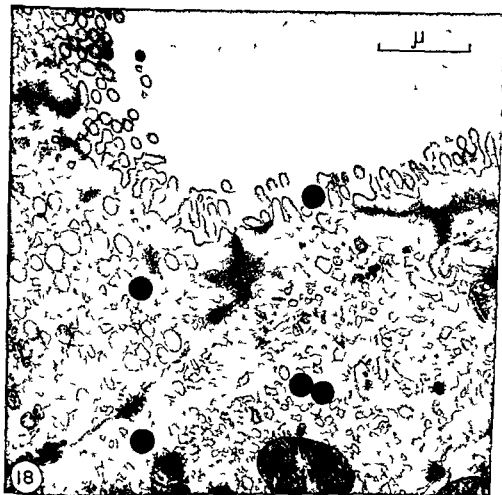




PLATE 8

EXPLANATION OF FIGURES

- 18 Apical portions of striated duct cells showing the microvilli on the luminal surface that are usually but not always present (cf fig 14) The cell on the left contains numerous secretion antecedents of various densities / 24 000
- 19 Section showing basal region of striated duct epithelium Two cells (A B) are present from which it can be inferred that the cell population in the walls of striated ducts is not a homogeneous aggregate of epithelial cells The cytoplasm of these cells is denser than that of ordinary striated duct cells Their profiles in section suggest a spindle like shape which in turn suggests that they may represent a transitional form between epithelial cell and myoepithelial cell / 9000



The Fine Structure of Capillaries in the Cerebral Cortex of the Rat at Various Stages of Development'

SHEILA DONAHUE AND GEORGE D. PAPPAS

Department of Pathology (Division of Neuropathology) and Department of Anatomy College of Physicians and Surgeons Columbia University and the Neurological Institute of the Presbyterian Hospital New York New York

The structure and the function of capillaries in the central nervous system have been of special interest since the existence of a selective barrier was described by Ehrlich (1885). An extensive literature exists on the differences between immature and mature animals in permeability of the central nervous system to substances entering it from the blood stream. After parenteral injection of certain aniline dyes into adult animals all the tissues of the body are stained except the major portion of the central nervous system. The meninges, the choroid plexus, the area postrema, the region of the tuber cinereum, the neurohypophysis and the pineal gland are stained. Trypan blue injected into young rats (two to 8 days postpartum) stains the same areas of the brain as it would in the adult but appears to penetrate to a greater distance beyond these areas (Mullen and Hess, '58). Similar observations have been made in the newborn mouse (Behnser, '27). The lack of staining of the central nervous system following injection of trypan blue into rat embryos ranging in age from 10½ days of gestation until birth suggests the presence of a barrier between the blood and the brain at this early stage of development (Grazer and Clemente, '57). Sodium fluorescein injected intravenously into adult animals does not enter the central nervous system. Stern and Peyrot ('27) showed, however, that it does enter the central nervous system of very young animals of many different species. They concluded that a barrier between the blood and the brain is not present until a certain stage of development is reached. This point in maturation varies with the species ex-

amined. Bakay ('56) has shown in rabbits that the embryonic and early postnatal brain concentrates more radioactive phosphate than the adult brain but the uptake is low when expressed in absolute values and when compared with other tissues. The concentration decreases steadily with increase in age and at about 7 weeks after birth it is the same as in the adult. He suggests that the different rate of uptake of phosphate is due to increased metabolic activity of the developing nervous system and to a greater permeability of the blood brain barrier in embryos and young animals.

Thus there is evidence that a selective barrier exists from an early age. This barrier increases in efficiency with age until the properties of the adult blood brain barrier become evident. It is probable that this selection takes place in or about the capillaries in the central nervous system. Examination of the cerebral cortex of late fetal, immature and adult rats with the electron microscope was undertaken to study the fine structure of the capillaries and their surroundings to determine whether there are also morphological changes with increasing age.

MATERIAL AND METHODS

Rats from our stock colony (Sherman strain) arbitrarily bred as a closed colony for at least 15 generations were used. They were sacrificed on the 20th day of

This work was supported in part by training grant 2B 5062 (C551) and research grant B 1620 from the National Institute of Neurological Diseases and Blindness, U.S.P.H.S. and by grants from the Association for the Aid of Crippled Children and the Life Insurance Medical Research Fund.

gestation on the day of birth and on each day thereafter up to the 15th postnatal day. Delivery was usually on the 22nd day. The skulls were opened rapidly and samples of dorsal parasagittal cerebral cortex were placed in cold 1% buffered osmic acid (Palade 52). The tissue was then cut into blocks of approximately 1 mm and fixed for a further 30 minutes in cold 1% buffered osmic acid pH 8.1 or 8.2. The tissues were dehydrated through an ethanol series and embedded in a mixture of 9 parts of butyl methacrylate to one part of methyl methacrylate with 2% Luperco added. Under nembutal anesthesia (4.3 mg per 100 gm body weight) similar samples were taken from adult rats approximately 5 months old and weighing about 250 gm. Sections were made with glass knives on Porter-Blum and LKB microtomes. Lead stains were made on all sections following the methods of Watson (58) and Dalton and Zeigel (60). They were studied with an RCA EMU 3C electron microscope.

OBSERVATIONS

This study was confined to the structure of the capillaries and their surroundings in the cerebral cortex of the adult and immature rat. Material from all ages i.e. 20 day fetus to 15 days after birth and adults 5 months old (approx. 250 gm) were examined but only selected ages are here described and illustrated to demonstrate the changes observed.

In the 20-day-old fetal rat (figs 1 and 2) the endothelial cell has abundant cytoplasm. The endoplasmic reticulum is widespread and consists of dilated canaliculi and vesicles. The ribonucleoprotein (RNP) granules (particles of Palade) (Palade 55) are usually unattached to these membranes and appear as particles scattered throughout the cytoplasm. The apposing endothelial cell membranes are thickened forming well defined tortuous terminal bars. The endothelial cells are separated from the cells and cell processes of the nervous system by a narrow region filled with an amorphous substance of variable electron density that forms the immature basement membrane. This region is delimited by the cell membranes of the endothelial cells and those of neural and glial cells. It has no marginal mem-

branes of its own. The basement membrane is usually slightly wider than the distance between other cells in the central nervous system. The intercellular distance is approximately of the same size in these animals as in the mature rats. Pericytes (pericapillary cells) are present although they are sometimes difficult to outline. The term pericytes in this study applies to cells embedded in the basement membrane but not forming part of the wall of the lumen.

In the newborn (fig 3) and the three-day old (fig 4) rat the changes in these structures are only in degree. The endothelial cell cytoplasm is abundant and contains numerous vesicles and many RNP granules. The basement membrane is generally broader and denser than in the fetal cortex. However it is often no wider than the adjacent intercellular distance and variation in density is evident. The bodies of cells in the neural tissues rather than their processes are more frequently in contiguity with the basement membrane in the immature rat.

In the 8 day old animal (fig 5) the endothelial cell cytoplasm is still thick. Microvilli which are present at all ages in this series of animals and are often associated with the terminal bars are prominent in this micrograph. Vesicles are numerous and the packed smooth surfaced membranes and vesicles of the Golgi complex can be distinguished from the rough surfaced endoplasmic reticulum. Dilated canaliculi and vesicles are not as numerous as in the fetal endothelial cells. The basement membrane is generally wider and denser as a result of this change the pericytes are more conspicuously outlined. Their cytoplasm remains similar in structure to the cytoplasm of the endothelial cells.

By 12 days of age (fig 6) the endothelial cell cytoplasm is less thick and contains fewer dilated vesicles. The basement membrane is usually denser and thicker than in younger animals. The capillaries are surrounded predominantly by cell processes but cell bodies are also in apposition to the basement membrane.

In the 14-day-old rat (fig 7) the basement membrane is usually well-defined and of intermediate density. The thick

ness of the endothelial cell and the thickness and density of the basement membrane are variable. There are places at which the basement membrane even at this age is as narrow as the distances between the cells of the neural tissue.

In the adult rat (fig. 8) the cytoplasm of the endothelial cell is thinner and contains fewer vesicles than in the immature animal. The terminal bars are less conspicuous. The basement membrane is now much thicker and denser than in the younger animal. It is also relatively uniform in its width and density around any given capillary although it varies in these respects from vessel to vessel.

DISCUSSION

Alterations in the structure of the cerebral cortical capillaries have been observed in rats ranging in age from the 20th fetal day to the 15th postnatal day and comparisons have been made with adults approximately 5 months of age. There is a generally progressive decrease in complexity and thickness of the endothelial cells with increasing age until the more uniform and thinner adult cell is seen. Microvilli are more numerous in the younger animals where they are often closely associated with the terminal bars. With the reduction in thickness of the cytoplasm in the adult animal the terminal bars are shorter and their structure simpler than the terminal bars of the endothelial cells in immature rats. Pericytes are present in the capillary walls of all of the age groups examined. Their cytoplasm alters gradually and always resembles endothelial cell cytoplasm. The basement membrane already present before birth gradually and irregularly increases in thickness and density with age until the adult stage is reached. In the younger animals it is sometimes as narrow as other intercellular distances in the nervous system. In the adult rat the thickness and density of the basement membrane which completely surrounds the capillary (Maynard Schultz and Pease 57) is more or less uniform in any single vessel. Variations in its width and density do not seem to be related to the caliber of the capillary. In the basement membrane of the immature rat cortex the thickness and density around any given capillary are variable.

The absence of pores in the endothelial cells of the central nervous system of the adult animal has been described (Maynard Schultz and Pease 57, Bennett Luft and Hampton 59). We have found no evidence of the presence of pores in the endothelial cells of the immature nervous system. Indeed the thin endothelial cell of the adult nervous system suggests a more favorable condition for the presence of pores but none was seen in our material.

The fine structure of elements surrounding the capillaries of the brain of the adult rat has been studied by Dempsey and Wislocki (55). These workers studying rats fed silver nitrate in their drinking water found that silver was deposited in the connective tissue around the basement membrane of the capillaries of the body and in known permeable sites in the central nervous system but not around the capillaries in other areas of the central nervous system. They demonstrated that there was no connective tissue around capillaries where silver was not deposited. Instead the cells and cell processes of the nervous system were separated from the endothelial cells of the capillaries by a narrow area filled with an amorphous substance of moderate density, the basement membrane. The close investment of the basement membrane by cell processes in the adult rat was also described by these authors. Our observations of the cerebral cortex in the immature rat are similar. A basement membrane is present in animals of all ages examined although it is often thin. There are no connective tissue cells or collagen fibers around these capillaries. Spaces and areas where a cell membrane is not in close proximity to the basement membrane are probably artifacts. Adequate preservation of structure is difficult to obtain in the central nervous system particularly in immature animals. When satisfactory preparations are obtained in the young animal the relation of cells and cell processes to the basement membrane appears to be the same as in the adult. Glial processes are not the only structures surrounding the capillaries. In the adult rat Luse (56) found that other neural elements such as nerve cell bodies, dendrites, myelinated axons and the cytoplasm of

glial cell bodies were also in close relation to the basement membrane. The glial cell processes however are the predominant structures that envelop the capillary. In immature rats these various structures are difficult to identify and as yet we can only state that cell bodies appear to be more often in close proximity to the basement membrane than are the cell processes at this age.

This description of the alterations related to age which are found in the structure of the capillaries in the cerebral cortex of the rat offers little toward an explanation of the changing permeability noted in these blood vessels. However some of the findings may be of interest in this connection. The possibility exists that the selection and the rejection of various substances are properties of the cells that surround the capillaries. In the adult there is a close approximation of cell processes and cells to the basement membrane. In the immature rat there is a similar close approximation. The basement membrane progresses from a small band of material of variable density unevenly distributed around the capillary to a larger band containing material of medium density which is more or less evenly distributed around any given capillary. It remains to be demonstrated whether or not these gradual alterations are in any way related to the decreased ability of various agents to enter the neural tissue from the circulation in the mature animal.

SUMMARY

A study has been made with the electron microscope of the capillaries in the cerebral cortex of immature and mature rats. Gradual changes with increase in age towards maturity are observed. The basement membrane progresses from a thin band of variable thickness and density to a thicker structure of more or less uniform width and density about any given capillary. The endothelial cells in the immature animal are relatively thick. These cells become attenuated in the adult. The

elements of the neural tissue that surround the capillaries are in the same intimate relationship with the basement membrane in the immature rat cerebral cortex as they are in the adult. Further studies may show whether the decreased ability of various substances to enter neural tissue from the blood stream in the mature animal is related to the changes described in the structure of the capillaries.

LITERATURE CITED

- Bakay L. 1956. *The Blood Brain Barrier*. Charles C. Thomas, Springfield, Illinois.
- Behnken G. 1927. Über die Farbstoffspeicherung im Zentralnervensystem der weissen Maus in verschiedenen Alterszuständen. *Z. Zellforsch. Mikr. Anat.* 4: 515-572.
- Bennett H. S., J. H. Luft and J. C. Hampton. 1959. Morphological classification of vertebrate blood capillaries. *Am. J. Physiol.* 196: 381-390.
- Dalton A. J. and R. F. Zeigel. 1960. A simplified method of staining thin sections of biological material with lead hydroxide for electron microscopy. *J. Biophys. Biochem. Cytol.* 7: 409-410.
- Dempsey E. W. and G. B. Wislocki. 1955. An electron microscopic study of the blood brain barrier in the rat employing silver nitrate as a vital stain. *Ibid.* 1: 245-256.
- Ehrlich P. 1885. *Das Sauerstoffbedürfnis des Organismus*. Ein Farbenanalytische Studie. A. Hirshwald, Berlin.
- Grazer F. M. and C. D. Clemente. 1957. Developing blood brain barrier to trypan blue. *Proc. Soc. Exp. Biol. Med.* 94: 758-760.
- Luse S. A. 1956. Electron microscopic observations on the central nervous system. *J. Biophys. Biochem. Cytol.* 2: 531-542.
- Maynard E. A., R. L. Schultz and D. C. Pesse. 1957. Electron microscopy of the vascular bed of the rat cerebral cortex. *Am. J. Anat.* 100: 409-433.
- Millen E. W. and A. Hess. 1958. The blood brain barrier: an experimental study with vital dyes. *Brain* 81, part II: 248-257.
- Palade G. E. 1952. A study of fixation for electron microscopy. *J. Exp. Med.* 9: 283-298.
- . 1955. A small particulate component of the cytoplasm. *J. Biophys. Biochem. Cytol.* 1: 59-68.
- Stern L. and R. Peyrot. 1927. Le fonctionnement de la Barrière Hémato-encéphalique aux divers stades de développement chez les diverses espèces animales. *C. R. Soc. Biol. Paris* 96: 1124-1126.
- Watson M. L. 1958. Staining of tissue sections for electron microscopy with heavy metals. *J. Biophys. Biochem. Cytol.* 4: 727-729.

PLATES

PLATE 2

EXPLANATION OF FIGURES

- 2 Electron micrograph of a capillary in the cerebral cortex of a 20-day-old rat fetus. The lumen contains a red blood cell (R). The endothelial cell (E) is not as thick as in figure 1 which shows a rat fetus of the same age or as the endothelial cell in figure 3 which shows material from a newborn rat. The cytoplasm of the endothelial cell contains many dilated vesicles. A terminal bar (T) is seen at the junction of two endothelial cells. The basement membrane (arrows) is not as thick or as dense as in figure 3 which shows material from a newborn rat. $\times 28,880$
- 3 Electron micrograph of part of a capillary in the cerebral cortex of a newborn rat. The lumen (L) is at the top of the picture. Two terminal bars (T) can be seen at the junctions of the endothelial cells. The cytoplasm of the endothelial cells is thick and contains mitochondria (M) and vesicles (V). The basement membrane (arrows) is of moderate thickness and intermediate density. The close relationship of the cells and the cell processes of neural tissue to the basement membrane can be seen. A small portion of the nucleus (N) of such a cell is at the side of the micrograph. A cell process (CP) partially separates this cell from the basement membrane. $\times 28,880$

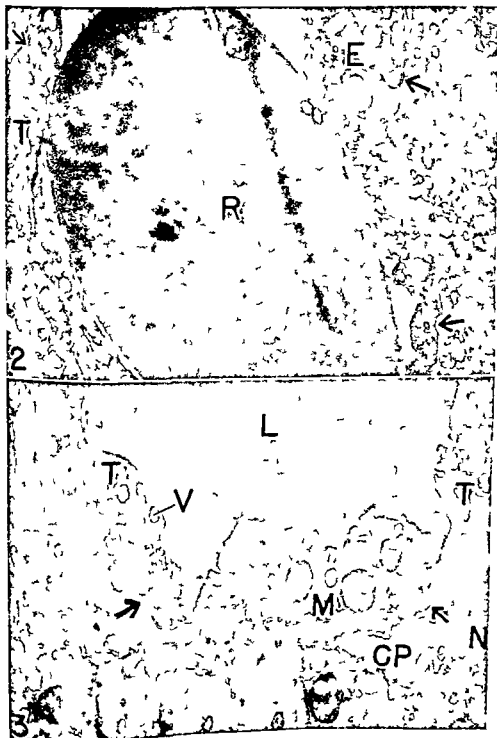


PLATE 3

EXPLANATION OF FIGURE

- 4 A longitudinal section of a capillary in the cerebral cortex of a 3-day-old rat. A terminal bar (T) is present at the junction of two endothelial cells (E). The endothelial cells are not as thick as is usual at this age (Compare figure 3 from a newborn rat and figure 5 from an 8-day-old rat where the cytoplasm is much thicker). The reduction in thickness is gradual, irregular and variable. Mitochondria (M) and dilated vesicles are seen in the endothelial cell cytoplasm. The basement membrane (arrows) varies in thickness and encloses a process of a pericyte (P). L lumen. $\times 28,880$



PLATE 4

EXPLANATION OF FIGURE

- 5 Electron micrograph of a cerebral cortical capillary of an 8 day-old rat. The lumen contains segments of red blood cells (R). Portions of three endothelial cells make up the lining of the lumen. The apposing cell membranes form terminal bars (T). The cytoplasm is plentiful and cell organelles are numerous. The Golgi complex (G) is present near the nucleus (N) of one of the endothelial cells. A process of a pericyte (P) embedded in basement membrane can be identified at the left side of the capillary. The cytoplasm of the pericyte resembles the cytoplasm of the endothelial cells. The basement membrane (arrows) is of variable thickness. The close relationship of the limiting membranes of the processes of cells in the surrounding tissue to the basement membrane can be observed. $\times 28,890$



PLATE 5

EXPLANATION OF FIGURE

- G Tangential section of a capillary in the cerebral cortex of a 12-day-old rat. The nucleus (N) of an endothelial cell is seen at the upper left of the micrograph. The basement membrane (see arrows) intervenes between the endothelial cells and the processes of the cells of the central nervous system. A process of a pericyte (P) can be identified. L lumen / 28 880

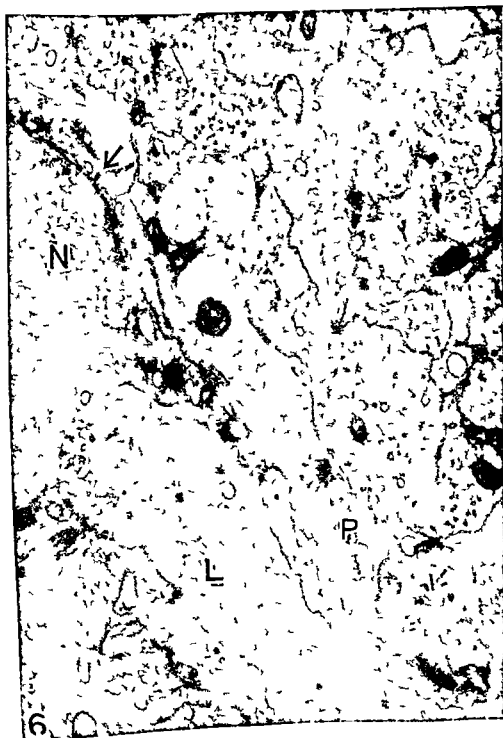
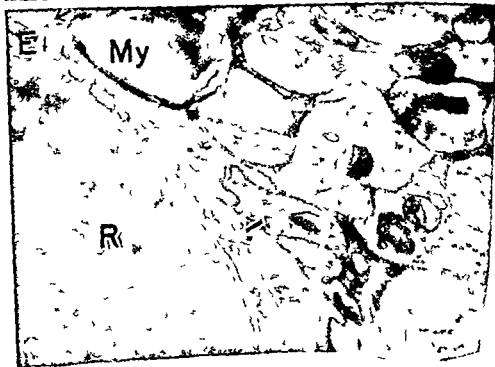
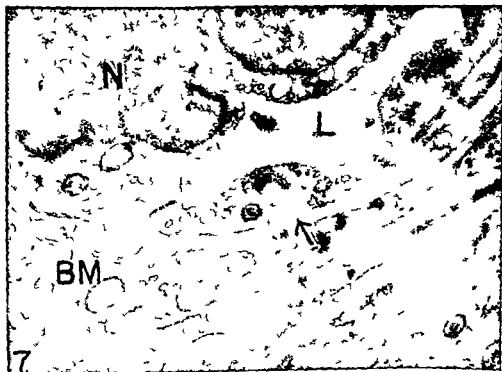


PLATE 6

EXPLANATION OF FIGURES

- 7 Electron micrograph of a capillary in the cerebral cortex of a 14 day-old rat. There is a moderate amount of endothelial cytoplasm although there is less than is found in some of the younger animals (cf figure 3 newborn rat). The increase in thickness of the basement membrane (BM) is gradual and irregular varying with increase in age. In one area at arrow the basement membrane is narrow its thickness is comparable with the distance between cell processes of the neural tissue i.e. approximately 200 Å. L. lumen $\times 28,880$
- 8 Electron micrograph of part of a capillary in the cerebral cortex of an adult (2.0 gm) rat. The lumen is filled by a red blood cell (R). The endothelial cell cytoplasm (E) is generally thinner and the basement membrane (arrow) thicker than in the younger animals. An exploded myelin sheath (MY) is shown close to the basement membrane. Cell processes occupy the right part of the picture their intimate relation to the basement membrane is evident. $\times 28,880$



Index

A

- acellular teleost fish bone osteogenesis of 99
 acid phosphatase nonspecific esterases and β -D-galactosidase in parotid and submaxillary glands of domestic and laboratory animals localization of 263
 adrenal transplantation studies on I Homologous and autogenous transplants 167
 anal glands of *Dasypus novemcinctus* the composition of the 295
 anatomy in various mammals a study of the subgross pulmonary 149
 anatomy of the sex cords and seminiferous tubules in growing and adult male albino rats microscopic 79
 ANDERSEN HELGE AND FREDE BRO-RAS 105
 sev Histochemical studie on the histogenesis of the joints in human fetuses with special reference to the development of the joint cavities in the hand and foot 111
 arterial variations in the limbs with special reference to symmetry of vascular patterns a study of the 245
 artery and its related vessels in the rat the development of the anterior cerebral 17
 Autogenous transplants I Homologous and Studies on adrenal transplantation 167

B

- BATTIG CHARLES G AND FRANK N LOW
 The ultrastructure of human cardiac muscle and its associated tissue space 199
 β -D-galactosidase in parotid and submaxillary glands of domestic and laboratory animals localization of acid phosphatase nonspecific esterases and 263
 BODEY GERALD P OLGA MIODUSZEWSKA AND GEORGE O GEY Studies on adrenal transplantation I Homologous and autogenous transplants 167
 bone osteogenesis of acellular teleost fish 99
 BRO-RASMUSSEN FREDE See Andersen Helge 111

C

- CANADA ROBERT O See McLaughlin Richard F 143
 Capillaries in the cerebral cortex of the rat at various stages of development the fine structure of 331
 Capsule in the rabbit the postnatal growth of the ear 1
 Cardiac muscle and its associated tissue space the ultrastructure of human 199
 CAVAZOS L F See Feagans W M 31
 Cerebral artery and its related vessels in the rat histology of the anterior 17
 Cerebral cortex of the rat at various stages of development the fine structure of capillaries in the 331

- CHANCEY HOWARD H AND GIULIANO
 QUINTARELLI Localization of acid phosphatase nonspecific esterases and β -D-galactosidase in parotid and submaxillary glands of domestic and laboratory animals 263
 CLERMONT Y AND CLAIRE HUCKINS Microscopic anatomy of the sex cords and seminiferous tubules in growing and adult male albino rats 79
 CLERMONT Y See Perey B 47
 COHEN ADOLPH I Electron microscopic observations of the internal limiting membrane and optic fiber layer of the retina of the Rhesus monkey (*M. mulatta*) 179
 Colchicine for the measurement of mitotic rate in the intestinal epithelium use of Cords and seminiferous tubules in growing and adult male albino rats microscopic anatomy of the sex 79
 Cortex of the rat at various stages of development the fine structure of capillaries in the cerebral 331

D

- Dasypus novemcinctus* the composition of the anal glands of 295
 Development of the anterior cerebral artery and its related vessels in the rat the 17
 Development of the joint cavities in the hand and foot histochemical studies on the histogenesis of the joints in human fetuses with special reference to the 111
D. podomys the ear apparatus of the kangaroo rat 111
 DONAHUE SHEILA AND GEORGE D PAPPAN 123
 The fine structure of capillaries in the cerebral cortex of the rat at various stages of development 331

E

- Ear apparatus of the kangaroo rat *Dipodomys* the 123
 Ear capsule in the rabbit the postnatal growth of the 1
 Electron microscopic observations of the internal limiting membrane and optic fiber layer of the retina of the Rhesus monkey (*M. mulatta*) 179
 ENDERS ALLEN C See Haynes Julian F 295
 Epithelium in the rat the wave of the seminiferous 4
 Epithelium use of colchicine for the measurement of mitotic rate in the intestinal 31
 Esterase and β -D-galactosidase in parotid and submaxillary glands of domestic and laboratory animals localization of acid phosphatase nonspecific 331

Estrogen induced lesions in the hamster male reproductive tract a morphological and histochemical study of
 EWALD A T See Feagans W M

F

FEAGANS W M L F CAVAZOS AND A T EWALD A morphological and histochemical study of estrogen induced lesions in the hamster male reproductive tract
 Fetuses with special reference to the development of the joint cavities in the hand and foot histochemical studies on the histogenesis of the joints in human
 Fiber layer of the retina of the Rhesus monkey (*M. mulatta*) electron microscopic observations of the internal limiting membrane and optic
 Fish bone osteogenesis of acellular teleost
 Foot histochemical studies on the histogenesis of the joints in human fetuses with special reference to the development of the joint cavities in the hand and

G

GEY GEORGE O See Bodley Gerald P
 Gland of mouse and rat on the fine structure of the parotid
 Glands of *Dasyproctus notomys* the composition of the anal
 Glands of domestic and laboratory animals localization of acid phosphatase non specific esterases and β D galactosidase in parotid and submaxillary
 Growth of the ear capsule in the rabbit the postnatal

H

Hamster male reproductive tract a morphological and histochemical study of estrogen induced lesions in the
 Hand and foot histochemical studies on the histogenesis of the joints in human fetuses with special reference to the development of the joint cavity in the
 HAYNES JULIAN F AND ALLEN C ENDERS The composition of the anal gland of *Dasyproctus notomys*
 Histochemical studies on the histogenesis of the joints in human fetuses with special reference to the development of the joint cavities in the hand and foot
 Histochemical study of estrogen induced lesions in the hamster male reproductive tract a morphological and
 Histogenesis of the joint in human fetuses with special reference to the development of the joint cavity in the hand and foot
 Homologous and autologous transplants
 I Studies on adrenal transplantation
 HOOVER CATHERINE E STEVENS Use of colchicine for the measurement of mitotic rate in the intestinal epithelium

HOYTE D A N The postnatal growth of the ear capsule in the rabbit
 HUCKINS CLAIRE See Clermont Y
 Human cardiac muscle and its associated tissue space the ultrastructure of
 Human fetuses with special reference to the development of the joint cavities in the hand and foot histochemical studies on the histogenesis of the joints in

I

Intestinal epithelium use of colchicine for the measurement of mitotic rate in the

J

Joints in human fetuses with special reference to the development of the joint cavities in the hand and foot histochemical studies on the histogenesis of the

K

Kangaroo rat *Dipodomys* the ear apparatus of the
 KEEN J A A study of the arterial variations in the limbs with special reference to symmetry of vascular patterns

L

LEBLOND C P See Percy B
 Lesions in the hamster male reproductive tract a morphological and histochemical study of estrogen induced
 Limbs with special reference to symmetry of vascular patterns a study of the arterial variations in the
 Localization of acid phosphatase non specific esterases and β D galactosidase in parotid and submaxillary glands of domestic and laboratory animals
 LOW FRANK N See Battig Charles C

M

(*M. mulatta*) electron microscopic observations of the internal limiting membrane and optic fiber layer of the retina of the Rhesus monkey
 Male reproductive tract a morphological and histochemical study of estrogen induced lesions in the hamster
 Mammals a study of the subgross pulmonary anatomy in various
 McLAUGHLIN RICHARD F WALTER S TYLER AND ROBERT O CANADA A study of the subgross pulmonary anatomy in various mammals
 Membrane and optic fiber layer of the retina of the Rhesus monkey (*M. mulatta*) electron microscopic observations of the internal limiting
 Microscopic anatomy of the sex cords and seminiferous tubules in growing and adult male albino rats

- Microscopic observations of the internal limiting membrane and optic fiber layer of the retina of the Rhesus monkey (*M. mulatta*) electron 179
- ALONCZAKOWSKA OLGA See Bodey Gerald P
- Mitotic rate in the intestinal epithelium use of colchicine for the measurement of 167
- MOFFAT D B The development of the anterior cerebral artery and its related vessels in the rat 231
- Monkey (*M. mulatta*) electron microscopic observations of the internal limiting membrane and optic fiber layer of the retina of the Rhesus 17
- Morphological and histochemical study of estrogen induced lesions in the hamster male reproductive tract A 179
- MOSS MELVIN L Osteogenesis of acellular teleost fish bone 31
- Mouse and rat on the fine structure of the parotid gland of 99
- Muscle and its associated tissue space the ultrastructure of human cardiac 303

O

- Optic fiber layer of the retina of the Rhesus monkey (*M. mulatta*) electron microscopic observations of the internal limiting membrane and 179
- Osteogenesis of acellular teleost fish bone 99

P

- PAPPAS GEORGE D See Donahue Sheila 331
- PARKS HAROLD F On the fine structure of the parotid gland of mouse and rat 303
- Parotid and submaxillary glands of domestic and laboratory animals localization of acid phosphatase nonspecific esterases and β -D-galactosidase in 263
- Parotid gland of mouse and rat on the fine structure of the 303
- PERRY B Y CLERMONT AND C P LEBLOND The wave of the seminiferous epithelium in the rat 47
- Phosphatase nonspecific esterase and β -D-galactosidase in parotid and submaxillary glands of domestic and laboratory animals localization of acid 263
- Postnatal growth of the ear capsule in the rabbit the 1
- Pulmonary anatomy in various mammals a study of the subgross 149

Q

- QUINTARELLI GIULIANO See Chauncey Howard H 263

R

- Rabbit the postnatal growth of the ear capsule in the 1
- Rat at various stages of development the fine structure of capillaries in the cerebral cortex of the 331

- Rat *Dipodomys* the ear apparatus of the kangaroo 123
- Rat on the fine structure of the parotid gland of mouse and 303
- Rat the development of the anterior cerebral artery and its related vessels in the 17
- Rat the wave of the seminiferous epithelium in the 47
- Rats microscopic anatomy of the sex cords and seminiferous tubules in growing and adult male albino 79
- Reproductive tract a morphological and histochemical study of estrogen induced lesions in the hamster male 31
- Retina of the Rhesus monkey (*M. mulatta*) electron microscopic observations of the internal limiting membrane and optic fiber layer of the 179
- Rhesus monkey (*M. mulatta*) electron microscopic observations of the internal limiting membrane and optic fiber layer of the retina of the 179

S

- Seminiferous epithelium in the rat the wave of the 47
- Seminiferous tubules in growing and adult male albino rats microscopic anatomy of the sex cords and 79
- Sex cords and seminiferous tubules in growing and adult male albino rats microscopic anatomy of the 79
- Structure of capillaries in the cerebral cortex of the rat at various stages of development the fine 331
- Structure of the parotid gland of mouse and rat on the fine 303
- Submaxillary glands of domestic and laboratory animals localization of acid phosphatase nonspecific esterases and β -D-galactosidase in parotid and 263
- Symmetry of vascular patterns a study of the arterial variations in the limbs with special reference to 213

T

- Teleost fish bone osteogenesis of acellular tissue space the ultrastructure of human cardiac muscle and its associated 99
- Transplantation studies on adrenal I homologous and autogenous transplants 109
- Transplants I homologous and autogenous studies on adrenal transplantation 167
- Tubules in growing and adult male albino rats microscopic anatomy of the sex cords and seminiferous 167
- TYLER WALTER S See McLaughlin Richard 79

U

- Ultrastructure of human cardiac muscle and its associated tissue space the 331

